

Notes on tokamak equilibrium*

BY YOUJUN HU

Institute of Plasma Physics, Chinese Academy of Sciences
Email: yjhu@ipp.cas.cn

Abstract

This document discusses the free boundary tokamak equilibrium fitting problem, fixed-boundary equilibrium problem, and magnetic coordinates.

1 Introduction

A routine in tokamak operation is to reconstruct magnetic field under the constraints of MHD force balance and experimental measurements. This kind of task can be done by various codes, e.g., **EFIT**. I developed a similar code, **heq** (github.com/youjunhu/heq). I will discuss details related to this code.

I also discuss the fixed-boundary equilibrium problem, where the boundary magnetic surface is given and one is asked to solve the force-balance equation within that boundray.

Another topic is how to construct spatial coordinates that conform to the shape of the magnetic surfaces and makes field line equation simple by defining suitable poloidal/toroidal angles, based on discrete numerical equilibrium data output by the equilibrium reconstructing codes.

Let us begin with the basics.

2 Axisymmetric magnetic field

Due to the divergence-free condition, i.e., $\nabla \cdot \mathbf{B} = 0$, magnetic field can be expressed as the curl of a vector field,

$$\mathbf{B} = \nabla \times \mathbf{A}, \quad (2.1)$$

where \mathbf{A} is called the vector potential of \mathbf{B} . (The usefulness of this representation is that, once \mathbf{B} is in this form, we do not need to worry about the divergence-free constraint.) In cylindrical coordinates (R, ϕ, Z) , the above expression is written

$$\mathbf{B} = \left(\frac{1}{R} \frac{\partial A_Z}{\partial \phi} - \frac{\partial A_\phi}{\partial Z} \right) \hat{\mathbf{R}} + \left(\frac{1}{R} \frac{\partial (R A_\phi)}{\partial R} - \frac{1}{R} \frac{\partial A_R}{\partial \phi} \right) \hat{\mathbf{Z}} + \left(\frac{\partial A_R}{\partial Z} - \frac{\partial A_Z}{\partial R} \right) \hat{\phi}. \quad (2.2)$$

*. This article has been written using GNU $\text{\TeX}_{\text{MACS}}$ [14].

We consider axisymmetric magnetic field, which means that, when expressed in the cylindrical coordinate system (R, ϕ, Z) , the components of \mathbf{B} , namely B_R , B_Z , and B_ϕ , are all independent of ϕ . For this case, it can be proved that an axisymmetric vector potential \mathbf{A} suffices for expressing the magnetic field, i.e., all the components of the vector potential \mathbf{A} can also be taken independent of ϕ . Using this, Eq. (2.2) is written

$$\mathbf{B} = -\frac{\partial A_\phi}{\partial Z} \hat{\mathbf{R}} + \frac{1}{R} \frac{\partial(RA_\phi)}{\partial R} \hat{\mathbf{Z}} + \left(\frac{\partial A_R}{\partial Z} - \frac{\partial A_Z}{\partial R} \right) \hat{\phi}. \quad (2.3)$$

In tokamak literature, $\hat{\phi}$ direction is called the toroidal direction, and (R, Z) planes (i.e., $\phi = \text{const}$ planes) are called poloidal planes.

2.1 Poloidal magnetic field

Equation (2.3) indicates that the two poloidal components of \mathbf{B} , namely B_R and B_Z , are determined by a single component of \mathbf{A} , namely A_ϕ . This motivates us to define a function $\Psi(R, Z)$:

$$\Psi(R, Z) \equiv RA_\phi(R, Z). \quad (2.4)$$

Then Eq. (2.3) implies the poloidal components, B_R and B_Z , can be written as

$$B_R = -\frac{1}{R} \frac{\partial \Psi}{\partial Z}, \quad (2.5)$$

$$B_Z = \frac{1}{R} \frac{\partial \Psi}{\partial R}. \quad (2.6)$$

(Note that it is the property of being axisymmetric and divergence-free that enables us to express the two components of \mathbf{B} , namely B_R and B_Z , in terms of a single function $\Psi(R, Z)$.) Furthermore, it is ready to prove that Ψ is constant along a magnetic field line, i.e. $\mathbf{B} \cdot \nabla \Psi = 0$. [Proof:

$$\begin{aligned} \mathbf{B} \cdot \nabla \Psi &= \mathbf{B} \cdot \left(\frac{\partial \Psi}{\partial R} \hat{\mathbf{R}} + \frac{\partial \Psi}{\partial Z} \hat{\mathbf{Z}} \right) \\ &= -\frac{1}{R} \frac{\partial \Psi}{\partial Z} \frac{\partial \Psi}{\partial R} + \frac{1}{R} \frac{\partial \Psi}{\partial R} \frac{\partial \Psi}{\partial Z} \\ &= 0. \end{aligned} \quad (2.7)$$

]

We note that Ψ is related to the poloidal magnetic flux, as we will discuss in Sec. 2.7.

Using Eqs. (2.5) and (2.6), the poloidal magnetic field \mathbf{B}_p is written as

$$\begin{aligned}
 \mathbf{B}_p &= B_R \hat{\mathbf{R}} + B_Z \hat{\mathbf{Z}} \\
 &= -\frac{1}{R} \frac{\partial \Psi}{\partial Z} \hat{\mathbf{R}} + \frac{1}{R} \frac{\partial \Psi}{\partial R} \hat{\mathbf{Z}} \\
 &= \frac{1}{R} \nabla \Psi \times \hat{\phi} \\
 &= \nabla \Psi \times \nabla \phi
 \end{aligned} \tag{2.8}$$

2.2 Toroidal magnetic field

Next, let's examine the toroidal component B_ϕ . Equation (2.3) indicates that B_ϕ involves both A_R and A_Z . This indicates that using the potential form does not enable useful simplification for B_ϕ . Therefore we will directly use B_ϕ . Define $g \equiv R B_\phi(R, Z)$ (the reason that we define this quantity will become clear when we discuss the force balance), then the toroidal magnetic field is written as

$$\mathbf{B}_\phi = B_\phi \hat{\phi} = \frac{g}{R} \hat{\phi} = g \nabla \phi. \tag{2.9}$$

2.3 General form of axisymmetric magnetic field

Combining Eqs. (2.8) and (2.9), we obtain

$$\begin{aligned}
 \mathbf{B} &= \mathbf{B}_p + \mathbf{B}_\phi \\
 &= \nabla \Psi \times \nabla \phi + g \nabla \phi,
 \end{aligned} \tag{2.10}$$

which is a general expression of axisymmetric magnetic field. Expression (2.10) is a famous formula in tokamak physics.

2.4 Gauge freedom of Ψ

Let us discuss the gauge freedom of \mathbf{A} in the axisymmetric case. Magnetic field remains the same under the following gauge transformation of the vector potential:

$$\mathbf{A}^{\text{new}} = \mathbf{A} + \nabla f, \tag{2.11}$$

where f is an arbitrary scalar field. Here we require that ∇f be axisymmetric because, as mentioned above, an axisymmetric vector potential suffices for describing an axisymmetric magnetic field. In cylindrical coordinates, ∇f is given by

$$\nabla f = \frac{\partial f}{\partial R} \hat{\mathbf{R}} + \frac{\partial f}{\partial Z} \hat{\mathbf{Z}} + \frac{1}{R} \frac{\partial f}{\partial \phi} \hat{\phi}. \tag{2.12}$$

Since ∇f is axisymmetric, it follows that all the three components of ∇f are independent of ϕ , i.e., $\partial^2 f / \partial R \partial \phi = 0$, $\partial^2 f / \partial Z \partial \phi = 0$, and $\partial^2 f / \partial \phi^2 = 0$, which implies that $\partial f / \partial \phi$ is independent of R , Z , and ϕ , i.e., $\partial f / \partial \phi$ is actually a spatial constant. Denote this constant by C . Then ϕ component of the gauge transformation (2.11) is written

$$\begin{aligned} A_\phi^{\text{new}} &= A_\phi + \frac{1}{R} \frac{\partial f}{\partial \phi} \\ &= A_\phi + \frac{C}{R}, \end{aligned} \quad (2.13)$$

(We see that the requirement of being axial symmetry greatly reduces gauge freedom of A_ϕ .) Multiplying Eq. (2.13) with R , we obtain the corresponding gauge transformation for Ψ ,

$$\Psi^{\text{new}} = \Psi + C, \quad (2.14)$$

which indicates Ψ is similar to that of electrostatic potential, i.e., adding a constant to it does not make difference. Note that the definition $\Psi(R, Z) \equiv R A_\phi$ does not imply $\Psi(R=0, Z)=0$ because A_ϕ can adopt $1/R$ dependence under the gauge transformation (2.13). If A_ϕ is finite at $R=0$, then Ψ is zero there. This is the case we encounter in the equilibrium reconstruction problem.

2.5 Contours of Ψ in the poloidal plane

Because Ψ is constant along a magnetic field line and Ψ is independent of ϕ , the projection of a magnetic field line onto (R, Z) plane is a contour of Ψ . Inversely, a contour of Ψ is also projections of a magnetic field line onto the plane. [Proof. A contour of Ψ on (R, Z) plane satisfies

$$d\Psi = 0, \quad (2.15)$$

i.e.,

$$\frac{\partial \Psi}{\partial R} dR + \frac{\partial \Psi}{\partial Z} dZ = 0. \quad (2.16)$$

$$\Rightarrow \frac{1}{R} \frac{\partial \Psi}{\partial R} dR + \frac{1}{R} \frac{\partial \Psi}{\partial Z} dZ = 0. \quad (2.17)$$

Using Eqs. (2.5) and (2.6), the above equation is written

$$B_Z dR - B_R dZ = 0, \quad (2.18)$$

i.e.,

$$\frac{dZ}{dR} = \frac{B_Z}{B_R}, \quad (2.19)$$

which is the equation of the projection of a magnetic field line in (R, Z) plane. This proves that contours of Ψ are projections of magnetic field lines in (R, Z) plane.]

Figure 2.1 shows typical contours of Ψ in a tokamak (CFETR tokamak as an example).

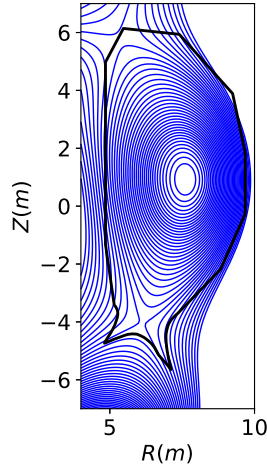


Figure 2.1. Blue lines are contours of Ψ . The black line is the machine wall.

Points where the poloidal field is zero (i.e., $\nabla\Psi=0$) are called (poloidal) magnetic null points. There are two types of magnetic null points : O-points and X-points, which can be visually identified by viewing contours of Ψ . Mathematically, O-points and X-points are distinguished by the sign of S defined by

$$S(R, Z) = \frac{\partial^2 \Psi}{\partial R^2} \frac{\partial^2 \Psi}{\partial Z^2} - \left(\frac{\partial^2 \Psi}{\partial R \partial Z} \right)^2, \quad (2.20)$$

where $S \geq 0$ corresponds to O-points and $S < 0$ corresponds to X-points.

2.6 Magnetic surfaces

Surfaces of revolution generated by rotating Ψ contours around the axis of symmetry (Z axis) are called magnetic surfaces or flux surfaces. No field line intersects these surfaces. We are only interested in flux surfaces within the machine wall. We note that some Ψ contours may intersect the wall before they can form closed curves. Field lines on the corresponding flux surfaces are called open field lines.

The value of Ψ is constant on a magnetic surface. Meanwhile, the values of Ψ on different magnetic surfaces are usually different. These two properties enable Ψ to be used as labels of magnetic surfaces. In cases that there are multiple magnetic surfaces of the same value of Ψ , the ambiguity can be resolved by specifying which region the flux surfaces lie in, e.g., within or outside the last-closed-flux surface region, near the high-field side or low-field side, in the Scrape-Off Layer or the private flux region (PFR, the area between the X-point and the material divertor., i.e, the region between divertor legs that is unconnected to the plasma).

2.7 Relation of Ψ with the poloidal magnetic flux

Note that Ψ is defined by $\Psi = RA_\phi$, which is just a component of the vector potential \mathbf{A} , thereby having no obvious physical meaning. Next, we show that Ψ has a simple relation with the poloidal magnetic flux that can be measured in experiments.

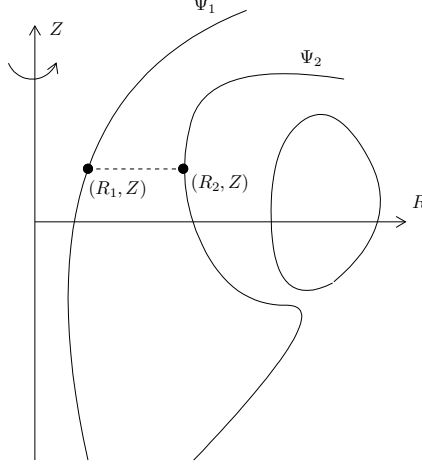


Figure 2.2. The poloidal magnetic flux $\Psi_p^{(12)}$ between the two magnetic surfaces Ψ_1 and Ψ_2 is given by $\Psi_p^{(12)} = 2\pi(\Psi_2 - \Psi_1)$, where the surface orientation for the poloidal flux definition is chosen to be $+\hat{\mathbf{Z}}$.

In Fig. 2.2, there are two magnetic surfaces labeled, respectively, by $\Psi = \Psi_1$ and $\Psi = \Psi_2$. The poloidal magnetic flux through any toroidal ribbons between the two magnetic surfaces is equal to each other (due to the magnetic Gauss theorem). Denote this poloidal magnetic flux by $\Psi_p^{(12)}$. Next, we calculate this flux. To make the calculation easy, we select a plane perpendicular to the Z axis, as is shown by the dash line in Fig. (2.2). In this case, only B_Z contribute to the poloidal magnetic flux: (the positive direction of the plane is chosen to be $\hat{\mathbf{Z}}$)

$$\begin{aligned}
 \Psi_p^{(12)} &= \int_{R_1}^{R_2} B_z(R, Z) 2\pi R dR \\
 &= \int_{R_1}^{R_2} \frac{1}{R} \frac{\partial \Psi}{\partial R} 2\pi R dR \\
 &= 2\pi \int_{R_1}^{R_2} \frac{\partial \Psi}{\partial R} dR \\
 &= 2\pi[\Psi_2 - \Psi_1].
 \end{aligned} \tag{2.21}$$

Equation (2.21) indicates that the difference of Ψ between two magnetic surfaces is equal to the poloidal flux divided by 2π .

In experiments, we measure the poloidal magnetic flux through toroidal loops around the central symmetric axis (discussed in Sec. 2.8). Consider one of the loops that located at point (R, Z) , then, using (2.21), the flux through the loop can be written as

$$\Psi_p = 2\pi[\Psi(R, Z) - \Psi(R=0, Z)], \quad (2.22)$$

The central symmetric axis ($R = 0$) is a field line. If A_ϕ is finite at $R = 0$, then $\Psi = A_\phi R$ is zero there. This is the case we encounter in the equilibrium reconstruction problem. Then this flux is written as

$$\Psi_p = 2\pi\Psi(R, Z). \quad (2.23)$$

Due to this relation, Ψ is often called the poloidal magnetic flux per radian (SI unit: web/rad), or simply “the poloidal flux”. This relation allows the poloidal flux measurements to be used to constrain the GS equation in the equilibrium reconstruction (discussed in Sec. 6). Note that the positive normal direction of the surface (where the magnetic flux Ψ_p is defined) is chosen in the $+\mathbf{Z}$ direction. This sign choice along with the 2π factor appearing in Eq. (2.23) are often confusing people when they try to relate the experimentally measured flux with the Ψ appearing in the GS equation. The 2π factor also appears when we relate the Green function of Ψ to the mutual inductance, i.e., $M = 2\pi G$ (discussed later).

2.8 Measuring poloidal magnetic flux in experiments

By measuring the voltage around a toroidal wire loop, we can obtain the time derivative of the poloidal flux and, after integrating over time, the flux itself.

Suppose that there is a toroidal wire loop located at (R, Z) and denote the magnetic flux through the loop by $\Psi_p(R, Z, t)$ (only the poloidal magnetic field contribute to this flux, hence this flux is called the poloidal flux). Then Faraday’s law

$$\oint \mathbf{E} \cdot d\mathbf{l} = - \int \frac{\partial \mathbf{B}}{\partial t} \cdot d\mathbf{S}, \quad (2.24)$$

where the direction of the loop integration and the direction of $d\mathbf{S}$ is related by the right-hand rule, is written as

$$\varepsilon = - \frac{d\Psi_p}{dt}, \quad (2.25)$$

where $\varepsilon = \oint \mathbf{E} \cdot d\mathbf{l}$ is often called electromotive force (emf). If the loop is a coil with N turns, the induced voltage V in the coil is N times the emf, i.e., $V = N\varepsilon$. Then Eq. (2.25) is written as

$$V = -N \frac{d\Psi_p}{dt}. \quad (2.26)$$

Integrating the above equation over time, we obtain

$$\Psi_p(R, Z, t) = \Psi_p(R, Z, 0) - \frac{1}{N} \int_0^t V dt. \quad (2.27)$$

The starting time $t = 0$ can be chosen as when $\Psi_p(R, Z, 0)$ is easy to know (e.g., when there is no plasma). Equation (2.27) tells us how to calculate Ψ_p from the measured loop voltage V . Then Ψ is obtained by $\Psi = \Psi_p / (2\pi)$.

There are usually many flux loops (e.g. 35 on EAST[32]) at different locations in the poloidal plane (see Fig. 2.3). They are outside of the plasma region and thus are “external magnetic measurements”. The measured poloidal flux, along with the poloidal field measurement by magnetic probes, can be used as constraints in reconstructing the magnetic field within the plasma region. This is discussed in Sec. 6.

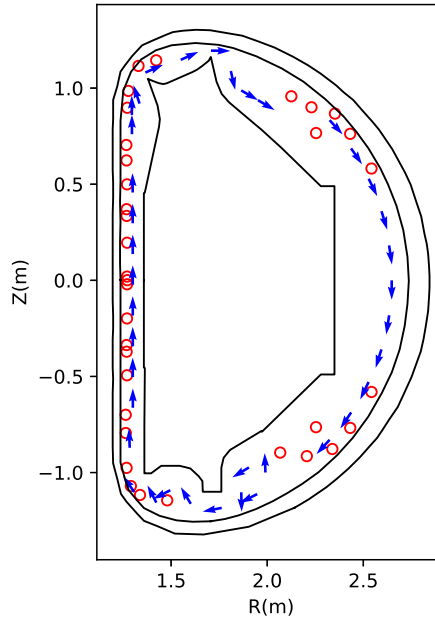


Figure 2.3. Flux loops (circles) and magnetic probes (blue arrows) on EAST tokamak. Arrows indicate the positive normal direction of the probes.

2.9 Closed magnetic surfaces

In most part of a tokamak plasma, contours of Ψ in (R, Z) plane are closed before they touch the machine wall. Figure 2.4 shows some examples of closed flux surfaces.

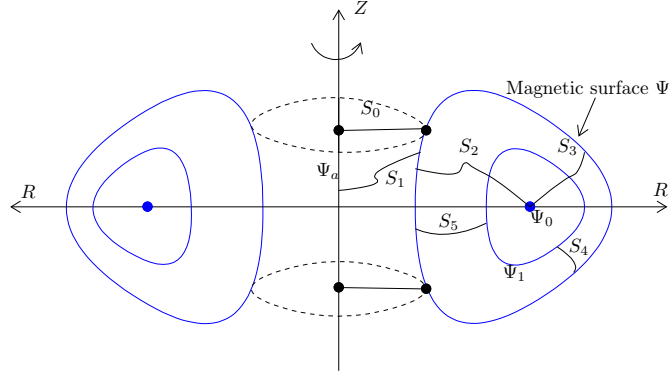


Figure 2.4. Closed magnetic surfaces (blue) and various toroidal surfaces used to define the poloidal magnetic flux. The magnetic flux through the toroidal surface S_2 and S_3 is equal to each other. Also the magnetic flux through S_4 and S_5 is equal to each other; the magnetic flux through S_0 and S_1 is equal to each other.

The innermost magnetic surface reduces to a curve, which is called magnetic axis (in Fig. 2.4, Ψ_0 labels the magnetic axis). $\nabla\Psi$ is zero at the magnetic axis since $\Psi(R, Z)$ reach maximum/minimum there. As a result, the poloidal magnetic field is zero there (refer to Eq. (2.8)).

As is discussed in Sec. 2.7, the poloidal magnetic flux enclosed by a magnetic surface Ψ (the poloidal magnetic flux through the toroidal surfaces S_2) is given by

$$\Psi_p^{(\text{axis})} = 2\pi (\Psi_0 - \Psi). \quad (2.28)$$

Here the positive direction of the surface S_2 is defined to be in the clockwise direction when an observer looks along the direction of $\hat{\phi}$. In practice, we need to pay attention to the positive direction chosen (there can be a sign difference when choosing different positive directions).

Also note, the poloidal magnetic flux enclosed by a closed magnetic surface can have another definitions: the poloidal magnetic flux through the central hole of the magnetic surface, i.e., the poloidal flux through S_1 in Fig. 2.4. In this case, as is discussed in Sec. 2.7, the poloidal magnetic flux is related to Ψ by

$$\Psi_p = 2\pi(\Psi - \Psi(R=0, Z)) = 2\pi\Psi, \quad (2.29)$$

where $\Psi(R=0, Z)=0$ is assumed and the positive direction of the surface S_1 is in the clockwise direction.

Also note that, since $\mathbf{B}_p = \nabla\Psi \times \nabla\phi$, the condition $\Psi_{\text{LCFS}} - \Psi_{\text{axis}} > 0$ means \mathbf{B}_p points in the anticlockwise direction (viewed along $\hat{\phi}$ direction), and $\Psi_{\text{LCFS}} - \Psi_{\text{axis}} < 0$ means \mathbf{B}_p points in the clockwise direction.

3 Non-axisymmetric magnetic perturbations

In the above, the magnetic field is assumed to be axisymmetric. With this assumption, the poloidal magnetic field (having two components) can be expressed in terms of a single component of the vector potential \mathbf{A} , A_ϕ (specifically via $\Psi \equiv A_\phi R$). This kind of simplification is not achievable if the axisymmetry assumption is dropped, because other components of the vector potential (namely A_R and A_Z) will appear in the expression of the poloidal magnetic field. Let us re-examine Eq. (2.2) for a general magnetic perturbation:

$$\begin{aligned} \delta \mathbf{B} = & \left(\frac{1}{R} \frac{\partial \delta A_Z}{\partial \phi} - \frac{\partial \delta A_\phi}{\partial Z} \right) \hat{\mathbf{R}} + \left(\frac{1}{R} \frac{\partial (R \delta A_\phi)}{\partial R} - \frac{1}{R} \frac{\partial \delta A_R}{\partial \phi} \right) \hat{\mathbf{Z}} \\ & + \left(\frac{\partial \delta A_R}{\partial Z} - \frac{\partial \delta A_Z}{\partial R} \right) \hat{\phi}. \end{aligned} \quad (3.1)$$

When studying tearing modes and electromagnetic turbulence, most authors narrow the possible perturbations by setting $\delta A_R = \delta A_Z = 0$, i.e.,

$$\delta B_R = -\frac{1}{R} \frac{\partial \delta \Psi}{\partial Z}, \quad (3.2)$$

$$\delta B_Z = \frac{1}{R} \frac{\partial \delta \Psi}{\partial R}, \quad (3.3)$$

$$\delta B_\phi = 0. \quad (3.4)$$

where $\delta \Psi = R \delta A_\phi$. Therefore this kind of magnetic perturbation can still be written in the same form as the equilibrium poloidal magnetic field:

$$\delta \mathbf{B} = \nabla \delta \Psi \times \nabla \phi. \quad (3.5)$$

The above approximation is widely used in practice, e.g., in turbulence simulation, where δA_ϕ is replaced by δA_\parallel . (Do we miss some magnetic perturbations that is important for plasma transport when using the above specific form?)

The total magnetic field is then written as

$$\mathbf{B} = \nabla(\Psi + \delta \Psi) \times \nabla \phi + g \nabla \phi. \quad (3.6)$$

****check**** Can the projection of the total magnetic field line in the poloidal plane can be traced by tracing the contour of $\Psi + \delta \Psi$? No. The contours of $\Psi + \delta \Psi$ will not show island structures in the poloidal plane. To show the expected island structures, we need to subtract non-reconnecting poloidal magnetic field from the total poloidal field? ****check**** The contours of the so-called helical flux will give the expected island structures near the resonant surfaces? ****check****

Next, we go back to discuss the 2D case (i.e., assuming axisymmetry).

4 Plasma current density in terms of Ψ and g

When the displacement current term is neglectable (the case we consider here), the conductive current is just another representation of the magnetic field. Specifically, the current density is proportional to the curl of the magnetic field (Ampère's law):

$$\begin{aligned}\mu_0 \mathbf{J} &= \nabla \times \mathbf{B} \\ &= -\frac{\partial B_\phi}{\partial Z} \hat{\mathbf{R}} + \frac{1}{R} \frac{\partial(RB_\phi)}{\partial R} \hat{\mathbf{Z}} + \left(\frac{\partial B_R}{\partial Z} - \frac{\partial B_Z}{\partial R} \right) \hat{\phi},\end{aligned}\quad (4.1)$$

where μ_0 is vacuum magnetic permeability.

4.1 Poloidal current density

Use Eq. (4.1) and the definition $g \equiv RB_\phi$, the poloidal components of the current density, J_Z and J_R , can be written as

$$\mu_0 J_R = -\frac{1}{R} \frac{\partial g}{\partial Z}, \quad (4.2)$$

and

$$\mu_0 J_Z = \frac{1}{R} \frac{\partial g}{\partial R}, \quad (4.3)$$

respectively.

4.2 Toroidal current density

Ampère's law (4.1) indicates the toroidal current density J_ϕ is given by

$$\begin{aligned}\mu_0 J_\phi &= \frac{\partial B_R}{\partial Z} - \frac{\partial B_Z}{\partial R} \\ &= -\frac{1}{R} \frac{\partial^2 \Psi}{\partial Z^2} - \frac{\partial}{\partial R} \left(\frac{1}{R} \frac{\partial \Psi}{\partial R} \right).\end{aligned}\quad (4.4)$$

Define Δ^* by

$$\Delta^* \equiv \frac{\partial^2}{\partial Z^2} + R \frac{\partial}{\partial R} \left(\frac{1}{R} \frac{\partial}{\partial R} \right), \quad (4.5)$$

which is the Laplace operator in cylindrical coordinates for the axisymmetric case, then Eq. (4.4) is written as

$$J_\phi = -\frac{1}{\mu_0 R} \Delta^* \Psi. \quad (4.6)$$

(Many authors refer to Eq. (4.6) as the Grad-Shafranov (GS) equation. No, it is not. It is just Ampère's law, which has nothing to do with the force-balance. Only after we express J_ϕ in terms of the plasma pressure, can Eq. (4.6) be called the GS equation, as is discussed Sec. 5.3.)

5 Constraint of force-balance on magnetic field

Let us consider what constraint the force balance imposes on the axisymmetric magnetic field discussed above. The MHD momentum equation is given by

$$\rho \left(\frac{\partial \mathbf{u}}{\partial t} + \mathbf{u} \cdot \nabla \mathbf{u} \right) = \rho_q \mathbf{E} + \mathbf{J} \times \mathbf{B} - \nabla \cdot \mathbb{P} \quad (5.1)$$

where ρ , ρ_q , \mathbb{P} , \mathbf{J} , \mathbf{E} , and \mathbf{B} are mass density, charge density, thermal pressure tensor, current density, electric field, and magnetic field, respectively. The electric field force $\rho_q \mathbf{E}$ is usually ignored due to either $\rho_q = 0$ or $\mathbf{E} = 0$. Further assume that there is no plasma flow ($\mathbf{u} = 0$, the flow effect is discussed in A.4) and the plasma pressure is isotropic, then the steady state momentum equation (force balance equation) is written as

$$\mathbf{J} \times \mathbf{B} = \nabla P, \quad (5.2)$$

where P is the scalar plasma pressure.

Is the force balance (5.2) always satisfied in a real tokamak discharge? To answer this question, we need to go back to the original momentum equation (5.1). The imbalance between $\mathbf{J} \times \mathbf{B}$ and ∇P will give rise to the compressional Alfvén waves, the time-scale of which, τ_A , is much shorter than the time-scale τ we are interested in. Therefore, on the time scale τ (and for slow flow with $\mathbf{u} < C_s$, where C_s is the sound speed), the leading order of the momentum equation is the force balance (5.2). [26].

5.1 Parallel force balance

Consider the force balance in the direction of \mathbf{B} . Dotting the equilibrium equation (5.2) by \mathbf{B} , we obtain

$$0 = \mathbf{B} \cdot \nabla P, \quad (5.3)$$

which implies that P is constant along a magnetic field line. Since Ψ is also constant along a magnetic field line, P can be expressed in terms of only Ψ on a single magnetic line. Note that this does not necessarily mean P is a single-valued function of Ψ , (i.e. $P = P(\Psi)$). This is because P still has the freedom of taking different values on different magnetic field lines with the same value of Ψ while still satisfying $\mathbf{B} \cdot \nabla P = 0$. This situation can appear when there are saddle points (X points) in Ψ contours (refer to Sec. A.14) and P takes different functions of Ψ in islands of Ψ separated by a X point. For pressure within a single island of Ψ , $P = P(\Psi)$ can be safely assumed.

On the other hand, if $P = P(\Psi)$, then we obtain

$$\mathbf{B} \cdot \nabla P = \frac{dP}{d\Psi} \mathbf{B} \cdot \nabla \Psi = 0,$$

i.e., Eq. (5.3) is satisfied, indicating $P = P(\Psi)$ is a sufficient condition for the force balance in the parallel (to the magnetic field) direction.

5.2 Toroidal force balance

Consider the force balance in the toroidal direction. The ϕ component of Eq. (5.2) is written

$$J_Z B_R - J_R B_Z = \frac{1}{R} \frac{\partial P}{\partial \phi}. \quad (5.4)$$

Since $P = P(\Psi)$, which implies $\partial P / \partial \phi = 0$, equation (5.4) reduces to

$$J_Z B_R - J_R B_Z = 0 \quad (5.5)$$

Using the expressions of the poloidal current density (4.2) and (4.3) in the force balance equation (5.5) yields

$$\frac{\partial g}{\partial R} B_R + \frac{\partial g}{\partial Z} B_Z = 0, \quad (5.6)$$

which can be further written

$$\mathbf{B} \cdot \nabla g = 0. \quad (5.7)$$

According to the same reasoning for the pressure, we conclude that $g = g(\Psi)$ is a sufficient condition for the toroidal force balance. (The function g defined here is usually called the “poloidal current function” in tokamak literature. The reason for this name is discussed in Sec. A.5.)

5.3 Force balance along the major radius

Consider the force balance in $\hat{\mathbf{R}}$ direction. The $\hat{\mathbf{R}}$ component of Eq. (5.2) is written

$$J_\phi B_Z - J_Z B_\phi = \frac{\partial P}{\partial R} \quad (5.8)$$

Using the expressions of the current density and magnetic field [Eqs. (2.6) and (4.3)], equation (5.8) is written

$$J_\phi \frac{1}{R} \frac{\partial \Psi}{\partial R} - \frac{1}{\mu_0 R} \frac{\partial g}{\partial R} \frac{g}{R} = \frac{\partial P}{\partial R}. \quad (5.9)$$

Assuming the sufficient condition discussed above, i.e., P and g are a function of only Ψ , i.e., $P = P(\Psi)$ and $g = g(\Psi)$, Eq. (5.9) is written

$$J_\phi \frac{1}{R} \frac{\partial \Psi}{\partial R} - \frac{1}{\mu_0 R} \frac{dg}{d\Psi} \frac{\partial \Psi}{\partial R} \frac{g}{R} = \frac{dP}{d\Psi} \frac{\partial \Psi}{\partial R}, \quad (5.10)$$

which can be simplified to

$$J_\phi = R \frac{dP}{d\Psi} + \frac{1}{\mu_0 R} \frac{dg}{d\Psi} g, \quad (5.11)$$

which is the requirement of force-balance along the major radius. On the other hand, we know J_ϕ can be expressed in Ψ via Eq. (4.6). Combining this with Eq. (5.11) yields

$$\Delta^* \Psi = -\mu_0 R^2 \frac{dP}{d\Psi} - \frac{dg}{d\Psi} g, \quad (5.12)$$

i.e.,

$$\frac{\partial^2 \Psi}{\partial Z^2} + R \frac{\partial}{\partial R} \left(\frac{1}{R} \frac{\partial \Psi}{\partial R} \right) = -\mu_0 R^2 \frac{dP}{d\Psi} - \frac{dg}{d\Psi} g. \quad (5.13)$$

Equation (5.13) is known as Grad-Shafranov (GS) equation.

[Note that the Z component of the force balance equation is written

$$\begin{aligned} J_R B_\phi - J_\phi B_R &= \frac{\partial P}{\partial Z} \\ \Rightarrow -\frac{\partial g}{\partial Z} \frac{1}{R} \frac{g}{R} - \frac{1}{R} \Delta^* \Psi \frac{1}{R} \frac{\partial \Psi}{\partial Z} &= \mu_0 \frac{dP}{d\Psi} \frac{\partial \Psi}{\partial Z} \\ \Rightarrow -\frac{dg}{d\Psi} \frac{\partial \Psi}{\partial Z} \frac{1}{R} \frac{g}{R} - \frac{1}{R} \Delta^* \Psi \frac{1}{R} \frac{\partial \Psi}{\partial Z} &= \mu_0 \frac{dP}{d\Psi} \frac{\partial \Psi}{\partial Z} \\ \Rightarrow -\frac{dg}{d\Psi} \frac{1}{R} \frac{g}{R} - \frac{1}{R} \Delta^* \Psi \frac{1}{R} &= \mu_0 \frac{dP}{d\Psi} \\ \Rightarrow \Delta^* \Psi &= -\mu_0 R^2 \frac{dP}{d\Psi} - \frac{dg}{d\Psi} g \end{aligned}$$

which turns out to be identical with the Grad-Shafranov equation. This is not a coincidence. The reason is that the force balance equation has been satisfied in three different directions (namely, $\hat{\phi}$, $\hat{\mathbf{R}}$, and \mathbf{B} direction) and thus it must be satisfied in all the directions.]

5.4 Axisymmetric equilibrium magnetic field

A general axisymmetric magnetic field (which does not necessarily satisfy the force balance), is given by Eq. (2.10), i.e.,

$$\mathbf{B} = \underbrace{\nabla \Psi \times \nabla \phi}_{\text{poloidal}} + \underbrace{g \nabla \phi}_{\text{toroidal}}, \quad (5.14)$$

For the above axisymmetric magnetic field to be consistent with the force balance equation (5.2), there are additional requirements for Ψ and g . Specifically, Ψ is restricted by the GS equation and g should be a function of only Ψ . Therefore an axisymmetric equilibrium magnetic field is fully determined by two functions, $\Psi = \Psi(R, Z)$ and $g = g(\Psi)$. The Ψ is determined by solving the GS equation with specified RHS source terms and boundary conditions.

The RHS source terms in the GS equation (5.13) are $P(\Psi)$ and $g(\Psi)$, both of which must be specified before the GS equation can be solved. For most cases, the source terms are nonlinear about Ψ and thus the GS equation is a two-dimensional (in R and Z) nonlinear partial differential equation for Ψ .

For most choices of $P(\Psi)$ and $g(\Psi)$, the GS equation (5.13) has to be solved numerically. For some particular choices of P and g profiles, analytical solutions are available, one of which is the Solovév equilibrium and is discussed in Appendix A.3.

Note that we solve the GS equation in order to obtain the poloidal magnetic flux Ψ and thus the poloidal magnetic field. The toroidal magnetic field must be specified in some way before we can solve the GS equation. There are several ways of specifying the toroidal magnetic field: (1) given $g(\Psi)$, (2) given $\langle j_{\parallel} \rangle$, (3) given the safety factor $q(\Psi)$. There are simple relations between g , $\langle j_{\parallel} \rangle$, and q , which allows translation from one to another (discussed later). In transport simulations, $\langle j_{\parallel} \rangle$ is obtained from current drive models and neoclassical bootstrap current models. Note that the specification of the source terms (P , g , q , and $\langle j_{\parallel} \rangle$) usually involve the unknown Ψ (via not only the explicit presence of Ψ , but also the flux-surface averaging which implicitly involves Ψ). This indicates that iterations are needed when numerically solving the GS equation.

6 Free-boundary fitting problem

Ampere's law in Eq. (4.6) can be generalized to include discrete toroidal currents:

$$\Delta^* \Psi = -\mu_0 R J_{\phi} - \mu_0 R \sum_i I_i \delta(R - R_i) \delta(Z - Z_i), \quad (6.1)$$

where J_{ϕ} is the plasma toroidal current density, I_i is a toroidal current filament located at $(R = R_i, Z = Z_i)$, $\delta(\cdot)$ is Dirac's delta function. The solution to the above equation is given by

$$\Psi(R, Z) = \int_{\Omega} G(R', Z', R, Z) J_{\phi}(R', Z') dR' dZ' + \sum_i G(R_i, Z_i, R, Z) I_i, \quad (6.2)$$

where G is the fundamental solution given by

$$G(R', Z', R, Z) = \frac{\mu_0 R}{4\pi} \int_0^{2\pi} \frac{R' \cos \phi' d\phi'}{\sqrt{(Z - Z')^2 + (R - R' \cos \phi')^2 + (R' \sin \phi')^2}}, \quad (6.3)$$

which is often called Green's function in this context (which is obtained by using a formula similar to the Biot-Savart Law, see B.14).

If all the toroidal currents (plasma current + coil/vessel currents) are known, then Ψ can be calculated by using Eq. (6.2). Unfortunately J_{ϕ} is usually unknown. Meanwhile the force-balance indicates that J_{ϕ} can be expressed in terms of Ψ via Eq. (5.11), i.e.,

$$J_{\phi} = R \frac{dP}{d\Psi} + \frac{1}{\mu_0 R} g \frac{dg}{d\Psi}. \quad (6.4)$$

Substituting this into Eq. (6.2) gives an implicit formula for Ψ , which can be iterated (with an initial guess of $\Psi(R, Z)$, and assuming the function forms, $P(\Psi)$ and $g(\Psi)$, as well as the coil currents I_i , are known). We can see that

this is a Picard iteration. Will the iteration converge? We do not know for sure. Numerical experiments indicate it does in some cases[18]. Let us discuss some specific cases. We assume that the 1D functions, $P(\Psi)$ and $g(\Psi)$ can be modeled as (following EFIT's model):

$$\frac{dP(\Psi)}{d\Psi} = \begin{cases} \sum_{j=0}^{N_P-1} \alpha_j (x^j - x^{N_P}) & \text{for } x \leq 1 \\ 0 & \text{for } x > 1 \end{cases} \quad (6.5)$$

$$g \frac{dg}{d\Psi} = \begin{cases} \sum_{j=0}^{N_F-1} \beta_j (x^j - x^{N_F}) & \text{for } x \leq 1 \\ 0 & \text{for } x > 1 \end{cases} \quad (6.6)$$

where

$$x \equiv \bar{\Psi} \equiv \Psi_N \equiv \frac{(\Psi - \Psi_A)}{\Psi_B - \Psi_A}, \quad (6.7)$$

Ψ_A and Ψ_B are values of Ψ at the magnetic axis and LCFS, the coefficients α_j and β_j are to be determined, N_p and N_F are integers chosen by users. One feature of expressions (6.5) and (6.6) is that they guarantee that $dP/d\Psi$ and $g dg/d\Psi$ are zero at and outside the LCFS, and thus no plasma current there. Also note that expressions (6.5) and (6.6) are nonlinear functions of Ψ even for $N_p = N_F = 1$. This is because the unknowns, Ψ_A and Ψ_B , appear in the denominator of expression (6.7). Another nonlinearity is related to the fact that the unknown Ψ determines where is the LCFS and thus determine region where the current density is set to zero. This also gives rise to the name “free-boundary” for this kind of problems.

Choosing an initial guess of $\Psi(R, Z)$ on gridpoints, we can get the values of α_j , β_j , and I_i by solving a least square problem that minimises the difference between quantities computed and the corresponding quantities measured in actual experiments. (Details are given in Sec. 6.1.)

After the coefficients α_j and β_j are obtained, J_ϕ can be updated by using Eqs. (6.4)-(6.6). Then, we use the latest J_ϕ and I_i in Eq. (6.2) to update the values of Ψ on gridpoints. The procedure is repeated until convergence in $\Psi(R, Z)$. This is called Picard iteration. (Alternatively, the values of Ψ on the inner gridpoints can be updated by inverting the Laplace operator Δ^* , see Sec. 6.4. The values of Ψ on the boundary still have to be obtained by using Eq. (6.2).)

I implemented the above method in a Python code (HEQ <https://github.com/youjunhu/heq>). The following subsections discuss details in the code: Sec. 6.1 discusses the least square problem. Sec. 6.3 discusses the vertical displacement instability stabilizer. Without the stabilizer, the Picard iteration diverges for many elongated configurations, due to the vertical displacement instability.

6.1 Response matrix Γ

For $x \leq 1$, plugging expressions (6.5) and (6.6) into (6.4), we obtain

$$J_\phi(R', Z') = R' \sum_{j=0}^{N_p-1} \alpha_j (x^j - x^{N_p}) + \frac{1}{\mu_0 R'} \sum_{j=0}^{N_F-1} \beta_j (x^j - x^{N_F}), \quad (6.8)$$

For notation ease, define the following basis functions:

$$b_j(x) = \begin{cases} R'(x^j - x^{N_p}) & \text{for } 0 \leq j < N_p \\ (x^{j-N_p} - x^{N_F}) / (\mu_0 R') & \text{for } N_p \leq j < N_p + N_F \end{cases} \quad (6.9)$$

and the corresponding expansion coefficients

$$c_j = \begin{cases} \alpha_j & \text{for } 0 \leq j < N_p \\ \beta_{j-N_p} & \text{for } N_p \leq j < N_p + N_F \end{cases} \quad (6.10)$$

then Eq. (6.8) is written as

$$J_\phi = \sum_{j=0}^{N_b-1} c_j b_j(x), \quad (6.11)$$

where $N_b = N_p + N_F$. Plugging expression (6.11) into Eq. (6.2), we obtain

$$\begin{aligned} \Psi(R, Z) &= \sum_{j=0}^{N_b-1} c_j \int_{\Omega} G(R', Z', R, Z) b_j(x) dR' dZ' \\ &+ \sum_{j=0}^{N_c-1} G(R_j^{(c)}, Z_j^{(c)}, R, Z) I_j. \end{aligned} \quad (6.12)$$

Collect all the free parameters as a column vector: $\mathbf{u} = (c_0, \dots, c_{N_b-1}, I_0, \dots, I_{N_c-1})^T$. Denote the size of vector \mathbf{u} by N , which is the number of free parameters, i.e., $N = N_b + N_c$, then the rhs of Eq. (6.12) can be written as matrix-vector product, $\Gamma \mathbf{u}$. Denote the total number of measurements of the poloidal flux by M_{FL} . Then matrix elements of Γ for $i = 0, \dots, M_{\text{FL}} - 1$ are given by:

$$\Gamma_{ij} = \int_{\Omega} G(R', Z', R_i^{(\text{FL})}, Z_i^{(\text{FL})}) b_j(x) dR' dZ', \quad (6.13)$$

for $j = 0, \dots, N_b - 1$, and

$$\Gamma_{ij} = G(R_{j-N_b}^{(c)}, Z_{j-N_b}^{(c)}, R_i^{(\text{FL})}, Z_i^{(\text{FL})}), \quad (6.14)$$

for $j = N_b, \dots, N - 1$. Here $(R_i^{(\text{FL})}, Z_i^{(\text{FL})})$ is the location where the i th flux measurement is made.

The matrix Γ , which is of shape (M, N) , is called “response matrix”. (In least square problems, this matrix is called “design matrix”.) The value of M is equal to number of measurements/constraints included (measurements/constraints are merged to Γ by row stacking). We will include M_{FL} measurements of the poloidal flux, M_B measurements of the poloidal magnetic field, 1 measurement of plasma current, a constraint for the on-axis safety factor. Then $M = M_{\text{FL}} + M_B + 1 + 1$. (For EAST, $M_{\text{FL}} = 35$, $M_B = 38$.)

Next, we consider the poloidal field measurement:

$$B_p(R_i, Z_i) = \mathbf{B}_p \cdot \hat{\mathbf{n}}_i = B_R \cos \theta_{pi} + B_Z \sin \theta_{pi}, \quad (6.15)$$

where (R_i, Z_i) is the location of the No. i probe, $\hat{\mathbf{n}}_i$ is a unit vector denoting the positive normal direction of the No. i magnetic probe, $\cos \theta_{pi} = \hat{\mathbf{n}}_i \cdot \mathbf{e}_R$, $\sin \theta_{pi} = \hat{\mathbf{n}}_i \cdot \mathbf{e}_Z$.

$B_p(R_i, Z_i)$ can be inferred from \mathbf{u} via

$$\begin{aligned} B_p(R_i, Z_i) = & \sum_{j=0}^{N_b-1} c_j \int_{\Omega} G_B(R', Z', R_i, Z_i) b_j(x) dR' dZ' \\ & + \sum_{j=0}^{N_c-1} G_B(R_j^{(c)}, Z_j^{(c)}, R_i, Z_i) I_j. \end{aligned} \quad (6.16)$$

where

$$G_B(R', Z', R_i, Z_i) = G_{B_R}(R', Z', R_i, Z_i) \cos \theta_{pi} + G_{B_Z}(R', Z', R_i, Z_i) \sin \theta_{pi}, \quad (6.17)$$

and G_{B_R} and G_{B_Z} is given by Eq. (B.18) and (B.19). The rhs of Eq. (6.16) indicates that the matrix elements of Γ are given by:

$$\Gamma_{ij} = \int_{\Omega} G_B(R', Z', R_i, Z_i) b_j(x) dR' dZ', \quad (6.18)$$

for $(j = 0, \dots, N_b - 1)$, and

$$\Gamma_{ij} = G_B(R_{j-N_b}^{(c)}, Z_{j-N_b}^{(c)}, R_i, Z_i), \quad (6.19)$$

for $(j = N_b, \dots, N - 1)$. I place the magnetic field equations after the flux equations, i.e the row number i is in the range $[M_{\text{FL}}, M_{\text{FL}} + M_B - 1]$.

Next, we consider the constraint of plasma current. The plasma current I_p can be inferred from \mathbf{u} via

$$I_p = \int_{\Omega} J_{\phi} dR' dZ' = \sum_{j=0}^{N_b-1} c_j \int_{\Omega} b_j(x) dR' dZ'. \quad (6.20)$$

The rhs of Eq. (6.20) indicates that the matrix elements of Γ are given by:

$$\Gamma_{ij} = \int_{\Omega} b_j(x) dR' dZ', \quad (6.21)$$

for $(j = 0, \dots, N_b - 1)$, and zero for $(j = N_b, \dots, N - 1)$. This equation is placed after the equations of flux and magnetic field measurement, i.e., its row number is $i = M_{\text{FL}} + M_B$.

Let us consider the constraint of on-axis safety factor. A formula for computing q_{axis} is given by [ref. P. M. Bellan's paper]:

$$q_{\text{axis}} = \frac{\epsilon^2 + 1}{\epsilon R_{\text{axis}}^2} \frac{g(0)}{\mu_0 J_{\phi \text{axis}}}, \quad (6.22)$$

where

$$\epsilon = \sqrt{\left(\frac{\partial^2 \Psi / \partial R^2}{\partial^2 \Psi / \partial Z^2} \right)_{\text{axis}}}, \quad (6.23)$$

is the elongation at the magnetic axis. Using

$$J_{\phi \text{axis}} = \sum_{j=0}^{N_b-1} c_j b_j(0)$$

expression (6.22) is written as

$$\frac{\epsilon R_{\text{axis}}^2 \mu_0}{(\epsilon^2 + 1)g(0)} \sum_{j=0}^{N_b-1} c_j b_j(0) = \frac{1}{q_{\text{axis}}}. \quad (6.24)$$

6.2 Algorithm summary

Step 0. Initial guess of Ψ : $\Psi^{(k)}$ with $k = 0$.

Step 1. Compute elements of response matrix Γ using $\Psi^{(k)}$.

Step 2. Solve linear least-square problem to get $(c_1, c_2, c_3, c_4, I_1, \dots, I_{N_c})$.

Step 3. Update Ψ using the Picard iteration:

$$\Psi^{(k+1)} = \int G J_{\phi}(R', \Psi^{(k)}, c_1, c_2, c_3, c_4) dR' dZ' + \sum_{n=1}^{N_c} G I_n, \quad (6.25)$$

or in its discrete form:

$$\Psi_{ij}^{(k+1)} = \sum_{i', j'} G_{i'j'ij} \left(\sum_{n=1}^4 c_n b_{n,i'j'} \right) dS_{i'j'} + \sum_{n=1}^{N_c} G_{n,ij}^{(c)} I_n. \quad (6.26)$$

Step 4: $k = k + 1$ and goto Step 1.

In Step 1, we first search for the magnetic axis and boundary surface of $\Psi^{(k)}$ so that we can get the values of $\Psi^{(k)}$ at those locations. These values are needed in computing $x = (\Psi^{(k)} - \Psi_M) / (\Psi_B - \Psi_M)$.

6.3 Vertical displacement instability stabilizer in free-boundary solver[17]

To stabilize the vertical displacement instability in the Picard iteration, we add two virtual coils that carry opposite currents (denoted by I_{vc} and $-I_{vc}$), and are up-down symmetric, located at (R_{vc}, Z_{vc}) and $(R_{vc}, -Z_{vc})$, respectively. And set the current I_{vc} by

$$I_{vc} = -g_z \frac{B_{R, \text{vacuum}}(R_{\text{cur}}, Z_{\text{cur}})}{G_{B_R}(R_{vc}, Z_{vc}, R_{\text{cur}}, Z_{\text{cur}}) - G_{B_R}(R_{vc}, -Z_{vc}, R_{\text{cur}}, Z_{\text{cur}})},$$

where $(R_{\text{cur}}, Z_{\text{cur}})$ is the location of plasma current center defined by

$$R_{\text{cur}} = \frac{1}{I_p} \int_{\Omega_{\text{pl}}} R J_\phi(R, Z) dR dZ,$$

$$Z_{\text{cur}} = \frac{1}{I_p} \int_{\Omega_{\text{pl}}} Z J_\phi(R, Z) dR dZ,$$

$B_{R, \text{vacuum}}$ is the B_R generated by all the real PF coils, g_z is a positive constant chosen by users. Note that $g = 1$ corresponds to that the B_R generated by the virtual coils exactly cancels the B_R generated by all the real coils. Usually we need value larger than 2, i.e., over compensation. The virtual coils locations, (R_{vc}, Z_{vc}) and $(R_{vc}, -Z_{vc})$, are usually chosen near the center of the top/bottom boundary of the computational box.

6.4 Solving by matrix inversion

If we want to invert the finite-difference version of the Laplace operator Δ^* to solve the GS equation for Ψ , we encounter two issues: (1) the RHS of the GS equation involves 2 unknown functions $P'(\Psi)$ and $g'g(\Psi)$, in addition to the main unknown function $\Psi(R, Z)$; (2) the boundary condition needs to be given: i.e., the values of Ψ on a rectangular computational boundary need to be provided.

To address issue (1): function forms of $P'(\Psi)$ and $g'g(\Psi)$ are chosen by users, often as polynomials in Ψ_N with coefficients that are assumed known (which are later obtained in the least-square method to make the resulting solution approximately match some measurements, as is discussed in the previous section).

To address issue (2): The value of Ψ on the rectangular boundary is updated using the Green's function method (assume that external coil currents are given), as is discussed in the previous section.

Guess values of Ψ on both the inner gridpoints and boundary points. After this, we can invert Δ^* to update Ψ within the computational box, and use the Green's function method to update values of Ψ on the boundary. Then iterate to converge.

Two iterations: one for Ψ values on the inner gridpoints, one over Ψ values on the computational boundary.

External PF coil currents enter the problem via the boundary condition: specifically via its contribution to Ψ on the boundary.

The above procedure is just a minor modification from the pure Green's function algorithm discussed in Sec. 6.2, i.e., replacing the Green's function method for the inner gridpoints with the finite-difference Laplace operator inverting.

For reference easy, the finite-difference schemes for the Laplace operator is listed below.

$$\Delta^* \Psi = -\mu_0 R J_\phi \quad (6.27)$$

$$\Delta^* = R \frac{\partial}{\partial R} \left(\frac{1}{R} \frac{\partial}{\partial R} \right) + \frac{\partial^2}{\partial Z^2} \quad (6.28)$$

$$= \frac{\partial}{\partial R^2} - \frac{1}{R} \frac{\partial}{\partial R} + \frac{\partial^2}{\partial Z^2} \quad (6.29)$$

Method 1: discretize Eq. (6.28) as

$$\begin{aligned} & R_i \frac{1}{\Delta_R} \left(\left(\frac{1}{R} \frac{\partial \Psi}{\partial R} \right)_{i+1/2} - \left(\frac{1}{R} \frac{\partial \Psi}{\partial R} \right)_{i-1/2} \right) \\ & + \frac{\Psi_{i,j+1} - 2\Psi_{i,j} + \Psi_{i,j-1}}{\Delta_Z^2} = -\mu_0 R_i J_{\phi i,j}, \end{aligned} \quad (6.30)$$

which can be further discretized as

$$\begin{aligned} & R_i \frac{1}{\Delta_R} \left(\frac{1}{R_{i+1/2}} \frac{\Psi_{i+1,j} - \Psi_{i,j}}{\Delta_R} - \frac{1}{R_{i-1/2}} \frac{\Psi_{i,j} - \Psi_{i-1,j}}{\Delta_R} \right) \\ & + \frac{\Psi_{i,j+1} - 2\Psi_{i,j} + \Psi_{i,j-1}}{\Delta_Z^2} = -\mu_0 R_i J_{\phi i,j}, \end{aligned} \quad (6.31)$$

which can be organized as

$$a\varphi_{i-1,j} + b\varphi_{i,j} + c\varphi_{i+1,j} + d\varphi_{i,j-1} + e\varphi_{i,j+1} = -\mu_0 R_i J_{\phi i,j},$$

where $b = -\frac{1}{\Delta_R^2} \left(\frac{R_i}{R_{i+1/2}} + \frac{R_i}{R_{i-1/2}} \right) - \frac{2}{\Delta_Z^2}$, $a = \frac{1}{\Delta_R^2} \frac{R_i}{R_{i-1/2}}$, $c = \frac{1}{\Delta_R^2} \frac{R_i}{R_{i+1/2}}$, $d = e = \frac{1}{\Delta_Z^2}$.

Method 2: discretize Eq. (6.29)

$$\begin{aligned} & \frac{\Psi_{i+1,j} - 2\Psi_{i,j} + \Psi_{i-1,j}}{\Delta_R^2} - \frac{1}{R} \frac{\Psi_{i+1,j} - \Psi_{i-1,j}}{2\Delta_R} + \frac{\Psi_{i,j+1} - 2\Psi_{i,j} + \Psi_{i,j-1}}{\Delta_Z^2} \\ & = -\mu_0 R_i J_{\phi i,j}, \end{aligned}$$

which can be organized as

$$a\varphi_{i-1,j} + b\varphi_{i,j} + c\varphi_{i+1,j} + d\varphi_{i,j-1} + e\varphi_{i,j+1} = -\mu_0 R_i J_{\phi i,j},$$

where $b = -\frac{2}{\Delta_R^2} - \frac{2}{\Delta_Z^2}$, $a = \frac{1}{\Delta_R^2} + \frac{1}{2R\Delta_R}$, $c = \frac{1}{\Delta_R^2} - \frac{1}{2R\Delta_R}$, $d = e = \frac{1}{\Delta_Z^2}$

My numerical experiments indicate this scheme is more stable than the first one (for the same grid size, and without the VDE stabilizer, the first scheme blow up while the latter scheme works well).

7 Semi-free boundary equilibrium problem

Semi-free boundary equilibrium problems refer to the problems where the LCFS shape and the value of Ψ on it are given and one is asked to solve the currents in the PF coils. This is similar to the fitting problem discussed above: we consider the control points on the LCFS as virtual flux loops that measure the poloidal flux.

8 Magnetic control (to be continued)

Using magnetic measurements, a realtime equilibrium reconstruction code (e.g., `rtefit`) can be used to infer the inner structure of Ψ (observer). PF coil currents can provide actions on Ψ (actuator). With the observer and actuator, we can feedback controll the magnetic configuration (flux map).

For example, consider controlling the shape of LCFS (often called iso-flux control). We choose a target surface. To make sure that the target surface is a magnetic surface, the value of Ψ on it should be made a spatial constant. Denote this constant by Ψ_t . To make sure that there is no closed flux surface outside the target surface, we select the target surface as a surface that is tangential to the first wall (for limiter configuration) or there is a X-point on it (for divertor configuration). Then discretize the target surface by a series of discrete coordinates (R_i, Z_i) with $i = 1, 2, \dots, M$. The actions (coil current changes) are chosen to minimise the following residual:

$$\sum_i^M \left(\Delta \Psi_i - \sum_j^{N_c} G(R'_j, Z'_j, R_i, Z_i) \Delta I_j \right)^2, \quad (8.1)$$

where

$$\Delta \Psi_i = \Psi^{(\text{target})} - \Psi_i^{(\text{old})}, \quad (8.2)$$

$$\Delta I_j = I_j^{(\text{new})} - I_j^{(\text{old})}, \quad (8.3)$$

the superscript (old) indicates values before the control actions, $\Psi_i^{(\text{old})}$ is obtained by a real-time equilibrium reconstruction code. This assumes that the plasma current density remains the same when the actions are imposed (i.e., no plasma response is included), so that only the coil current changes contribute to the Ψ change.

If we need to feedback control X points to desired positions, then the above sum can be extended to include the following:

$$\begin{aligned} & \sum_i^{M_X} \left(B_R(R_i^{(X)}, Z_i^{(X)}) + \sum_j^{N_c} G_{BR}(R'_j, Z'_j, R_i^{(X)}, Z_i^{(X)}) \Delta I_j \right)^2 \\ & + \sum_i^{M_X} \left(B_Z(R_i^{(X)}, Z_i^{(X)}) + \sum_j^{N_c} G_{BZ}(R'_j, Z'_j, R_i^{(X)}, Z_i^{(X)}) \Delta I_j \right)^2, \end{aligned} \quad (8.4)$$

where $(R_i^{(X)}, Z_i^{(X)})$ are desired positions of X points.

8.1 Circuit equation for PF coil currents

Faraday's law

$$\nabla \times \mathbf{E} = -\frac{\partial \mathbf{B}}{\partial t}, \quad (8.5)$$

can be written in the integral form:

$$\oint \mathbf{E} \cdot d\mathbf{l} = - \int \frac{\partial \mathbf{B}}{\partial t} \cdot d\mathbf{S} = - \frac{\partial}{\partial t} \int \mathbf{B} \cdot d\mathbf{S} = - \frac{\partial \Psi_p}{\partial t} \quad (8.6)$$

where the direction of the loop integration is related to the surface orientation by the right-hand rule. (For a PF coil, if we choose the loop integration along anti-clockwise direction viewed from above, then the surface orientation for the surface integration must point vertically up. This is the convention I adopt in HEQ.)

For the No. k coil, $\partial \Psi_p / \partial t$ can be expressed as

$$\frac{\partial \Psi_p}{\partial t} = \sum_{j=1}^{N_c} M_{jk} \frac{dI_j}{dt} + \frac{d}{dt} \int M_k(\mathbf{r}) J_\phi dS, \quad (8.7)$$

where M_{jk} is the mutual inductance between the No. j coil and No. k coil, $M_k(\mathbf{r})$ is the mutual inductance between the No. k coil and a plasma filament located at \mathbf{r} , and $J_\phi dS$ is the current carried by the filament. The integration is over a fixed region (time independent) that is large enough to include all the plasma and small enough to not include any coil.

Define the effective mutual inductance between the plasma and the No. k coil by

$$M_{k,p} = \frac{1}{I_p} \int M_k(\mathbf{r}) J_\phi dS, \quad (8.8)$$

where I_p is the plasma current, then expression (8.7) is written as

$$\begin{aligned} \frac{\partial \Psi_p}{\partial t} &= \left(\sum_{j=1}^{N_c} M_{jk} \frac{dI_j}{dt} \right) + \frac{d}{dt} (I_p M_{k,p}) \\ &= \left(\sum_{j=1}^{N_c} M_{jk} \frac{dI_j}{dt} \right) + M_{k,p} \frac{dI_p}{dt} + I_p \frac{dM_{k,p}}{dt} \\ &\approx \left(\sum_{j=1}^{N_c} M_{jk} \frac{dI_j}{dt} \right) + M_{k,p} \frac{dI_p}{dt}, \end{aligned} \quad (8.9)$$

where the term proportional to the time derivative of $M_{ck,p}$ is ignored (is this a good approximation?). Including the above emf in the circuit equation, we get

$$V_k - \left(\sum_{j=1}^{N_c} M_{jk} \frac{dI_j}{dt} \right) - M_{k,p} \frac{dI_p}{dt} = I_k \mathcal{R}_k, \quad (8.10)$$

where \mathcal{R}_k is the resistance of the coil, I_k is the current in the present coil, V_k is the voltage imposed on the coil by the power supply. (Here the positive direction of V_k and I_k must be chosen consistent with the loop integration discussed above i.e., anti-clockwise in top view.)

Using the Euler implicit scheme, the above equation is written as

$$V_k^{(n)} - \sum_{j=1}^{N_c} M_{jk} \frac{I_j^{(n+1)} - I_j^{(n)}}{\Delta t} - M_{k,p} \frac{I_p^{(n+1)} - I_p^{(n)}}{\Delta t} = I_k^{(n+1)} \mathcal{R}_k.$$

Moving all the unknown (coil currents $I_j^{(n+1)}$ and plasma current $I_p^{(n+1)}$) to the left-hand side, we get

$$\begin{aligned} & \mathcal{R}_k I_k^{(n+1)} + \sum_{j=1}^{N_c} M_{jk} \frac{I_j^{(n+1)}}{\Delta t} + M_{k,p} \frac{I_p^{(n+1)}}{\Delta t} \\ &= V_k^{(n)} + \sum_{j=1}^{N_c} M_{jk} \frac{I_j^{(n)}}{\Delta t} + M_{k,p} \frac{I_p^{(n)}}{\Delta t}. \end{aligned} \quad (8.11)$$

For each coil, we get a linear equation like the above. For N_c coils, we get N_c equations.

(If we use value of $M_{ck,p}$ at the No. $n+1$ time step in the above equation, then we need to iterate because $M_{k,p}^{(n+1)}$ is unknown. If we use the value at the No. n time step, then no iteration is needed, which is the case used in HEQ).

8.2 Circuit equation for total plasma current

Because mutual inductance between two objects is symmetric (i.e., $M_{AB} = M_{BA}$), the mutual inductance $M_{k,p}$ given by expression (8.8) can also be used to calculate the effective emf induced in the plasma by the coils:

$$\begin{aligned} & \frac{d}{dt} \left(\sum_{k=1}^{N_c} M_{k,p} I_k \right) \\ &= - \sum_{k=1}^{N_c} \left(M_{k,p} \frac{dI_k}{dt} + I_k \frac{d}{dt} M_{k,p} \right). \\ &\approx - \sum_{k=1}^{N_c} M_{k,p} \frac{dI_k}{dt}. \end{aligned}$$

(here $M_{k,p}$ can be understood as J_ϕ weighted average of $M_k(\mathbf{r})$. Why to use J_ϕ weighted, rather than just equal-weighted spatial average? This is to ensure energy conservation: the power is $\mathbf{E} \cdot \mathbf{J}$, so the current density should serve as a weight.)

Similarly, the effective emf self-induced in the plasma is given by

$$-\frac{d}{dt} \left(\frac{1}{I_p} \iint J_{\phi i'j'} M_{i'j'ij} J_{\phi ij} dS_{ij} dS_{i'j'} \right), \quad (8.12)$$

where $M_{i'j'ij}$ is the mutual inductance between ij filament and $i'j'$ filament; both the 2D integrations are over a fixed region that includes the plasma but does not include any coil; one of the two 2D integrations can be regarded as J_ϕ weighted average and the other is the integration over the source. Expression (8.12) motivates us to define the effective self-inductance of plasma by

$$L_p = \frac{1}{I_p^2} \iint J_{\phi i'j'} M_{i'j'ij} J_{\phi ij} dS_{ij} dS_{i'j'}, \quad (8.13)$$

Then the effective emf in expression (8.12) is written as

$$\begin{aligned} & -\frac{d}{dt}(L_p I_p) \\ & = -L_p \frac{dI_p}{dt} - I_p \frac{d}{dt}(L_p) \\ & \approx -L_p \frac{dI_p}{dt}, \end{aligned}$$

where the term proportional to the time derivative of L_p is ignored (is this a good approximation?).

Then the circuit equation for the plasma current is written as

$$-L_p \frac{dI_p}{dt} - \sum_{k=1}^{N_c} M_{k,p} \frac{dI_k}{dt} = I_p \mathcal{R}_p, \quad (8.14)$$

which can be time discretized using the Euler implicit scheme as

$$-L_p \frac{I_p^{(n+1)} - I_p^{(n)}}{\Delta t} - \sum_{k=1}^{N_c} M_{k,p} \frac{I_k^{(n+1)} - I_k^{(n)}}{\Delta t} = I_p^{(n+1)} \mathcal{R}_p, \quad (8.15)$$

i.e.,

$$\sum_{k=1}^{N_c} M_{k,p} \frac{I_k^{(n+1)}}{\Delta t} + \left(\mathcal{R}_p + \frac{L_p}{\Delta t} \right) I_p^{(n+1)} = L_p \frac{I_p^{(n)}}{\Delta t} + \sum_{k=1}^{N_c} M_{k,p} \frac{I_k^{(n)}}{\Delta t}. \quad (8.16)$$

****Reinforcement learning****

Define the plasma state by the position of the magnetic axis (R_a, Z_a), total plasma current I_p , and the shape of the LCFS. Discretize the LCFS in the cylindrical coordinates by N_s points. Then the plasma state can be represented by $2N_s + 3$ real numbers: R_a, Z_a, I_p , and (R_i, Z_i) for $i = 1, 2, \dots, N_s$.

Inputs to the policy network: target plasma state (provided by the designer) and the magnetic measurements at the present time step t_n (which serves as a proxy to the actual plasma state).

Output of the policy network: voltage command to the coils imposed at t_n which can hopefully make the plasma reach the target state in a future time step.

How to train the policy network on a plasma simulator?

9 Safety factor

A magnetic field line on a closed magnetic surface travel a closed curve in a poloidal plane. For these field lines, we can define the safety factor q : the number of toroidal loops a magnetic field line travels when it makes one poloidal loop, i.e.

$$q \equiv \frac{\Delta\phi}{2\pi}, \quad (9.1)$$

where $\Delta\phi$ as the change of the toroidal angle when a magnetic field line travels a full poloidal loop.

For open field line region (where a field line touches the wall before its poloidal projection can close itself), the “connection length” is often used to characterize the magnetic field.

9.0.1 Expression of safety factor in terms of magnetic field

The equation of magnetic field lines is given by

$$\frac{Rd\phi}{d\ell_p} = \frac{B_\phi}{B_p}, \quad (9.2)$$

where $d\ell_p$ is the line element along the direction of \mathbf{B}_p on the poloidal plane. Equation (9.2) can be arranged in the form

$$d\phi = \frac{1}{R} \frac{B_\phi}{B_p} d\ell_p, \quad (9.3)$$

which can be integrated over $d\ell_p$ to give

$$\Delta\phi = \oint \frac{1}{R} \frac{B_\phi}{B_p} d\ell_p, \quad (9.4)$$

where the line integration is along the poloidal magnetic field (the contour of Ψ on the poloidal plane). Using this, Eq. (9.1) is written

$$q = \frac{1}{2\pi} \oint \frac{1}{R} \frac{B_\phi}{B_p} d\ell_p. \quad (9.5)$$

9.1 Expression of safety factor in terms of magnetic flux

The safety factor given by Eq. (9.5) is expressed in terms of the components of the magnetic field. The safety factor can also be expressed in terms of the magnetic flux. Define $\Delta\Psi_p$ as the poloidal magnetic flux enclosed by two neighboring magnetic surface, then $\Delta\Psi_p$ is given by

$$\Delta\Psi_p = 2\pi R \Delta x B_p \quad (9.6)$$

where Δx is the length of a line segment in the poloidal plane between the two magnetic surfaces, which is perpendicular to the first magnetic surface (so perpendicular to the \mathbf{B}_p). Note that Δx , as well as R and B_p , generally depends on the poloidal location whereas $\Delta\Psi_p$ is independent of the poloidal location.

Using Eq. (9.6), the poloidal magnetic field is written as

$$B_p = \frac{1}{2\pi R} \frac{\Delta\Psi_p}{\Delta x}. \quad (9.7)$$

Substituting Eq. (9.7) into Eq. (9.5), we obtain

$$q = \frac{1}{2\pi} \oint \frac{1}{R} \frac{B_\phi}{B_p} d\ell_p = \frac{1}{2\pi} \oint \frac{1}{R} \frac{2\pi R \Delta x B_\phi}{\Delta\Psi_p} d\ell_p = \oint \frac{\Delta x B_\phi}{\Delta\Psi_p} d\ell_p. \quad (9.8)$$

We know $\Delta\Psi_p$ is a constant independent of the poloidal location, so $\Delta\Psi_p$ can be taken outside the integration to give

$$q = \frac{1}{\Delta\Psi_p} \oint \Delta x B_\phi d\ell_p \quad (9.9)$$

It is ready to realise that the integral appearing in Eq. (9.9) is the toroidal magnetic flux enclosed by the two magnetic surfaces, $\Delta\Psi_t$. Using this, Eq. (9.9) is written as

$$q = \frac{\Delta\Psi_t}{\Delta\Psi_p} \quad (9.10)$$

Equation (9.10) indicates that the safety factor of a magnetic surface is equal to the differential of the toroidal magnetic flux with respect to the poloidal magnetic flux enclosed by the magnetic surface.

9.2 Rational surfaces vs. irrational surfaces

If the safety factor of a magnetic surface is a rational number, i.e., $q = m/n$, where m and n are integers, then this magnetic surface is called a rational surface, otherwise an irrational surface. A field line on a rational surface with $q = m/n$ closes itself after it travels n poloidal loops. An example of a field line on a rational surface is shown in Fig. 9.1.

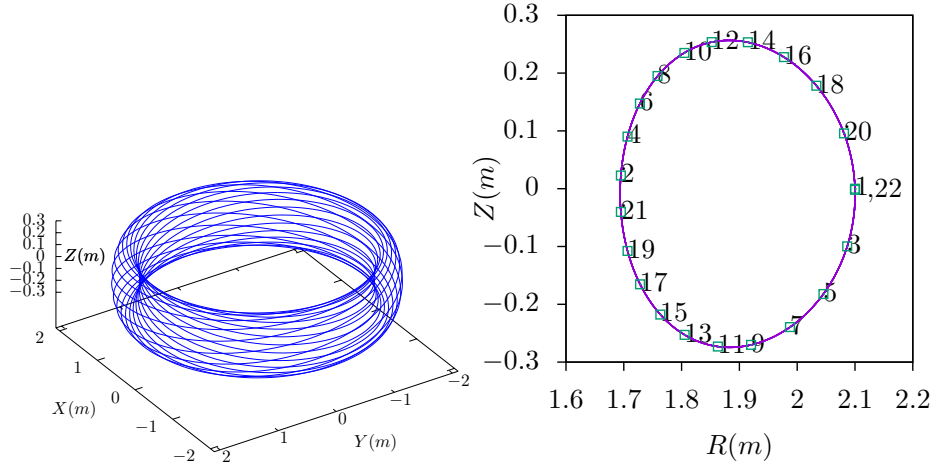


Figure 9.1. Left: A magnetic field line (blue) on a rational surface with $q = 2.1 = 21/10$ (magnetic field is from EAST discharge #59954@3.1s). This field line closes itself after traveling 21 toroidal loops (meanwhile, it travels 10 poloidal loops). Right: The intersecting points of the magnetic field line with the $\phi = 0$ plane when it is traveling toroidally. The sequence of the intersecting points is indicated by the number labels. The 22nd intersecting point coincides with the 1st point and then the intersecting points repeat themselves.

10 Coordinates based on magnetic field structure

In many studies of tokamak plasmas, one need construct a curvilinear coordinate system based on a given magnetic configuration in order to make the problem amenable to analytical methods or numerical methods. Specifically, many theories and numerical codes use the curvilinear coordinate systems that are constructed with one coordinate surface coinciding with magnetic surfaces. In these coordinate systems, we need to choose a poloidal coordinate θ and a toroidal coordinate ζ . A particular choice for θ and ζ is one that makes the magnetic field lines be straight lines in (θ, ζ) plane. These kinds of coordinates are often called magnetic coordinates. That is, “magnetic coordinates are defined so they conform to the shape of the magnetic surfaces and trivialize the equations for the field lines.”

A further tuned magnetic coordinate system is the so-called field aligned (or field-line following) coordinate system, in which changing one of the three coordinates with the other two fixed would correspond to following a magnetic field line. The field aligned coordinates are discussed in Sec. 15.

Next, let us discuss some general properties about coordinates transformation[4].

10.1 Coordinates transformation

In the Cartesian coordinates, a point is described by its coordinates (x, y, z) , which, in the vector form, is written as

$$\mathbf{r} = x\hat{\mathbf{x}} + y\hat{\mathbf{y}} + z\hat{\mathbf{z}}, \quad (10.1)$$

where \mathbf{r} is the location vector of the point; $\hat{\mathbf{x}}$, $\hat{\mathbf{y}}$, and $\hat{\mathbf{z}}$ are the basis vectors of the Cartesian coordinates, which are constant, independent of spacial location. The transformation between the Cartesian coordinates system, (x, y, z) , and a general coordinates system, (x_1, x_2, x_3) , can be expressed as

$$\mathbf{r} = x(x_1, x_2, x_3)\hat{\mathbf{x}} + y(x_1, x_2, x_3)\hat{\mathbf{y}} + z(x_1, x_2, x_3)\hat{\mathbf{z}}. \quad (10.2)$$

For example, cylindrical coordinates (R, ϕ, Z) can be considered as a general coordinate systems, which are defined by $\mathbf{r} = R \cos \phi \hat{\mathbf{x}} + R \sin \phi \hat{\mathbf{y}} + Z \hat{\mathbf{z}}$.

The transformation function in Eq. (10.2) can be written as

$$\begin{aligned} x &= x(x_1, x_2, x_3) \\ y &= y(x_1, x_2, x_3) \\ z &= z(x_1, x_2, x_3) \end{aligned} \quad (10.3)$$

10.2 Jacobian

A useful quality characterizing coordinate transformation is the Jacobian determinant (or simply called Jacobian), which, for the transformation in Eq. (10.3), is defined by

$$\mathcal{J} = \begin{vmatrix} \frac{\partial x}{\partial x_1} & \frac{\partial x}{\partial x_2} & \frac{\partial x}{\partial x_3} \\ \frac{\partial y}{\partial x_1} & \frac{\partial y}{\partial x_2} & \frac{\partial y}{\partial x_3} \\ \frac{\partial z}{\partial x_1} & \frac{\partial z}{\partial x_2} & \frac{\partial z}{\partial x_3} \end{vmatrix}, \quad (10.4)$$

which can also be written as

$$\mathcal{J} = \frac{\partial \mathbf{r}}{\partial x_1} \times \frac{\partial \mathbf{r}}{\partial x_2} \cdot \frac{\partial \mathbf{r}}{\partial x_3}. \quad (10.5)$$

It is easy to prove that the Jacobian \mathcal{J} in Eq. (10.5) can also be written (the derivation is given in my notes on Jacobian)

$$\mathcal{J} = (\nabla x_1 \times \nabla x_2 \cdot \nabla x_3)^{-1}. \quad (10.6)$$

Conventionally, the Jacobian of the transformation from the Cartesian coordinates to a particular coordinate system σ is called the Jacobian of σ , without explicitly mentioning that this transformation is with respect to the Cartesian coordinates.

Using the definition in Eq. (10.4), the Jacobian \mathcal{J} of the Cartesian coordinates can be calculated, yielding 1. Likewise, the Jacobian of the cylindrical coordinates (R, ϕ, Z) can be calculated as follows:

$$\begin{aligned}\mathcal{J} &= \begin{vmatrix} \frac{\partial x}{\partial R} & \frac{\partial x}{\partial \phi} & \frac{\partial x}{\partial Z} \\ \frac{\partial y}{\partial R} & \frac{\partial y}{\partial \phi} & \frac{\partial y}{\partial Z} \\ \frac{\partial z}{\partial R} & \frac{\partial z}{\partial \phi} & \frac{\partial z}{\partial Z} \end{vmatrix} = \begin{vmatrix} \frac{\partial R \cos \phi}{\partial R} & \frac{\partial R \cos \phi}{\partial \phi} & \frac{\partial R \cos \phi}{\partial Z} \\ \frac{\partial R \sin \phi}{\partial R} & \frac{\partial R \sin \phi}{\partial \phi} & \frac{\partial R \sin \phi}{\partial Z} \\ \frac{\partial Z}{\partial R} & \frac{\partial Z}{\partial \phi} & \frac{\partial Z}{\partial Z} \end{vmatrix} \\ &= \begin{vmatrix} \cos \phi & -R \sin \phi & 0 \\ \sin \phi & R \cos \phi & 0 \\ 0 & 0 & 1 \end{vmatrix} = R\end{aligned}$$

If the Jacobian of a coordinate system is greater than zero, it is called a right-handed coordinate system. Otherwise it is called a left-handed system.

10.3 Orthogonality relation between two sets of basis vectors

In a curvilinear coordinate system (x_1, x_2, x_3) , there are two kinds of basis vectors: ∇x_i and $\partial \mathbf{r} / \partial x_i$, with $i = 1, 2, 3$. These two kinds of basis vectors satisfy the following orthogonality relation:

$$\nabla x_i \cdot \frac{\partial \mathbf{r}}{\partial x_j} = \delta_{ij}, \quad (10.7)$$

where δ_{ij} is the Kronecker delta function. [Proof: Working in a Cartesian coordinate system (x, y, z) with the corresponding basis vectors denoted by $(\hat{\mathbf{x}}, \hat{\mathbf{y}}, \hat{\mathbf{z}})$, then the left-hand side of Eq. (10.7) can be written as

$$\begin{aligned}\nabla x_i \cdot \frac{\partial \mathbf{r}}{\partial x_j} &= \left[\left(\frac{\partial x_i}{\partial x} \right) \hat{\mathbf{x}} + \left(\frac{\partial x_i}{\partial y} \right) \hat{\mathbf{y}} + \left(\frac{\partial x_i}{\partial z} \right) \hat{\mathbf{z}} \right] \cdot \left[\frac{\partial x}{\partial x_j} \hat{\mathbf{x}} + x \frac{\partial \hat{\mathbf{x}}}{\partial x_j} + \frac{\partial y}{\partial x_j} \hat{\mathbf{y}} + y \frac{\partial \hat{\mathbf{y}}}{\partial x_j} + \frac{\partial z}{\partial x_j} \hat{\mathbf{z}} + z \frac{\partial \hat{\mathbf{z}}}{\partial x_j} \right] \\ &= \left[\left(\frac{\partial x_i}{\partial x} \right) \hat{\mathbf{x}} + \left(\frac{\partial x_i}{\partial y} \right) \hat{\mathbf{y}} + \left(\frac{\partial x_i}{\partial z} \right) \hat{\mathbf{z}} \right] \cdot \left[\frac{\partial x}{\partial x_j} \hat{\mathbf{x}} + 0 + \frac{\partial y}{\partial x_j} \hat{\mathbf{y}} + 0 + \frac{\partial z}{\partial x_j} \hat{\mathbf{z}} + 0 \right] \\ &= \frac{\partial x_i}{\partial x} \frac{\partial x}{\partial x_j} + \frac{\partial x_i}{\partial y} \frac{\partial y}{\partial x_j} + \frac{\partial x_i}{\partial z} \frac{\partial z}{\partial x_j} \\ &= \frac{\partial x_i}{\partial x_j} \\ &= \delta_{ij},\end{aligned} \quad (10.8)$$

$$\begin{aligned}&= \frac{\partial x_i}{\partial x} \frac{\partial x}{\partial x_j} + \frac{\partial x_i}{\partial y} \frac{\partial y}{\partial x_j} + \frac{\partial x_i}{\partial z} \frac{\partial z}{\partial x_j} \\ &= \frac{\partial x_i}{\partial x_j} \\ &= \delta_{ij},\end{aligned} \quad (10.9)$$

where the second equality is due to $\partial \hat{\mathbf{x}} / \partial x^j = 0$, $\partial \hat{\mathbf{y}} / \partial x^j = 0$, $\partial \hat{\mathbf{z}} / \partial x^j = 0$ since $\hat{\mathbf{x}}, \hat{\mathbf{y}}, \hat{\mathbf{z}}$ are constant vectors independent of spatial location; the chain rule has been used in obtaining Eq. (10.9)]

[The cylindrical coordinate system (R, ϕ, Z) is an example of general coordinates. As an exercise, we can verify that the cylindrical coordinates have the property given in Eq. (10.7). In this case, $x = x_1 \cos x_2$, $y = x_1 \sin x_2$, $z = x_3$, where $x_1 \equiv R$, $x_2 \equiv \phi$, $x_3 \equiv Z$.]

It can be proved that ∇x^i is a contravariant vector while $\partial \mathbf{r} / \partial x^i$ is a covariant vector (I do not prove this and do not bother with the meaning of these names, just using this as a naming scheme for easy reference).

The orthogonality relation in Eq. (10.7) is fundamental to the theory of general coordinates. The orthogonality relation allows one to write the covariant basis vectors in terms of contravariant basis vectors and vice versa. For example, the orthogonality relation tells that $\partial \mathbf{r} / \partial x_1$ is orthogonal to ∇x_2 and ∇x_3 , thus, $\partial \mathbf{r} / \partial x_1$ can be written as

$$\frac{\partial \mathbf{r}}{\partial x_1} = A \nabla x_2 \times \nabla x_3, \quad (10.10)$$

where A is a unknown variable to be determined. To determine A , dotting Eq. (10.10) by ∇x_1 , and using the orthogonality relation again, we obtain

$$1 = A (\nabla x_2 \times \nabla x_3) \cdot \nabla x_1, \quad (10.11)$$

which gives

$$\begin{aligned} A &= \frac{1}{(\nabla x_2 \times \nabla x_3) \cdot \nabla x_1} \\ &= \mathcal{J} \end{aligned} \quad (10.12)$$

Thus $\partial \mathbf{r} / \partial x_1$ is written, in terms of ∇x_1 , ∇x_2 , and ∇x_3 , as

$$\frac{\partial \mathbf{r}}{\partial x_1} = \mathcal{J} \nabla x_2 \times \nabla x_3. \quad (10.13)$$

Similarly, we obtain

$$\frac{\partial \mathbf{r}}{\partial x_2} = \mathcal{J} \nabla x_3 \times \nabla x_1 \quad (10.14)$$

and

$$\frac{\partial \mathbf{r}}{\partial x_3} = \mathcal{J} \nabla x_1 \times \nabla x_2. \quad (10.15)$$

Equations (10.13)-(10.15) can be generally written

$$\frac{\partial \mathbf{r}}{\partial x_i} = \mathcal{J} \nabla x_j \times \nabla x_k, \quad (10.16)$$

where (i, j, k) represents the cyclic order in the variables (x_1, x_2, x_3) . Equation (10.16) expresses the covariant basis vectors in terms of the contravariant basis vectors. On the other hand, from Eq. (10.13)-(10.15), we obtain

$$\nabla x_i = \mathcal{J}^{-1} \frac{\partial \mathbf{r}}{\partial x_j} \times \frac{\partial \mathbf{r}}{\partial x_k}, \quad (10.17)$$

which expresses the contravariant basis vectors in terms of the covariant basis vectors.

10.4 An example: (ψ, θ, ζ) coordinates

Suppose (ψ, θ, ζ) is an arbitrary general coordinate system. Following Einstein's notation, contravariant basis vectors are denoted with upper indices as

$$\mathbf{e}^\psi \equiv \nabla \psi; \quad \mathbf{e}^\theta \equiv \nabla \theta; \quad \mathbf{e}^\zeta \equiv \nabla \zeta. \quad (10.18)$$

and the covariant basis vectors are denoted with low indices as

$$\mathbf{e}_\psi \equiv \frac{\partial \mathbf{r}}{\partial \psi}; \quad \mathbf{e}_\theta \equiv \frac{\partial \mathbf{r}}{\partial \theta}; \quad \mathbf{e}_\zeta \equiv \frac{\partial \mathbf{r}}{\partial \zeta}. \quad (10.19)$$

Then the orthogonality relation, Eq. (10.7), is written as

$$\mathbf{e}^\alpha \cdot \mathbf{e}_\beta = \delta_{\alpha\beta}. \quad (10.20)$$

In term of the contravariant basis vectors, \mathbf{A} is written

$$\mathbf{A} = A_\psi \mathbf{e}^\psi + A_\theta \mathbf{e}^\theta + A_\zeta \mathbf{e}^\zeta, \quad (10.21)$$

where the components are easily obtained by taking scalar product with $\mathbf{e}_\psi, \mathbf{e}_\theta$, and \mathbf{e}_ζ , yielding $A_\psi = \mathbf{A} \cdot \mathbf{e}_\psi$, $A_\theta = \mathbf{A} \cdot \mathbf{e}_\theta$, and $A_\zeta = \mathbf{A} \cdot \mathbf{e}_\zeta$. Similarly, in term of the covariant basis vectors, \mathbf{A} is written

$$\mathbf{A} = A^\psi \mathbf{e}_\psi + A^\theta \mathbf{e}_\theta + A^\zeta \mathbf{e}_\zeta, \quad (10.22)$$

where $A^\psi = \mathbf{A} \cdot \mathbf{e}^\psi$, $A^\theta = \mathbf{A} \cdot \mathbf{e}^\theta$, and $A^\zeta = \mathbf{A} \cdot \mathbf{e}^\zeta$.

Using the above notation, the relation in Eq. (10.16) is written as

$$\mathbf{e}_\psi = \mathcal{J} \mathbf{e}^\theta \times \mathbf{e}^\zeta \quad (10.23)$$

$$\mathbf{e}_\theta = \mathcal{J} \mathbf{e}^\zeta \times \mathbf{e}^\psi \quad (10.24)$$

$$\mathbf{e}_\zeta = \mathcal{J} \mathbf{e}^\psi \times \mathbf{e}^\theta \quad (10.25)$$

where $\mathcal{J} = [(\nabla \psi \times \nabla \theta) \cdot \nabla \zeta]^{-1}$. Similarly, the relation in Eq. (10.17) is written as

$$\mathbf{e}^\psi = \mathcal{J}^{-1} \mathbf{e}_\theta \times \mathbf{e}_\zeta \quad (10.26)$$

$$\mathbf{e}^\theta = \mathcal{J}^{-1} \mathbf{e}_\zeta \times \mathbf{e}_\psi \quad (10.27)$$

$$\mathbf{e}^\zeta = \mathcal{J}^{-1} \mathbf{e}_\psi \times \mathbf{e}_\theta \quad (10.28)$$

10.5 Gradient and directional derivative in general coordinates (ψ, θ, ζ)

The gradient of a scalar function $f(\psi, \theta, \zeta)$ is readily calculated from the chain rule,

$$\nabla f = \frac{\partial f}{\partial \psi} \nabla \psi + \frac{\partial f}{\partial \theta} \nabla \theta + \frac{\partial f}{\partial \zeta} \nabla \zeta. \quad (10.29)$$

Note that the gradient of a scalar function is in the covariant representation. The inverse form of this expression is obtained by dotting the above equation respectively by the three contravariant basis vectors, yielding

$$\frac{\partial f}{\partial \psi} = (\mathcal{J} \nabla \theta \times \nabla \zeta) \cdot \nabla f = \frac{\partial \mathbf{r}}{\partial \psi} \cdot \nabla f \quad (10.30)$$

$$\frac{\partial f}{\partial \theta} = (\mathcal{J} \nabla \zeta \times \nabla \psi) \cdot \nabla f = \frac{\partial \mathbf{r}}{\partial \theta} \cdot \nabla f \quad (10.31)$$

$$\frac{\partial f}{\partial \zeta} = (\mathcal{J} \nabla \psi \times \nabla \theta) \cdot \nabla f = \frac{\partial \mathbf{r}}{\partial \zeta} \cdot \nabla f \quad (10.32)$$

Using Eq. (10.29), the directional derivative in the direction of $\nabla \psi$ is written as

$$\nabla \psi \cdot \nabla f = |\nabla \psi|^2 \frac{\partial f}{\partial \psi} + (\nabla \theta \cdot \nabla \psi) \frac{\partial f}{\partial \theta} + (\nabla \zeta \cdot \nabla \psi) \frac{\partial f}{\partial \zeta}. \quad (10.33)$$

10.6 Divergence operator in general coordinates (ψ, θ, ζ)

To calculate the divergence of a vector, it is desired that the vector should be in the contravariant form because we can make use of the fact:

$$\nabla \cdot (\nabla \alpha \times \nabla \beta) = 0, \quad (10.34)$$

for any scalar quantities α and β . Therefore we write vector \mathbf{A} as

$$\mathbf{A} = A^{(\psi)} \mathcal{J} \nabla \theta \times \nabla \zeta + A^{(\theta)} \mathcal{J} \nabla \zeta \times \nabla \psi + A^{(\zeta)} \mathcal{J} \nabla \psi \times \nabla \theta, \quad (10.35)$$

where $A^{(\psi)} = \mathbf{A} \cdot \nabla \psi$, $A^{(\theta)} = \mathbf{A} \cdot \nabla \theta$, $A^{(\zeta)} = \mathbf{A} \cdot \nabla \zeta$. Then the divergence of \mathbf{A} is readily calculated as

$$\nabla \cdot \mathbf{A} = (\nabla \theta \times \nabla \zeta) \cdot \nabla (A^{(\psi)} \mathcal{J}) + (\nabla \zeta \times \nabla \psi) \cdot \nabla (A^{(\theta)} \mathcal{J}) + (\nabla \psi \times \nabla \theta) \cdot \nabla (A^{(\zeta)} \mathcal{J}) \quad (10.36)$$

$$= \frac{1}{\mathcal{J}} \left(\frac{\partial A^{(\psi)} \mathcal{J}}{\partial \psi} + \frac{\partial A^{(\theta)} \mathcal{J}}{\partial \theta} + \frac{\partial A^{(\zeta)} \mathcal{J}}{\partial \zeta} \right), \quad (10.37)$$

where the second equality is obtained by using Eqs. (10.30), (10.31), and (10.32).

10.7 Laplacian operator in general coordinates (ψ, θ, ζ)

The Laplacian operator is defined by $\nabla^2 \equiv \nabla \cdot \nabla$. Then $\nabla^2 f$ is written as (f is an arbitrary function)

$$\begin{aligned} \nabla^2 f &= \nabla \cdot \nabla f \\ &= \nabla \cdot \left(\frac{\partial f}{\partial \psi} \nabla \psi + \frac{\partial f}{\partial \theta} \nabla \theta + \frac{\partial f}{\partial \zeta} \nabla \zeta \right). \end{aligned} \quad (10.38)$$

To proceed, we can use the divergence formula (10.37) to express the divergence in the above expression. However, the vector in the above (blue term) is not in the covariant form desired by the divergence formula (10.37). If we want to directly use the formula (10.37), we need to transform the vector (blue term in expression (10.38)) to the covariant form. This process seems to be a little complicated. Therefore, I choose not to use this method. Instead, I try to simplify expression (10.38) by using basic vector identities:

$$\begin{aligned}\nabla^2 f &= \nabla \left(\frac{\partial f}{\partial \psi} \right) \cdot \nabla \psi + \nabla \left(\frac{\partial f}{\partial \theta} \right) \cdot \nabla \theta + \nabla \left(\frac{\partial f}{\partial \zeta} \right) \cdot \nabla \zeta \\ &\quad + \frac{\partial f}{\partial \psi} \nabla^2 \psi + \frac{\partial f}{\partial \theta} \nabla^2 \theta + \frac{\partial f}{\partial \zeta} \nabla^2 \zeta.\end{aligned}\tag{10.39}$$

Using the gradient formula, the above expression is further written as

$$\begin{aligned}\nabla^2 f &= \frac{\partial^2 f}{\partial \psi^2} |\nabla \psi|^2 + \frac{\partial^2 f}{\partial \psi \partial \theta} \nabla \psi \cdot \nabla \theta + \frac{\partial^2 f}{\partial \psi \partial \zeta} \nabla \psi \cdot \nabla \zeta \\ &\quad + \frac{\partial^2 f}{\partial \theta \partial \psi} \nabla \theta \cdot \nabla \psi + \frac{\partial^2 f}{\partial \theta^2} |\nabla \theta|^2 + \frac{\partial^2 f}{\partial \theta \partial \zeta} \nabla \theta \cdot \nabla \zeta \\ &\quad + \frac{\partial^2 f}{\partial \zeta \partial \psi} \nabla \zeta \cdot \nabla \psi + \frac{\partial^2 f}{\partial \zeta \partial \theta} \nabla \zeta \cdot \nabla \theta + \frac{\partial^2 f}{\partial \zeta^2} |\nabla \zeta|^2 \\ &\quad + \frac{\partial f}{\partial \psi} \nabla^2 \psi + \frac{\partial f}{\partial \theta} \nabla^2 \theta + \frac{\partial f}{\partial \zeta} \nabla^2 \zeta,\end{aligned}\tag{10.40}$$

and can be simplified as

$$\begin{aligned}\nabla^2 f &= \frac{\partial^2 f}{\partial \psi^2} |\nabla \psi|^2 + 2 \frac{\partial^2 f}{\partial \psi \partial \theta} \nabla \psi \cdot \nabla \theta + 2 \frac{\partial^2 f}{\partial \psi \partial \zeta} \nabla \psi \cdot \nabla \zeta \\ &\quad + \frac{\partial^2 f}{\partial \theta^2} |\nabla \theta|^2 + 2 \frac{\partial^2 f}{\partial \theta \partial \zeta} \nabla \theta \cdot \nabla \zeta \\ &\quad + \frac{\partial^2 f}{\partial \zeta^2} |\nabla \zeta|^2 \\ &\quad + \frac{\partial f}{\partial \psi} \nabla^2 \psi + \frac{\partial f}{\partial \theta} \nabla^2 \theta + \frac{\partial f}{\partial \zeta} \nabla^2 \zeta.\end{aligned}\tag{10.41}$$

Assume (ψ, θ, ζ) are field-line following coordinates with $\partial \mathbf{r} / \partial \theta$ along the field line direction, then neglect all the parallel derivatives, i.e., derivative over θ , then the above expression is reduced to

$$\begin{aligned}\nabla^2 f &= \frac{\partial^2 f}{\partial \psi^2} |\nabla \psi|^2 + 2 \frac{\partial^2 f}{\partial \psi \partial \zeta} \nabla \psi \cdot \nabla \zeta + \frac{\partial^2 f}{\partial \zeta^2} |\nabla \zeta|^2 \\ &\quad + \frac{\partial f}{\partial \psi} \nabla^2 \psi + \frac{\partial f}{\partial \zeta} \nabla^2 \zeta.\end{aligned}\tag{10.42}$$

This approximation reduces the Laplacian operator from being three-dimensional to being two-dimensional. This approximation is often called the high- n approximation, where n is the toroidal mode number (mode number along ζ direction).

10.8 Curl operator in general coordinates (ψ, θ, ζ)

To take the curl of a vector, it should be in the covariant representation since we can make use of the fact that $\nabla \times \nabla \alpha = 0$. Thus the curl of \mathbf{A} is written as

$$\begin{aligned}
 \nabla \times \mathbf{A} &= \nabla \times (A_1 \nabla \psi + A_2 \nabla \theta + A_3 \nabla \zeta) \\
 &= \nabla A_1 \times \nabla \psi + \nabla A_2 \times \nabla \theta + \nabla A_3 \times \nabla \zeta \\
 &= \left(\frac{\partial A_1}{\partial \theta} \nabla \theta + \frac{\partial A_1}{\partial \zeta} \nabla \zeta \right) \times \nabla \psi + \left(\frac{\partial A_2}{\partial \psi} \nabla \psi + \frac{\partial A_2}{\partial \zeta} \nabla \zeta \right) \times \nabla \theta + \\
 &\quad \left(\frac{\partial A_3}{\partial \psi} \nabla \psi + \frac{\partial A_3}{\partial \theta} \nabla \theta \right) \times \nabla \zeta \\
 &= \frac{1}{\mathcal{J}} \left(\frac{\partial A_2}{\partial \psi} - \frac{\partial A_1}{\partial \theta} \right) \mathcal{J} \nabla \psi \times \nabla \theta + \frac{1}{\mathcal{J}} \left(\frac{\partial A_1}{\partial \zeta} - \frac{\partial A_3}{\partial \psi} \right) \mathcal{J} \nabla \zeta \times \nabla \psi + \\
 &\quad \frac{1}{\mathcal{J}} \left(\frac{\partial A_3}{\partial \theta} - \frac{\partial A_2}{\partial \zeta} \right) \mathcal{J} \nabla \theta \times \nabla \zeta.
 \end{aligned} \tag{10.43}$$

Note that taking the curl of a vector in the covariant form leaves the vector in the contravariant form.

10.9 Metric tensor for general coordinate system

Consider a general coordinate system (ψ, θ, ζ) . I define the metric tensor as the transformation matrix between the covariant basis vectors and the contravariant ones. Equations (10.16) and (10.17) express the relation between the two sets of basis vectors using cross product. Next, let us express the relation in matrix form. To obtain the metric matrix, we write the contravariant basis vectors in terms of the covariant ones, such as

$$\nabla \psi = a^1 \mathcal{J} \nabla \theta \times \nabla \zeta + a^2 \mathcal{J} \nabla \zeta \times \nabla \psi + a^3 \mathcal{J} \nabla \psi \times \nabla \theta. \tag{10.44}$$

Taking the scalar product respectively with $\nabla \psi$, $\nabla \theta$, and $\nabla \zeta$, Eq. (10.44) is written as

$$a^1 = |\nabla \psi|^2, \tag{10.45}$$

$$a^2 = \nabla \psi \cdot \nabla \theta, \tag{10.46}$$

$$a^3 = \nabla \psi \cdot \nabla \zeta. \tag{10.47}$$

Similarly, we write

$$\nabla \theta = b^1 \mathcal{J} \nabla \theta \times \nabla \zeta + b^2 \mathcal{J} \nabla \zeta \times \nabla \psi + b^3 \mathcal{J} \nabla \psi \times \nabla \theta, \tag{10.48}$$

Taking the scalar product with $\nabla \psi$, $\nabla \theta$, and $\nabla \zeta$, respectively, the above becomes

$$b^1 = \nabla \theta \cdot \nabla \psi \tag{10.49}$$

$$b^2 = |\nabla \theta|^2, \tag{10.50}$$

$$b^3 = \nabla \theta \cdot \nabla \zeta. \tag{10.51}$$

The same situation applies for the $\nabla\zeta$ basis vector,

$$\nabla\zeta = c^1\nabla\theta \times \nabla\zeta\mathcal{J} + c^2\nabla\zeta \times \nabla\psi\mathcal{J} + c^3\nabla\psi \times \nabla\theta\mathcal{J}, \quad (10.52)$$

Taking the scalar product with $\nabla\psi$, $\nabla\theta$, and $\nabla\zeta$, respectively, the above equation becomes

$$c^1 = \nabla\zeta \cdot \nabla\psi \quad (10.53)$$

$$c^2 = \nabla\zeta \cdot \nabla\theta \quad (10.54)$$

$$c^3 = |\nabla\zeta|^2 \quad (10.55)$$

Summarizing the above results in matrix form, we obtain

$$\begin{pmatrix} \nabla\psi \\ \nabla\theta \\ \nabla\zeta \end{pmatrix} = \begin{pmatrix} |\nabla\psi|^2 & \nabla\psi \cdot \nabla\theta & \nabla\psi \cdot \nabla\zeta \\ \nabla\theta \cdot \nabla\psi & |\nabla\theta|^2 & \nabla\theta \cdot \nabla\zeta \\ \nabla\zeta \cdot \nabla\psi & \nabla\zeta \cdot \nabla\theta & |\nabla\zeta|^2 \end{pmatrix} \begin{pmatrix} \nabla\theta \times \nabla\zeta\mathcal{J} \\ \nabla\zeta \times \nabla\psi\mathcal{J} \\ \nabla\psi \times \nabla\theta\mathcal{J} \end{pmatrix} \quad (10.56)$$

Similarly, to convert contravariant basis vector to covariant one, we write

$$\nabla\theta \times \nabla\zeta\mathcal{J} = d_1\nabla\psi + d_2\nabla\theta + d_3\nabla\zeta \quad (10.57)$$

Taking the scalar product respectively with $\nabla\theta \times \nabla\zeta\mathcal{J}$, $\nabla\zeta \times \nabla\psi\mathcal{J}$, and $\nabla\psi \times \nabla\theta\mathcal{J}$, the above equation becomes

$$d_1 = |\nabla\theta \times \nabla\zeta|^2 \mathcal{J}^2 \quad (10.58)$$

$$d_2 = (\nabla\theta \times \nabla\zeta\mathcal{J}) \cdot (\nabla\zeta \times \nabla\psi\mathcal{J}) \quad (10.59)$$

$$d_3 = (\nabla\theta \times \nabla\zeta\mathcal{J}) \cdot (\nabla\psi \times \nabla\theta\mathcal{J}) \quad (10.60)$$

For the second contravariant basis vector

$$\nabla\phi \times \nabla\psi\mathcal{J} = e_1\nabla\psi + e_2\nabla\theta + e_3\nabla\zeta \quad (10.61)$$

$$e_1 = (\nabla\zeta \times \nabla\psi) \cdot (\nabla\theta \times \nabla\zeta) \mathcal{J}^2 \quad (10.62)$$

$$e_2 = (\nabla\zeta \times \nabla\psi) \cdot (\nabla\zeta \times \nabla\psi) \mathcal{J}^2 \quad (10.63)$$

$$e_3 = (\nabla\zeta \times \nabla\psi) \cdot (\nabla\psi \times \nabla\theta) \mathcal{J}^2 \quad (10.64)$$

For the third contravariant basis vector

$$\nabla\psi \times \nabla\theta\mathcal{J} = f_1\nabla\psi + f_2\nabla\theta + f_3\nabla\zeta \quad (10.65)$$

$$f_1 = (\nabla\psi \times \nabla\theta) \cdot (\nabla\theta \times \nabla\zeta) \mathcal{J}^2 \quad (10.66)$$

$$f_2 = (\nabla\psi \times \nabla\theta) \cdot (\nabla\zeta \times \nabla\psi) \mathcal{J}^2 \quad (10.67)$$

$$f_3 = (\nabla\psi \times \nabla\theta) \cdot (\nabla\psi \times \nabla\theta) \mathcal{J}^2 \quad (10.68)$$

Summarizing these results, we obtain

$$\begin{pmatrix} \nabla\theta \times \nabla\zeta\mathcal{J} \\ \nabla\zeta \times \nabla\psi\mathcal{J} \\ \nabla\psi \times \nabla\theta\mathcal{J} \end{pmatrix} = M \begin{pmatrix} \nabla\psi \\ \nabla\theta \\ \nabla\zeta \end{pmatrix}, \quad (10.69)$$

where

$$M = \begin{pmatrix} |\nabla\theta \times \nabla\zeta|^2 \mathcal{J}^2 & (\nabla\theta \times \nabla\zeta) \cdot (\nabla\zeta \times \nabla\psi) \mathcal{J}^2 & (\nabla\theta \times \nabla\zeta) \cdot (\nabla\psi \times \nabla\theta) \mathcal{J}^2 \\ (\nabla\zeta \times \nabla\psi) \cdot (\nabla\theta \times \nabla\zeta) \mathcal{J}^2 & (\nabla\zeta \times \nabla\psi) \cdot (\nabla\zeta \times \nabla\psi) \mathcal{J}^2 & (\nabla\zeta \times \nabla\psi) \cdot (\nabla\psi \times \nabla\theta) \mathcal{J}^2 \\ (\nabla\psi \times \nabla\theta) \cdot (\nabla\theta \times \nabla\zeta) \mathcal{J}^2 & (\nabla\psi \times \nabla\theta) \cdot (\nabla\zeta \times \nabla\psi) \mathcal{J}^2 & (\nabla\psi \times \nabla\theta) \cdot (\nabla\psi \times \nabla\theta) \mathcal{J}^2 \end{pmatrix},$$

This matrix and the matrix in Eqs. (10.56) should be the inverse of each other. It is ready to prove this by directly calculating the product of the two matrix.

10.9.1 Special case: metric tensor for (ψ, θ, ϕ) coordinate system

Suppose that (ψ, θ, ϕ) are arbitrary general coordinates except that ϕ is the usual toroidal angle in cylindrical coordinates. Then $\nabla\phi = 1/R\hat{\phi}$ is perpendicular to both $\nabla\psi$ and $\nabla\theta$. Using this, Eq. (10.56) is simplified to

$$\begin{pmatrix} \nabla\psi \\ \nabla\theta \\ \nabla\phi \end{pmatrix} = \begin{pmatrix} |\nabla\psi|^2 & \nabla\psi \cdot \nabla\theta & 0 \\ \nabla\psi \cdot \nabla\theta & |\nabla\theta|^2 & 0 \\ 0 & 0 & 1/R^2 \end{pmatrix} \begin{pmatrix} \nabla\theta \times \nabla\phi \mathcal{J} \\ \nabla\phi \times \nabla\psi \mathcal{J} \\ \nabla\psi \times \nabla\theta \mathcal{J} \end{pmatrix} \quad (10.70)$$

Similarly, Eq. (10.69) is simplified to

$$\begin{pmatrix} \nabla\theta \times \nabla\phi \mathcal{J} \\ \nabla\phi \times \nabla\psi \mathcal{J} \\ \nabla\psi \times \nabla\theta \mathcal{J} \end{pmatrix} = \begin{pmatrix} |\nabla\theta|^2 \mathcal{J}^2 / R^2 & -\nabla\theta \cdot \nabla\psi \mathcal{J}^2 / R^2 & 0 \\ -\nabla\psi \cdot \nabla\theta \mathcal{J}^2 / R^2 & |\nabla\psi|^2 \mathcal{J}^2 / R^2 & 0 \\ 0 & 0 & R^2 \end{pmatrix} \begin{pmatrix} \nabla\psi \\ \nabla\theta \\ \nabla\phi \end{pmatrix} \quad (10.71)$$

[Note that the matrix in Eqs. (10.70) and (10.71) should be the inverse of each other. The product of the two matrix,

$$\begin{pmatrix} |\nabla\theta|^2 \mathcal{J}^2 / R^2 & -\nabla\theta \cdot \nabla\psi \mathcal{J}^2 / R^2 & 0 \\ -\nabla\psi \cdot \nabla\theta \mathcal{J}^2 / R^2 & \frac{\mathcal{J}^2}{R^2} |\nabla\psi|^2 & 0 \\ 0 & 0 & R^2 \end{pmatrix} \begin{pmatrix} |\nabla\psi|^2 & \nabla\psi \cdot \nabla\theta & 0 \\ \nabla\psi \cdot \nabla\theta & |\nabla\theta|^2 & 0 \\ 0 & 0 & 1/R^2 \end{pmatrix}, \quad (10.72)$$

can be calculated to give

$$\begin{pmatrix} A & 0 & 0 \\ 0 & A & 0 \\ 0 & 0 & 1 \end{pmatrix},$$

where

$$A = |\nabla\theta|^2 |\nabla\psi|^2 \mathcal{J}^2 / R^2 - (\nabla\theta \cdot \nabla\psi)^2 \mathcal{J}^2.$$

By using the definition of the Jacobian in Eq. (10.6), it is easy to verify that $A = 1$, i.e.,

$$|\nabla\theta|^2 |\nabla\psi|^2 - (\nabla\theta \cdot \nabla\psi)^2 = \frac{R^2}{\mathcal{J}^2}, \quad (10.73)$$

]

10.10 Covariant/contravariant representation of equilibrium magnetic field

The axisymmetric equilibrium magnetic field is given by Eq. (5.14), i.e.,

$$\mathbf{B} = \nabla \Psi \times \nabla \phi + g \nabla \phi. \quad (10.74)$$

In a general coordinate system (ψ, θ, ϕ) (not necessarily magnetic surface coordinates), the above expression can be written as

$$\mathbf{B} = -\Psi_\psi \nabla \phi \times \nabla \psi - \Psi_\theta \nabla \phi \times \nabla \theta + g \nabla \phi, \quad (10.75)$$

where the subscripts denote the partial derivatives with the corresponding subscripts. Note that Eq. (10.75) is a mixed representation, which involves both covariant and contravariant basis vectors. Equation (10.75) can be converted to the contravariant form by using the metric tensor, giving

$$\mathbf{B} = -\Psi_\psi \nabla \phi \times \nabla \psi - \Psi_\theta \nabla \phi \times \nabla \theta + g \frac{\mathcal{J}}{R^2} \nabla \psi \times \nabla \theta. \quad (10.76)$$

Similarly, Eq. (10.75) can also be transformed to the covariant form, giving

$$\mathbf{B} = \left(\Psi_\psi \frac{\mathcal{J}}{R^2} \nabla \psi \cdot \nabla \theta + \Psi_\theta \frac{\mathcal{J}}{R^2} |\nabla \theta|^2 \right) \nabla \psi + \left(-\Psi_\psi \frac{\mathcal{J}}{R^2} |\nabla \psi|^2 - \Psi_\theta \frac{\mathcal{J}}{R^2} \nabla \theta \cdot \nabla \psi \right) \nabla \theta + g \nabla \phi. \quad (10.77)$$

For the convenience of notation, define

$$h^{\alpha\beta} = \frac{\mathcal{J}}{R^2} \nabla \alpha \cdot \nabla \beta, \quad (10.78)$$

then Eq. (10.77) is written as

$$\mathbf{B} = (\Psi_\psi h^{\psi\theta} + \Psi_\theta h^{\theta\theta}) \nabla \psi + (-\Psi_\psi h^{\psi\psi} - \Psi_\theta h^{\psi\theta}) \nabla \theta + g \nabla \phi. \quad (10.79)$$

10.11 Magnetic surface coordinates (ψ, θ, ϕ)

A coordinate system (ψ, θ, ϕ) , where ϕ is the usual cylindrical toroidal angle, is called a magnetic surface coordinate system if Ψ is a function of only ψ , i.e., $\partial \Psi / \partial \theta = 0$ (we also have $\partial \Psi / \partial \phi = 0$ since we are considering axially symmetrical case). In terms of (ψ, θ, ϕ) coordinates, the contravariant form of the magnetic field, Eq. (10.76), is written as

$$\mathbf{B} = -\Psi' \nabla \phi \times \nabla \psi + g \frac{\mathcal{J}}{R^2} \nabla \psi \times \nabla \theta, \quad (10.80)$$

where $\Psi' \equiv d\Psi / d\psi$. The covariant form of the magnetic field, Eq. (10.77), is written as

$$\mathbf{B} = \left(\Psi' \frac{\mathcal{J}}{R^2} \nabla \psi \cdot \nabla \theta \right) \nabla \psi + \left(-\Psi' \frac{\mathcal{J}}{R^2} |\nabla \psi|^2 \right) \nabla \theta + g \nabla \phi. \quad (10.81)$$

10.12 Local safety factor

The local safety factor \hat{q} is defined by

$$\hat{q} = \frac{\mathbf{B} \cdot \nabla \phi}{\mathbf{B} \cdot \nabla \theta}, \quad (10.82)$$

which characterizes the local pitch angle of a magnetic field line in (θ, ϕ) plane of a magnetic surface. Substituting the contravariant representation of the magnetic field, Eq. (10.80), into the above equation, the local safety factor is written

$$\hat{q}(\psi, \theta) = -\frac{g}{R^2} \frac{\mathcal{J}}{\Psi'}. \quad (10.83)$$

Note that the expression \hat{q} in Eq. (10.83) depends on the Jacobian \mathcal{J} . This is because the definition of \hat{q} depends on the definition of θ , which in turn depends on the the Jacobian \mathcal{J} .

In terms of \hat{q} , the contravariant form of the magnetic field, Eq. (10.80), is written

$$\mathbf{B} = -\Psi'(\nabla \phi \times \nabla \psi + \hat{q} \nabla \psi \times \nabla \theta). \quad (10.84)$$

and the parallel differential operator $\mathbf{B}_0 \cdot \nabla$ is written as

$$\mathbf{B}_0 \cdot \nabla = -\Psi'(\nabla \phi \times \nabla \psi + \hat{q} \nabla \psi \times \nabla \theta) \cdot \nabla = -\Psi' \mathcal{J}^{-1} \left(\frac{\partial}{\partial \theta} + \hat{q} \frac{\partial}{\partial \phi} \right). \quad (10.85)$$

If \hat{q} happens to be independent of θ (i.e., field lines are straight in (θ, ϕ) plane), then the above operator becomes a constant coefficient differential oprator (after divided by \mathcal{J}^{-1}). This simplification is useful because different poloidal harmonics are decoupled in this case. We will discuss this issue futher in Sec. 14.

10.13 Global safety factor

The global safety factor defined in Eq. (9.5) is actually the poloidal average of the local safety factor, i.e.,

$$q(\psi) \equiv \frac{1}{2\pi} \int_0^{2\pi} \hat{q} d\theta \quad (10.86)$$

$$= -\frac{1}{2\pi} \frac{g}{\Psi'} \int_0^{2\pi} \frac{\mathcal{J}}{R^2} d\theta. \quad (10.87)$$

Note that q and \hat{q} defined this way can be negative, which depends on the choice of the positive direction of ϕ and θ coordinates (note that the safety factor given in G-eqds file is always positive, i.e. it is the absolute value of the safety factor defined here).

Next, let us transform the θ integration in expression (10.87) to a curve integral in the poloidal plane. Using the relation $d\ell_p$ and $d\theta$ [Eq. (10.95)], expression (10.87) is further written

$$\begin{aligned} q(\psi) &= -\frac{1}{2\pi} \frac{g}{\Psi'} \oint \text{sign}(\mathcal{J}) \frac{d\ell_p}{R|\nabla\psi|} \\ &= -\frac{1}{2\pi} g \frac{\text{sign}(\mathcal{J})}{\text{sign}(\Psi')} \oint \frac{d\ell_p}{R|\nabla\Psi|}. \end{aligned} \quad (10.88)$$

Expression (10.88) is used in the GTAW code to numerically calculate the value of q on magnetic surfaces (as a benchmarking of the q profile specified in the G-eqdisk file). Expression (10.88) can also be considered as a relation between q and g . In the equilibrium problem where q is given (fixed- q equilibrium), we can use expression (10.88) to obtain the corresponding g (which explicitly appears in the GS equation):

$$g = -2\pi q \left(\oint \frac{d\ell_p}{R|\nabla\Psi|} \right)^{-1} \frac{\text{sign}(\Psi')}{\text{sign}(\mathcal{J})}. \quad (10.89)$$

We note that expression (10.89) involves magnetic surface averaging, which is unknown before we know Ψ . Therefore iteration is usually needed in solving the fixed- q equilibrium (i.e., we guess the unknown Ψ , so that the magnetic surface averaging in expression (10.89) can be performed, yielding the values of g .)

Using $B_p = |\nabla\Psi|/R$ and $B_\phi = g/R$, the absolute value of q in expression (10.88) is written

$$|q| = \frac{1}{2\pi} g \oint \frac{d\ell_p}{R|\nabla\Psi|}. \quad (10.90)$$

$$= \frac{1}{2\pi} \oint \frac{1}{R} \frac{|B_\phi|}{B_p} d\ell_p \quad (10.91)$$

which is the familiar formula we see in textbooks.

10.14 Relation between Jacobian and poloidal angle θ

Given the definition of a magnetic surface coordinate system (ψ, θ, ϕ) , the Jacobian of this system is fully determined. On the other hand, given the definition of ψ , ϕ , and the Jacobian, the definition of θ is fully determined (can have some trivial shifting freedoms). Next, let us discuss how to calculate θ in this case. In (ψ, θ, ϕ) coordinates, a line element is written

$$d\mathbf{l} = \frac{\partial \mathbf{r}}{\partial \psi} d\psi + \frac{\partial \mathbf{r}}{\partial \theta} d\theta + \frac{\partial \mathbf{r}}{\partial \phi} d\phi \quad (10.92)$$

The line element that lies on a magnetic surface (i.e., $d\psi=0$) and in a poloidal plane (i.e., $d\phi=0$) is then written

$$\begin{aligned} d\ell_p &= \frac{\partial \mathbf{r}}{\partial \theta} d\theta \\ &= \mathcal{J} \nabla \phi \times \nabla \psi d\theta. \end{aligned} \quad (10.93)$$

We use the convention that $d\ell_p$ and $d\theta$ take the same sign, i.e.,

$$d\ell_p = |\mathcal{J}\nabla\phi \times \nabla\psi| d\theta. \quad (10.94)$$

Using the fact that $\nabla\psi$ and $\nabla\phi$ are orthogonal and $\nabla\phi = \hat{\phi}/R$, the above equation is written as

$$d\theta = \frac{R}{|\mathcal{J}\nabla\psi|} dl_p \quad (10.95)$$

Given $|\mathcal{J}\nabla\psi|$, Eq. (10.95) can be integrated to determine the θ coordinate of points on a magnetic surface.

$$\bar{\delta} = \int_0^\theta \hat{q} d\theta = - \int_0^\theta \frac{g}{R^2} \frac{\mathcal{J}}{\Psi'} d\theta \quad (10.96)$$

10.15 Calculating poloidal angle

Once $|\mathcal{J}\nabla\psi|$ is known, the value of θ of a point can be obtained by integrating expression (10.95), i.e.,

$$\theta_{i,j} = \theta_{\text{ref},j} + \int_{\mathbf{x}_{\text{ref},j}}^{\mathbf{x}_{i,j}} \frac{R}{|\mathcal{J}\nabla\psi|} dl_p, \quad (10.97)$$

where the curve integration is along the contour $\Psi = \Psi_j$, $\mathbf{x}_{\text{ref},j}$ is a reference point on the contour, where value of the poloidal angle is chosen as $\theta_{\text{ref},j}$. The choice of the positive direction of θ is up to users. Depending on the positive direction chosen, the sign of the Jacobian of the constructed coordinates can have a sign difference from the \mathcal{J} appearing in Eq. (10.97). Denote the Jacobian of the constructed coordinates by \mathcal{J}' , then

$$\mathcal{J}' = \pm \mathcal{J} \quad (10.98)$$

This sign can be determined after the radial coordinate and the positive direction of the poloidal angle are chosen. In GTAW code, I choose the positive direction of θ to be in anticlockwise direction when observers look along the direction of $\hat{\phi}$. To achieve this, the line integration in Eq. (10.97) should be along the anticlockwise direction. (I use the determination of the direction matrix, a well known method in graphic theory, to determine the direction from a given set of discrete points on a magnetic surface.)

10.15.1 Normalized poloidal angle

The span of θ defined by Eq. (10.97) is usually not 2π in one poloidal loop. This poloidal angle can be scaled by $s(\psi)$ to define a new poloidal coordinate $\bar{\theta}$, whose span is 2π in one poloidal loop, where $s(\psi)$ is a magnetic surface function given by

$$s(\psi) = \frac{2\pi}{\oint \frac{R}{|\mathcal{J}\nabla\psi|} dl_p}. \quad (10.99)$$

Then $\bar{\theta}$ is written as

$$\begin{aligned}
 \bar{\theta}_{i,j} &= s(\psi_j)\theta_{i,j} \\
 &= s(\psi_j)\left(\theta_{\text{ref},j} + \int_{\mathbf{x}_{\text{ref},j}}^{\mathbf{x}_{i,j}} \frac{R}{|\mathcal{J}\nabla\psi|} dl_p\right) \\
 &= \bar{\theta}_{\text{ref},j} + s(\psi_j) \int_{\mathbf{x}_{\text{ref},j}}^{\mathbf{x}_{i,j}} \frac{R}{|\mathcal{J}\nabla\psi|} dl_p,
 \end{aligned} \tag{10.100}$$

where $\bar{\theta}_{\text{ref},j} = s(\psi_j)\theta_{\text{ref},j}$. Since we have modified the definition of the poloidal angle, the Jacobian of the new coordinates $(\psi, \bar{\theta}, \phi)$ is different from that of (ψ, θ, ϕ) . The Jacobian \mathcal{J}_{new} of the new coordinates $(\psi, \bar{\theta}, \phi)$ is written as

$$\begin{aligned}
 \mathcal{J}_{\text{new}} &\equiv \frac{1}{(\nabla\psi \times \nabla\bar{\theta}) \cdot \nabla\phi} \\
 &= \frac{1}{\{\nabla\psi \times \nabla[s(\psi)\theta]\} \cdot \nabla\phi} \\
 &= \frac{1}{s(\psi)} \frac{1}{(\nabla\psi \times \nabla\theta) \cdot \nabla\phi} \\
 &= \frac{1}{s(\psi)} \mathcal{J}' \\
 &= \pm \frac{1}{s(\psi)} \mathcal{J}
 \end{aligned} \tag{10.101}$$

The Jacobian \mathcal{J} can be set to various forms to achieve various poloidal coordinates, which will be discussed in the next section. After the Jacobian and the radial coordinate ψ is chosen, all the quantities on the right-hand side of Eq. (10.100) are known and the integration can be performed to obtain the value of $\bar{\theta}_{i,j}$ of each point on each flux surface.

[The reference points $\mathbf{x}_{\text{ref},j}$ and the values of poloidal angle at these points can be chosen by users. One choice of the reference points $\mathbf{x}_{\text{ref},j}$ are those points on the horizontal ray in the midplane that starts from the magnetic axis and points to the low field side of the device and $\bar{\theta}_{\text{ref},j}$ at these points is chosen as zero (this is my choice in the GTAW code). In the TEK code, the reference points are chosen at the high-field side of the midplane and $\bar{\theta}_{\text{ref},j} = -\pi$ at the reference points.]

10.15.2 Jacobian for equal-arc-length poloidal angle

If the Jacobian \mathcal{J} is chosen to be of the following form

$$\mathcal{J} = \frac{R}{|\nabla\psi|}. \tag{10.102}$$

Then $\bar{\theta}_{i,j}$ in Eq. (10.100) is written

$$\bar{\theta}_{i,j} = \bar{\theta}_{\text{ref},j} + \frac{2\pi}{\oint dl_p} \int_{\mathbf{x}_{\text{ref},j}}^{\mathbf{x}_{i,j}} dl_p. \quad (10.103)$$

and the Jacobian of new coordinates $(\psi, \bar{\theta}, \phi)$, \mathcal{J}_{new} , which is given by Eq. (10.101), now takes the form

$$\mathcal{J}_{\text{new}} = \pm \frac{\oint dl_p}{2\pi} \frac{R}{|\nabla\psi|} = \pm \frac{\oint dl_p}{2\pi} \frac{R}{|\nabla\Psi|} \frac{d\Psi}{d\psi}. \quad (10.104)$$

Equation (10.103) indicates a set of poloidal points with equal arc intervals corresponds to a set of uniform θ_i points. Therefore this choice of the Jacobian is called the equal-arc-length Jacobian. Note that Eq. (10.103) does not involve the radial coordinate ψ . Therefore the values of θ of points on any magnetic surface can be determined before the radial coordinate is chosen.

10.15.3 Jacobian for equal-volume poloidal angle (Hamada coordinate)

The volume element in (ψ, θ, ϕ) coordinates is given by $dV = |\mathcal{J}|d\theta d\phi d\psi$. If we choose a Jacobian that is independent of θ , then uniform θ grids will correspond to grids with uniform volume interval. In this case, \mathcal{J} is written as

$$\mathcal{J} = h(\psi), \quad (10.105)$$

where $h(\psi)$ is a function independent of θ . Then $\bar{\theta}_{i,j}$ in Eq. (10.100) is written

$$\bar{\theta}_{i,j} = \bar{\theta}_{\text{ref},j} + \frac{2\pi}{\oint \frac{R}{|\nabla\psi|} dl_p} \int_{\mathbf{x}_{\text{ref},j}}^{\mathbf{x}_{i,j}} \frac{R}{|\nabla\psi|} dl_p \quad (10.106)$$

and the Jacobian of the new coordinates $(\psi, \bar{\theta}, \phi)$, \mathcal{J}_{new} , is given by Eq. (10.101), which now takes the following form:

$$\mathcal{J}_{\text{new}} = \pm \frac{1}{2\pi} \oint \frac{R}{|\nabla\psi|} dl_p. \quad (10.107)$$

Note that both $\bar{\theta}_{i,j}$ and \mathcal{J}_{new} are independent of the function $h(\psi)$ introduced in Eq. (10.105). ($h(\psi)$ is eliminated by the normalization procedure specified in Sec. 10.15.1 due to the fact that $h(\psi)$ is constant on a magnetic surface.) The equal-volume poloidal angle is also called Hamada poloidal angle.

The equal-volume poloidal angle is useful in achieving loading balance for parallel particle simulations. Assume that markers are loaded uniform in space and the poloidal angle is domain decomposed and assigned to different MPI process. Then the equal-volume poloidal angle can make marker number in

each MPI process be equal to each other and thus work loading to each process be equal. (**check**If the domain decomposition is also applied to the radial direction, to achieve loading balance, then the radial coordinate ψ should be chosen in a way that makes $\oint (R/\nabla\psi)dl_p$ be independent of ψ , so that \mathcal{J}_{new} in Eq. (10.107) is constant in space.**)

10.15.4 Jacobian of Boozer's poloidal angle

If the Jacobian \mathcal{J} is chosen to be of the Boozer form:

$$\mathcal{J}(\psi, \theta) = \frac{h(\psi)}{B^2}. \quad (10.108)$$

then the poloidal angle in Eq. (10.100) is written as

$$\theta_{i,j} = \theta_{\text{ref},j} + \frac{2\pi}{\oint \frac{B^2 R}{|\nabla\psi|} dl_p} \int_{\mathbf{x}_{\text{ref},j}}^{\mathbf{x}_{i,j}} \frac{B^2 R}{|\nabla\psi|} dl_p. \quad (10.109)$$

The final Jacobian is given by

$$\mathcal{J}_{\text{new}} = \pm \frac{\oint \frac{B^2 R}{|\nabla\psi|} dl_p}{2\pi} \frac{1}{B^2}. \quad (10.110)$$

The usefulness of Boozer poloidal angle will be further discussed in Sec. 14.8 after we introduce a generalized toroidal angle.

10.15.5 Jacobian for PEST poloidal angle (straight-field-line poloidal angle)

If the Jacobian \mathcal{J} is chosen to be of the following form

$$\mathcal{J}(\psi, \theta) = R^2,$$

then Eq. (10.83) implies that the local safety factor, $\hat{q}(\psi, \theta) = -g/\Psi'$, is a magnetic surface function, i.e., the magnetic field lines are straight in (ψ, θ) plane. Then the poloidal angle in Eq. (10.100) is written

$$\bar{\theta}_{i,j} = \bar{\theta}_{\text{ref},j} + \frac{2\pi}{\oint \frac{1}{R|\nabla\psi|} dl_p} \int_{\mathbf{x}_{\text{ref},j}}^{\mathbf{x}_{i,j}} \frac{1}{R|\nabla\psi|} dl_p, \quad (10.111)$$

The Jacobian \mathcal{J}_{new} given by Eq. (10.101) now takes the form

$$\mathcal{J}_{\text{new}} = \pm R^2 \frac{\oint \frac{1}{R|\nabla\psi|} dl_p}{2\pi}. \quad (10.112)$$

Let us denote an arbitrary poloidal angle by θ and the above straight-field-line poloidal angle by ϑ , then it is ready to find the following relation between θ and ϑ :

$$\vartheta = \vartheta_{\text{ref},j} + \frac{1}{q} \int_{\theta_{\text{ref},j}}^{\theta} \hat{q} d\theta, \quad (10.113)$$

where \hat{q} is the local safety factor corresponding to the arbitrary poloidal angle θ , i.e., $\hat{q} = \mathbf{B} \cdot \nabla \phi / (\mathbf{B} \cdot \nabla \theta)$. [Proof: Using $d\theta = \frac{R}{|\mathcal{J} \nabla \psi|} dl_p$, the poloidal angle ϑ given in Eq. (10.111) is written as

$$\begin{aligned} \vartheta &= \vartheta_{\text{ref},j} + \frac{2\pi}{\oint \frac{1}{R|\nabla \psi|} dl_p} \int_{\mathbf{x}_{\text{ref},j}}^{\mathbf{x}_{i,j}} \frac{1}{R|\nabla \psi|} dl_p \\ &= \vartheta_{\text{ref},j} + \frac{2\pi}{\oint \frac{1}{R|\nabla \psi|} \frac{|\mathcal{J} \nabla \psi|}{R} d\theta} \int_{\mathbf{x}_{\text{ref},j}}^{\mathbf{x}_{i,j}} \frac{1}{R|\nabla \psi|} \frac{|\mathcal{J} \nabla \psi|}{R} d\theta \\ &= \vartheta_{\text{ref},j} + \frac{2\pi}{\oint \frac{|\mathcal{J}|}{R^2} d\theta} \int_{\mathbf{x}_{\text{ref},j}}^{\mathbf{x}_{i,j}} \frac{|\mathcal{J}|}{R^2} d\theta. \end{aligned} \quad (10.114)$$

Using $\hat{q} = -\frac{g}{R^2} \frac{\mathcal{J}}{\Psi'}$, where \mathcal{J} is the Jacobian of (ψ, θ, ϕ) coordinates, then the above ϑ is reduced to expression (10.113).]

Note that Boozer poloidal angle is very close to the poloidal angle discussed here because the two Jacobians are very similar:

$$\mathcal{J} = \frac{1}{B^2} \sim R^2. \quad (10.115)$$

10.15.6 Comparison between different types of poloidal angle

All Jacobians introduced above can be written in a general form:

$$\mathcal{J} = \frac{R^i}{|\nabla \psi|^j B^k}, \quad (10.116)$$

The choice of $(i = 2, j = k = 0)$ gives the PEST coordinate, $(i = j = 0, k = 2)$ give the Boozer coordinate, $(i = j = 1, k = 0)$ gives the equal-arc coordinate, $(i = j = k = 0)$ gives the Hammada coordinate.

Figure 10.1 compares the equal-arc-poloidal angle and the straight-line poloidal angle, which shows that the resolution of the straight-line poloidal angle is not good near the low-field-side midplane. Since ballooning modes take larger amplitude near the low-field-side midplane, better resolution is desired there. This is one reason that I often avoid using the straight-line poloidal angle in my numerical codes.

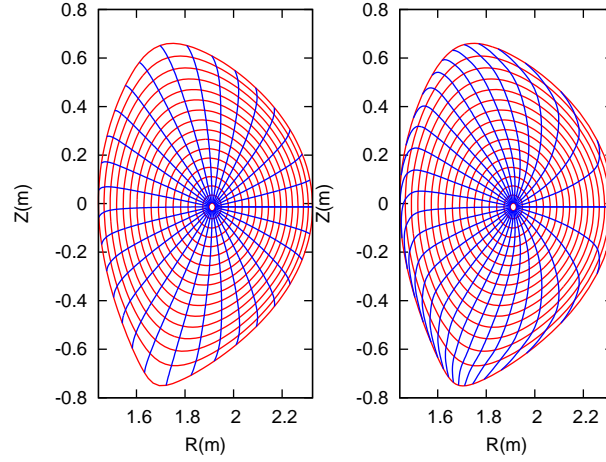


Figure 10.1. The equal-arc poloidal angle (left) and the straight-line poloidal angle (right) for EAST equilibrium #38300@3.9s. The blue lines correspond to the equal- θ lines, with uniform θ interval between neighbour lines. The red lines correspond to the magnetic surfaces, which start from $\sqrt{\Psi_t} = 0.01714$ (the innermost magnetic surface) and end at $\sqrt{\Psi_t} = 0.9851$ (the boundary magnetic surface), and are equally spaced in $\sqrt{\Psi_t}$.

10.15.7 Verification of Jacobian

After the magnetic coordinates are constructed, we can evaluate the Jacobian \mathcal{J}_{new} by using directly the definition of the Jacobian, i.e.,

$$\mathcal{J}_{\text{new}} = \frac{1}{(\nabla\psi \times \nabla\bar{\theta}) \cdot \nabla\phi}, \quad (10.117)$$

which can be further written as

$$\mathcal{J}_{\text{new}} = R(R_{\bar{\theta}}Z_{\psi} - R_{\psi}Z_{\bar{\theta}}), \quad (10.118)$$

where the partial differential can be evaluated by using numerical differential schemes. The results obtained by this way should agree with results obtained from the analytical form of the Jacobian. This consistency check provide a verification for the correctness of the theory derivation and numerical implementation. In evaluating the Jacobian by using the analytical form, we may need to evaluate $\nabla\psi$, which finally reduces to evaluating $\nabla\Psi$. The value of $|\nabla\Psi|$ is obtained numerically based on the numerical data of Ψ given in cylindrical coordinate grids. Then the cubic spline interpolating formula is used to obtain the value of $|\nabla\Psi|$ at desired points. (\mathcal{J}_{new} calculated by the second method (i.e. using analytic form) is used in the GTAW code; the first methods are also implemented in the code for the benchmark purpose.) In the following sections, for notation ease, the Jacobian of the constructed coordinate system will be denoted by \mathcal{J} , rather than \mathcal{J}_{new} .

10.15.8 Radial coordinate

The radial coordinate ψ can be chosen to be various surface function, e.g., volume, poloidal or toroidal magnetic flux within a magnetic surface. The frequently used radial coordinates include $\bar{\Psi}$, and $\sqrt{\bar{\Psi}}$, where $\bar{\Psi}$ is defined by

$$\bar{\Psi} = \frac{\Psi - \Psi_0}{\Psi_a - \Psi_0}, \quad (10.119)$$

where Ψ_0 and Ψ_a are the values of Ψ at the magnetic axis and LCFS, respectively. Other choices of the radial coordinates: the toroidal magnetic flux and its square root, $\bar{\Psi}_t$, and $\sqrt{\bar{\Psi}_t}$, where Ψ_t and $\bar{\Psi}_t$ are defined by

$$\frac{d\Psi_t}{d\Psi} = 2\pi q, \Psi_t(0) = 0 \quad (10.120)$$

and

$$\bar{\Psi}_t = \frac{\Psi_t}{\Psi_t(1)}, \quad (10.121)$$

respectively, where $\Psi_t(0)$ and $\Psi_t(1)$ are the values of Ψ_t at the magnetic axis and LCFS, respectively.

If $\psi = \sqrt{\bar{\Psi}_t}$, then

$$\frac{d\Psi}{d\psi} = \frac{d\Psi}{d\Psi_t} \frac{d\Psi_t}{d\psi} = \frac{1}{2\pi q} \frac{d\Psi_t}{d\psi} = \frac{1}{2\pi q} \frac{d\Psi_t}{d\bar{\Psi}_t} \frac{d\bar{\Psi}_t}{d\psi} = \frac{1}{2\pi q} \Psi_t(1) 2\psi \quad (10.122)$$

The cylindrical coordinates (R, ϕ, Z) is a right-hand system, with the positive direction of Z pointing vertically up. In GTAW code, the positive direction of θ is chosen in the anticlockwise direction when observers look along the direction of $\hat{\phi}$. Then the definition $\mathcal{J}^{-1} = \nabla\psi \times \nabla\theta \cdot \nabla\phi$ indicates that (1) \mathcal{J} is negative if $\nabla\psi$ points from the magnetic axis to LCFS; (2) \mathcal{J} is positive if $\nabla\psi$ points from the LCFS to the magnetic axis. This can be used to determine the sign of Jacobian after using the analytical formula to obtain the absolute value of Jacobian.

If $\psi = \bar{\Psi}$ or $\psi = \sqrt{\bar{\Psi}}$, $\nabla\psi$ points from the magnetic axis to LCFS.

The volume between magnetic surfaces can also be used as a radial coordinate. The differential volume element is written as

$$d^3V = \mathcal{J} d\psi d\theta d\phi. \quad (10.123)$$

Integrating over the toroidal angle, we obtain

$$d^2V = 2\pi \mathcal{J} d\psi d\theta \quad (10.124)$$

Further integrating over the poloidal angle, we obtain

$$d^1V = 2\pi d\psi \oint \mathcal{J} d\theta, \quad (10.125)$$

i.e.,

$$\frac{d^1V}{d\psi} = 2\pi \oint \mathcal{J} d\theta. \quad (10.126)$$

In codes I wrote, I stick to using $\bar{\Psi}$ as the radial coordinate when doing computation, and transform to other radial coordinates when presenting the results if needed.

11 Constructing magnetic surface coordinate system from discrete $\Psi(R, Z)$ data

Given an axisymmetric tokamak equilibrium in (R, ϕ, Z) coordinates (e.g., 2D data $\Psi(R, Z)$ on a rectangular grids (R, Z) in G-file), we can construct a magnetic surface coordinates (ψ, θ, ϕ) by the following two steps. (1) Find out a series of magnetic surfaces on (R, Z) plane and select radial coordinates for each magnetic surface (e.g. the poloidal flux within each magnetic surface). (2) Specify the Jacobian or some property that we want the poloidal angle to have. Then calculate the poloidal angle of each point on each flux surface (on the $\phi = \text{const}$ plane) by using Eq. (10.95) (if the Jacobian is specified) or some method specified by us to achieve some property we prefer for the poloidal angle (if a Jacobian is not directly specified). Then we obtain the magnetic surface coordinates system (ψ, θ, ϕ) .

11.1 Finding magnetic surfaces

Two-dimensional data $\Psi(R, Z)$ on a rectangular grids (R, Z) is read from the G_EQDSK file (G-file) of EFIT code. Based on the 2D array data, I use 2D cubic spline interpolation to construct a interpolating function $\Psi = \Psi(R, Z)$. To construct a magnetic surface coordinate system, I need to find the contours of Ψ , i.e., magnetic surfaces. The values of Ψ on the magnetic axis, Ψ_0 , and the value of Ψ on the last closed flux surface (LCFS), Ψ_b , are given in G-file. Using these two values, I construct a 1D array “psival” with value of elements changing uniform from Ψ_0 to Ψ_b . Then I try to find the contours of Ψ with contour level value ranging from Ψ_0 to Ψ_b . This is done in the following way: construct a series of straight line (in the poloidal plane) that starts from the location of the magnetic axis and ends at one of the points on the LCFS. Combine the straight line equation, $Z = Z(R)$, with the interpolating function $\Psi(R, Z)$, we obtain a one variable function $h = \Psi(R, Z(R))$. Then finding the location where Ψ is equal to a specified value Ψ_i , is reduced to finding the root of the equation $\Psi(R, Z(R)) - \Psi_i = 0$. Since this is a one variable equation, the root can be easily found by using simple root finding scheme, such as bisection method (bisection method is used in GTAW code). After finding the roots for each value in the array “psival” on each straight lines, the process of finding the contours of Ψ is finished. The contours of Ψ found this way are plotted in Fig. 11.1.

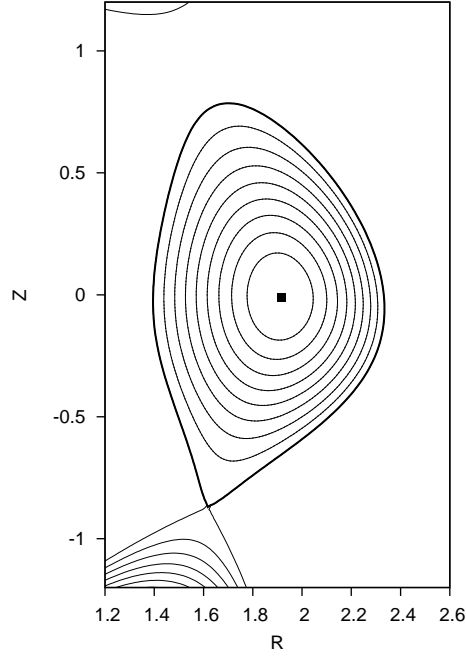


Figure 11.1. Verification of the numerical code that calculates the contours of the poloidal flux Ψ . The bold line in the figure indicates the LCFS. The contour lines (solid lines) given by the gnuplot program agrees well with the results I calculate by using interpolation and root-finding method (the two sets of contours are indistinguishable in this scale). My code only calculate the contour lines within the LCFS, while those given by gnuplot contains additional contour lines below the X point and on the left top in the figure. Eqdisk file of the equilibrium was provided by Dr. Guoqiang Li (filename: g013606.07104).

In the above, we mentioned that the point of magnetic axis and points on the LCFS are needed to construct the straight lines. In G-file, points on LCFS are given explicitly in an array. The location of magnetic axis is also explicitly given in G-file. It is obvious that some of the straight lines $Z = Z(R)$ that pass through the location of magnetic axis and points on the LCFS will have very large or even infinite slope. On these lines, finding the accurate root of the equation $\Psi(R, Z(R)) - \Psi_i = 0$ is difficult or even impossible. The way to avoid this situation is obvious: switch to use function $R = R(Z)$ instead of $Z = Z(R)$ when the slope of $Z = Z(R)$ is large (the switch condition I used is $|dZ/dR| > 1$).

In constructing the flux surface coordinate with desired Jacobian, we will need the absolute value of the gradient of Ψ , $|\nabla\Psi|$, on some specified spatial points. To achieve this, we need to construct a interpolating function for $|\nabla\Psi|$.

The $|\nabla\Psi|$ can be written as

$$|\nabla\Psi| = \sqrt{\left(\frac{\partial\Psi}{\partial R}\right)^2 + \left(\frac{\partial\Psi}{\partial Z}\right)^2}, \quad (11.1)$$

By using the center difference scheme to evaluate the partial derivatives with respect to R and Z in the above equation (using one side difference scheme for the points on the rectangular boundary), we can obtain an 2D array for the value of $|\nabla\Psi|$ on the rectangular (R, Z) grids. Using this 2D array, we can construct an interpolating function for $\nabla\Psi$ by using the cubic spline interpolation scheme.

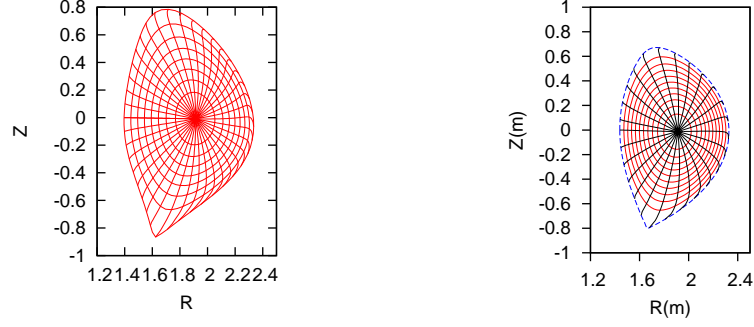


Figure 11.2. Grid points (the intersecting points of two curves in the figure) corresponding to uniform poloidal flux and uniform poloidal arc length for EAST equilibrium shot 13606 at 7.1s (left) (G-file name: g013606.07104) and shot 38300 at 3.9s (right) (G-file name: g038300.03900).

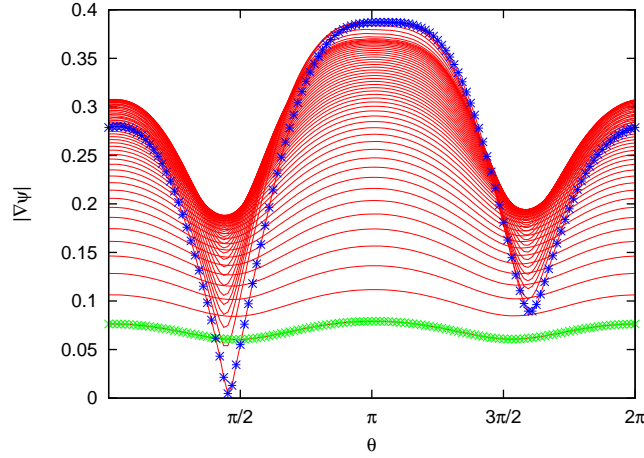


Figure 11.3. $|\nabla\Psi|$ as a function of the poloidal angle. The different lines corresponds to the values of $|\nabla\Psi|$ on different magnetic surfaces. The stars correspond to the values on the boundary magnetic surface while the plus signs correspond to the value on the innermost magnetic surface (the magnetic surface adjacent to the magnetic axis). The equilibrium is for EAST shot 38300 at 3.9s.

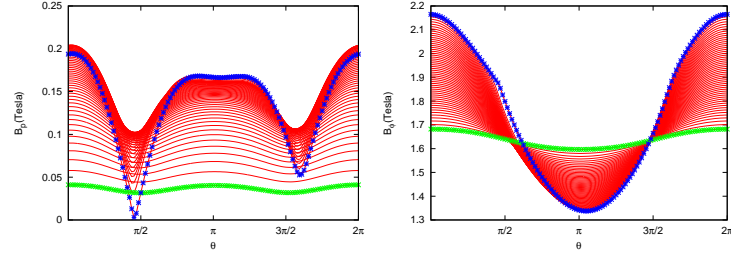


Figure 11.4. The Poloidal magnetic field $B_p = |\nabla\Psi|/R$ (left) and toroidal magnetic field $B_\phi = g/R$ (right) as a function of the poloidal angle. The different lines corresponds to the values on different magnetic surfaces. The stars correspond to the values on the boundary magnetic surface while the plus signs correspond to the value on the innermost magnetic surface (the magnetic surface adjacent to the magnetic axis). The equilibrium is for EAST shot 38300 at 3.9s.

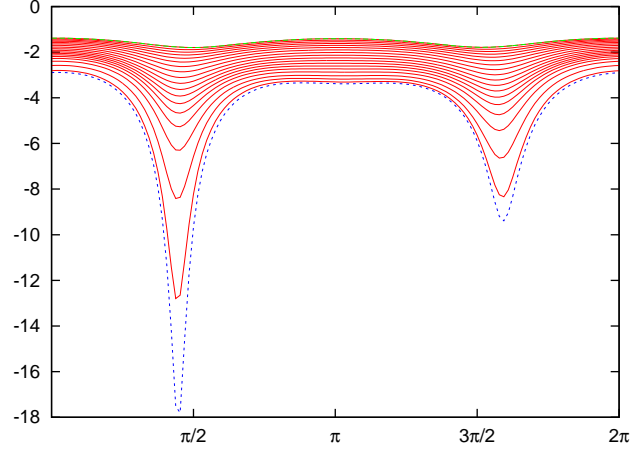


Figure 11.5. Equal-arc Jacobian as a function of the poloidal angle on different magnetic surfaces. The dotted line corresponds to the values of Jacobian on the boundary magnetic surface. The equilibrium is for EAST shot 38300 at 3.9s.

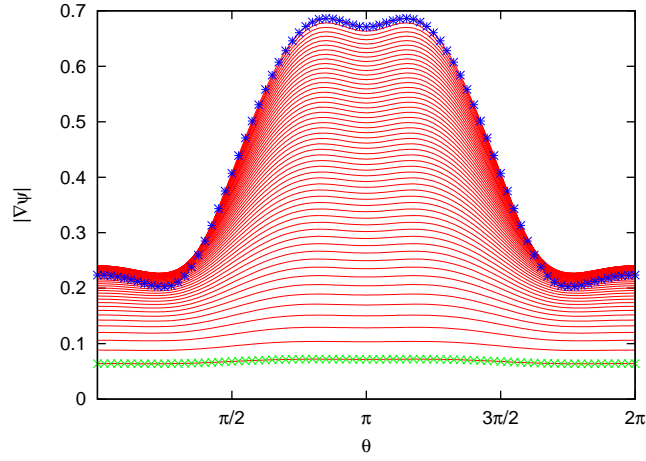


Figure 11.6. $|\nabla\Psi|$ as a function of the poloidal angle. The different lines corresponds to values of $|\nabla\Psi|$ on different magnetic surfaces. The stars correspond to the values of $|\nabla\Psi|$ on the boundary magnetic surface while the plus signs correspond to the value on the innermost magnetic surface (the magnetic surface adjacent to the magnetic axis). The equilibrium is a Solovév equilibrium.

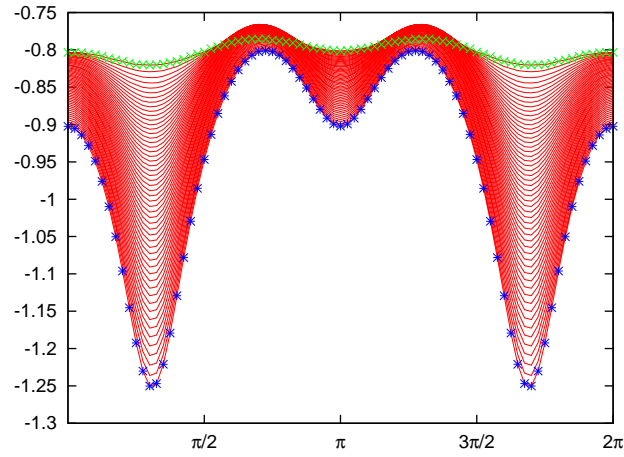


Figure 11.7. Jacobian on different magnetic surfaces as a function of the poloidal angle. The equilibrium is a Solovév equilibrium and the Jacobian is an equal-arc Jacobian. The stars correspond to the values of Jacobian on the boundary magnetic surface while the plus signs correspond to the value on the innermost magnetic surface (the magnetic surface adjacent to the magnetic axis).

11.2 Expression of metric elements of magnetic coordinates (ψ, θ, ϕ)

Metric elements of the (ψ, θ, ϕ) coordinates, e.g., $\nabla\psi \cdot \nabla\theta$, are often needed in practical calculations. Next, we express these metric elements in terms of the cylindrical coordinates (R, Z) and their partial derivatives with respect to ψ and θ . Note that, in this case, the coordinate system is (ψ, θ, ϕ) while R and Z are functions of ψ and θ , i.e.,

$$R = R(\psi, \theta), \quad (11.2)$$

$$Z = Z(\psi, \theta). \quad (11.3)$$

Then ∇R and ∇Z are written as

$$\nabla R = \hat{\mathbf{R}} = R_\psi \nabla\psi + R_\theta \nabla\theta, \quad (11.4)$$

$$\nabla Z = \hat{\mathbf{Z}} = Z_\psi \nabla\psi + Z_\theta \nabla\theta, \quad (11.5)$$

where $R_\psi \equiv \partial R / \partial \psi$, etc. Equations (11.4) and (11.5) can be solved to give

$$\nabla\psi = \frac{1}{R_\psi Z_\theta - Z_\psi R_\theta} (Z_\theta \hat{\mathbf{R}} - R_\theta \hat{\mathbf{Z}}), \quad (11.6)$$

$$\nabla\theta = \frac{1}{Z_\psi R_\theta - R_\psi Z_\theta} (Z_\psi \hat{\mathbf{R}} - R_\psi \hat{\mathbf{Z}}). \quad (11.7)$$

Using the above expressions, the Jacobian of (ψ, θ, ϕ) coordinates, \mathcal{J} , is written as

$$\begin{aligned} \mathcal{J}^{-1} &= \nabla\psi \times \nabla\theta \cdot \nabla\phi \\ &= -\frac{1}{(R_\psi Z_\theta - Z_\psi R_\theta)^2} (Z_\theta R_\psi \hat{\phi} - R_\theta Z_\psi \hat{\phi}) \times \frac{\hat{\phi}}{R} \\ &= -\frac{1}{(Z_\theta R_\psi - R_\theta Z_\psi)R}, \end{aligned} \quad (11.8)$$

i.e.,

$$\mathcal{J} = R(R_\theta Z_\psi - R_\psi Z_\theta). \quad (11.9)$$

Using this, Expressions (11.6) and (11.7) are written as

$$\nabla\psi = -\frac{R}{\mathcal{J}} (Z_\theta \hat{\mathbf{R}} - R_\theta \hat{\mathbf{Z}}) \quad (11.10)$$

and

$$\nabla\theta = \frac{R}{\mathcal{J}} (Z_\psi \hat{\mathbf{R}} - R_\psi \hat{\mathbf{Z}}). \quad (11.11)$$

Then the elements of the metric matrix are written as

$$|\nabla\psi|^2 = \frac{R^2}{\mathcal{J}^2} (Z_\theta^2 + R_\theta^2), \quad (11.12)$$

$$|\nabla\theta|^2 = \frac{R^2}{\mathcal{J}^2} (Z_\psi^2 + R_\psi^2), \quad (11.13)$$

and

$$\nabla\psi \cdot \nabla\theta = -\frac{R^2}{\mathcal{J}^2}(Z_\theta Z_\psi + R_\theta R_\psi). \quad (11.14)$$

Equations (11.12), (11.13), and (11.14) are the expressions of the metric elements in terms of R , R_ψ , R_θ , Z_ψ , and Z_θ . [Combining the above results, we obtain

$$\frac{\nabla\psi \cdot \nabla\theta}{|\nabla\psi|^2} = -\frac{Z_\theta Z_\psi + R_\theta R_\psi}{Z_\theta^2 + R_\theta^2}. \quad (11.15)$$

Equation (11.14) is used in GTAW code. Using the above results, $h^{\alpha\beta} = \frac{\mathcal{J}}{R^2} \nabla\alpha \cdot \nabla\beta$ are written as

$$h^{\psi\psi} = \frac{\mathcal{J}}{R^2} |\nabla\psi|^2 = \frac{1}{\mathcal{J}} (Z_\theta^2 + R_\theta^2) \quad (11.16)$$

$$h^{\theta\theta} = \frac{\mathcal{J}}{R^2} |\nabla\theta|^2 = \frac{1}{\mathcal{J}} (Z_\psi^2 + R_\psi^2), \quad (11.17)$$

$$h^{\psi\theta} = \frac{\mathcal{J}}{R^2} \nabla\psi \cdot \nabla\theta = -\frac{1}{\mathcal{J}} (Z_\theta Z_\psi + R_\theta R_\psi) \quad (11.18)$$

As a side product of the above results, we can calculate the arc length in the poloidal plane along a constant ψ surface, $d\ell_p$, which is expressed as

$$\begin{aligned} d\ell_p &= \sqrt{(dR)^2 + (dZ)^2} \\ &= \sqrt{(R_\psi d\psi + R_\theta d\theta)^2 + (Z_\psi d\psi + Z_\theta d\theta)^2}. \end{aligned}$$

Note that $d\psi = 0$ since we are considering the arc length along a constant ψ surface in (R, Z) plane. Then the above expression is reduced to

$$\begin{aligned} d\ell_p &= \sqrt{(R_\theta d\theta)^2 + (Z_\theta d\theta)^2} \\ &= \sqrt{R_\theta^2 + Z_\theta^2} d\theta \\ &= \frac{|\mathcal{J} \nabla\psi|}{R} d\theta, \end{aligned} \quad (11.19)$$

which agrees with Eq. (10.95).]

12 Constructing model tokamak magnetic field

In some cases (e.g., turbulence simulation), model tokamak magnetic field, which is not an exact solution to the GS equation, is often used. In the model, the safety factor profile $q(\psi)$, toroidal field function $g(\psi)$, and the magnetic surface shape $(R(\psi, \theta), Z(\psi, \theta))$ are given. To use this model in a simulation, we need to calculate its poloidal magnetic field, which is determined by the poloidal magnetic flux function Ψ . To determine Ψ , we need to use Eq. (10.87), i.e.,

$$q(\psi) = -\frac{1}{2\pi} \frac{g}{\Psi'} \int_0^{2\pi} \frac{\mathcal{J}}{R^2} d\theta, \quad (12.1)$$

and re-organize the formula as

$$\frac{d\Psi}{d\psi} = -\frac{1}{2\pi} \frac{g(\psi)}{q(\psi)} \int_0^{2\pi} \frac{\mathcal{J}}{R^2} d\theta, \quad (12.2)$$

which can be integrated to obtain Ψ and thus the poloidal magnetic field $\mathbf{B}_p = \nabla\Psi \times \nabla\phi$, where $\mathcal{J} = [(\nabla\psi \times \nabla\theta) \cdot \nabla\phi]^{-1}$. The toroidal magnetic field can be obtained from $g(\psi)$ by $B_\phi = g/R$. In most papers, $g(\psi)$ is chosen to be a constant.

A typical magnetic surface shape used in simulations is the Miller shape, which is given by

$$\begin{aligned} R(r, \theta) &= R_0(r) + r \cos[\theta + (\sin^{-1}\delta(r)) \sin\theta] \\ Z(r, \theta) &= \kappa(r) r \sin\theta \end{aligned} \quad (12.3)$$

where $r = \psi$ is the radial coordinate, $R_0(r)$, $\delta(r)$, and $\kappa_r(r)$ are the Shafranov shift, triangularity, and elongation profiles, which can be arbitrarily specified. For the special case of R_0 being a constant, $\delta(r) = 0$, and $\kappa(r) = 1$, this shape reduces to a concentric-circular magnetic field. An example of calculating the poloidal field of the model field is given in Sec. 16. This kind of model field can be called theoretical physicists' tokamak. Computational physicists often use this model for code benchmarking purpose. The famous DIII-D cyclone base case is an example, which was extensively used for benchmarking gyrokinetic simulation of ion temperature driven turbulence.

13 Magnetic surface averaging

13.1 Definition

The magnetic surface average of a physical quantity $G(\psi, \theta, \phi)$ is defined by

$$\langle G \rangle \equiv \lim_{\Delta\Psi \rightarrow 0} \left(\frac{\iint \iint_{\Delta\Psi} G d^3V}{\iint \iint_{\Delta\Psi} d^3V} \right), \quad (13.1)$$

where the volume integration is over a small volume between two adjacent flux surfaces with Ψ differing by $\Delta\Psi$. [This formula (with finite $\Delta\Psi$) is used in TEK code to calculate the radial heat flux.]

The above 3D volume integration can also be written as a 2D surface integration. The differential volume element is given by $d^3V = |\mathcal{J}| d\psi d\theta d\phi$, where \mathcal{J} is the Jacobian of (ψ, θ, ϕ) coordinates. Using this, equation (13.1) is written as

$$\begin{aligned} \langle G \rangle &= \lim_{\Delta\Psi \rightarrow 0} \left(\frac{\iint \iint_{\Delta\Psi} G |\mathcal{J}| d\psi d\theta d\phi}{\iint \iint_{\Delta\Psi} |\mathcal{J}| d\psi d\theta d\phi} \right) \\ &= \frac{\iint G |\mathcal{J}| d\theta d\phi}{\iint |\mathcal{J}| d\theta d\phi}, \end{aligned} \quad (13.2)$$

which is a 2D averaging over a magnetic surface and thus is called magnetic surface average. Note that the surface averaging of any $n \neq 0$ harmonic is zero (n is the toroidal mode number). Therefore the magnetic surface average contains only the contribution from the $n = 0$ component, i.e., axisymmetric component. (On the other hand, $m \neq 0$ poloidal harmonics of G can contribute to the surface average since the Jacobian has a poloidal angle dependence.) Using this and noting that \mathcal{J} is axisymmetric, then expression (13.2) is written as

$$\langle G \rangle = \frac{\int G_0(\psi, \theta) |\mathcal{J}| d\theta}{\int |\mathcal{J}| d\theta}, \quad (13.3)$$

where $G_0(\theta)$ is defined by the following Fourier expansion:

$$G = \sum_{n=-\infty}^{+\infty} G_n(\psi, \theta) \exp(-in\phi). \quad (13.4)$$

“Zonal” and “mean” components

$\langle G \rangle$ is sometimes called the “zonal” component of G if the radial wavelength of $\langle G \rangle$ is much smaller than the equilibrium scale length. If the radial wavelength of $\langle G \rangle$ is comparable to the equilibrium scale length, $\langle G \rangle$ is usually called “mean” component in tokamak literature. For example, mean flows are of system space scale and thus are easy to be observed in experiments. On the other hand, the “zonal” flow, which usually refers to the turbulence generated secondary flow, is of much smaller radial scale (the radial wavelength of zonal flow is of several Larmor radius) and thus is difficult to observe in experiments.

Sometimes, we do not want the Jacobian to explicitly appear in the formula. This can be achieved by writing the differential volume element as

$$d^3V = R d\phi \frac{d\Psi}{|\nabla\Psi|} dl_p. \quad (13.5)$$

Using $B_p = |\nabla\Psi|/R$, the volume element is further written as

$$d^3V = d\phi \frac{d\Psi}{B_p} dl_p \quad (13.6)$$

Using this, the averaging defined in Eq. (13.1) is written as

$$\begin{aligned} \langle G \rangle &= \lim_{\Delta\Psi \rightarrow 0} \frac{\iint \int_{\Delta\Psi} G d\phi \frac{d\Psi}{B_p} dl_p}{\iint \int_{\Delta\Psi} d\phi \frac{d\Psi}{B_p} dl_p} \\ &= \frac{\iint G \frac{1}{B_p} d\phi dl_p}{\iint \frac{1}{B_p} d\phi dl_p}. \end{aligned} \quad (13.7)$$

If G is axisymmetric, then the above equation is written as

$$\langle G \rangle = \frac{\oint G \frac{1}{B_p} dl_p}{\oint \frac{1}{B_p} dl_p}. \quad (13.8)$$

(Equation (13.8) is used in the GTAW code to calculate the magnetic surface averaging.) Using Eq. (10.95) and $B_p = |\nabla \Psi|/R$, equation (13.8) can also be written as

$$\langle G \rangle = \frac{\int_0^{2\pi} G |\mathcal{J}| d\theta}{\int_0^{2\pi} |\mathcal{J}| d\theta}. \quad (13.9)$$

Using the expression of the volume element $d\tau = |\mathcal{J}| d\theta d\phi d\psi$, the volume within a magnetic surface is written

$$V(\psi) = \int d\tau = \int |\mathcal{J}| d\theta d\phi d\psi = 2\pi \int_{\psi_0}^{\psi} \int_0^{2\pi} |\mathcal{J}| d\theta d\psi. \quad (13.10)$$

Using this, the differential of V with respect to ψ is written as

$$V' \equiv \frac{dV}{d\psi} = 2\pi \int_0^{2\pi} |\mathcal{J}| d\theta. \quad (13.11)$$

Using this, Eq. (13.9) is written as

$$\langle G \rangle = \frac{2\pi}{V'} \int_0^{2\pi} G |\mathcal{J}| d\theta$$

14 Magnetic coordinates (ψ, θ, ζ) with general toroidal angle ζ

14.1 General toroidal angle ζ

In Sec. 10.12, we introduced the local safety factor $\hat{q}(\psi, \theta)$. Equation (10.83) indicates that if the Jacobian is chosen to be of the particular form $\mathcal{J} = h(\psi)R^2$, then the local safety factor is independent of θ , i.e., magnetic line is straight in (θ, ϕ) plane. On the other hand, if we want to make field line straight in (θ, ϕ) plane, the Jacobian must be chosen to be of the specific form $\mathcal{J} = h(\psi)R^2$. We note that, as mentioned in Sec. 10.14, the poloidal angle is fully determined by the choice of the Jacobian. The specific choice of $\mathcal{J} = \alpha(\psi)R^2$ is usually too restrictive for achieve a desired poloidal resolution (for example, the equal-arc poloidal angle can not be achieved by this choice of Jacobian). Is there any way that we can make the field line straight in a coordinate system at the same time ensure that the Jacobian can be freely adjusted to obtain desired poloidal angle? The answer is yes. The obvious way to achieve this is to define a new toroidal angle ζ that generalizes the usual toroidal angle ϕ . Define a new toroidal angle ζ by[10]

$$\zeta = \phi - q(\psi)\delta(\psi, \theta), \quad (14.1)$$

where $\delta = \delta(\psi, \theta)$ is a unknown function to be determined by the constraint of field line being straight in (θ, ζ) plane. Using Eq. (10.84), the new local safety factor in (ψ, θ, ζ) coordinates is written as

$$\begin{aligned}
 \hat{q}_{\text{new}} &\equiv \frac{\mathbf{B} \cdot \nabla \zeta}{\mathbf{B} \cdot \nabla \theta} \\
 &= \frac{(\nabla \phi \times \nabla \psi + \hat{q} \nabla \psi \times \nabla \theta) \cdot \nabla \zeta}{(\nabla \phi \times \nabla \psi + \hat{q} \nabla \psi \times \nabla \theta) \cdot \nabla \theta} \\
 &= \frac{\nabla \phi \times \nabla \psi \cdot \nabla \zeta + \hat{q} \nabla \psi \times \nabla \theta \cdot \nabla \zeta}{(\nabla \phi \times \nabla \psi) \cdot \nabla \theta} \\
 &= \frac{\nabla \phi \times \nabla \psi \cdot \nabla(-q\delta) + \hat{q} \nabla \psi \times \nabla \theta \cdot \nabla \phi}{(\nabla \phi \times \nabla \psi) \cdot \nabla \theta} \\
 &= -q \frac{\partial \delta}{\partial \theta} + \hat{q}.
 \end{aligned} \tag{14.2}$$

To make the new local safety factor be independent of θ , the right-hand side of Eq. (14.2) should be independent of θ , i.e.,

$$-q \frac{\partial \delta}{\partial \theta} + \hat{q} = c(\psi), \tag{14.3}$$

where $c(\psi)$ can be an arbitrary function of ψ . A convenient choice for $c(\psi)$ is $c(\psi) = q$, i.e., making the new local safety factor be equal to the original global safety factor, i.e., $\hat{q}_{\text{new}} = q$. In this case, equation (14.3) is written as

$$\frac{\partial \delta}{\partial \theta} = \frac{\hat{q}}{q} - 1, \tag{14.4}$$

which, on a magnetic surface labeled by ψ , can be integrated over θ to give

$$\delta(\psi, \theta) = \delta(\psi, \theta_{\text{ref}}) - (\theta - \theta_{\text{ref}}) + \frac{1}{q} \int_{\theta_{\text{ref}}}^{\theta} \hat{q} d\theta, \tag{14.5}$$

where θ_{ref} is an starting poloidal angle arbitrarily chosen for the integration, and $\delta(\psi, \theta_{\text{ref}})$ is the constant of integration. In the following, both θ_{ref} and $\delta(\psi, \theta_{\text{ref}})$ will be chosen to be zero. Then the above equations is written

$$\delta = -\theta + \frac{1}{q} \int_0^{\theta} \hat{q} d\theta. \tag{14.6}$$

Substituting the above expression into the definition of ζ (Eq. 14.1), we obtain

$$\zeta = \phi + q\theta - \int_0^{\theta} \hat{q} d\theta, \tag{14.7}$$

which is the formula for calculating the general toroidal angle. If θ is a straight-field line poloidal angle, then ζ in Eq. (14.7) reduces to the usual toroidal angle ϕ .

In summary, magnetic field line is straight in (θ, ζ) plane with slope being q if ζ is defined by Eq. (14.7). In this method, we make the field line straight by defining a new toroidal angle, instead of requiring the Jacobian to take particular forms. Thus, the freedom of choosing the form of the Jacobian is still available to be used later to choose a good poloidal angle coordinate. Note that the Jacobian of the new coordinates (ψ, θ, ζ) is equal to that of (ψ, θ, ϕ) . [Proof:

$$\begin{aligned}\mathcal{J}_{\text{new}}^{-1} &= \nabla\psi \times \nabla\theta \cdot \nabla\zeta \\ &= \nabla\psi \times \nabla\theta \cdot \nabla(\phi - q\delta) \\ &= \nabla\psi \times \nabla\theta \cdot \nabla\phi - \nabla\psi \times \nabla\theta \cdot \nabla(q\delta) \\ &= \nabla\psi \times \nabla\theta \cdot \nabla\phi - 0 \\ &= \mathcal{J}^{-1}.\end{aligned}$$

] Also note that $\delta(\psi, \theta)$ defined by Eq. (14.6) is a periodic function of θ . [Proof: Equation (14.6) implies that

$$\begin{aligned}\delta(\psi, \theta + 2\pi) &= \frac{1}{q} \int_0^{\theta+2\pi} \hat{q} d\theta - (\theta - \theta_{\text{ref}}) - 2\pi \\ &= \frac{1}{q} \int_0^{\theta} \hat{q} d\theta - (\theta - \theta_{\text{ref}}) - 2\pi + \frac{1}{q} \int_{\theta}^{\theta+2\pi} \hat{q} d\theta \\ &= \delta(\psi, \theta) - 2\pi + \frac{1}{q} \int_{\theta}^{\theta+2\pi} \hat{q} d\theta \\ &= \delta(\psi, \theta).\end{aligned}\tag{14.8}$$

]

[In numerical implementation, the term $\int_0^{\theta} \frac{\mathbf{B} \cdot \nabla \phi}{\mathbf{B} \cdot \nabla \theta} d\theta$ appearing in δ is computed by using

$$\begin{aligned}\int_0^{\theta} \frac{\mathbf{B} \cdot \nabla \phi}{\mathbf{B} \cdot \nabla \theta} d\theta &= \int_0^{\theta} \frac{g}{R^2} \frac{\mathcal{J}}{\Psi'} d\theta = \int_0^{\theta} \frac{g}{R^2} \frac{1}{\Psi'} \frac{R}{|\nabla\psi|} dl_p \\ &= \int_0^{\theta} \frac{g}{R} \frac{1}{|\nabla\Psi|} dl_p \\ &= \int_0^{\theta} \frac{1}{R} \frac{B_{\phi}}{B_p} d\ell_p.\end{aligned}\tag{14.9}$$

For later use, from Eq. (14.6), we obtain

$$\frac{\partial(\delta q)}{\partial\psi} = -\frac{d}{d\psi} \left(\frac{g}{\Psi'} \right) \int_0^{\theta} \frac{\mathcal{J}}{R^2} d\theta - \frac{g}{\Psi'} \frac{\partial}{\partial\psi} \int_0^{\theta} \frac{\mathcal{J}}{R^2} d\theta - \frac{dq}{d\psi} \theta.\tag{14.10}$$

This formula is used in GTAW code, where the derivative $\partial(g / \Psi') / \partial\psi$ is calculated numerically by using the central difference scheme.]

14.2 Contravariant form of magnetic field in (ψ, θ, ζ) coordinates

Recall that the contravariant form of the magnetic field in (ψ, θ, ϕ) coordinates is given by Eq. (10.84), i.e.,

$$\mathbf{B} = -\Psi'(\nabla\phi \times \nabla\psi + \hat{q}\nabla\psi \times \nabla\theta). \quad (14.11)$$

Next, let us derive the corresponding form in (ψ, θ, ζ) coordinates. Using the definition of ζ , equation (14.11) is written as

$$\begin{aligned} \mathbf{B} &= -\Psi'\nabla(\zeta + q\delta) \times \nabla\psi - \Psi'\hat{q}\nabla\psi \times \nabla\theta \\ &= -\Psi'\nabla\zeta \times \nabla\psi - \Psi'\nabla(q\delta) \times \nabla\psi - \Psi'\hat{q}\nabla\psi \times \nabla\theta \\ &= -\Psi'\nabla\zeta \times \nabla\psi - \Psi'q\frac{\partial\delta}{\partial\theta}\nabla\theta \times \nabla\psi - \Psi'\hat{q}\nabla\psi \times \nabla\theta \end{aligned} \quad (14.12)$$

Using Eq. (14.4), the above equation is simplified as

$$\mathbf{B} = -\Psi'(\nabla\zeta \times \nabla\psi + q\nabla\psi \times \nabla\theta). \quad (14.13)$$

Equation (14.13) is the contravariant form of the magnetic field in (ψ, θ, ζ) coordinates.

The expression of the magnetic field in Eq. (14.13) can be rewritten in terms of the flux function Ψ_p and Ψ_t discussed in Sec. (). Equation (14.13) is

$$\mathbf{B} = \nabla\Psi \times \nabla\zeta + q\nabla\theta \times \nabla\Psi, \quad (14.14)$$

which, by using Eq. (), i.e., $\nabla\Psi = \nabla\Psi_p/(2\pi)$, is rewritten as

$$\mathbf{B} = \frac{1}{2\pi}(\nabla\zeta \times \nabla\Psi_p + q\nabla\Psi_p \times \nabla\theta), \quad (14.15)$$

which, by using Eq. (), i.e., $q = d\Psi_t/d\Psi_p$, is further written as

$$\mathbf{B} = \frac{1}{2\pi}(\nabla\zeta \times \nabla\Psi_p + \nabla\Psi_t \times \nabla\theta). \quad (14.16)$$

14.3 Relation between the partial derivatives in (ψ, θ, ϕ) and (ψ, θ, ζ) coordinates

Noting the simple fact that

$$\frac{d}{dx} = \frac{d}{d(x+c)}, \quad (14.17)$$

where c is a constant, we conclude that

$$\left(\frac{\partial f}{\partial \zeta}\right)_{\psi, \theta} = \left(\frac{\partial f}{\partial \phi}\right)_{\psi, \theta}, \quad (14.18)$$

(since $\phi = \zeta + q(\psi)\delta(\psi, \theta)$, where the part $q(\psi)\delta(\psi, \theta)$ acts as a constant when we hold ψ and θ constant), i.e., the symmetry property with respect to the new toroidal angle ζ is identical with the one with respect to the old toroidal angle ϕ . On the other hand, generally,

$$\left(\frac{\partial f}{\partial \psi}\right)_{\theta, \zeta} \neq \left(\frac{\partial f}{\partial \psi}\right)_{\theta, \phi} \quad (14.19)$$

and

$$\left(\frac{\partial f}{\partial \theta}\right)_{\psi, \zeta} \neq \left(\frac{\partial f}{\partial \theta}\right)_{\psi, \phi}. \quad (14.20)$$

In the special case that f is axisymmetric (i.e., f is independent of ϕ in (ψ, θ, ϕ) coordinates), then two sides of Eqs. (14.19) and (14.20) are equal to each other. Note that the partial derivatives $\partial/\partial\psi$ and $\partial/\partial\theta$ in Sec. 14.1 and 14.2 are taken in (ψ, θ, ϕ) coordinates. Because the quantities involved in Sec. 14.1 and 14.2 are axisymmetric, these partial derivatives are equal to their counterparts in (ψ, θ, ζ) coordinates.

14.4 Steps to construct a straight-line magnetic coordinate system

In Sec. 11, we have provided the steps to construct the magnetic surface coordinate system (ψ, θ, ϕ) . Only one additional step is needed to construct the straight-line flux coordinate system (ψ, θ, ζ) . The additional step is to calculate the generalized toroidal angle ζ according to Eq. (14.1), where δ is obtained from Eq. (14.6). Also note that the Jacobian of (ψ, θ, ζ) coordinates happens to be equal to that of (ψ, θ, ϕ) coordinates.

14.5 Form of operator $\mathbf{B} \cdot \nabla$ in (ψ, θ, ζ) coordinates

The usefulness of the contravariant form [Eq. (14.13)] of the magnetic field lies in that it allows a simple form of $\mathbf{B} \cdot \nabla$ operator in a coordinate system. (The operator $\mathbf{B}_0 \cdot \nabla$ is usually called magnetic differential operator.) In (ψ, θ, ζ) coordinate system, by using the contravariant form Eq. (14.13), the operator is written as

$$\begin{aligned} \mathbf{B} \cdot \nabla f &= -\Psi'(\nabla \zeta \times \nabla \psi) \cdot \nabla f(\psi, \theta, \zeta) - \Psi'q(\nabla \psi \times \nabla \theta) \cdot \nabla f(\psi, \theta, \zeta) \\ &= -\Psi' \mathcal{J}^{-1} \left(\frac{\partial}{\partial \theta} + q \frac{\partial}{\partial \zeta} \right) f. \end{aligned} \quad (14.21)$$

Next, consider the solution of the following magnetic differential equation:

$$\mathbf{B} \cdot \nabla f = h. \quad (14.22)$$

where $h = h(\psi, \theta, \zeta)$ is some known function. Using Eq. (14.21), the magnetic differential equation is written as

$$\left(\frac{\partial}{\partial \theta} + q(\psi) \frac{\partial}{\partial \zeta} \right) f = -\frac{1}{\Psi'} \mathcal{J} h(\psi, \theta, \zeta). \quad (14.23)$$

Note that the coefficients before the two partial derivatives of the above equation are all independent of θ and ζ . This indicates that different Fourier harmonics in θ and ζ are decoupled. As a result of this fact, if f is Fourier expanded as

$$f(\psi, \theta, \zeta) = \sum_{m,n} f_{mn}(\psi) e^{i(m\theta - n\zeta)}, \quad (14.24)$$

(note that, following the convention adopted in tokamak literature[10], the Fourier harmonics are chosen to be $e^{i(m\theta - n\zeta)}$, instead of $e^{i(m\theta + n\zeta)}$), and the right-hand side is expanded as

$$-\frac{1}{\Psi'} \mathcal{H}(\psi, \theta, \zeta) = \sum_{m,n} \gamma_{mn}(\psi) e^{i(m\theta - n\zeta)}, \quad (14.25)$$

then Eq. (14.23) can be readily solved to give

$$f_{mn} = \frac{\gamma_{mn}}{i[m - nq]}. \quad (14.26)$$

The usefulness of the straight line magnetic coordinates (ψ, θ, ζ) lies in that, as mentioned previously, it makes the coefficients before the two partial derivatives both independent of θ and ζ , thus, allowing a simple solution to the magnetic differential equation.

14.6 Resonant surface of a perturbation

Equation (14.26) indicates that, for the differential equation (14.22), there is a resonant response to a perturbation $e^{i(m\theta - n\zeta)}$ on a magnetic surface with $m - nq = 0$. Therefore, the magnetic surface with $q = m/n$ is called the “resonant surface” for the perturbation $e^{i(m\theta - n\zeta)}$.

The phase change of the perturbation $e^{i(m\theta - n\zeta)}$ along a magnetic field is given by $m\Delta\theta - n\Delta\zeta$, which can be written as $\Delta\theta(m - nq)$. Since $m - nq = 0$ on a resonant surface, this indicates that there is no phase change along a magnetic field line on a resonant surface, i.e., the parallel wavenumber k_{\parallel} is zero on a resonant surface.

14.7 Helical angle used in tearing mode theory

Next, we discuss a special poloidal angle, which is useful in describing a perturbation of single harmonic (m, n) . This poloidal angle is defined by

$$\chi = \theta - \frac{n}{m}\zeta, \quad (14.27)$$

where (m, n) are the mode numbers of the perturbation. The poloidal angle χ is often called helical angle and is special in that its definition is associated with a perturbation (the mode numbers of the perturbation appear in the definition) while the definition of the poloidal angles discussed previously only involve the equilibrium quantities.

The poloidal angle χ is designed to make 3D perturbations of the form $\sim f(\psi, m\theta - n\zeta)$ reduce to 2D perturbations, i.e.,

$$\left. \frac{\partial f}{\partial \zeta} \right|_{\psi, \chi} = 0. \quad (14.28)$$

It is ready to verify that the Jacobian of coordinates (ψ, χ, ζ) is equal to that of coordinates (ψ, θ, ζ) [proof: $(\mathcal{J}')^{-1} = \nabla\psi \times \nabla\chi \cdot \nabla\zeta = \nabla\psi \times \nabla(\theta - n\zeta/m) \cdot \nabla\zeta = \nabla\psi \times \nabla\theta \cdot \nabla\zeta = \mathcal{J}^{-1}$].

The component of \mathbf{B} along $\nabla\chi$ direction (i.e., the covariant component) is written

$$\begin{aligned} B^{(\chi)} &\equiv \mathbf{B} \cdot \nabla\chi \\ &= -\Psi'(\nabla\zeta \times \nabla\psi + q\nabla\psi \times \nabla\theta) \cdot \nabla(\theta - n\zeta/m) \\ &= -\Psi'(\nabla\zeta \times \nabla\psi \cdot \nabla\theta) + \Psi' \frac{n}{m} (q\nabla\psi \times \nabla\theta \cdot \nabla\zeta) \\ &= -\Psi' \mathcal{J}^{-1} + \Psi' \frac{n}{m} q \mathcal{J}^{-1} \\ &= \Psi' \mathcal{J}^{-1} \left(\frac{nq}{m} - 1 \right). \end{aligned} \quad (14.29)$$

At the resonant surface $q = m/n$, equation (14.29) implies $B^{(\chi)} = 0$. The direction $\nabla\chi$ defines the reconnecting component of the magnetic field?

On the other hand, the component of \mathbf{B} along $\nabla\theta$ direction is written

$$\begin{aligned} B^{(\theta)} &\equiv \mathbf{B} \cdot \nabla\theta \\ &= -\Psi'(\nabla\zeta \times \nabla\psi + q\nabla\psi \times \nabla\theta) \cdot \nabla\theta \\ &= -\Psi' \nabla\zeta \times \nabla\psi \cdot \nabla\theta \\ &= -\Psi' \mathcal{J}^{-1}. \end{aligned} \quad (14.30)$$

Using (14.30) and (14.29), the relation between $B^{(\theta)}$ and $B^{(\chi)}$ is written as

$$B^{(\chi)} = B^{(\theta)} \left(1 - \frac{nq}{m} \right). \quad (14.31)$$

14.8 Covariant form of magnetic field in (ψ, θ, ζ) coordinate system

In the above, we have obtained the covariant form of the magnetic field in (ψ, θ, ϕ) coordinates (i.e., Eq. (10.81)). Next, we derive the corresponding form in $(\psi,$

θ, ζ) coordinate. In order to do this, we need to express the $\nabla\phi$ basis vector in terms of $\nabla\psi$, $\nabla\theta$, and $\nabla\zeta$ basis vectors. Using the definition of the generalized toroidal angle, we obtain

$$\begin{aligned}
g\nabla\phi &= g\nabla(\zeta + q\delta) \\
&= g\nabla\zeta + gq\nabla\delta + g\delta\nabla q \\
&= g\nabla\zeta + gq\left(\frac{\partial\delta}{\partial\psi}\nabla\psi + \frac{\partial\delta}{\partial\theta}\nabla\theta\right) + g\delta q'\nabla\psi \\
&= \left(gq\frac{\partial\delta}{\partial\psi} + g\delta q'\right)\nabla\psi + gq\frac{\partial\delta}{\partial\theta}\nabla\theta + g\nabla\zeta \\
&= g\frac{\partial(q\delta)}{\partial\psi}\nabla\psi + gq\frac{\partial\delta}{\partial\theta}\nabla\theta + g\nabla\zeta.
\end{aligned} \tag{14.32}$$

Using Eq. (14.32), the covariant form of the magnetic field, Eq. (10.81), is written as

$$\mathbf{B} = \left(\Psi' \frac{\mathcal{J}}{R^2} \nabla\psi \cdot \nabla\theta + g \frac{\partial(q\delta)}{\partial\psi}\right) \nabla\psi + \left(gq \frac{\partial\delta}{\partial\theta} - \Psi' \frac{\mathcal{J}}{R^2} |\nabla\psi|^2\right) \nabla\theta + g\nabla\zeta. \tag{14.33}$$

This expression can be further simplified by using equation (14.4) to eliminate $\partial\delta/\partial\theta$, which gives

$$\begin{aligned}
\mathbf{B} &= \left(\Psi' \frac{\mathcal{J}}{R^2} \nabla\psi \cdot \nabla\theta + g \frac{\partial(q\delta)}{\partial\psi}\right) \nabla\psi + \left(-\frac{g^2}{\Psi'} - gq \frac{R^2}{\mathcal{J}} - \Psi' |\nabla\psi|^2\right) \frac{\mathcal{J}}{R^2} \nabla\theta + g\nabla\zeta \\
&= \left(\Psi' \frac{\mathcal{J}}{R^2} \nabla\psi \cdot \nabla\theta + g \frac{\partial(q\delta)}{\partial\psi}\right) \nabla\psi + \left(-\frac{g^2 + |\nabla\Psi|^2}{\Psi'} - gq \frac{R^2}{\mathcal{J}}\right) \frac{\mathcal{J}}{R^2} \nabla\theta + g\nabla\zeta.
\end{aligned} \tag{14.34}$$

Using $B^2 = (|\nabla\Psi|^2 + g^2)/R^2$, the above equation is written as

$$\begin{aligned}
\mathbf{B} &= \left(\Psi' \frac{\mathcal{J}}{R^2} \nabla\psi \cdot \nabla\theta + g \frac{\partial(q\delta)}{\partial\psi}\right) \nabla\psi + \left(-\frac{B^2 R^2}{\Psi'} - gq \frac{R^2}{\mathcal{J}}\right) \frac{\mathcal{J}}{R^2} \nabla\theta + g\nabla\zeta \\
&= \left(\Psi' \frac{\mathcal{J}}{R^2} \nabla\psi \cdot \nabla\theta + g \frac{\partial(q\delta)}{\partial\psi}\right) \nabla\psi + \left(-\frac{B^2}{\Psi'} \mathcal{J} - gq\right) \nabla\theta + g\nabla\zeta.
\end{aligned} \tag{14.35}$$

Equation (14.35) is the covariant form of the magnetic field in (ψ, θ, ζ) coordinate system. For the particular choice of the radial coordinate $\psi = -\Psi$ and the Jacobian $\mathcal{J} = h(\psi)/B^2$ (i.e., Boozer's Jacobian, discussed in Sec. 14.9), equation (14.35) reduces to

$$\mathbf{B} = \left(-\frac{\mathcal{J}}{R^2} \nabla\psi \cdot \nabla\theta + g \frac{\partial(q\delta)}{\partial\psi}\right) \nabla\psi + I(\psi) \nabla\theta + g(\psi) \nabla\zeta, \tag{14.36}$$

with $I(\psi) = h(\psi) - gq$. The magnetic field expression in Eq. (14.36) frequently appears in tokamak literature[30]. In this form, the coefficients before both $\nabla\theta$ and $\nabla\zeta$ depends on only the radial coordinate. In terms of $I(\psi)$, the Jacobian can also be written as

$$\mathcal{J} = \frac{gq + I}{B^2}. \quad (14.37)$$

14.9 Form of operator $(\mathbf{B} \times \nabla\psi / B^2) \cdot \nabla$ in (ψ, θ, ζ) coordinates

In solving the MHD eigenmode equations in toroidal geometries, besides the $\mathbf{B} \cdot \nabla$ operator, we will also encounter another surface operator $(\mathbf{B} \times \nabla\psi / B^2) \cdot \nabla$. Next, we derive the form of this operator in (ψ, θ, ζ) coordinate system. Using the covariant form of the equilibrium magnetic field [Eq. (14.35)], we obtain

$$\frac{\mathbf{B} \times \nabla\psi}{B^2} = \frac{1}{B^2} \left(-\frac{B^2}{\Psi'} \mathcal{J} - gq \right) \nabla\theta \times \nabla\psi + \frac{g}{B^2} \nabla\zeta \times \nabla\psi. \quad (14.38)$$

Using this, the $(\mathbf{B} \times \nabla\psi / B^2) \cdot \nabla$ operator is written as

$$\frac{\mathbf{B} \times \nabla\psi}{B^2} \cdot \nabla = \frac{1}{B^2} \left(\frac{B^2}{\Psi'} \mathcal{J} + gq \right) \mathcal{J}^{-1} \frac{\partial}{\partial\zeta} + \frac{g}{B^2} \mathcal{J}^{-1} \frac{\partial}{\partial\theta} \quad (14.39)$$

$$= \left(\frac{1}{\Psi'} + g \frac{\mathcal{J}^{-1}}{B^2} q \right) \frac{\partial}{\partial\zeta} + g \frac{\mathcal{J}^{-1}}{B^2} \frac{\partial}{\partial\theta}, \quad (14.40)$$

which is the form of the operator in (ψ, θ, ζ) coordinate system.

Examining Eq. (14.40), we find that the coefficients before the two partial derivatives will be independent of θ and ζ if the Jacobian \mathcal{J} is chosen to be of the form $\mathcal{J} = h(\psi) / B^2$, where h is some magnetic surface function. It is obvious that the independence of the coefficients on θ and ζ will be advantageous to some applications. The coordinate system (ψ, θ, ζ) with the particular choice of $\mathcal{J} = h(\psi) / B^2$ is called the Boozer coordinates. The usefulness of the new toroidal angle ζ is highlighted in Boozer's choice of the Jacobian, which makes both $\mathbf{B} \cdot \nabla$ and $(\mathbf{B} \times \nabla\psi / B^2) \cdot \nabla$ be a constant-coefficient differential operator. For other choices of the Jacobian, only the $\mathbf{B} \cdot \nabla$ operator is a constant-coefficient differential operator.

14.10 Radial differential operator

In solving the MHD eigenmode equations in toroidal geometry, we also need the radial differential operator $\nabla\psi \cdot \nabla$. Next, we derive the form of the operator in (ψ, θ, ζ) coordinates. Using

$$\nabla f = \frac{\partial f}{\partial\psi} \nabla\psi + \frac{\partial f}{\partial\theta} \nabla\theta + \frac{\partial f}{\partial\zeta} \nabla\zeta,$$

the radial differential operator is written as

$$\begin{aligned}
\nabla\psi \cdot \nabla f &= |\nabla\psi|^2 \frac{\partial f}{\partial\psi} + (\nabla\theta \cdot \nabla\psi) \frac{\partial f}{\partial\theta} + (\nabla\zeta \cdot \nabla\psi) \frac{\partial f}{\partial\zeta} \\
&= |\nabla\psi|^2 \frac{\partial f}{\partial\psi} + (\nabla\theta \cdot \nabla\psi) \frac{\partial f}{\partial\theta} + \{\nabla[\phi - q\delta(\psi, \theta)] \cdot \nabla\psi\} \frac{\partial f}{\partial\zeta} \\
&= |\nabla\psi|^2 \frac{\partial f}{\partial\psi} + (\nabla\theta \cdot \nabla\psi) \frac{\partial f}{\partial\theta} - \nabla[q\delta] \cdot \nabla\psi \frac{\partial f}{\partial\zeta} \\
&= |\nabla\psi|^2 \frac{\partial f}{\partial\psi} + (\nabla\theta \cdot \nabla\psi) \frac{\partial f}{\partial\theta} - [q\nabla\delta + \delta\nabla q] \cdot \nabla\psi \frac{\partial f}{\partial\zeta} \\
&= |\nabla\psi|^2 \frac{\partial f}{\partial\psi} + (\nabla\theta \cdot \nabla\psi) \frac{\partial f}{\partial\theta} - \left[q \left(\frac{\partial\delta}{\partial\psi} \nabla\psi + \frac{\partial\delta}{\partial\theta} \nabla\theta \right) + \delta q' \nabla\psi \right] \cdot \nabla\psi \frac{\partial f}{\partial\zeta} \\
&= |\nabla\psi|^2 \frac{\partial f}{\partial\psi} + (\nabla\theta \cdot \nabla\psi) \frac{\partial f}{\partial\theta} - \left[\frac{\partial(q\delta)}{\partial\psi} |\nabla\psi|^2 + q \frac{\partial\delta}{\partial\theta} \nabla\theta \cdot \nabla\psi \right] \frac{\partial f}{\partial\zeta},
\end{aligned} \tag{14.41}$$

where $\partial(q\delta)/\partial\psi$ and $q\partial\delta/\partial\theta$ are given respectively by Eqs. (14.10) and (14.4). Using the above formula, $\nabla\psi \cdot \nabla\zeta$ is written as

$$\nabla\psi \cdot \nabla\zeta = - \left[\frac{\partial(q\delta)}{\partial\psi} |\nabla\psi|^2 + q \frac{\partial\delta}{\partial\theta} \nabla\theta \cdot \nabla\psi \right]. \tag{14.42}$$

This formula is used in GTAW code.

15 Field-line-following coordinates

15.1 Definition

In (ψ, θ, ζ) coordinates, a magnetic field line is straight in (θ, ζ) plane with the slope being q . So the equation for magnetic field lines is given by $\zeta = q\theta + \alpha$, where α is a constant in (θ, ζ) plane. Note that α can be used to label different magnetic field lines on a magnetic surface. This motivates us to use α , i.e.,

$$\alpha \equiv \zeta - q\theta, \tag{15.1}$$

to as a new coordinate to replace ζ . Then we obtain a new set of coordinate: (ψ, θ, α) , which are called field-line-following coordinates. Using Eqs. (15.1) and (14.7), α can be written as

$$\alpha = \phi - \int_0^\theta \hat{q} d\theta, \tag{15.2}$$

where $\hat{q} = \mathbf{B} \cdot \nabla \phi / \mathbf{B} \cdot \nabla \theta$ is the local safety factor. (If we choose the straight-field-line θ , then α is written as $\alpha = \phi - q\theta$.) Define $\bar{\delta} = \int_0^\theta \hat{q} d\theta$, which is called `tor_shift` in TEK code, then $\alpha = \phi - \bar{\delta}$.

In TEK, I choose $\theta \in [-\pi, \pi)$ with $\theta = \pm\pi$ corresponding to the high-field-side midplane, and θ is increasing along the counter-clockwise direction when viewed along $\nabla \phi$. There are two reasons why θ is chosen this way: 1. The toroidal shift $\bar{\delta}$ remain small near the low-field-side $\theta = 0$. This may be good for spatial resolution in this important region where ballooning modes often have larger amplitude. 2. The θ cut, i.e., $\theta = \pm\pi$, is far away from the important low-field-side. The gyrokinetic field equations are not solved at $\theta = +\pi$. Perturbations there need to be obtained by using interpolations at the θ cut, i.e., infer values of perturbations on α gridpoints at $\theta = +\pi$ from the corresponding values at $\theta = -\pi$. Numerical errors more likely appear there. So we prefer that the θ cut is located in less important area (area where mode amplitude is small).

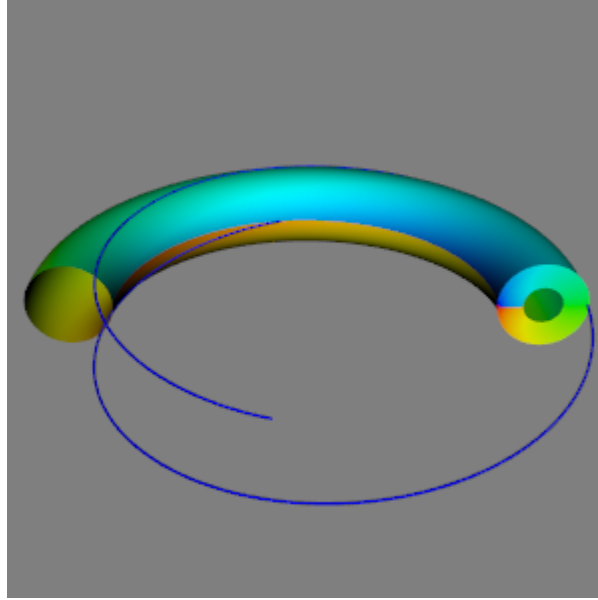


Figure 15.1. Values (color) of α on a magnetic surface and a poloidal plane ($\phi = 0$ plane). A field line on the surface is also plotted, which passes the point $(\phi = 0, \theta = 0)$, with one half going along the positive θ direction to reach $\theta = +\pi$ and another half going along negative θ direction to reach $\theta = -\pi$. The values of α plotted here is for the $0 < \phi < \pi$.

This field line is on a $q = 1.5$ surface, so it travels 1.5 toroidal loops when it finishes one poloidal loop.

Why does the value of α along the field line shown above seem not constant? This is because the $\theta < 0$ half of the field line belongs to a different branch ($\phi < 0$ branch) from the branch shown here ($\phi > 0$ branch).

15.2 Properties of field-line-following coordinates

In (ψ, θ, α) coordinates, the magnetic field in Eq. (14.13) is written as

$$\mathbf{B} = \Psi' \nabla \psi \times \nabla \alpha, \quad (15.3)$$

which is called the Clebsch form. The direction

$$\frac{\partial \mathbf{r}}{\partial \theta}|_{\psi, \alpha} = \mathcal{J} \nabla \alpha \times \nabla \psi, \quad (15.4)$$

is parallel (or anti-parallel) to the magnetic field direction. Due to this fact, (ψ, θ, α) coordinates are usually called “field-line-following coordinates” or “field-aligned coordinates” [2, 6].

Equation (15.3) implies that

$$\mathbf{B} \cdot \nabla \alpha = 0, \quad (15.5)$$

and

$$\mathbf{B} \cdot \nabla \psi = 0, \quad (15.6)$$

i.e., both α and ψ are constant along a magnetic field line. Taking scalar product of Eq. (15.3) with $\nabla \theta$, we obtain

$$\mathbf{B} \cdot \nabla \theta = -\frac{\Psi'}{\mathcal{J}}, \quad (15.7)$$

which is nonzero, i.e., only θ among (ψ, θ, α) is changing along a magnetic field line. (Here $\mathcal{J} = (\nabla \psi \times \nabla \theta \cdot \nabla \alpha)^{-1}$ is the Jacobian of the coordinate system (ψ, θ, α) , which happens to be equal to the Jacobian of (ψ, θ, ζ) coordinates.)

Using Eq. (15.3), the magnetic differential operator $\mathbf{B} \cdot \nabla$ in the new coordinate system (ψ, θ, α) is written

$$\mathbf{B} \cdot \nabla f = -\frac{\Psi'}{\mathcal{J}} \frac{\partial}{\partial \theta} f, \quad (15.8)$$

which is just a partial derivative over θ , as is expected, since only θ is changing along a magnetic field line.

By the way, note that $(\mathbf{B} \cdot \nabla \alpha) / (\mathbf{B} \cdot \nabla \theta) = 0$, i.e., the magnetic field lines are

straight with zero slope on (θ, α) plane.

15.3 Some discussions

The fact $\mathbf{B} \cdot \nabla \alpha = 0$ implies that α is constant along a magnetic field line. At first glance, a magnetic line on an irrational surface seems to sample all the points on the surface. This seems to indicate that α is a constant on irrational surfaces. However, α must be varying so that it can provide a suitable toroidal coordinate. I had once been confused by this conflict for a long time. The key point to resolve this confusion is to realize that it is wrong to say there is only one magnetic line on an irrational surface, i.e. it is wrong to say a magnetic line on an irrational surface samples all the points on the surface. There are still infinite number of magnetic field lines that can not be connected with each other on an irrational surface. Then the fact $\mathbf{B} \cdot \nabla \alpha = 0$ does not imply that α must be the same on these different magnetic field lines. In fact, although $\mathbf{B} \cdot \nabla \alpha = 0$, the gradient of α on a flux-surface along the perpendicular direction is nonzero, i.e., $\frac{\mathbf{B} \times \nabla \Psi}{|\mathbf{B} \times \nabla \Psi|} \cdot \nabla \alpha \neq 0$. [Proof:

$$\begin{aligned} \frac{\mathbf{B} \times \nabla \Psi}{|\mathbf{B} \times \nabla \Psi|} \cdot \nabla \alpha &= \frac{\nabla \Psi \times \nabla \alpha \cdot \mathbf{B}}{|\mathbf{B} \times \nabla \Psi|} \\ &= \frac{B^2}{|\mathbf{B} \times \nabla \Psi|} \end{aligned} \quad (15.9)$$

$$= \frac{B}{|\nabla \Psi|}, \quad (15.10)$$

which is obviously nonzero.] This indicates that α is not constant on a flux-surface. Equation (15.10) also indicates that the perpendicular gradient becomes infinity at points where $\nabla \Psi = 0$ (i.e., X-points).

In (ψ, θ, ϕ) coordinates, $\nabla \phi$ is perpendicular to $\nabla \psi$. However, in field-line-following coordinates (ψ, θ, α) , $\nabla \alpha$ is not perpendicular to $\nabla \psi$. Therefore $\nabla \alpha$ is not along the binormal direction $\mathbf{B} \times \nabla \psi$.

It is widely believed that turbulence responsible for energy transport in tokamak plasmas usually has $k_{\parallel} \ll k_{\perp}$, where k_{\parallel} and k_{\perp} are the parallel and perpendicular wavenumbers, respectively. Due to this elongated structure along the parallel direction, less grids can be used in the parallel direction than that in the perpendicular direction in turbulence simulation. In this case, the field-aligned coordinates (ψ, θ, α) provide suitable coordinates to be used, where less gridpoints can be used for θ coordinate in simulations and even some $\partial / \partial \theta$ derivatives can be neglected (high-n approximation), which simplifies the equations that need to be solved. There is another reason why almost all gyrokinetic codes use field-aligned coordinates: the stability of numerical algorithms is improved when we use coarse grids in the parallel direction because the parallel Courant condition (for explicit schemes) $\Delta t \leq \Delta L_{\parallel} / v_{\parallel}$ can be more easily satisfied (especially for the cases with kinetic electrons), where ΔL_{\parallel} is the parallel grid spacing, which is larger when coarse grids are used in the parallel

direction. This is also mentioned in Ref. [23] and it seems right from my experiences of testing several algorithms. This can also be understood in the following way: the coarse parallel grid automatically filters out physically irrelevant but numerically problematic high- k_{\parallel} modes, permitting much longer time steps for explicit time stepping, in both particle and fluid codes[12].

15.4 Expression of $\nabla\alpha$, $\nabla\psi \cdot \nabla\alpha$, and $\nabla\alpha \cdot \nabla\theta$

The generalized toroidal angle α is defined by Eq. (15.2), i.e., $\alpha = \phi - \bar{\delta}$, where $\bar{\delta} = \int_0^{\theta} \hat{q} d\theta$. The gradient of α is then written as

$$\begin{aligned}\nabla\alpha &= \nabla\phi - \nabla\bar{\delta} \\ &= \frac{\hat{\phi}}{R} - \frac{\partial\bar{\delta}}{\partial\psi}\nabla\psi - \frac{\partial\bar{\delta}}{\partial\theta}\nabla\theta.\end{aligned}\quad (15.11)$$

Then

$$\nabla\psi \cdot \nabla\alpha = -\frac{\partial\bar{\delta}}{\partial\psi}|\nabla\psi|^2 - \frac{\partial\bar{\delta}}{\partial\theta}\nabla\psi \cdot \nabla\theta \quad (15.12)$$

$$\nabla\alpha \cdot \nabla\theta = -\frac{\partial\bar{\delta}}{\partial\psi}\nabla\psi \cdot \nabla\theta - \frac{\partial\bar{\delta}}{\partial\theta}|\nabla\theta|^2 \quad (15.13)$$

Another method of computing the above quantities: Using Eqs. (11.10) and (11.11), expression (15.11) is written as

$$\begin{aligned}\nabla\alpha &= \frac{\hat{\phi}}{R} + \frac{\partial\bar{\delta}}{\partial\psi}\frac{R}{\mathcal{J}}(Z_{\theta}\hat{\mathbf{R}} - R_{\theta}\hat{\mathbf{Z}}) - \frac{\partial\bar{\delta}}{\partial\theta}\frac{R}{\mathcal{J}}(Z_{\psi}\hat{\mathbf{R}} - R_{\psi}\hat{\mathbf{Z}}) \\ &= \frac{\hat{\phi}}{R} + \left(\frac{\partial\bar{\delta}}{\partial\psi}\frac{R}{\mathcal{J}}Z_{\theta} - \frac{\partial\bar{\delta}}{\partial\theta}\frac{R}{\mathcal{J}}Z_{\psi}\right)\hat{\mathbf{R}} + \left(\frac{\partial\bar{\delta}}{\partial\theta}\frac{R}{\mathcal{J}}R_{\psi} - \frac{\partial\bar{\delta}}{\partial\psi}\frac{R}{\mathcal{J}}R_{\theta}\right)\hat{\mathbf{Z}}.\end{aligned}\quad (15.14)$$

(Note that $\partial\bar{\delta}/\partial\psi$ is discontinuous across the θ cut.) Then

$$\begin{aligned}\nabla\psi \cdot \nabla\alpha &= \left(-\frac{R}{\mathcal{J}}Z_{\theta}\hat{\mathbf{R}} + \frac{R}{\mathcal{J}}R_{\theta}\hat{\mathbf{Z}}\right) \cdot \left[\frac{\hat{\phi}}{R} + \left(\frac{\partial\bar{\delta}}{\partial\psi}\frac{R}{\mathcal{J}}Z_{\theta} - \frac{\partial\bar{\delta}}{\partial\theta}\frac{R}{\mathcal{J}}Z_{\psi}\right)\hat{\mathbf{R}} + \left(\frac{\partial\bar{\delta}}{\partial\theta}\frac{R}{\mathcal{J}}R_{\psi} - \frac{\partial\bar{\delta}}{\partial\psi}\frac{R}{\mathcal{J}}R_{\theta}\right)\hat{\mathbf{Z}}\right] \\ &= -\frac{R}{\mathcal{J}}Z_{\theta}\left(\frac{\partial\bar{\delta}}{\partial\psi}\frac{R}{\mathcal{J}}Z_{\theta} - \frac{\partial\bar{\delta}}{\partial\theta}\frac{R}{\mathcal{J}}Z_{\psi}\right) + \frac{R}{\mathcal{J}}R_{\theta}\left(\frac{\partial\bar{\delta}}{\partial\theta}\frac{R}{\mathcal{J}}R_{\psi} - \frac{\partial\bar{\delta}}{\partial\psi}\frac{R}{\mathcal{J}}R_{\theta}\right).\end{aligned}\quad (15.15)$$

$$\begin{aligned}\nabla\alpha \cdot \nabla\theta &= \left[\frac{\hat{\phi}}{R} + \left(\frac{\partial\bar{\delta}}{\partial\psi}\frac{R}{\mathcal{J}}Z_{\theta} - \frac{\partial\bar{\delta}}{\partial\theta}\frac{R}{\mathcal{J}}Z_{\psi}\right)\hat{\mathbf{R}} + \left(\frac{\partial\bar{\delta}}{\partial\theta}\frac{R}{\mathcal{J}}R_{\psi} - \frac{\partial\bar{\delta}}{\partial\psi}\frac{R}{\mathcal{J}}R_{\theta}\right)\hat{\mathbf{Z}}\right] \cdot \\ &\quad \left(\frac{R}{\mathcal{J}}Z_{\psi}\hat{\mathbf{R}} - \frac{R}{\mathcal{J}}R_{\psi}\hat{\mathbf{Z}}\right)\end{aligned}$$

$$= \left(\frac{\partial \bar{\delta}}{\partial \psi} \frac{R}{\mathcal{J}} Z_\theta - \frac{\partial \bar{\delta}}{\partial \theta} \frac{R}{\mathcal{J}} Z_\psi \right) \frac{R}{\mathcal{J}} Z_\psi - \left(\frac{\partial \bar{\delta}}{\partial \theta} \frac{R}{\mathcal{J}} R_\psi - \frac{\partial \bar{\delta}}{\partial \psi} \frac{R}{\mathcal{J}} R_\theta \right) \frac{R}{\mathcal{J}} R_\psi. \quad (15.16)$$

The figures below plot the spatial variation of some quantities.

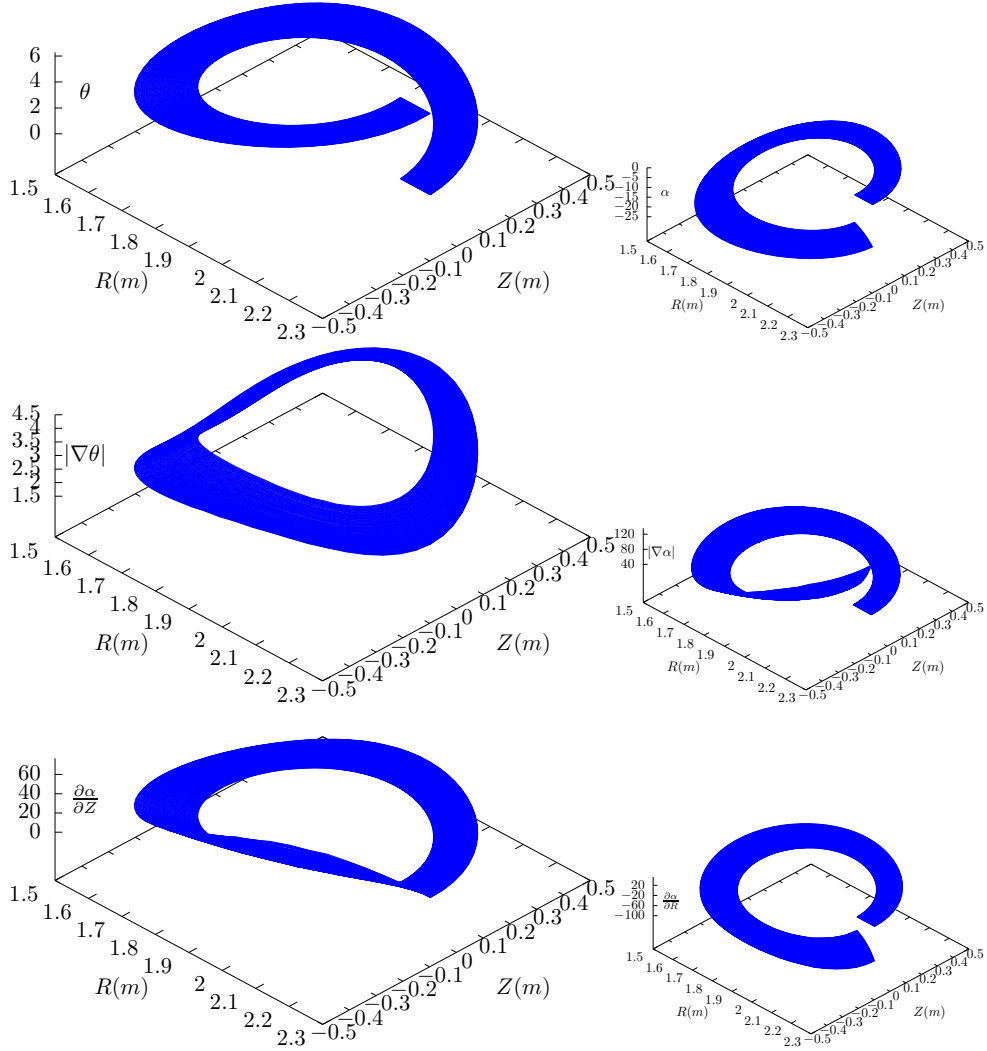


Figure 15.2. The value of θ , α and their gradients on an annulus on the poloidal plane (R, Z) . Note that $\nabla\theta$ is single-valued while $\partial\alpha/\partial R$ and $\nabla\alpha$ are multi-valued and thus there is a jump near the branch cut when a single branch is chosen.

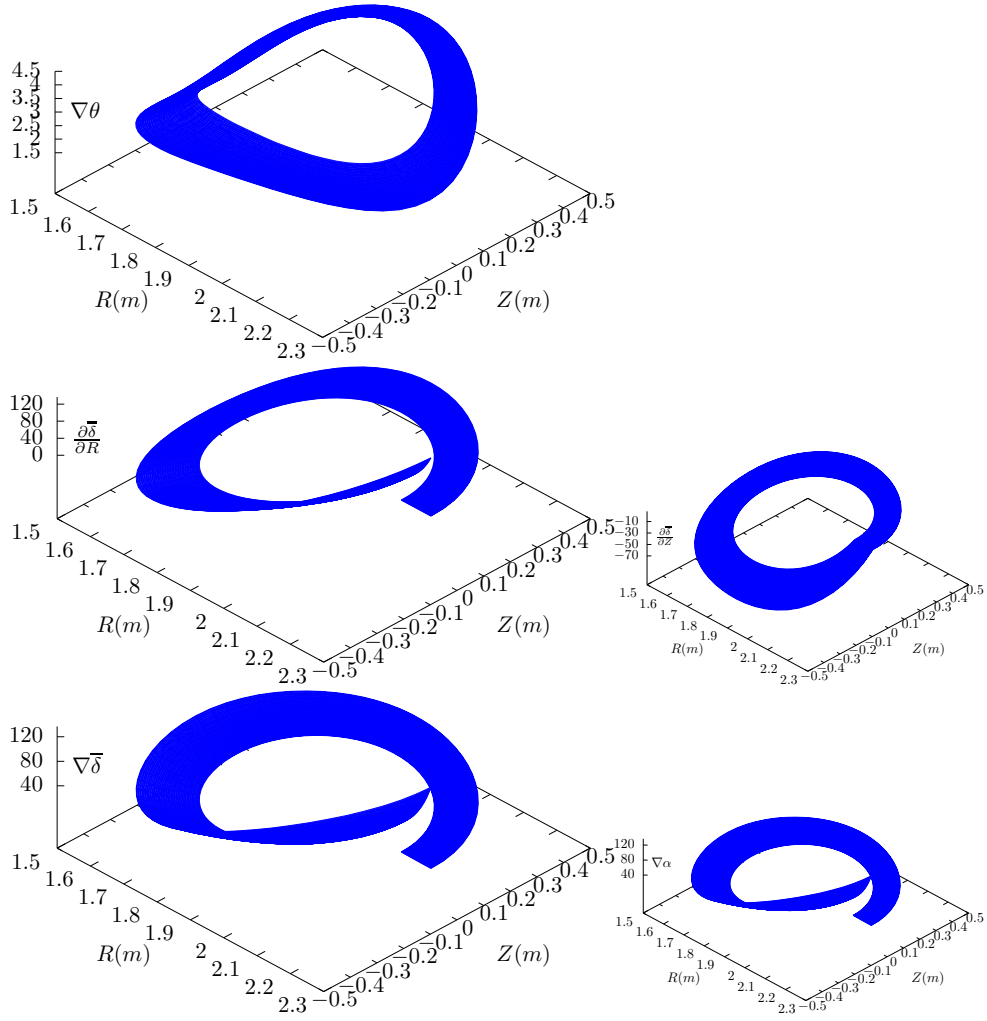


Figure 15.3. The same as Fig. 15.2, but gradients are computed in cylindrical coordinates. The results agrees with those of Fig. 15.2, which provides the confidence in the correctness of the numerical implementation.

15.5 Field-aligned coordinates in GEM[7] and GENE[13] codes

In GEM[7] and GENE[13] codes, the field-aligned coordinates (x, y, z) are

defined by

$$x = r - r_0, \quad (15.17)$$

$$y = \alpha \frac{r_0}{q_0}, \quad (15.18)$$

$$z = \theta q_0 R_0, \quad (15.19)$$

where r is an arbitrary flux surface label with length dimension, which is often chosen in GEM to be the minor radius of a magnetic surface in the midplane. Here r_0 and R_0 are constant quantities of length dimension, r_0 is the minor radius of a reference magnetic surface (usually corresponding to the center of the radial simulation box), R_0 is the major radius of the magnetic axis, q_0 is the safety factor value on the $r = r_0$ surface. The constant length $q_0 R_0$ introduced in the definition of z is to make z approximately correspond to the length along the field line in the large-aspect ratio limit. The constant length r_0/q_0 introduced in the definition of y is to make y corresponds to the arc-length in the poloidal plane traced by a field line when its usual toroidal angle increment $\Delta\phi$ is α . This explanation makes y look like a poloidal coordinate whereas y is actually a toroidal coordinate.

Next, let us calculate the wave number along the y direction, k_y , for a mode with toroidal wave number n . The wavelength along the y direction, λ_y , is given by

$$\lambda_y = \frac{2\pi}{n} \frac{r_0}{q_0}. \quad (15.20)$$

Then the wavenumber k_y is written as

$$k_y = \frac{2\pi}{\lambda_y} = \frac{nq_0}{r_0}. \quad (15.21)$$

On the other hand, the poloidal wavenumber k_θ is given by

$$k_\theta = \frac{2\pi}{\lambda_\theta} \approx \frac{2\pi}{2\pi r_0/m} = \frac{m}{r_0}. \quad (15.22)$$

where m is the poloidal mode number of the mode in (ψ, θ, ϕ) coordinates. If the mode has the property $k_\parallel \approx 0$, i.e., $m \approx nq_0$, then k_θ is equal to the k_y . The motivation of introducing the constant length r_0/q_0 in the definition of y is to make $k_y \approx k_\theta$ for a mode with $k_\parallel \approx 0$.

Some authors call k_y or k_θ by the name “binormal wavenumber”, which is not an appropriate name in my opinion. Some authors call y the binormal direction, which is also an inappropriate name since neither ∇y nor $\partial \mathbf{r} / \partial y$ is along the binormal direction $\mathbf{B}_0 \times \nabla \psi$.

15.6 Visualization of gridpoints in field aligned coordinate system

In this section, I try to visualize gridpoints in the field aligned coordinates. The directions of the covariant basis vectors of (ψ, θ, α) coordinates are as follows:

$$\frac{\partial \mathbf{r}}{\partial \alpha} |_{\psi, \theta} \longrightarrow \text{usual toroidal direction, } \hat{\phi}, \quad (15.23)$$

$$\frac{\partial \mathbf{r}}{\partial \theta} |_{\psi, \alpha} \longrightarrow (\text{parallel or antiparallel to}) \text{ field line direction} \quad (15.24)$$

$$\frac{\partial \mathbf{r}}{\partial \psi} |_{\theta, \alpha} \longrightarrow \text{combination of the usual radial and toroidal direction} \quad (15.25)$$

Here $\partial \mathbf{r} / \partial \psi |_{\theta, \alpha}$ is a combination of the usual radial and toroidal direction, which needs some clarification. Note that, ϕ is related to α by Eq. (15.2), i.e.,

$$\phi = \alpha + \int_0^\theta \frac{\mathbf{B} \cdot \nabla \phi}{\mathbf{B} \cdot \nabla \theta} d\theta \approx \alpha + q(\psi)\theta, \quad (15.26)$$

(where the second equality becomes exact if θ is the straight-field-line poloidal angle defined in Sec. 10.15.5.), which indicates that, for $q'(\psi) \neq 0$ and $\theta \neq 0$, the usual toroidal angle ϕ is changing when changing ψ and holding θ and α fixed. Figure 15.4b shows how the usual toroidal angle ϕ changes when we change ψ

and hold θ and α fixed.

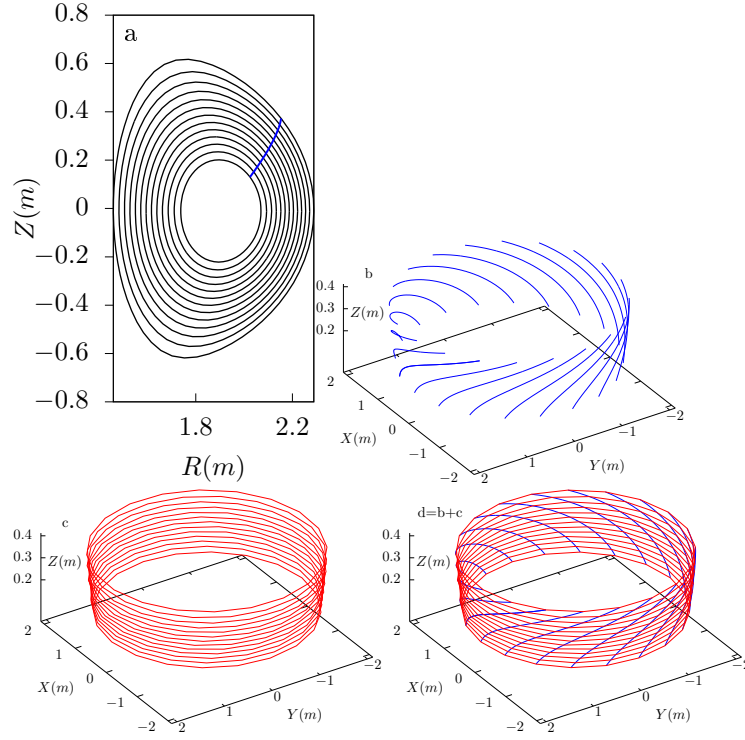


Figure 15.4. (a): A θ contour on $\phi = 0$ plane. Here $\theta = 9 \times 2\pi/63$. This is the direction of $\partial\mathbf{r}/\partial\psi|_{\theta,\phi}$. (b): ψ coordinate lines in (ψ, θ, α) coordinates ($\partial\mathbf{r}/\partial\psi|_{\theta,\alpha}$ are the tangent lines to these curves) on the isosurface of $\theta = 9 \times 2\pi/63$. Here different lines correspond to different values of α . (c): α coordinate lines ($\partial\mathbf{r}/\partial\alpha|_{\psi,\theta}$ are tangent lines to these curves), which are along the usual toroidal direction $\hat{\phi}$. (d): Grid on the isosurface of $\theta = 9 \times 2\pi/63$, where the red lines are α coordinate lines while the blue lines are ψ coordinate lines. Magnetic field from EAST discharge #59954@3.03s.

The relation $\phi \approx \alpha + q(\psi)\theta$ given by Eq. (15.26) indicates that the toroidal shift along $\partial\mathbf{r}/\partial\psi|_{\alpha,\theta}$ for a radial change from ψ_1 to ψ_2 is given by $(q(\psi_2) - q(\psi_1))\theta$, which is larger on θ isosurface with larger value of θ . An example for this is shown in Fig. 15.5 for $\theta = 19 \times 2\pi/63$, where $\partial\mathbf{r}/\partial\psi|_{\alpha,\theta}$ has larger toroidal shift than that in Fig. 15.4 for $\theta = 9 \times 2\pi/63$.

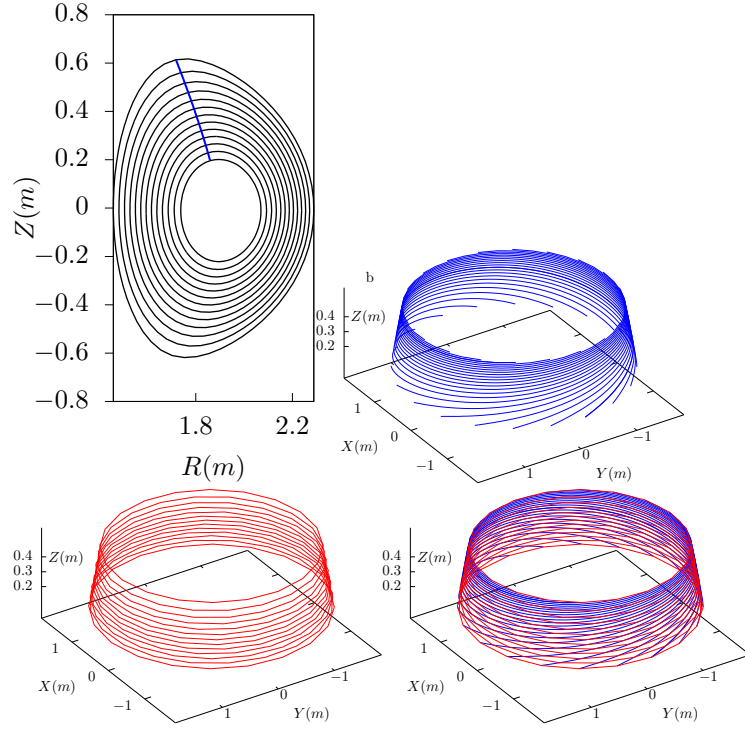


Figure 15.5. (a) $\theta = 19 \times 2\pi/63$ contour on $\phi=0$ plane, (b) $\partial\mathbf{r}/\partial\psi$ curves, (c) $\partial\mathbf{r}/\partial\alpha$ curves on isosurface of $\theta = 19 \times 2\pi/63$. $\partial\mathbf{r}/\partial\alpha$ lines are identical with $\partial\mathbf{r}/\partial\phi$ lines. (d): Grid on the isosurface of $\theta = 19 \times 2\pi/63$, which are the combinations of $\partial\mathbf{r}/\partial\psi$ curves and $\partial\mathbf{r}/\partial\alpha$ curves.

The $\partial\mathbf{r}/\partial\psi|_{\theta,\alpha}$ curves can be understood from another perspective. Examine a family of magnetic field lines that start from $\theta = 0$ and $\phi = \phi_1$ but different radial coordinates. These starting points all have the same value of α , which is equal to ϕ_1 . When following these field lines to another isosurface of θ , the intersecting points of these field lines with the θ isosurface will trace out a $\partial\mathbf{r}/\partial\psi|_{\theta,\alpha}$ line with $\alpha = \phi_1$. Examine another family of magnetic field lines similar to the above but with the starting toroidal angle $\phi = \phi_2$. They will trace out another $\partial\mathbf{r}/\partial\psi|_{\theta,\alpha}$ line (with $\alpha = \phi_2$) on the θ isosurface. Continue the process, we finally get those curves in Fig. 15.4b and Fig. 15.5b.

15.6.1 Radial wavenumber in field-aligned coordinates (ψ, θ, α)

For a harmonic in (ψ, θ, ϕ) coordinates given by $A(\psi, \theta, \phi) = \exp(i k_\psi \psi + i m \theta + i n \phi)$, the radial wave number is k_ψ . Let us calculate the corresponding radial wavenumber k_ψ^* in the new coordinates (ψ, θ, α) , which is defined by

$$k_\psi^* = \left. \frac{\partial \text{phase}}{\partial \psi} \right|_{\theta, \alpha}, \quad (15.27)$$

where the phase is given by $\text{phase} = k_\psi \psi + m\theta + n\phi$. Then the above expression is written as

$$\begin{aligned} k_\psi^* &= \left. \frac{\partial(k_\psi \psi + m\theta + n\phi)}{\partial \psi} \right|_{\theta, \alpha} \\ &= k_\psi + n \left. \frac{\partial \phi}{\partial \psi} \right|_{\theta, \alpha} \end{aligned} \quad (15.28)$$

Using $\phi \approx \alpha + q(\psi)\theta$, the above expression is written as

$$k_\psi^* = k_\psi + n q' \theta, \quad (15.29)$$

where $q' = dq/d\psi$. This result indicates that, compared with the radial wavenumber in coordinate system (ψ, θ, ϕ) , the radial wavenumber in the new coordinate system (ψ, θ, α) has an increment $n\theta q'$. For nonzero magnetic shear ($q' \neq 0$) and nonzero poloidal location ($\theta \neq 0$), the increment $n\theta q'$ can be large for modes with toroidal mode number $n \gg 1$. Then we need to use more radial grid number (compared what is needed in (ψ, θ, ϕ) coordinates) to resolve the radial variation. This is one of disadvantage of using field-aligned coordinates. If the saving associated with using less parallel grid number out-weights the cost associated with using more radial grid number, we obtain a net saving in using the field-aligned coordinates.

Let us examine how many ψ grid points are needed to resolve the ψ dependence in (ψ, θ, α) coordinates on the high-field side ($\theta = \pi$). Assume $k_\psi \approx 0$, then k_ψ^* at $\theta = \pi$ is given by $k_\psi^* = n\pi q'$. The corresponding wave-length is given by $\lambda_\psi^* = 2\pi/k_\psi^*$. The grid spacing $\Delta\psi$ should be less than half of this wave-length (sampling theorem). Then the grid number should satisfy that

$$N_\psi^* = \frac{L_\psi}{\Delta\psi} \geq \frac{L_\psi}{\lambda_\psi^*/2} = n q' L_\psi, \quad (15.30)$$

where L_ψ is the radial width of the computational domain.

The number of Fourier harmonics that need to be included is given by

$$N_{k_\psi^*} = \frac{k_\psi^*}{2\pi/L_\psi} = \frac{n q' L_\psi}{2}. \quad (15.31)$$

For DIII-D cyclone base case, choose the radial coordinate ψ as r . At the radial location $\psi = r_0 = 0.24m$, $q_0 = 1.4$, $\hat{s}_0 = 0.78$, then $q'_0 = s_0 q_0 / r_0 = 4.5m^{-1}$. Then $N_r^* = n \times 0.45$ for the radial width $L_r = 0.10m$.

Figure 15.6 plots $\partial \mathbf{r} / \partial \psi|_{\theta, \alpha}$ lines on the $\theta = 0, 2\pi$ isosurfaces, which are chosen to be on the low-field-side midplane. On $\theta = 0$ surface, $\partial \mathbf{r} / \partial \psi|_{\theta, \alpha}$ lines are identical to $\partial \mathbf{r} / \partial \psi|_{\theta, \phi}$ lines. On $\theta = 2\pi$ surface, each $\partial \mathbf{r} / \partial \psi|_{\theta, \alpha}$ line has large ϕ shift. In old version of my code, $\theta = 0, 2\pi$ surfaces are chosen as the θ cuts (in the

new version $\theta = [-\pi, \pi]$). A connection condition for the perturbations is needed between these two surfaces. This connection condition is discussed in Sec. 15.6.2.

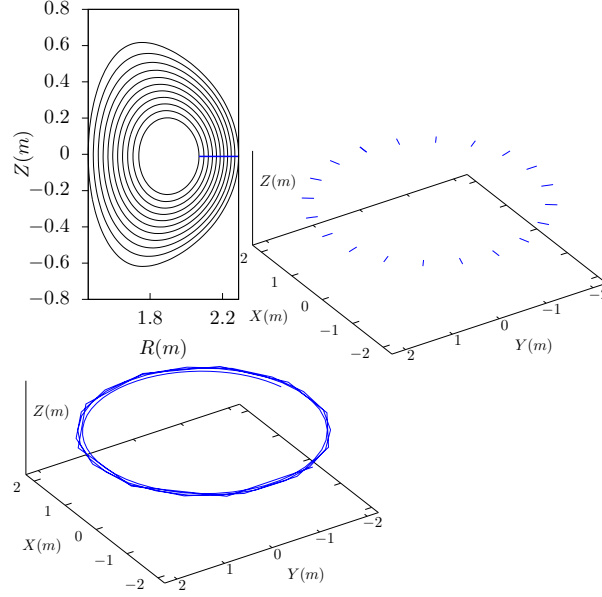


Figure 15.6. (a) $\theta = 0$ contour (blue line) in $\phi = 0$ plane; (b) a series of $\partial \mathbf{r} / \partial \psi|_{\theta, \alpha}$ curves (with $\alpha_j = j2\pi/20$, $j = 0, 1, 2, \dots, 20$) on $\theta = 0$ isosurface, (c) a single $\partial \mathbf{r} / \partial \psi|_{\theta, \alpha}$ curve (with $\alpha = 0$) on $\theta = 2\pi$ isosurface. This curve finish about 4 torodial loops because $(q_{\max} - q_{\min})2\pi = (5.56 - 1.79) \times 2\pi \approx 4 \times 2\pi$. The radial range is $\psi = 0.2 \rightarrow 0.9$, where ψ is the normalized poloidal magnetic flux. Magnetic field from EAST discharge #59954@3.03s (gfile g059954.003030 provided by Hao BaoLong).

15.6.2 Periodic conditions of physical quantity along θ and α in field-line-following coordinates (ψ, θ, α)

Since (ψ, θ, ϕ) and $(\psi, \theta + 2\pi, \phi)$ correspond to the same spatial point, a real space continuous quantity f expressed in terms of coordinates (ψ, θ, ϕ) , i.e., $f = f(\psi, \theta, \phi)$, must satisfy the following periodic conditions along θ :

$$f(\psi, \theta + 2\pi, \phi) = f(\psi, \theta, \phi). \quad (15.32)$$

Since (ψ, θ, ϕ) and $(\psi, \theta, \phi + 2\pi)$ correspond to the same spatial point, f must satisfy the following periodic conditions along ϕ :

$$f(\psi, \theta, \phi + 2\pi) = f(\psi, \theta, \phi). \quad (15.33)$$

Since (ψ, θ, α) and $(\psi, \theta, \alpha + 2\pi)$ correspond to the same spatial point, a real space continuous quantity g expressed in terms of field-line-following coordinates

(ψ, θ, α) , i.e., $g = g(\psi, \theta, \alpha)$, must satisfy the following periodic condition along α :

$$g(\psi, \theta, \alpha + 2\pi) = g(\psi, \theta, \alpha). \quad (15.34)$$

However, generally there is no periodic condition along θ ,

$$g(\psi, \theta + 2\pi, \alpha) \neq g(\psi, \theta, \alpha), \quad (15.35)$$

because $P_1 = (\psi, \theta, \alpha)$ and $P_2 = (\psi, \theta + 2\pi, \alpha)$ are generally not the same spatial point. In fact, equation (15.2) implies, for point P_1 , its toroidal angle ϕ_1 is given by

$$\phi_1 = \alpha + \int_0^\theta \frac{\mathbf{B} \cdot \nabla \phi}{\mathbf{B} \cdot \nabla \theta} d\theta, \quad (15.36)$$

while for point P_2 , its toroidal angle ϕ_2 is given by

$$\phi_2 = \alpha + \int_0^{\theta+2\pi} \frac{\mathbf{B} \cdot \nabla \phi}{\mathbf{B} \cdot \nabla \theta} d\theta = \phi_1 + 2\pi q, \quad (15.37)$$

i.e., ϕ_1 and ϕ_2 are different by $2\pi q$. From this, we know that (ψ, θ, α) and $(\psi, \theta + 2\pi, \alpha - 2\pi q)$ correspond to the same spatial point. Therefore we have the following periodic condition:

$$g(\psi, \theta, \alpha) = g(\psi, \theta + 2\pi, \alpha - 2\pi q), \quad (15.38)$$

or equivalently

$$g(\psi, \theta + 2\pi, \alpha) = g(\psi, \theta, \alpha + 2\pi q). \quad (15.39)$$

15.6.3 Numerical implementation of periodic condition (15.38)

For the fully kinetic ion module of GEM code that I am developing, θ is chosen in the range $[0:2\pi]$. The condition (15.39) imposes the following boundary condition:

$$g(\psi, 2\pi, \alpha) = g(\psi, 0, \alpha + 2\pi q). \quad (15.40)$$

If α is on a grid, $\alpha + 2\pi q$ is usually not on a grid. Therefore, to get the value of $g(\psi, 0, \alpha + 2\pi q)$, an interpolation of the discrete data over the generalized toroidal angle α (or equivalently ϕ) is needed, as is shown in Fig. 15.7.

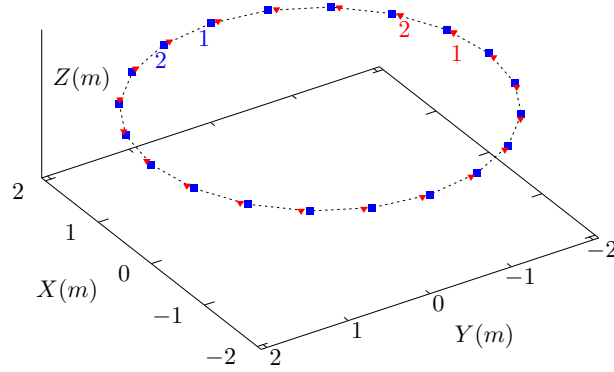


Figure 15.7. Twenty magnetic field lines (on $\psi = 0.2$ magnetic surface) starting at different toroidal angle (blue points) on the midplane ($\theta = 0$) go a full poloidal loop (i.e., $\Delta\theta = 2\pi$), arriving at a toroidal angle (red points) which are different from their respective starting toroidal angle. The field values on the red points can be obtained by interpolating the field values on the blue points. The safety factor of the magnetic surface $q = 1.79$. Magnetic field from EAST discharge #59954@3.03s.

15.6.4 α contours on a magnetic surface

Figure 15.8 compares a small number of ϕ contours and α contours on a magnetic surface.

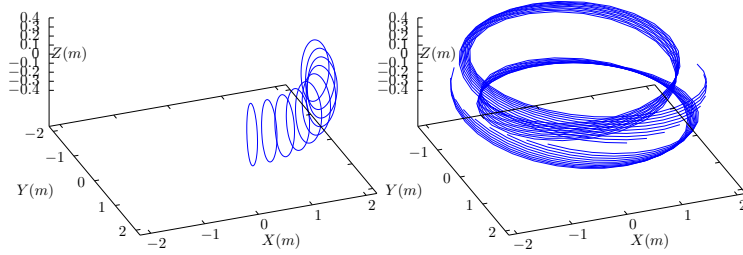


Figure 15.8. Comparison between a series of ϕ contours (left) and a series of α contours (right) on a magnetic surface. Here contour levels are $\phi_j = \alpha_j = (j - 1)2\pi/4/(10 - 1)$ with $j = 1, 2, \dots, 10$, i.e., only $1/4$ of the full torus. Every ϕ and α contour start from the lower-field-side midplane and go one poloidal loop. Magnetic field from EAST discharge #59954@3.03s.

As is shown in the left panel of Fig. 15.8, with ϕ fixed, an θ curve reaches its starting point when θ changes from zero to 2π . However, as shown in the right panel of Fig. 15.8, with α fixed, an θ curve (i.e. a magnetic field line) does not necessarily reach its starting point when θ changes from zero to 2π . There is a toroidal shift, $2\pi q$, between the starting point and ending point. Therefore there is generally no periodic condition along θ since q is not always an integer. A mixed periodic condition involves both θ and α is given in (15.38).

In field-line-following coordinates (ψ, θ, α) , a toroidal harmonic of a physical perturbation can be written as

$$\delta A(\psi, \theta, \alpha) = \delta A_0(\psi) \cos(m'\theta + n\alpha + \alpha_0) \quad (15.41)$$

where n is the toroidal mode number, m' , which is not necessary an integer, is introduced to describe the variation along a field line. The periodic condition given by Eq. (15.38) requires that

$$\cos(m'\theta + n\alpha + \alpha_0) = \cos[m'(\theta + 2\pi) + n(\alpha - 2\pi q) + \alpha_0], \quad (15.42)$$

To satisfy the above condition, we can choose

$$m'2\pi - n2\pi q = N2\pi, \quad (15.43)$$

where N is an arbitrary integer, i.e.,

$$m' = N + nq. \quad (15.44)$$

We are interested in perturbation with a slow variation along the field line direction (i.e., along $\partial \mathbf{r} / \partial \theta|_{\psi, \alpha}$) and thus we want the value of m' to be small. One of the possible small values given by expression (15.44) is to choose $N = -n \times \text{NINT}((q_{\max} + q_{\min})/2)$, so that m' is given by

$$m'(\psi) = nq - n \times \text{NINT}\left(\frac{q_{\max} + q_{\min}}{2}\right), \quad (15.45)$$

where NINT is a function that return the nearest integer of its argument, q_{\max} and q_{\min} is the maximal and minimal value of the safety factor in the radial region in which we are interested. [In the past, I choose $m'(\psi) = nq - \text{NINT}(nq)$. However, $m'(\psi)$ in this case is not a continuous function of ψ and thus is not physical.] This form is used to set the initial density perturbation in the fully kinetic code I am developing. Note that m' in Eq. (15.45) depends on the radial coordinate ψ through $q(\psi)$. Also note that m' here is different from the poloidal mode number m in (ψ, θ, ϕ) coordinate system. It is ready to show that the perturbation given by Eq. (15.41) with $m' \sim 1$ and $n \gg 1$ has large poloidal mode number m when expressed in (ψ, θ, ϕ) coordinates. [Proof: Expression (15.41) can be written as

$$\delta A = \delta A_0(\psi) \cos[m'\theta + n(\phi - \bar{\delta}(\psi, \theta)) + \alpha_0] \quad (15.46)$$

Assume that θ is the straight-field-line poloidal angle in (ψ, θ, ϕ) coordinate system, then $\bar{\delta}(\psi, \theta) = q\theta$ and the above equation is written as

$$\delta A = \delta A_0(\psi) \cos[(m' - nq)\theta + n\phi + \alpha_0], \quad (15.47)$$

which indicates the poloidal mode number m in (ψ, θ, ϕ) coordinates is given by $m = m' - nq$. For the case with $m' \sim 1$ and $n \gg 1$, m is much larger than one.]

Since α contours on a magnetic surface are magnetic field lines, they span out the 3D shape of magnetic surface when there are many α contours on a magnetic surface, as is shown by the right-panel of Fig. 15.9.

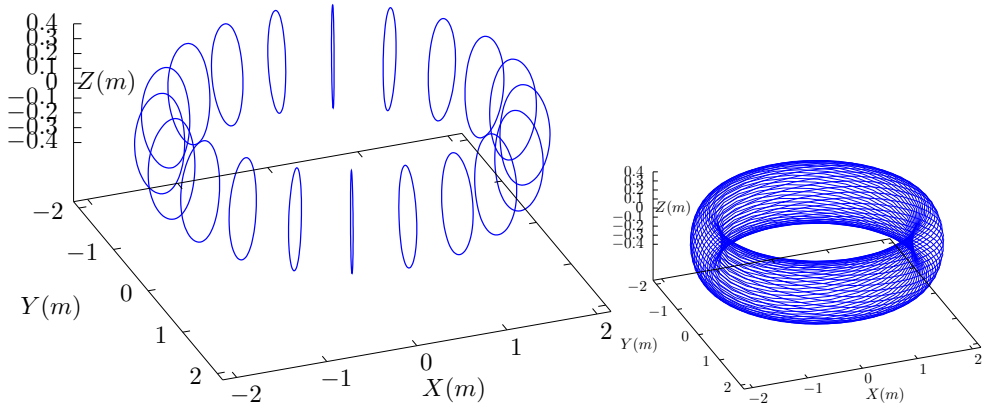


Figure 15.9. Comparison between a series of ϕ contours(left) and a series of α contours (left) on a magnetic surface. The α contours correspond to magnetic field lines. Here the α values of adjacent α contours differ by $d\alpha = 2\pi/20$ and each α contour goes one full poloidal loop. Magnetic field from EAST discharge #59954@3.03s.

15.6.5 α contours in a toroidal annulus

Figure 15.10 compares the ϕ coordinate surface of (ψ, θ, ϕ) coordinates with the α coordinate surface of (ψ, θ, α) coordinates.

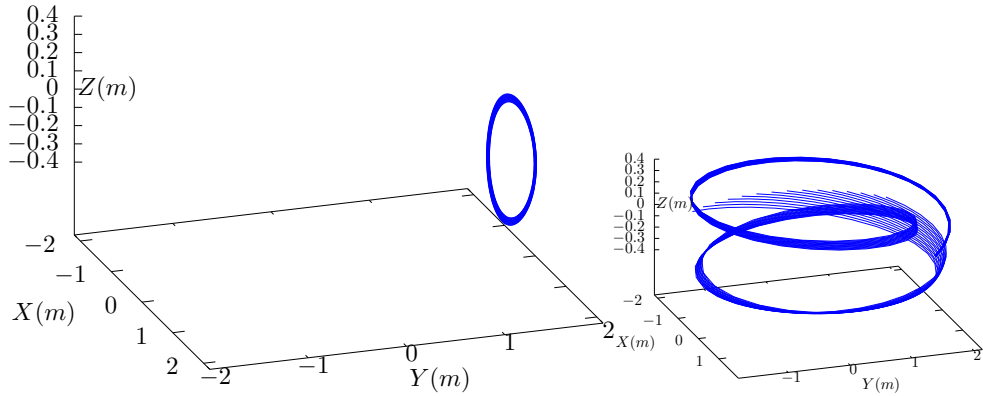


Figure 15.10. Comparison between isosurface of $\phi = 2\pi/8$ (projection of magnetic field lines onto $\phi = 2\pi/8$ plane) and isosurface of $\alpha = 2\pi/8$. The α isosurface is made of a family of contours of $\alpha = 2\pi/8$, which are all magnetic field lines. These field lines are traced by starting from a series of points on the low-field-side midplane ($\theta = 0$) at different radial locations and the field lines are followed by one poloidal loop. The radial range is given by $\psi_N \in [0.4; 0.5]$, where ψ_N is the normalized poloidal magnetic flux. Magnetic field from EAST discharge #59954@3.03s.

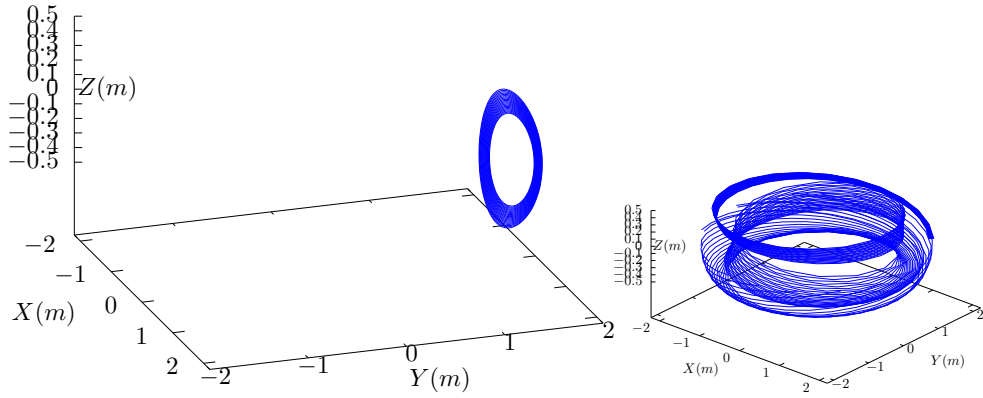


Figure 15.11. The same plot as in Fig. 15.10 but with a larger radial range. $\psi_N \in [0.4: 0.7]$, where ψ_N is the normalized poloidal magnetic flux.

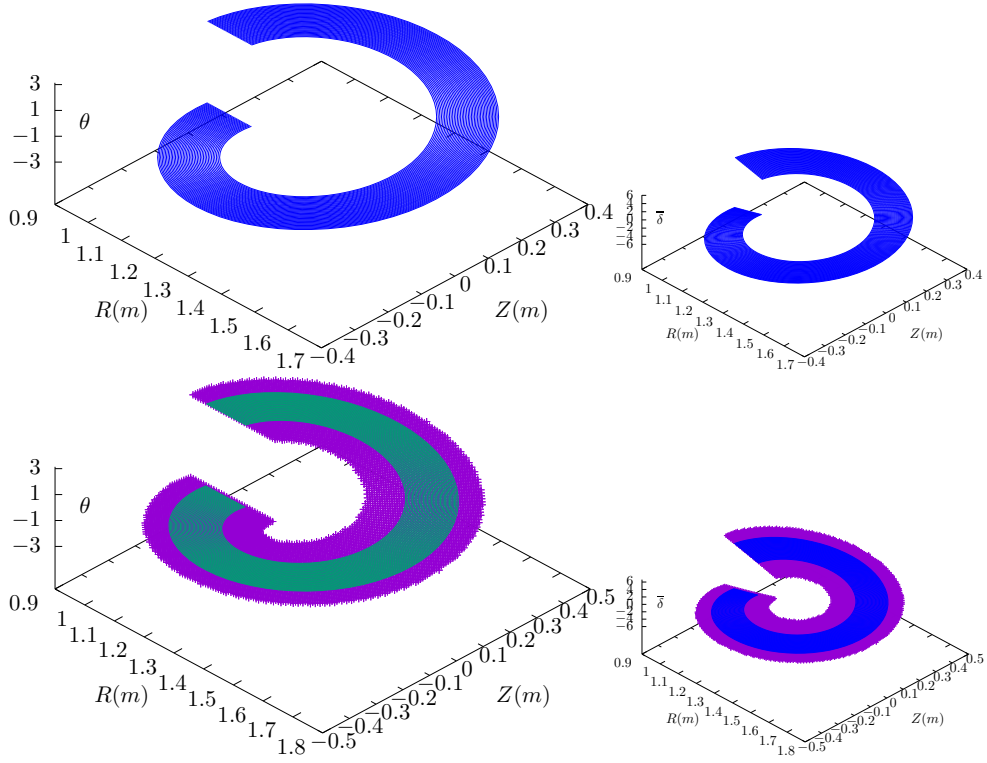


Figure 15.12. Values of θ and $\bar{\delta} \equiv \int_0^\theta \hat{q} d\theta$ on an annulus in the poloidal plane (R, Z) . Upper panel: using magnetic coordinates. Lower panel: comparison with the results computed in cylindrical coordinates. Both θ and $\bar{\delta}$ are discontinuous at the θ cut, $\theta = \pm\pi$, which is chosen on the high-field-side.

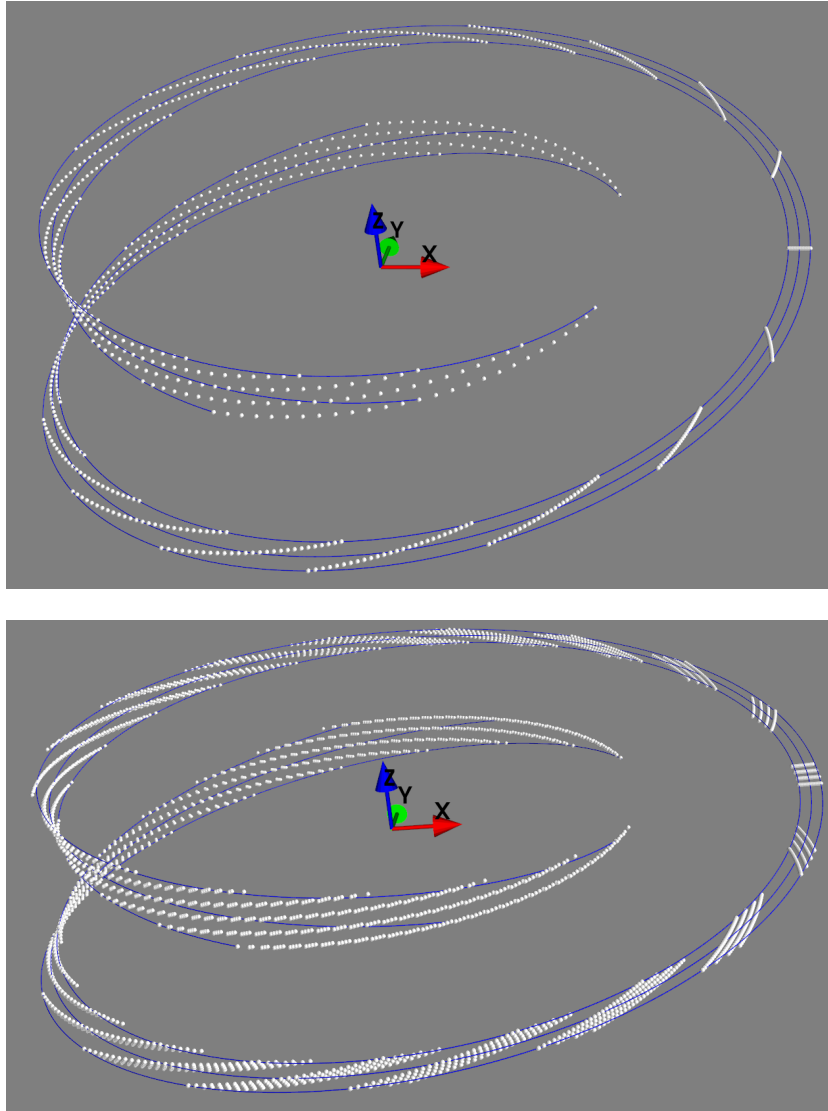


Figure 15.13. Upper panel: 2D grid (ψ, θ) of resolution $(27, 33)$ for a fixed value of α . Lower panel: 3D grid (ψ, α, θ) of resolution $(27, 4, 33)$ for a toroidal wedge of $2\pi/40$. The 3D grid is generated by rotating the 2D grid toroidally. The blue lines are examples of field lines.

The above grid is often called “flux-tube”, since it is created by following field lines, and it looks like a tube if the field lines are very near to each other (e.g., when we choose a very narrow radial and toroidal region to start from). Since no magnetic field line passes through the sides of the tube, the flux through any cross section of the tube is equal. The term “flux tube” is often used in astrophysics.

15.7 Field-line-following mesh in gyrokinetic turbulence simulation codes

Most gyrokinetic simulation codes use field-line-following coordinates in constructing spatial mesh. The mesh is conceptually generated by the following three steps: (1) selecting some initial points; (2) tracing out magnetic-field-lines passing through these points; (3) choose the intersecting points of these field-lines with a series of chosen surfaces as the final grid-points. The initial points and the chosen surfaces differ among various codes and thus the resulting grid differs. Next, let us discuss some examples.

15.7.1 Mesh in GENE, GYRO, and GEM codes

Given the definition of (ψ, θ) coordinates, first choose N_ψ points at $(\psi_j, \theta = 0, \phi = 0)$ with $j = 0, 1, \dots, N_r - 1$. (The $\theta = 0$ plane is chosen to be near the low-field-side midplane.) Then trace out the magnetic-field-lines passing through these points for one poloidal circuit (poloidal angle range: $\theta \in [-\pi, \pi]$) and record the intersection points of these field-lines with various $\theta = \text{const}$ planes. This gives a 2D grid $[(\psi, \theta)$ surface for a fixed value of $\alpha]$. After this, we rotate the 2D grid toroidally to get the 3D grid. Usually we consider a toroidal wedge rather than a full torus (to reduce computational cost). So the 2D grid is rotated toroidally by $\Delta\phi_k = k(2\pi / N_{\text{wedge}}) / N_\varphi$, where $k = 0, 1, \dots, N_\varphi - 1$.

Note that the gridpoints on $\theta = -\pi$ surface usually do not coincide those on $\theta = +\pi$ surface due to the toroidal shift along the field line arising when the safety factor is irrational. Interpolation can be used to map physical variables defined on gridpoints in $\theta = -\pi$ plane to those in $\theta = +\pi$ plane.

15.7.2 Mesh in GTC and GTS codes[28]

Given the definition of (ψ, θ) coordinates, 2D grid-points can be chosen on $\phi = 0$ plane based on (ψ, θ) coordinates. Then trace out the magnetic-field-lines starting from these points for one toroidal circuit and record the intersection points of these field-lines with $\phi_j = j\Delta\phi$ planes, where $j = 1, 2, \dots, N_t - 1$,

$\Delta\phi = 2\pi / (N_t - 1)$. It is obvious that the resulting mesh are not toroidally symmetrical. And also the grids on $\phi=0$ plane differ from those on $\phi=2\pi$ plane. Interpolation can be used to mapping physical variables defined on grid-points of $\phi=0$ to those of $\phi=2\pi$ plane. In this case, the number of “toroidal grid-points” N_t (i.e., the number of poloidal planes) is actually the number of grid-points in the parallel direction within one toroidal circuit.

15.7.3 Mesh in XGC1 code ***check**

XGC1 can handle the region outside of the LCFS. Here we only discuss the region inside the LCFS. At each radial gridpoint on $\phi = 0$ plane, follow the magnetic field line starting from this point for one poloidal loop and record the intersection points of this field-line with $\phi_j = j\Delta\phi$ planes, where $j = 1, 2, \dots, N_t$, $\Delta\phi = 2\pi / N_t$. For the case $q > 1$, one magnetic-field-line will have more than one intersection points on some poloidal planes. Repeat tracing the field line for each radial location. Then project (toroidally) all the intersection points on different poloidal planes to a single poloidal plane and rotate (toroidally) these 2D grids to define a 3D grid that are toroidally symmetrical.

15.8 Numerical verification of the field-aligned coordinates

The generalized toroidal angle α is numerically calculated in my code. To verify $\mathbf{B} \cdot \nabla\alpha = 0$ along a magnetic field-line, figure 15.14 plots the values of α along a magnetic field line, which indicates that α is constant. This indicates the numerical implementation of the field-aligned coordinates is correct.

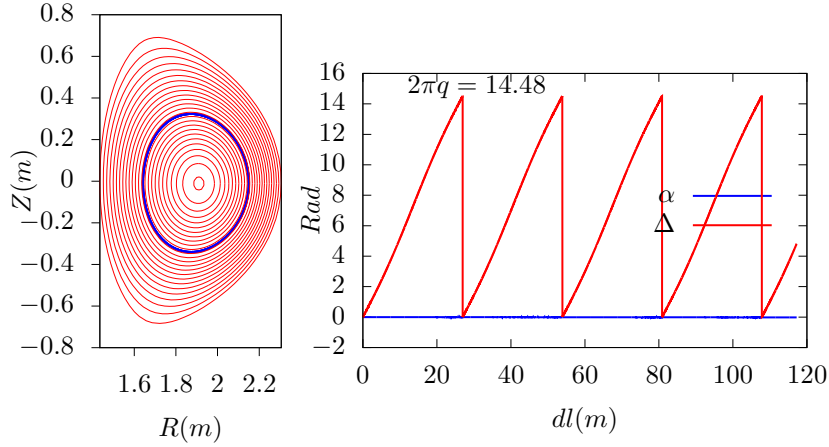


Figure 15.14. Left: Projection of a field line on the poloidal plane. Right: the value of Δ and α along the magnetic field line. Here α is defined by $\alpha = \phi - \Delta$, where ϕ is the usual cylindrical toroidal angle and $\Delta = \int_0^\theta \frac{\mathbf{B} \cdot \nabla \phi}{\mathbf{B} \cdot \nabla \theta} d\theta$.

15.8.1 Binormal wavenumber

Let us introduce the binormal wavenumber, which is frequently used in presenting turbulence simulation results. Define the binormal direction \mathbf{s} by

$$\mathbf{s} = \frac{\mathbf{B} \times \nabla \Psi}{|\mathbf{B} \times \nabla \Psi|},$$

which is a unit vector lying on a magnetic surface and perpendicular to \mathbf{B} . The binormal wavenumber of a mode is defined by

$$k_{bn} = \mathbf{s} \cdot \nabla p, \quad (15.48)$$

where p is the phase of the mode. Consider a mode given by $\exp(ik_\psi\psi + im\theta - in\zeta)$, then the phase $p = k_\psi\psi + m\theta - n\zeta$. Then k_{bn} is written as

$$\begin{aligned} k_{bn} &= \frac{\mathbf{B} \times \nabla \Psi}{|\mathbf{B} \times \nabla \Psi|} \cdot \nabla(k_\psi\psi + m\theta - n\zeta) \\ &= \frac{\mathbf{B} \times \nabla \Psi}{|\mathbf{B} \times \nabla \Psi|} \cdot \nabla(m\theta - n\zeta), \end{aligned} \quad (15.49)$$

where the radial phase $k_\psi\psi$ does not appear since $\mathbf{B} \times \nabla \Psi \cdot \nabla \psi = 0$. The above expression can be further written as

$$\begin{aligned} k_{bn} &= \frac{1}{|\mathbf{B} \times \nabla \Psi|} [m\mathbf{B} \times \nabla \Psi \cdot \nabla \theta - n\mathbf{B} \times \nabla \Psi \cdot \nabla \zeta] \\ &= \frac{1}{|\mathbf{B} \times \nabla \Psi|} [m\mathbf{B} \cdot \nabla \Psi \times \nabla \theta - n\mathbf{B} \cdot \nabla \Psi \times \nabla \zeta] \\ &= \frac{n\mathbf{B} \cdot}{|\mathbf{B} \times \nabla \Psi|} \left[\frac{m}{n} \nabla \Psi \times \nabla \theta - \nabla \Psi \times \nabla \zeta \right]. \end{aligned} \quad (15.50)$$

Equation (15.50) is the general expression of the binormal wavenumber. On the resonant surface of the mode, i.e., $q(\psi) = m/n$, then the above expression is written as

$$k_{bn} = \frac{n\mathbf{B} \cdot}{|\mathbf{B} \times \nabla \Psi|} [q\nabla \Psi \times \nabla \theta - \nabla \Psi \times \nabla \zeta]. \quad (15.51)$$

Using Eq. (14.12), i.e., $\mathbf{B} = -(\nabla \zeta \times \nabla \Psi + q\nabla \Psi \times \nabla \theta)$, the above expression is written as

$$\begin{aligned} k_{bn} &= \frac{-n\mathbf{B} \cdot}{|\mathbf{B} \times \nabla \Psi|} \mathbf{B} \\ &= -n \frac{B}{|\nabla \Psi|} \end{aligned}$$

Using $B_p = |\nabla \Psi|/R$, the above equation is written

$$k_{bn} = -n \frac{B}{RB_p} \quad (15.52)$$

which indicates the binormal wavenumber generally depends on the poloidal angle. For large aspect-ratio tokamak, we have $B_\phi \approx B$, $q \approx B_\phi r / (B_p R)$. Then Eq. (15.52) is written

$$k_{bn} \approx -\frac{nq}{r}, \quad (15.53)$$

which indicates the binormal wavenumber are approximately independent of the poloidal angle. Since $m = nq$ on a resonant surface, the above equation is written $|k_{bn}| \approx m/r$, which is the usual poloidal wave number. Due to this relation, the binormal wavenumber k_{bn} is often called the poloidal wavenumber and denoted by k_θ in papers on tokamak turbulence. In the GENE code, y coordinate is defined by $y = \alpha r_0 / q_0$. Then the k_y of a mode of toroidal mode number n is given by $k_y = 2\pi / \lambda_y$ where $\lambda_y = \lambda_\alpha r_0 / q_0$ and $\lambda_\alpha = 2\pi / n$. Then k_y is written as $k_y = nq_0 / r_0$, which is similar to the binormal defined above. For this reason, k_y of GENE code is also called binormal wave-vector, which is in fact not reasonable because neither $\partial \mathbf{r} / \partial y$ or ∇y is along the binormal direction.

16 Concentric-circular magnetic configuration with a given safety factor profile

Assume magnetic surfaces of a magnetic configuration are known and given by

$$R(r, \theta) = R_0 + r \cos \theta, \quad (16.1)$$

$$Z(r, \theta) = r \sin \theta, \quad (16.2)$$

where (r, θ) are two parameters and r is magnetic surface label (i.e., $\partial \Psi / \partial \theta|_{r=0}$). The above parametric equations specify a series of concentric-circular magnetic surfaces.

Assume the toroidal field function $g(r) = RB_\phi$ is given. Then the toroidal magnetic field is determined by $B_\phi = g/R$. Further assume the safety factor profile $q(r)$ is given, then the magnetic field is fully determined. Next, let us derive the explicit form of the poloidal magnetic field \mathbf{B}_p , which is given by

$$\mathbf{B}_p = \nabla \Psi \times \nabla \phi = \frac{1}{2\pi} \nabla \Psi_p \times \nabla \phi, \quad (16.3)$$

which involves the poloidal magnetic flux Ψ_p . Therefore our task is to express Ψ_p in terms of q and g . Using $q(r) = d\Psi_t / d\Psi_p$, we obtain

$$d\Psi_p = \frac{1}{q} d\Psi_t,$$

Integrate the above equation over r , we obtain

$$\int_0^r d\Psi_p = \int_0^r \frac{1}{q} d\Psi_t, \quad (16.4)$$

which can be written as

$$\Psi_p(r) - \Psi_p(0) = \int_0^r \frac{1}{q(r)} d\left(\int_0^r \int_{-\pi}^{\pi} B_\phi r dr d\theta\right), \quad (16.5)$$

where use has been made of $\Psi_t = \int_0^r \int_{-\pi}^{\pi} B_\phi r dr d\theta$. Using $B_\phi = g / R$ and $R = R_0 + r \cos\theta$, the above equation is written

$$\Psi_p(r) - \Psi_p(0) = \int_0^r \frac{1}{q(r)} d\left(\int_0^r \int_{-\pi}^{\pi} \frac{g}{R_0 + r \cos\theta} r dr d\theta\right) \quad (16.6)$$

Using **maxima** (an open-source computer algebra system), the above integration over θ can be performed analytically, giving

$$\int_{-\pi}^{\pi} \frac{1}{R_0 + r \cos\theta} d\theta = \frac{2\pi}{\sqrt{R_0^2 - r^2}}. \quad (16.7)$$

Using this, equation (16.6) is written as

$$\Psi_p(r) - \Psi_p(0) = \int_0^r \frac{1}{q(r)} d\left(\int_0^r \frac{2\pi g r}{\sqrt{R_0^2 - r^2}} dr\right), \quad (16.8)$$

which can be simplified as

$$\Psi_p(r) - \Psi_p(0) = \int_0^r \frac{1}{q(r)} \frac{2\pi g r}{\sqrt{R_0^2 - r^2}} dr. \quad (16.9)$$

This is what we want—the expression of the poloidal magnetic flux in terms of q and g . [Another way of obtaining Eq. (16.9) is to use Eq. (10.87), i.e.,

$$\frac{d\Psi_p}{dr} = -\frac{g}{q} \int_0^{2\pi} \frac{\mathcal{J}}{R^2} d\theta, \quad (16.10)$$

where \mathcal{J} is the Jacobian of the (r, θ, ϕ) coordinates and is given by $\mathcal{J} = R(R_\theta Z_r - R_r Z_\theta) = -Rr$. Then Eq. (16.10) is simplified as

$$\frac{d\Psi_p}{dr} = \frac{g}{q} \int_0^{2\pi} \frac{r}{R} d\theta = \frac{g}{q} \int_0^{2\pi} \frac{r}{R_0 + r \cos\theta} d\theta = \frac{g}{q} r \frac{2\pi}{\sqrt{R_0^2 - r^2}}, \quad (16.11)$$

which, after being integrated over r , gives Eq. (16.9).]

Using Eq. (16.9), the poloidal magnetic field in Eq. (16.3) is written as

$$\begin{aligned}\mathbf{B}_p &= \frac{\nabla r \times \nabla \phi}{2\pi} \frac{\partial}{\partial r} \left(\int_0^r \frac{1}{q(r)} \frac{2\pi g r}{\sqrt{R_0^2 - r^2}} dr \right) \\ &= \nabla r \times \nabla \phi \frac{1}{q(r)} \frac{gr}{\sqrt{R_0^2 - r^2}}.\end{aligned}\quad (16.12)$$

[Using the formulas $\nabla r = -\frac{R}{\mathcal{J}}(Z_\theta \hat{\mathbf{R}} - R_\theta \hat{\mathbf{Z}})$ and $\mathcal{J} = R(R_\theta Z_r - R_r Z_\theta)$, where \mathcal{J} is the Jacobian of the (r, θ, ϕ) coordinates, we obtain $\mathcal{J} = -Rr$ and $\nabla r = \cos\theta \hat{\mathbf{R}} + \sin\theta \hat{\mathbf{Z}}$, $\nabla \phi = \hat{\phi}/R$. Then Eq. (16.12) is written as

$$\mathbf{B}_p = \frac{\cos\theta \hat{\mathbf{Z}} - \sin\theta \hat{\mathbf{R}}}{R} \frac{1}{q(r)} \frac{gr}{\sqrt{R_0^2 - r^2}} \quad (16.13)$$

This is the explicit form of the poloidal magnetic field in terms of g and q . The magnitude of \mathbf{B}_p is written as

$$B_p = \frac{1}{(R_0 + r \cos\theta)} \frac{1}{q(r)} \frac{gr}{\sqrt{R_0^2 - r^2}} \quad (16.14)$$

Note that both B_p and B_ϕ depend on the poloidal angle θ .]

I use Eq. (16.9) to compute the 2D data of Ψ ($\Psi = \Psi_p / 2\pi$) on the poloidal plane when creating a numerical G-eqds file for the above magnetic configuration (Fortran code is at `/home/yj/project_new/circular_configuration_with_q_given`).

Assume that the poloidal plasma current is zero, then $g(r) = RB_\phi$ is a constant independent of r . This is always assumed by the authors who use concentric-circular configuration but is seldom explicitly mentioned.

In analytical work, $1/R$ dependence on (r, θ) is often approximated as

$$\frac{1}{R} = \frac{1}{R_0 + r \cos\theta} = \frac{1}{R_0} \frac{1}{1 + \varepsilon \cos\theta} \approx \frac{1}{R_0} (1 - \varepsilon \cos\theta),$$

where $\varepsilon = r/R_0$ is the local inverse aspect ratio.

16.1 Is the above \mathbf{B} divergence-free?

Since the above field is derived from the general form given by Eq. (2.10), it is guaranteed that the field is divergence-free. In case of any doubt, let us directly verify this. Write \mathbf{B} as

$$\mathbf{B} = B^{(1)} \mathcal{J} \nabla \theta \times \nabla \phi + B^{(2)} \mathcal{J} \nabla \phi \times \nabla r + B^{(3)} \mathcal{J} \nabla r \times \nabla \theta, \quad (16.15)$$

where \mathcal{J} is the Jacobian of (r, θ, ϕ) coordinates; $B^{(1)}$, $B^{(2)}$, and $B^{(3)}$ are given by

$$B^{(1)} = \mathbf{B} \cdot \nabla r \quad (16.16)$$

$$B^{(2)} = \mathbf{B} \cdot \nabla \theta \quad (16.17)$$

$$B^{(3)} = \mathbf{B} \cdot \nabla \phi \quad (16.18)$$

Use \mathbf{B}_p given by (16.12), then $B^{(1)}$, $B^{(2)}$, and $B^{(3)}$ are written as

$$B^{(1)} = 0, \quad (16.19)$$

$$B^{(2)} = -\frac{1}{\mathcal{J}} \frac{1}{q(r)} \frac{g_0 r}{\sqrt{R_0^2 - r^2}}, \quad (16.20)$$

and

$$B^{(3)} = \frac{B_\phi}{R}, \quad (16.21)$$

respectively. Then, by using the divergence formula in (r, θ, ϕ) coordinates, $\nabla \cdot \mathbf{B}$ is written as

$$\begin{aligned} \nabla \cdot \mathbf{B} &= \frac{1}{\mathcal{J}} \left(\frac{\partial B^{(1)} \mathcal{J}}{\partial r} + \frac{\partial B^{(2)} \mathcal{J}}{\partial \theta} + \frac{\partial B^{(3)} \mathcal{J}}{\partial \phi} \right) \\ &= \frac{1}{\mathcal{J}} \left(0 + \frac{\partial B^{(2)} \mathcal{J}}{\partial \theta} + 0 \right) \\ &= \frac{1}{\mathcal{J}} \frac{\partial}{\partial \theta} \left(-\frac{1}{q(r)} \frac{g_0 r}{\sqrt{R_0^2 - r^2}} \right) \\ &= 0 \end{aligned} \quad (16.22)$$

i.e., \mathbf{B} in this case is indeed divergence-free.

16.2 Is the above \mathbf{B} a solution to the GS equation?

The answer is no. It is ready to verify that the poloidal magnetic flux function $\Psi = \Psi_p / 2\pi$ given by Eq. (16.9) is not a solution to the GS equation (A.99) even if the plasma pressure in the GS equation is set to zero. The above expression is a solution to the GS equation in the limit of infinite aspect ratio and zero plasma pressure. The finite aspect ratio and plasma pressure requires the magnetic surfaces to have the Shafranov shift in order to satisfy the GS equation (see Sec. A.19).

16.3 Explicit expression for the generalized toroidal angle

For the above magnetic field, the toroidal shift involved in the definition of the generalized toroidal angle can be expressed in simple analytical form. The toroidal shift is given by

$$\bar{\delta} = \int_0^\theta \hat{q} d\theta, \quad (16.23)$$

where the local safety factor \hat{q} can be written as

$$\hat{q} = -\frac{g_0}{R^2} \frac{\mathcal{J}}{\Psi'}. \quad (16.24)$$

Using $\mathcal{J} = -Rr$ and

$$\Psi' = \frac{1}{q(r)} \frac{g_0 r}{\sqrt{R_0^2 - r^2}} \quad (16.25)$$

The local safety factor \hat{q} in Eq. (16.24) is written as

$$\hat{q} = q \sqrt{R_0^2 - r^2} \frac{1}{R}. \quad (16.26)$$

Using this, expression (16.23) is written

$$\bar{\delta} = q \sqrt{R_0^2 - r^2} \int_0^\theta \frac{1}{R} d\theta \quad (16.27)$$

Assume $\theta \in (-\pi, \pi)$, then the integration $\int_0^\theta 1/R d\theta$ can be analytically performed (using maxima), yielding

$$\int_0^\theta \frac{1}{R} d\theta = \frac{2 \arctan\left(\frac{\sin\theta(R_0 - r)}{(\cos\theta + 1)\sqrt{R_0^2 - r^2}}\right)}{\sqrt{R_0^2 - r^2}}. \quad (16.28)$$

Then expression (16.27) is written

$$\bar{\delta} = 2q \arctan\left(\frac{(R_0 - r)}{\sqrt{R_0^2 - r^2}} \tan\left(\frac{\theta}{2}\right)\right), \quad (16.29)$$

where use has been made of $\sin\theta / (\cos\theta + 1) = \tan(\theta/2)$. Using this, the generalized toroidal angle can be written as

$$\begin{aligned} \alpha &= \phi - \bar{\delta} \\ &= \phi - 2q \arctan\left(\frac{(R_0 - r)}{\sqrt{R_0^2 - r^2}} \tan\left(\frac{\theta}{2}\right)\right). \end{aligned} \quad (16.30)$$

The results given by the formula (16.29) are compared with the results from my code that assumes a general numerical configuration. The results from the two methods agree with each other, as is shown in Fig. 16.1, which provides confidence in both the analytical formula and the numerical code.

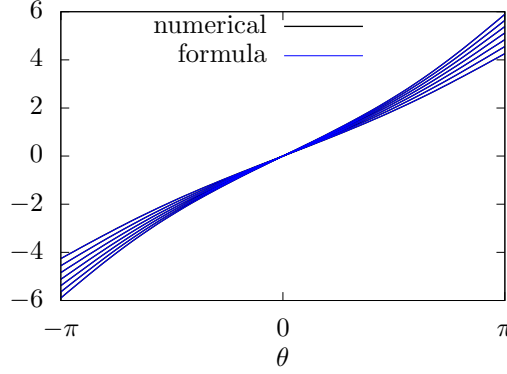


Figure 16.1. The results of $\bar{\delta} = \int_0^\theta \hat{q} d\theta$ computed by using formula (16.29) and the numerical code agree with each other. The different lines correspond to values of $\bar{\delta}$ on different magnetic surfaces. In the numerical code, two kinds of poloidal angles can be selected: one is the equal-volume poloidal angle, and another is the equal-arc-length angle. Make sure that the latter is selected when doing the comparison because the the poloidal angle θ appearing in the analytical formula is the equal-arc-length poloidal angle.

In passing, we note that the straight-field-line poloidal angle θ_f can also be considered to be defined by

$$\alpha = \phi - q\theta_f, \quad (16.31)$$

i.e.,

$$\theta_f = \frac{1}{q}(\phi - \alpha) = \frac{\bar{\delta}}{q}. \quad (16.32)$$

Then using Eq. (16.30), θ_f is written as

$$\theta_f = 2 \arctan \left(\frac{(R_0 - r)}{\sqrt{R_0^2 - r^2}} \tan \left(\frac{\theta}{2} \right) \right), \quad (16.33)$$

which agrees with Eq. (A2) in Gorler's paper[13].

16.4 Metric elements

Let $\psi = r$ and define $h^{\psi R} = \nabla \psi \cdot \hat{\mathbf{R}}$, $h^{\alpha R} = \nabla \alpha \cdot \hat{\mathbf{R}}$, etc. Explicit expressions for these elements can be written as

$$\begin{aligned} h^{\psi R} &= \nabla \psi \cdot \hat{\mathbf{R}} \\ &= \nabla r \cdot \hat{\mathbf{R}} \\ &= -\frac{R}{\mathcal{J}}(Z_\theta \hat{\mathbf{R}} - R_\theta \hat{\mathbf{Z}}) \cdot \hat{\mathbf{R}} \end{aligned}$$

$$\begin{aligned}
&= -\frac{R}{\mathcal{J}}Z_\theta \\
&= \cos\theta
\end{aligned} \tag{16.34}$$

$$\begin{aligned}
h^{\psi Z} &= \nabla\psi \cdot \hat{\mathbf{Z}} \\
&= \nabla r \cdot \hat{\mathbf{Z}} \\
&= -\frac{R}{\mathcal{J}}(Z_\theta \hat{\mathbf{R}} - R_\theta \hat{\mathbf{Z}}) \cdot \hat{\mathbf{Z}} \\
&= \frac{R}{\mathcal{J}}R_\theta \\
&= \sin\theta
\end{aligned}$$

$$\begin{aligned}
h^{\psi\phi} &= \nabla\psi \cdot \hat{\phi} \\
&= 0
\end{aligned}$$

$$\begin{aligned}
h^{\theta R} &= \nabla\theta \cdot \hat{\mathbf{R}} \\
&= \frac{R}{\mathcal{J}}(Z_\psi \hat{\mathbf{R}} - R_\psi \hat{\mathbf{Z}}) \cdot \hat{\mathbf{R}} \\
&= \frac{R}{\mathcal{J}}Z_\psi \\
&= -\frac{1}{r}\sin\theta
\end{aligned}$$

$$\begin{aligned}
h^{\theta Z} &= \nabla\theta \cdot \hat{\mathbf{Z}} \\
&= \frac{R}{\mathcal{J}}(Z_\psi \hat{\mathbf{R}} - R_\psi \hat{\mathbf{Z}}) \cdot \hat{\mathbf{Z}} \\
&= -\frac{R}{\mathcal{J}}R_\psi \\
&= \frac{1}{r}\cos\theta
\end{aligned}$$

$$\begin{aligned}
h^{\theta\phi} &= \nabla\theta \cdot \hat{\phi} \\
&= 0
\end{aligned}$$

$$\begin{aligned}
h^{\alpha R} &= \nabla\alpha \cdot \hat{\mathbf{R}} \\
&= \left[\frac{\hat{\phi}}{R} + \left(\frac{\partial\bar{\delta}}{\partial\psi} \frac{R}{\mathcal{J}}Z_\theta - \frac{\partial\bar{\delta}}{\partial\theta} \frac{R}{\mathcal{J}}Z_\psi \right) \hat{\mathbf{R}} + \left(\frac{\partial\bar{\delta}}{\partial\theta} \frac{R}{\mathcal{J}}R_\psi - \frac{\partial\bar{\delta}}{\partial\psi} \frac{R}{\mathcal{J}}R_\theta \right) \hat{\mathbf{Z}} \right] \cdot \hat{\mathbf{R}} \\
&= \frac{\partial\bar{\delta}}{\partial\psi} \frac{R}{\mathcal{J}}Z_\theta - \frac{\partial\bar{\delta}}{\partial\theta} \frac{R}{\mathcal{J}}Z_\psi \\
&= \frac{\partial\bar{\delta}}{\partial\psi} \frac{R}{\mathcal{J}}r \cos\theta - \frac{\partial\bar{\delta}}{\partial\theta} \frac{R}{\mathcal{J}}\sin\theta
\end{aligned}$$

$$\begin{aligned}
 &= -\frac{\partial \bar{\delta}}{\partial \psi} \cos \theta + \frac{\partial \bar{\delta}}{\partial \theta} \frac{1}{r} \sin \theta \\
 &= -\frac{\partial \bar{\delta}}{\partial r} \cos \theta + \hat{q} \frac{1}{r} \sin \theta \\
 h^{\alpha Z} &= \nabla \alpha \cdot \hat{\mathbf{Z}} \\
 &= \left[\frac{\hat{\phi}}{R} + \left(\frac{\partial \bar{\delta}}{\partial \psi} \frac{R}{\mathcal{J}} Z_\theta - \frac{\partial \bar{\delta}}{\partial \theta} \frac{R}{\mathcal{J}} Z_\psi \right) \hat{\mathbf{R}} + \left(\frac{\partial \bar{\delta}}{\partial \theta} \frac{R}{\mathcal{J}} R_\psi - \frac{\partial \bar{\delta}}{\partial \psi} \frac{R}{\mathcal{J}} R_\theta \right) \hat{\mathbf{Z}} \right] \cdot \hat{\mathbf{Z}} \\
 &= \frac{\partial \bar{\delta}}{\partial \theta} \frac{R}{\mathcal{J}} R_\psi - \frac{\partial \bar{\delta}}{\partial \psi} \frac{R}{\mathcal{J}} R_\theta \\
 &= -\hat{q} \frac{1}{r} \cos \theta - \frac{\partial \bar{\delta}}{\partial r} \sin \theta \\
 h^{\alpha \phi} &= \frac{1}{R}. \tag{16.35}
 \end{aligned}$$

Using expression (16.29), $d\bar{\delta}/dr$ can be evaluated analytically, yielding

$$\begin{aligned}
 \frac{d\bar{\delta}}{dr} &= 2 \frac{dq}{dr} \arctan \left(\frac{(R_0 - r)}{\sqrt{R_0^2 - r^2}} \tan \left(\frac{\theta}{2} \right) \right) + 2q \frac{1}{1 + \left(\frac{(R_0 - r)}{\sqrt{R_0^2 - r^2}} \tan \left(\frac{\theta}{2} \right) \right)^2} \tan \left(\frac{\theta}{2} \right) \frac{d}{dr} \left[\frac{(R_0 - r)}{\sqrt{R_0^2 - r^2}} \right] \\
 &= 2 \frac{dq}{dr} \arctan \left(\frac{(R_0 - r)}{\sqrt{R_0^2 - r^2}} \tan \left(\frac{\theta}{2} \right) \right) \\
 &\quad + 2q \frac{1}{1 + \left(\frac{(R_0 - r)}{\sqrt{R_0^2 - r^2}} \tan \left(\frac{\theta}{2} \right) \right)^2} \tan \left(\frac{\theta}{2} \right) \frac{-R_0}{(R_0 + r) \sqrt{R_0^2 - r^2}}
 \end{aligned}$$

where use has been made of

$$\frac{d}{dx} \arctan(x) = \frac{1}{1 + x^2}$$

(I did not remember this formula and I use SymPy to obtain this.) These expressions are used to benchmark the numerical code that assume general flux surface shapes. The results show that the code gives correct result when concentric circular flux surfaces are used.

Taking the θ derivative of $\bar{\delta}$, equation (16.29) is written as (using SymPy)

$$\frac{\partial \bar{\delta}}{\partial \theta} = 2qA \left(\frac{\tan^2 \left(\frac{\theta}{2} \right)}{2} + \frac{1}{2} \right) \frac{1}{A^2 \tan^2 \left(\frac{\theta}{2} \right) + 1} \tag{16.36}$$

where

$$A = \frac{(R_0 - r)}{\sqrt{R_0^2 - r^2}} \quad (16.37)$$

Equation (16.26) should be equal to \hat{q} given by Eq. (16.26). This was verified numerically.

Taking the r derivative of Eq. (16.9), we obtain

$$\frac{d\Psi_p}{dr} = \frac{1}{q(r)} \frac{2\pi g_0 r}{\sqrt{R_0^2 - r^2}} \quad (16.38)$$

i.e.,

$$\frac{d\Psi}{dr} = \frac{1}{q(r)} \frac{g_0 r}{\sqrt{R_0^2 - r^2}}. \quad (16.39)$$

$$\frac{d\psi}{dr} = \frac{1}{\Psi(a) - \Psi(0)} \frac{1}{q(r)} \frac{g_0 r}{\sqrt{R_0^2 - r^2}}. \quad (16.40)$$

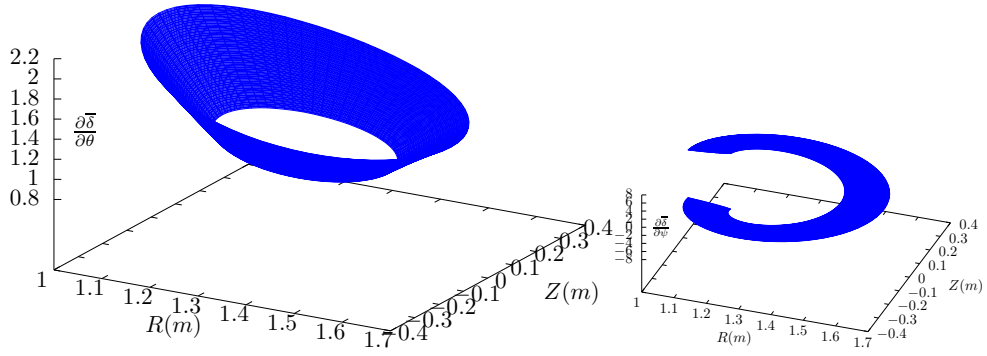


Figure 16.2. $\partial\bar{\delta}/\partial\theta$ and $\partial\bar{\delta}/\partial\psi$. Numerical and analytical results are plotted, which are so close to each other that they can not be distinguished by eyes. $\partial\bar{\delta}/\partial\theta$ is equal to the local safety factor \hat{q} . Note that $\partial\bar{\delta}/\partial\psi$ is discontinuous at the θ cut, which in this case is on the high-field-side.

16.5 Safety factor profile

The magnetic shear for a concentric-circular configuration is defined by

$$\hat{s} = \frac{dq}{dr} \frac{r}{q}, \quad (16.41)$$

where r is the minor radius of a magnetic surface. The above expression can be re-arranged as

$$\hat{s} \frac{dr}{r} = \frac{dq}{q} \quad (16.42)$$

Integrating the above equation over r and assuming \hat{s} is a constant, we obtain

$$\hat{s} \int_{r_0}^r \frac{dr}{r} = \int_{r_0}^r \frac{dq}{q}, \quad (16.43)$$

Performing the integration, the above equation is written as

$$\hat{s}(\ln r - \ln r_0) = \ln q - \ln q_0, \quad (16.44)$$

where $q_0 = q(r_0)$. Equation (16.44) can be finally written as

$$q = q_0 \left(\frac{r}{r_0} \right)^{\hat{s}}. \quad (16.45)$$

This is a profile with a constant magnetic shear s . In Ben's toroidal ITG simulation, the following q profile is used:

$$q = q_0 + (r - r_0)q'(r_0), \quad (16.46)$$

with $q'(r_0) = \hat{s}q_0/r_0$. This is a linear profile over r , with the values of q and the shear at $r = r_0$ being q_0 and \hat{s} , respectively.

17 Fixed boundary tokamak equilibrium problem

The fixed boundary equilibrium problem (also called the “inverse equilibrium problem” by some authors) refers to the case where the shape of a boundary magnetic surface is given and one is asked to solve the equilibrium within this magnetic surface. To make it convenient to deal with the shape of the boundary, one usually uses a general coordinates system which has one coordinate surface coinciding with the given magnetic surface. This makes it trivial to deal with the irregular boundary. To obtain the equilibrium, one needs to solve the GS equation in the general coordinate system.

17.1 Toroidal elliptic operator in general coordinates

Next we derive the form of the GS equation in a general coordinate system. The main task is to derive the form of the toroidal elliptic operator in the general coordinate system. The toroidal elliptic operator takes the form

$$\Delta^* \Psi \equiv R^2 \nabla \cdot \left(\frac{1}{R^2} \nabla \Psi \right) \quad (17.1)$$

For an arbitrary general coordinate system (ψ, θ, ϕ) (the (ψ, θ, ϕ) coordinate system here is an arbitrary general coordinate system except that $\nabla\phi$ is perpendicular to both $\nabla\psi$ and $\nabla\theta$), the toroidal elliptic operator is written

$$\Delta^*\Psi = \frac{R^2}{\mathcal{J}} \left\{ \left[\Psi_\psi \frac{\mathcal{J}}{R^2} |\nabla\psi|^2 \right]_\psi + \left[\Psi_\theta \frac{\mathcal{J}}{R^2} |\nabla\theta|^2 \right]_\theta + \left[\Psi_\psi \frac{\mathcal{J}}{R^2} (\nabla\psi \cdot \nabla\theta) \right]_\theta + \left[\Psi_\theta \frac{\mathcal{J}}{R^2} \nabla\theta \cdot \nabla\psi \right]_\psi \right\}, \quad (17.2)$$

where the subscripts denotes partial derivatives, \mathcal{J} is the Jacobian of the coordinate system (ψ, θ, ϕ) . [Next, we provide the proof of Eq. (17.2). The gradient of Ψ is written as (note that Ψ is independent of ϕ)

$$\nabla\Psi = \frac{\partial\Psi}{\partial\psi} \nabla\psi + \frac{\partial\Psi}{\partial\theta} \nabla\theta \quad (17.3)$$

Using this expression and the divergence formula (10.37), the elliptic operator in Eq. (17.1) is written

$$\begin{aligned} \Delta^*\Psi &= R^2 \nabla \cdot \left(\frac{1}{R^2} \frac{\partial\Psi}{\partial\psi} \nabla\psi + \frac{1}{R^2} \frac{\partial\Psi}{\partial\theta} \nabla\theta \right) \\ &= R^2 \frac{1}{\mathcal{J}} \frac{\partial}{\partial\psi} \left(\mathcal{J} \frac{1}{R^2} \frac{\partial\Psi}{\partial\psi} \nabla\psi \cdot \nabla\psi + \mathcal{J} \frac{1}{R^2} \frac{\partial\Psi}{\partial\theta} \nabla\theta \cdot \nabla\psi \right) \\ &\quad + R^2 \frac{1}{\mathcal{J}} \frac{\partial}{\partial\theta} \left(\mathcal{J} \frac{1}{R^2} \frac{\partial\Psi}{\partial\psi} \nabla\psi \cdot \nabla\theta + \mathcal{J} \frac{1}{R^2} \frac{\partial\Psi}{\partial\theta} \nabla\theta \cdot \nabla\theta \right) \\ &= \frac{R^2}{\mathcal{J}} \left[\left(\Psi_\psi \frac{\mathcal{J}}{R^2} |\nabla\psi|^2 \right)_\psi + \left(\Psi_\theta \frac{\mathcal{J}}{R^2} |\nabla\theta|^2 \right)_\theta + \left(\Psi_\psi \frac{\mathcal{J}}{R^2} \nabla\psi \cdot \nabla\theta \right)_\theta + \right. \\ &\quad \left. \left(\Psi_\theta \frac{\mathcal{J}}{R^2} \nabla\theta \cdot \nabla\psi \right)_\psi \right], \end{aligned} \quad (17.4)$$

which is Eq. (17.2).]

Using Eq. (17.2), the GS equation (5.13) is written

$$\begin{aligned} \frac{R^2}{\mathcal{J}} \left[\left(\Psi_\psi \frac{\mathcal{J}}{R^2} |\nabla\psi|^2 \right)_\psi + \left(\Psi_\theta \frac{\mathcal{J}}{R^2} |\nabla\theta|^2 \right)_\theta + \left(\Psi_\psi \frac{\mathcal{J}}{R^2} \nabla\psi \cdot \nabla\theta \right)_\theta + \left(\Psi_\theta \frac{\mathcal{J}}{R^2} \nabla\theta \cdot \nabla\psi \right)_\psi \right] \\ = -\mu_0 R^2 \frac{dP}{d\Psi} - \frac{dg}{d\Psi} g, \end{aligned} \quad (17.5)$$

which is the form of the GS equation in (ψ, θ, ϕ) coordinate system.

17.2 Finite difference form of toroidal elliptic operator in general coordinate system

The toroidal elliptic operator in Eq. (17.2) can be written

$$\Delta^*\Psi = \frac{R^2}{\mathcal{J}} [(h^{\psi\psi}\Psi_\psi)_\psi + (h^{\theta\theta}\Psi_\theta)_\theta + (h^{\psi\theta}\Psi_\theta)_\psi + (h^{\theta\psi}\Psi_\psi)_\theta], \quad (17.6)$$

where $h^{a\beta}$ is defined by Eq. (10.78), i.e.,

$$h^{\alpha\beta} = \frac{\mathcal{J}}{R^2} \nabla \alpha \cdot \nabla \beta. \quad (17.7)$$

Next, we derive the finite difference form of the toroidal elliptic operator. The finite difference form of the term $(h^{\psi\psi}\Psi_\psi)_\psi$ is written

$$\begin{aligned} (h^{\psi\psi}\Psi_\psi)_\psi|_{i,j} &= \frac{1}{\delta\psi} \left[h_{i,j+1/2}^{\psi\psi} \left(\frac{\Psi_{i,j+1} - \Psi_{i,j}}{\delta\psi} \right) - h_{i,j-1/2}^{\psi\psi} \left(\frac{\Psi_{i,j} - \Psi_{i,j-1}}{\delta\psi} \right) \right] \\ &= H_{i,j+1/2}^{\psi\psi} (\Psi_{i,j+1} - \Psi_{i,j}) - H_{i,j-1/2}^{\psi\psi} (\Psi_{i,j} - \Psi_{i,j-1}), \end{aligned} \quad (17.8)$$

where

$$H^{\psi\psi} = \frac{h^{\psi\psi}}{(\delta\psi)^2}. \quad (17.9)$$

The finite difference form of $(h^{\theta\theta}\Psi_\theta)_\theta$ is written

$$\begin{aligned} (h^{\theta\theta}\Psi_\theta)_\theta|_{i,j} &= \frac{1}{\delta\theta} \left[h_{i+1/2,j}^{\theta\theta} \left(\frac{\Psi_{i+1,j} - \Psi_{i,j}}{\delta\theta} \right) - h_{i-1/2,j}^{\theta\theta} \left(\frac{\Psi_{i,j} - \Psi_{i-1,j}}{\delta\theta} \right) \right] \\ &= H_{i+1/2,j}^{\theta\theta} (\Psi_{i+1,j} - \Psi_{i,j}) - H_{i-1/2,j}^{\theta\theta} (\Psi_{i,j} - \Psi_{i-1,j}), \end{aligned} \quad (17.10)$$

where

$$H^{\theta\theta} = \frac{h^{\theta\theta}}{(\delta\theta)^2}. \quad (17.11)$$

The finite difference form of $(h^{\psi\theta}\Psi_\theta)_\psi$ is written as

$$\begin{aligned} (\Psi_\theta h^{\psi\theta})_\psi|_{i,j} &= \frac{1}{\delta\psi} \left[h_{i,j+1/2}^{\psi\theta} \left(\frac{\Psi_{i+1,j+1/2} - \Psi_{i-1,j+1/2}}{2\delta\theta} \right) - h_{i,j-1/2}^{\psi\theta} \left(\frac{\Psi_{i+1,j-1/2} - \Psi_{i-1,j-1/2}}{2\delta\theta} \right) \right]. \end{aligned} \quad (17.12)$$

Approximating the value of Ψ at the grid centers by the average of the value of Ψ at the neighbor grid points, Eq. (17.12) is written as

$$\begin{aligned} (\Psi_\theta h^{\psi\theta})_\psi|_{i,j} &= H_{i,j+1/2}^{\psi\theta} (\Psi_{i+1,j} + \Psi_{i+1,j+1} - \Psi_{i-1,j} - \Psi_{i-1,j+1}) - H_{i,j-1/2}^{\psi\theta} (\Psi_{i+1,j-1} + \Psi_{i+1,j} - \Psi_{i-1,j-1} - \Psi_{i-1,j}). \end{aligned} \quad (17.13)$$

where

$$H^{\psi\theta} = \frac{h^{\psi\theta}}{4\delta\psi d\theta}. \quad (17.14)$$

Similarly, the finite difference form of $(h^{\psi\theta}\Psi_\psi)_\theta$ is written as

$$\begin{aligned}
 (\Psi_\psi h^{\psi\theta})_\theta|_{i,j} &= \frac{1}{\delta\theta} \left[h_{i+1/2,j}^{\psi\theta} \left(\frac{\Psi_{i+1/2,j+1} - \Psi_{i+1/2,j-1}}{2\delta\psi} \right) - \right. \\
 &\quad \left. h_{i-1/2,j}^{\psi\theta} \left(\frac{\Psi_{i-1/2,j+1} - \Psi_{i-1/2,j-1}}{2\delta\psi} \right) \right] \\
 &= H_{i+1/2,j}^{\psi\theta} (\Psi_{i+1,j+1} + \Psi_{i,j+1} - \Psi_{i+1,j-1} - \Psi_{i,j-1}) - \\
 &\quad H_{i-1/2,j}^{\psi\theta} (\Psi_{i,j+1} + \Psi_{i-1,j+1} - \Psi_{i,j-1} - \Psi_{i-1,j-1}). \quad (17.15)
 \end{aligned}$$

Using the above results, the finite difference form of the operator $\mathcal{J}\Delta^*\Psi/R^2$ is written as

$$\begin{aligned}
 \frac{\mathcal{J}}{R^2} \Delta^* \Psi \Big|_{i,j} &= (h^{\psi\theta}\Psi_\theta)_\psi + (h^{\psi\psi}\Psi_\psi)_\psi + (h^{\theta\theta}\Psi_\theta)_\theta + (h^{\psi\theta}\Psi_\psi)_\theta \\
 &= H_{i,j+1/2}^{\psi\psi} (\Psi_{i,j+1} - \Psi_{i,j}) - H_{i,j-1/2}^{\psi\psi} (\Psi_{i,j} - \Psi_{i,j-1}) \\
 &\quad + H_{i+1/2,j}^{\theta\theta} (\Psi_{i+1,j} - \Psi_{i,j}) - H_{i-1/2,j}^{\theta\theta} (\Psi_{i,j} - \Psi_{i-1,j}) \\
 &\quad + H_{i,j+1/2}^{\psi\theta} (\Psi_{i+1,j} + \Psi_{i+1,j+1} - \Psi_{i-1,j} - \Psi_{i-1,j+1}) - \\
 &\quad H_{i,j-1/2}^{\psi\theta} (\Psi_{i+1,j-1} + \Psi_{i+1,j} - \Psi_{i-1,j-1} - \Psi_{i-1,j}) \\
 &\quad + H_{i+1/2,j}^{\psi\theta} (\Psi_{i+1,j+1} + \Psi_{i,j+1} - \Psi_{i+1,j-1} - \Psi_{i,j-1}) - \\
 &\quad H_{i-1/2,j}^{\psi\theta} (\Psi_{i,j+1} + \Psi_{i-1,j+1} - \Psi_{i-1,j-1} - \Psi_{i,j-1}) \\
 &= \Psi_{i,j} (-H_{i,j+1/2}^{\psi\psi} - H_{i,j-1/2}^{\psi\psi} - H_{i+1/2,j}^{\theta\theta} - H_{i-1/2,j}^{\theta\theta}) \\
 &\quad + \Psi_{i-1,j-1} (H_{i,j-1/2}^{\psi\theta} + H_{i-1/2,j}^{\psi\theta}) + \Psi_{i,j-1} (H_{i,j-1/2}^{\psi\psi} - H_{i+1/2,j}^{\psi\theta} + \\
 &\quad H_{i-1/2,j}^{\psi\theta}) \\
 &\quad + \Psi_{i+1,j-1} (-H_{i,j-1/2}^{\psi\theta} - H_{i+1/2,j}^{\psi\theta}) + \Psi_{i-1,j} (H_{i-1/2,j}^{\theta\theta} - H_{i,j+1/2}^{\psi\theta} + \\
 &\quad H_{i,j-1/2}^{\psi\theta}) \\
 &\quad + \Psi_{i+1,j} (H_{i+1/2,j}^{\theta\theta} + H_{i,j+1/2}^{\psi\theta} - H_{i,j-1/2}^{\psi\theta}) + \Psi_{i-1,j+1} (-H_{i,j+1/2}^{\psi\theta} - \\
 &\quad H_{i-1/2,j}^{\psi\theta}) \\
 &\quad + \Psi_{i,j+1} (H_{i,j+1/2}^{\psi\psi} + H_{i+1/2,j}^{\psi\theta} - H_{i-1/2,j}^{\psi\theta}) + \Psi_{i+1,j+1} (H_{i,j+1/2}^{\psi\theta} + \\
 &\quad H_{i+1/2,j}^{\psi\theta})
 \end{aligned}$$

The coefficients are given by

$$h^{\psi\psi} = \frac{\mathcal{J}}{R^2} |\nabla\psi|^2 = \frac{1}{\mathcal{J}} (R_\theta^2 + Z_\theta^2), \quad (17.16)$$

$$h^{\theta\theta} = \frac{\mathcal{J}}{R^2} |\nabla\theta|^2 = \frac{1}{\mathcal{J}} (R_\psi^2 + Z_\psi^2), \quad (17.17)$$

and

$$h^{\psi\theta} = \frac{\mathcal{J}}{R^2} \nabla\psi \cdot \nabla\theta = -\frac{1}{\mathcal{J}} (R_\theta R_\psi + Z_\theta Z_\psi), \quad (17.18)$$

where the Jacobian

$$\mathcal{J} = R(R_\theta Z_\psi - R_\psi Z_\theta). \quad (17.19)$$

The partial derivatives, R_θ , R_ψ , Z_θ , and Z_ψ , appearing in Eqs. (17.16)-(17.19) are calculated by using the central difference scheme. The values of $h^{\psi\psi}$, $h^{\theta\theta}$, $h^{\psi\theta}$ and \mathcal{J} at the middle points are approximated by the linear average of their values at the neighbor grid points.

17.3 Special treatment at coordinate origin, wrong! to be deleted

$$\Psi \approx a^{00} + a^{10}R + a^{01}Z + a^{11}RZ + a^{20}R^2 + a^{02}Z^2. \quad (17.20)$$

$$R = R_0 + b^{11}\sqrt{\psi}\cos\theta \quad (17.21)$$

$$Z = Z_0 + c^{11}\sqrt{\psi}\sin\theta \quad (17.22)$$

$$\begin{aligned} \Psi &\approx a^{00} + a^{10}(R_0 + b^{11}\sqrt{\psi}\cos\theta) + a^{01}c^{11}\sqrt{\psi}\sin\theta + a^{11}(R_0 + b^{11}\sqrt{\psi}\cos\theta)c^{11}\sqrt{\psi}\sin\theta + a^{20}(R_0 + b^{11}\sqrt{\psi}\cos\theta)^2 + a^{02}(c^{11}\sqrt{\psi}\sin\theta)^2 \\ &= a^{00} + a^{10}R_0 + a^{10}b^{11}\sqrt{\psi}\cos\theta + a^{01}c^{11}\sqrt{\psi}\sin\theta + a^{11}R_0c^{11}\sqrt{\psi}\sin\theta + \frac{1}{2}a^{11}b^{11}\sqrt{\psi}c^{11}\sqrt{\psi}\sin 2\theta + 2a^{20}R_0^2 + a^{20}(b^{11})^2\psi\cos^2\theta + 2a^{20}R_0b^{11}\sqrt{\psi}\cos\theta + a^{02}(c^{11})^2\psi\sin^2\theta \\ &= d_0 + d_1\sqrt{\psi}\cos\theta + d_2\sqrt{\psi}\sin\theta + d_3\psi\sin 2\theta + d_4\psi\cos^2\theta + d_5\psi\sin^2\theta \end{aligned}$$

$$\Psi = d_0 + d_1\sqrt{\psi}\cos\theta + d_2\sqrt{\psi}\sin\theta$$

$$R = R_0 + b^{11}\sqrt{\psi}\cos\theta + b^{12}\sqrt{\psi}\cos 2\theta + b^{21}(\sqrt{\psi})^2\cos\theta + b^{22}(\sqrt{\psi})^2\cos 2\theta \quad (17.23)$$

$$Z = Z_0 + c^{11}\sqrt{\psi}\sin\theta + c^{12}\sqrt{\psi}\sin 2\theta + c^{21}(\sqrt{\psi})^2\sin\theta + c^{22}(\sqrt{\psi})^2\sin 2\theta \quad (17.24)$$

17.4 Pressure and toroidal field function profile

The function $p(\Psi)$ and $g(\Psi)$ in the GS equation are free functions which must be specified by users before solving the GS equation. Next, we discuss one way to specify the free functions. Following Ref. [16], we take $P(\Psi)$ and $g(\Psi)$ to be of the forms

$$P(\Psi) = P_0 - (P_0 - P_b)\hat{p}(\bar{\Psi}), \quad (17.25)$$

$$\frac{1}{2}g^2(\Psi) = \frac{1}{2}g_0^2(1 - \gamma\hat{g}(\bar{\Psi})), \quad (17.26)$$

with \hat{p} and \hat{g} chosen to be of polynomial form:

$$\hat{p}(\bar{\Psi}) = \bar{\Psi}^\alpha, \quad (17.27)$$

$$\hat{g}(\bar{\Psi}) = \bar{\Psi}^\beta, \quad (17.28)$$

where

$$\bar{\Psi} \equiv \frac{\Psi - \Psi_a}{\Psi_b - \Psi_a}, \quad (17.29)$$

with Ψ_b the value of Ψ on the boundary, Ψ_a the value of Ψ on the magnetic axis, α , β , γ , P_0 , P_b , and g_0 are free parameters. Using the profiles of P and g given by Eqs. (17.25) and (17.26), we obtain

$$\frac{dP(\Psi)}{d\Psi} = -\frac{1}{\Delta}(P_0 - P_b)\alpha\bar{\Psi}^{\alpha-1} \quad (17.30)$$

where $\Delta = \Psi_b - \Psi_a$, and

$$g \frac{dg}{d\Psi} = -\frac{1}{2}g_0^2\gamma\frac{1}{\Delta}\beta\bar{\Psi}^{\beta-1}. \quad (17.31)$$

Then the term on the r.h.s (nonlinear source term) of the GS equation is written

$$-\mu_0 R^2 \frac{dP}{d\Psi} - \frac{dg}{d\Psi} g = \mu_0 R^2 \left[\frac{1}{\Delta}(P_0 - P_b)\alpha\bar{\Psi}^{\alpha-1} \right] + \frac{1}{2}g_0^2\gamma\frac{1}{\Delta}\beta\bar{\Psi}^{\beta-1}. \quad (17.32)$$

The value of parameters P_0 , P_b , and g_0 in Eqs. (17.25) and (17.26), and the value of α and β in Eqs. (17.27) and (17.28) can be chosen arbitrarily. The parameter γ is used to set the value of the total toroidal current. The toroidal current density is given by Eq. (A.59), i.e.,

$$J_\phi = R \frac{dP}{d\Psi} + \frac{1}{\mu_0} \frac{dg}{d\Psi} \frac{g}{R}, \quad (17.33)$$

which can be integrated over the poloidal cross section within the boundary magnetic surface to give the total toroidal current,

$$\begin{aligned} I_\phi &= \int J_\phi dS \\ &= \int \left(R \frac{dP}{d\Psi} + \frac{1}{\mu_0} \frac{dg}{d\Psi} \frac{g}{R} \right) dR dZ \\ &= \int \left[R \left(-\frac{1}{\Delta} \right) (P_0 - P_b) \hat{p}'(\bar{\Psi}) - \frac{1}{\mu_0 R} \frac{1}{2} g_0^2 \gamma \frac{1}{\Delta} \hat{g}'(\bar{\Psi}) \right] dR dZ \end{aligned} \quad (17.34)$$

Using

$$dRdZ = \frac{1}{R} \mathcal{J} d\psi d\theta, \quad (17.35)$$

Eq. (17.34) is written as

$$I_\phi = \int \left[\left(-\frac{1}{\Delta} \right) (P_0 - P_b) \hat{p}'(\bar{\Psi}) - \frac{1}{\mu_0 R^2} \frac{1}{2} g_0^2 \gamma \frac{1}{\Delta} \hat{g}'(\bar{\Psi}) \right] \mathcal{J} d\psi d\theta, \quad (17.36)$$

from which we solve for γ , giving

$$\gamma = \frac{-\Delta I_\phi - (P_0 - P_b) \int [\hat{p}'(\bar{\Psi})] \mathcal{J} d\psi d\theta}{\frac{1}{2\mu_0} g_0^2 \int \left[\frac{1}{R^2} \hat{g}'(\bar{\Psi}) \right] \mathcal{J} d\psi d\theta}. \quad (17.37)$$

If the total toroidal current I_ϕ is given, Eq. (17.37) can be used to determine the value of γ .

17.5 Boundary magnetic surface and initial coordinates

In the fixed boundary equilibrium problem, the shape of the boundary magnetic surface (it is also the boundary of the computational region) is given while the shape of the inner flux surface is to be solved. A simple analytical expression for a D-shaped magnetic surface takes the form

$$R = R_0 + a \cos(\theta + \Delta \sin \theta), \quad (17.38)$$

$$Z = \kappa a \sin \theta, \quad (17.39)$$

with θ changing from 0 to 2π . According to the definition in Eqs. (A.1), (A.2), and (A.4) we can readily verify that the parameters a , R_0 , κ appearing in Eqs. (17.38) and (17.39) are indeed the minor radius, major radius, and ellipticity, respectively. According to the definition of triangularity Eq. (A.3), the triangularity δ for the magnetic surface defined by Eqs. (17.38) and (17.39) is written as

$$\delta = \sin \Delta. \quad (17.40)$$

Another common expression for the shape of a magnetic surface was given by Miller[8, 22], which is written as

$$R = R_0 + a \cos[\theta + \arcsin(\Delta \sin \theta)], \quad (17.41)$$

$$Z = \kappa a \sin \theta. \quad (17.42)$$

Note that Miller's formula is only slightly different from the formula (17.38). For Miller's formula, it is easy to prove that the triangularity δ is equal to Δ (instead of $\delta = \sin \Delta$ as given in Eq. (17.40)).

In the iterative metric method[11] for solving the fixed boundary equilibrium problem, we need to provide an initial guess of the shape of the inner flux surface (this initial guess is used to construct a initial generalized coordinates system). A common guess of the inner flux surfaces is given by

$$R = \psi^\alpha (R_{\text{LCFS}} - R_0) + R_0, \quad (17.43)$$

$$Z = \psi^\alpha Z_{\text{LCFS}}, \quad (17.44)$$

where α is a parameter, ψ is a label parameter of flux surface. If the shape of the LCFS is given by Eqs. (17.38) and (17.39), then Eqs. (17.43) and (17.44) are written as

$$R = R_0 + \psi^\alpha a \cos(\theta + \Delta \sin \theta), \quad (17.45)$$

$$Z = \psi^\alpha \kappa a \sin \theta. \quad (17.46)$$

Fig. 17.1 plots the shape given by Eqs. (17.45) and (17.46) for $a = 0.4$, $R_0 = 1.7$, $\kappa = 1.7$, $\Delta = \arcsin(0.6)$, and $\alpha = 1$ with ψ varying from zero to one.

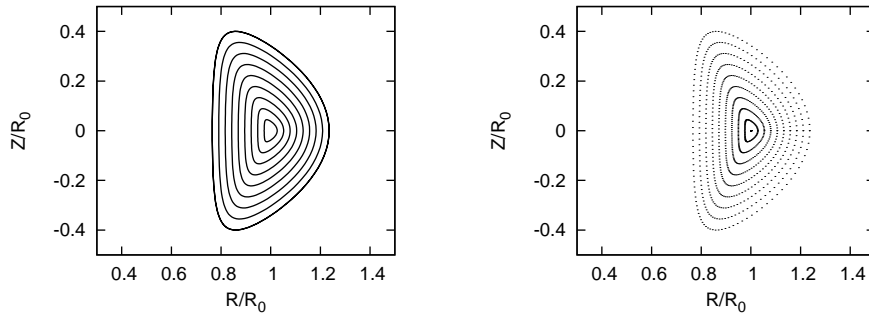


Figure 17.1. Shape of flux surface given by Eqs. (17.45) and (17.46). Left figure: points with the same value of ψ are connected to show ψ coordinate surface; Right figure: dot plot. Parameters are $a = 0.4\text{m}$, $R_0 = 1.7\text{m}$, $\kappa = 1.7$, $\Delta = \arcsin(0.6)$, $\alpha = 1$ with ψ varying from zero (center) to one (boundary). The shape parameters of LCFS are chosen according to the parameters of EAST tokamak.

17.6 Fixed boundary equilibrium numerical code

The tokamak equilibrium problem where the shape of the LCFS is given is called fixed boundary equilibrium problem. I wrote a numerical code that uses the iterative metric method[11] to solve this kind of equilibrium problem. Figure 17.2 describes the steps involved in the iterative metric method.

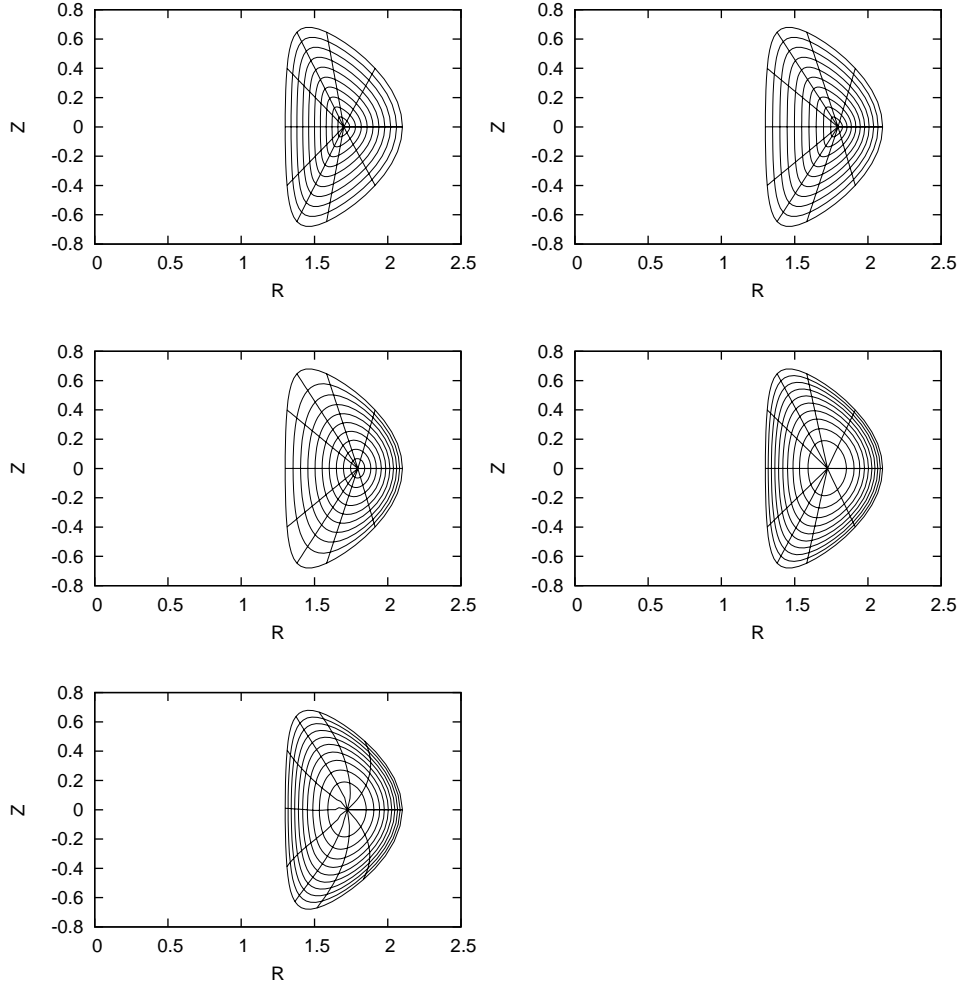


Figure 17.2. Upper left figure plots the initial coordinate surfaces. After solving the GS equation to obtain the location of the magnetic axis, I shift the origin point of the initial coordinate system to the location of the magnetic axis (upper right figure). Then, reshape the coordinate surface so that the coordinate surfaces $\psi = \text{const}$ lies on magnetic surfaces (middle left figure). Recalculate the radial coordinate ψ that is consistent with the Jacobian constraint and interpolate flux surface to uniform ψ coordinates (middle right figure). Recalculate the poloidal coordinate θ that is consistent with the Jacobian constraint and interpolate poloidal points on every flux surface to uniform θ coordinates (bottom left figure).

17.7 Benchmark of the code

To benchmark the numerical code, I set the profile of P and g according to Eqs. (A.11) and (A.12) with the parameters $c_2 = 0$, $c_1 = B_0(\kappa_0^2 + 1) / (R_0^2 \kappa_0 q_0)$, $\kappa_0 = 1.5$,

and $q_0 = 1.5$. The comparison of the analytic and numerical results are shown in Fig. 17.3.

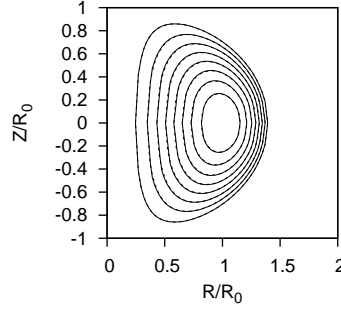


Figure 17.3. Agreement between the magnetic surfaces (contours of Ψ) given by the Solovév analytic formula and those calculated by the numerical code. The two sets of magnetic surfaces are indistinguishable at this scale. The boundary magnetic surface is selected by the requirement that $\bar{\Psi} = 0.11022$ in the Solovév formula (A.17). Parameters: $\kappa_0 = 1.5$, $q_0 = 1.5$.

Note that the parameter c_0 in the Solovév equilibrium seems to be not needed in the numerical calculation. In fact this impression is wrong: the c_0 parameter is actually needed in determining the boundary magnetic surface of the numerical equilibrium (in the case considered here c_0 is chosen as $c_0 = B_0 / (R_0^2 \kappa_0 q_0)$).

17.8 Low-beta equilibrium vs. high-beta equilibrium

With the pressure increasing, the magnetic axis usually shifts to the low-field-side of the device, as is shown in Fig. 17.4.

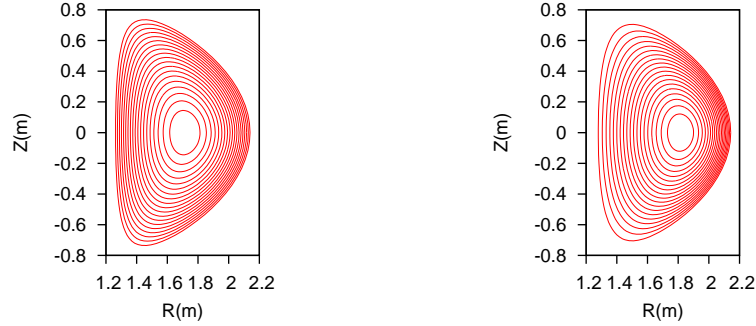


Figure 17.4. Comparison of two equilibria obtained with $P_0 = 10^4$ Pasca (left) and $P_0 = 10^5$ Pasca (right), respectively, where P_0 is the pressure at the magnetic axis. All the other parameters are the same for the two equilibria, $\alpha = 1.0$, $\beta = 1.0$, $P_b = 10^{-1}$ Pasca, $g_0 = 1.0Tm$, $I_\phi = 500kA$, and the LCFS is given by miller's formulas (17.41) and (17.42) with $R_0 = 1.7$, $a = 0.45$, $\kappa = 1.7$, and $\delta = 0.6$.

17.9 Analytical form of Jacobian (need cleaning up)

Consider the Jacobian of the form

$$\mathcal{J} = \mu \left(\frac{R}{R_0} \right)^m \psi^n, \quad (17.47)$$

where m and n are arbitrary integers which can be appropriately chosen by users, μ_0 and R_0 are constants included for normalization. In the iterative metric method of solving fixed boundary equilibrium problem, we first construct a coordinates transformation $(\theta, \psi) \rightarrow (R(\theta, \psi), Z(\theta, \psi))$ (this transformation is arbitrary except for that surface $\psi = 1$ coincides with the last closed flux surface), then solve the GS equation in (θ, ψ) coordinate system to get the value of Ψ at grid points, and finally adjust the value of $(R(\theta, \psi), Z(\theta, \psi))$ to make surface $\psi = \text{const}$ lies on a magnetic surface. It is obvious the Jacobian of the final transformation we obtained usually does not satisfy the constraint given by Eq. (17.47) since we do not use any information of Eq. (17.47) in the above steps. Now comes the question: how to make the transformation obtained above satisfy the constraint Eq. (17.47) through adjusting the values of θ ? To make the constraint Eq. (17.47) satisfied, θ and ψ should satisfy the relation

$$\mathcal{J}(\theta, \psi) = \mu \left[\frac{R(\theta, \psi)}{R_0} \right]^m \psi^n, \quad (17.48)$$

which

Using Eq. (), we obtain

$$\begin{aligned} \int_0^\theta d\theta &= \int_0^\theta d\theta \frac{\mathcal{J}}{\psi^n \mu} \left(\frac{R_0}{R} \right)^m \\ \theta &= \int_0^\theta d\theta \frac{\mathcal{J}}{\psi^n \mu} \left(\frac{R_0}{R} \right)^m \end{aligned} \quad (17.49)$$

normalized to 2π , the normalized θ is written as

$$\theta = 2\pi \frac{\int_0^\theta d\theta \frac{\mathcal{J}}{\psi^n \mu} \left(\frac{R_0}{R} \right)^m}{\int_0^{2\pi} d\theta \frac{\mathcal{J}}{\psi^n \mu} \left(\frac{R_0}{R} \right)^m} = 2\pi \frac{\int_0^\theta d\theta \mathcal{J} \left(\frac{1}{R} \right)^m}{\int_0^{2\pi} d\theta \mathcal{J} \left(\frac{1}{R} \right)^m} \quad (17.50)$$

17.10 Grad-Shafranov equation with prescribed safety factor profile (to be finished)

In the GS equation, $g(\Psi)$ is one of the two free functions which can be prescribed by users. In some cases, we want to specify the safety factor profile $q(\Psi)$, instead of $g(\Psi)$, in solving the GS equation. Next, we derive the form of the GS equation that contains $q(\Psi)$, rather than $g(\Psi)$, as a free function. The safety factor defined

in Eq. (10.87) can be written

$$q(\psi) = -\frac{1}{2\pi} \frac{g}{\Psi'} \int_0^{2\pi} \frac{\mathcal{J}}{R^2} d\theta \quad (17.51)$$

$$= -\frac{1}{2\pi} \frac{g}{\Psi'} \frac{\int_0^{2\pi} R^{-2} \mathcal{J} d\theta}{\int_0^{2\pi} \mathcal{J} d\theta} \int_0^{2\pi} \mathcal{J} d\theta$$

$$= -\frac{1}{2\pi} \frac{g}{\Psi'} \langle R^{-2} \rangle \int_0^{2\pi} \mathcal{J} d\theta \quad (17.52)$$

$$= -\text{sgn}(\mathcal{J}) \frac{V'}{(2\pi)^2} \frac{\langle R^{-2} \rangle}{\Psi'} g. \quad (17.53)$$

Equation (17.53) gives the relation between the safety factor q and the toroidal field function g . This relation can be used in the GS equation to eliminate g in favor of q , which gives

$$g = -\text{sgn}(\mathcal{J}) \frac{(2\pi)^2}{V' \langle R^{-2} \rangle} \Psi' q. \quad (17.54)$$

$$\Rightarrow \frac{dg}{d\Psi} g = \frac{(2\pi)^2}{V' \langle R^{-2} \rangle} q \left[\frac{(2\pi)^2}{V' \langle R^{-2} \rangle} q \Psi' \right]_{\psi}. \quad (17.55)$$

Note that this expression involves the flux surface average, which depends on the flux surface shape and the shape is unknown before Ψ is determined.

Multiplying Eq. (A.82) by R^{-2} gives

$$\frac{1}{\mathcal{J}} \left[\left(\Psi' \frac{\mathcal{J}}{R^2} |\nabla \psi|^2 \right)_{\psi} + \left(\Psi' \frac{\mathcal{J}}{R^2} (\nabla \psi \cdot \nabla \theta) \right)_{\theta} \right] + \mu_0 \frac{dp}{d\Psi} + R^{-2} \frac{dg}{d\Psi} g = 0. \quad (17.56)$$

Surface-averaging the above equation, we obtain

$$\frac{2\pi}{V'} \int d\theta \left[\left(\Psi' \frac{\mathcal{J}}{R^2} |\nabla \psi|^2 \right)_{\psi} + \left(\Psi' \frac{\mathcal{J}}{R^2} (\nabla \psi \cdot \nabla \theta) \right)_{\theta} \right] + \mu_0 \frac{dp}{d\Psi} + \langle R^{-2} \rangle \frac{dg}{d\Psi} g = 0, \quad (17.57)$$

$$\Rightarrow \frac{2\pi}{V'} \int d\theta \left(\Psi' \frac{\mathcal{J}}{R^2} |\nabla \psi|^2 \right)_{\psi} + \mu_0 \frac{dp}{d\Psi} + \langle R^{-2} \rangle \frac{dg}{d\Psi} g = 0, \quad (17.58)$$

$$\Rightarrow \frac{2\pi}{V'} \left[\Psi' \int d\theta \left(\mathcal{J} \frac{|\nabla \psi|^2}{R^2} \right) \right]_{\psi} + \mu_0 \frac{dp}{d\Psi} + \langle R^{-2} \rangle \frac{dg}{d\Psi} g = 0, \quad (17.59)$$

$$\Rightarrow \frac{1}{V'} \left[V' \Psi' \left\langle \frac{|\nabla \psi|^2}{R^2} \right\rangle \right]_{\psi} + \mu_0 \frac{dp}{d\Psi} + \langle R^{-2} \rangle \frac{dg}{d\Psi} g = 0. \quad (17.60)$$

$$\Rightarrow \left[V' \Psi' \left\langle \frac{|\nabla \psi|^2}{R^2} \right\rangle \right]_{\psi} + \mu_0 V' \frac{dp}{d\Psi} + \langle R^{-2} \rangle V' \frac{dg}{d\Psi} g = 0, \quad (17.61)$$

Substitute Eq. (17.55) into the above equation to eliminate $gdg/d\Psi$, we obtain

$$\Rightarrow \left[V' \Psi' \left\langle \frac{|\nabla \psi|^2}{R^2} \right\rangle \right]_{\psi} + \mu_0 V' \frac{dp}{d\Psi} + q(2\pi)^4 \left[\frac{q \Psi'}{V' \langle R^{-2} \rangle} \right]_{\psi} = 0, \quad (17.62)$$

Eq. (17.62) agrees with Eq. (5.55) in Ref. [16].

$$\Rightarrow V' \left\langle \frac{|\nabla \psi|^2}{R^2} \right\rangle \Psi'' + \left[V' \left\langle \frac{|\nabla \psi|^2}{R^2} \right\rangle \right]_{\psi} \Psi' + \mu_0 V' \frac{dp}{d\Psi} + q(2\pi)^4 \left[\frac{q}{V' \langle R^{-2} \rangle} \right] \Psi'' + q(2\pi)^4 \left[\frac{q}{V' \langle R^{-2} \rangle} \right]_{\psi} \Psi' = 0 \quad (17.63)$$

$$\Rightarrow \Psi'' = - \frac{1}{V'D} \left\{ \left[V' \left\langle \frac{|\nabla \psi|^2}{R^2} \right\rangle \right]_{\psi} \Psi' + q(2\pi)^4 \left[\frac{q}{V' \langle R^{-2} \rangle} \right]_{\psi} \Psi' + \mu_0 V' \frac{dp}{d\Psi} \right\} \quad (17.64)$$

where

$$D = \left\langle \frac{|\nabla \psi|^2}{R^2} \right\rangle + \frac{(2\pi)^4}{\langle R^{-2} \rangle} \left(\frac{q}{V'} \right)^2 \quad (17.65)$$

The GS equation is

$$\Delta^* \Psi = -\mu_0 R^2 \frac{dp}{d\Psi} - g \frac{dg}{d\Psi} \quad (17.66)$$

$$\Rightarrow \Delta^* \Psi = -\mu_0 R^2 \frac{dp}{d\Psi} - \frac{q(2\pi)^4}{V' \langle R^{-2} \rangle} \left[\frac{q \Psi'}{V' \langle R^{-2} \rangle} \right]_{\psi} \quad (17.67)$$

$$\Rightarrow \Delta^* \Psi = -\mu_0 R^2 \frac{dp}{d\Psi} - \frac{q(2\pi)^4}{V' \langle R^{-2} \rangle} \left\{ \left[\frac{q}{V' \langle R^{-2} \rangle} \right]_{\psi} \Psi' + \left[\frac{q}{V' \langle R^{-2} \rangle} \right] \Psi'' \right\} \quad (17.68)$$

Using Eq. (17.64) to eliminate Ψ'' in the above equation, the coefficients before $(-\mu_0 dp/d\Psi)$ is written as

$$\begin{aligned} B &= R^2 - \frac{q(2\pi)^4}{V' \langle R^{-2} \rangle} \left\{ \left[\frac{q}{V' \langle R^{-2} \rangle} \right] \frac{1}{V'D} V' \right\} \\ &= \frac{1}{D} \left\{ R^2 D - \left(\frac{q}{V'} \right)^2 \frac{(2\pi)^4}{\langle R^{-2} \rangle^2} \right\}. \end{aligned} \quad (17.69)$$

Substituting the expression of D into the above equation, we obtain

$$\begin{aligned} B &= \frac{1}{D} \left\{ R^2 \left\langle \frac{|\nabla \psi|^2}{R^2} \right\rangle + R^2 \frac{(2\pi)^4}{\langle R^{-2} \rangle} \left(\frac{q}{V'} \right)^2 - \left(\frac{q}{V'} \right)^2 \frac{(2\pi)^4}{\langle R^{-2} \rangle^2} \right\} \\ &= \frac{1}{D} \left\{ R^2 \left\langle \frac{|\nabla \psi|^2}{R^2} \right\rangle + \left(\frac{q}{V'} \right)^2 \frac{(2\pi)^4}{\langle R^{-2} \rangle} \left(R^2 - \frac{1}{\langle R^{-2} \rangle} \right) \right\}, \end{aligned} \quad (17.70)$$

which is equal to the expression (5.58) in Ref. [16]. The coefficient before Ψ' is written as

$$\begin{aligned} A &= - \frac{q(2\pi)^4}{V' \langle R^{-2} \rangle} \left\{ \left[\frac{q}{V' \langle R^{-2} \rangle} \right]_{\psi} - \left[\frac{q}{V' \langle R^{-2} \rangle} \right] \frac{1}{V'D} \left(V' \left\langle \frac{|\nabla \psi|^2}{R^2} \right\rangle \right)_{\psi} + \right. \\ &\quad \left. q(2\pi)^4 \left[\frac{q}{V' \langle R^{-2} \rangle} \right]_{\psi} \right\} \end{aligned}$$

Define

$$\alpha = \left\langle \frac{|\nabla \psi|^2}{R^2} \right\rangle,$$

$$\beta = \frac{q}{V' \langle R^{-2} \rangle}.$$

$$\begin{aligned} A &= -(2\pi)^4 \beta \left\{ \beta_\psi - \beta \frac{1}{V'D} [(V'\alpha)_\psi + q(2\pi)^4 \beta_\psi] \right\} \\ \Rightarrow \frac{D}{-(2\pi)^4 \beta} A &= D\beta_\psi - \beta \frac{1}{V'} [(V'\alpha)_\psi + q(2\pi)^4 \beta_\psi] \end{aligned} \quad (17.71)$$

$$\Rightarrow \frac{D}{-\beta(2\pi)^4} A = D\beta_\psi - \beta \frac{1}{V'} [V''\alpha + V'\alpha_\psi + q(2\pi)^4 \beta_\psi] \quad (17.72)$$

Using

$$D = \alpha + (2\pi)^4 \langle R^{-2} \rangle \beta^2 \quad (17.73)$$

Eq. () is written as

$$\begin{aligned} \Rightarrow \frac{D}{-\beta(2\pi)^4} A &= \alpha\beta_\psi + (2\pi)^4 \langle R^{-2} \rangle \beta^2 \beta_\psi - \beta \frac{1}{V'} V''\alpha - \beta \frac{1}{V'} V'\alpha_\psi - \\ &\quad \beta \frac{1}{V'} q(2\pi)^4 \beta_\psi \end{aligned} \quad (17.74)$$

$$\begin{aligned} \Rightarrow \frac{D}{-\beta(2\pi)^4} A &= \alpha\beta_\psi + (2\pi)^4 \langle R^{-2} \rangle \beta^2 \beta_\psi - \beta \frac{1}{V'} V''\alpha - \beta\alpha_\psi - \\ &\quad \beta \frac{1}{V'} q(2\pi)^4 \beta_\psi \end{aligned} \quad (17.75)$$

$$\begin{aligned} \frac{A}{-\beta(2\pi)^4} D &= \alpha\beta_\psi + (2\pi)^4 \langle R^{-2} \rangle \beta^2 \beta_\psi - \beta \frac{1}{V'} V''\alpha - \beta\alpha_\psi - \\ &\quad \beta^2 \langle R^{-2} \rangle (2\pi)^4 \beta_\psi \end{aligned} \quad (17.76)$$

$$\Rightarrow \frac{A}{-\beta(2\pi)^4} D = \alpha\beta_\psi - \beta \frac{1}{V'} V''\alpha - \beta\alpha_\psi \quad (17.77)$$

$$\Rightarrow \frac{A}{-\beta(2\pi)^4} D = -\beta^2 \left(\frac{\alpha}{\beta} \right)_\psi - \beta \frac{1}{V'} V''\alpha \quad (17.78)$$

$$\Rightarrow \frac{A}{-\beta(2\pi)^4} D = -\beta^2 \left(\frac{\alpha}{\beta} \right)_\psi - \beta^2 \frac{1}{V'} V''\frac{\alpha}{\beta} \quad (17.79)$$

$$\Rightarrow \frac{A}{-\beta(2\pi)^4} D = -\beta^2 \left[\left(\frac{\alpha}{\beta} \right)_\psi + \frac{1}{V'} V''\frac{\alpha}{\beta} \right] \quad (17.80)$$

$$\Rightarrow \frac{A}{-\beta(2\pi)^4} D = -\beta^2 \frac{1}{V'} \left[\left(\frac{\alpha}{\beta} \right)_\psi V' + V'' \frac{\alpha}{\beta} \right] \quad (17.81)$$

$$\Rightarrow \frac{A}{-\beta(2\pi)^4} D = -\beta^2 \frac{1}{V'} \left(\frac{\alpha}{\beta} V' \right)_\psi \quad (17.82)$$

$$\Rightarrow A = \frac{(2\pi)^4}{D} \left(\frac{q}{V' \langle R^{-2} \rangle} \right)^3 \frac{1}{V'} \left[\left\langle \frac{|\nabla \psi|^2}{R^2} \right\rangle \frac{\langle R^{-2} \rangle}{q} V'^2 \right]_\psi \quad (17.83)$$

But the expression of A is slightly different from that given in Ref. [16] [Eq. (5.57)]. Using the above coefficients, the GS equation with the q -profile held fixed is written as

$$\left(\Delta^* - A \frac{\partial}{\partial \psi} \right) \Psi = -B\mu_0 \frac{dp}{d\Psi}. \quad (17.84)$$

18 Misc contents

18.1 Equilibrium scaling

The GS equation is given by Eq. (5.13), i.e.,

$$\frac{\partial^2 \Psi}{\partial Z^2} + R \frac{\partial}{\partial R} \left(\frac{1}{R} \frac{\partial \Psi}{\partial R} \right) = -\mu_0 R^2 \frac{dP}{d\Psi} - \frac{dg}{d\Psi} g. \quad (18.1)$$

If a solution to the GS equation is obtained, the solution can be scaled to obtain a family of solutions. Given an equilibrium with $\Psi(R, Z)$, $P(\Psi)$, $g(\Psi)$, then it is ready to prove that $\Psi_2 = s\Psi$, $P_2 = s^2 P(\Psi)$, and $g_2 = \pm s g(\Psi)$ is also a solution to the GS equation, where s is a constant. In this case, both the poloidal and toroidal magnetic fields are increased by a factor of s , and thus the safety factor remains unchanged. Also note that the pressure is increased by s^2 factor and thus the value of β (the ratio of the therm pressure to magnetic pressure) remains unchanged. Note that $g_2 = \pm s g(\Psi)$, which indicates that the direction of the toroidal magnetic field can be reversed without breaking the force balance. Also note that $\Psi_2 = s\Psi$ and s can be negative, which indicates that the direction of the toroidal current can also be reversed without breaking the force balance.

The second kind of scaling is to set $\Psi_2 = \Psi$, $P_2 = P(\Psi)$, and $g_2^2 = g^2(\Psi) + c$. It is ready to prove that the scaled expression is still a solution to the GS equation because $g_2 g_2' = g g'$. This scaling keep the pressure and the poloidal field unchanged and thus the poloidal beta β_p remains unchanged. This scaling scales the toroidal field and thus can be used to generate a family of equilibria with different profiles of safety factor.

Another scaling, which is trivial, is to set $\Psi_2 = \Psi$, $P_2 = P(\Psi) + c$, and $g_2 = g(\Psi)$. This scaling can be used to test the effects of the pressure (not the pressure gradient) on various physical processes.

When a numerical equilibrium is obtained, one can use these scaling methods

together to generate new equilibria that satisfy particular global conditions. Note that the shape of magnetic surfaces of the scaled equilibrium remains the same as the original one.

The above scaling is made under the constraint that the the GS equation (18.1), is satisfied. In practice, we may scale Ψ by a factor while fixing g and P . This does not satisfy the GS equation, but allows more flexibility in changing the the safety factor profile. Scaling Ψ by a factor corresponds to scaling the plasma current and the poloidal magnetic field.

18.2 Expression of current density

Let us derive the contravariant expression for the current density. Using

$$\mu_0 \mathbf{J} = \nabla \times \mathbf{B},$$

along with magnetic field expression (10.81) and the curl formula (10.43), we obtain

$$\mu_0 \mathbf{J} = - \left[\left(\Psi' \frac{\mathcal{J}}{R^2} |\nabla \psi|^2 \right)_{\psi} + \left(\Psi' \frac{\mathcal{J}}{R^2} \nabla \psi \cdot \nabla \theta \right)_{\theta} \right] \nabla \psi \times \nabla \theta - g' \nabla \phi \times \nabla \psi, \quad (18.2)$$

which is the contravariant form of the current density vector. Next, for later use, calculate the parallel current. By using Eqs. (10.81) and (18.2), the parallel current density is written as

$$\begin{aligned} \mu_0 \mathbf{J} \cdot \mathbf{B} &= - \left[\left(\Psi' \frac{\mathcal{J}}{R^2} |\nabla \psi|^2 \right)_{\psi} + \left(\Psi' \frac{\mathcal{J}}{R^2} \nabla \psi \cdot \nabla \theta \right)_{\theta} \right] g \nabla \psi \times \nabla \theta \cdot \nabla \phi - \\ &\quad g' \left(-\Psi' \frac{\mathcal{J}}{R^2} |\nabla \psi|^2 \right) \nabla \phi \times \nabla \psi \cdot \nabla \theta \\ &= - \left[\left(\Psi' \frac{\mathcal{J}}{R^2} |\nabla \psi|^2 \right)_{\psi} + \left(\Psi' \frac{\mathcal{J}}{R^2} \nabla \psi \cdot \nabla \theta \right)_{\theta} \right] g \mathcal{J}^{-1} + g' \mathcal{J}^{-1} \Psi' \frac{\mathcal{J}}{R^2} |\nabla \psi|^2 \\ &= -g^2 \mathcal{J}^{-1} \left\{ \frac{1}{g} \left(\Psi' \frac{\mathcal{J}}{R^2} |\nabla \psi|^2 \right)_{\psi} + \frac{1}{g} \left(\Psi' \frac{\mathcal{J}}{R^2} \nabla \psi \cdot \nabla \theta \right)_{\theta} - \frac{g'}{g^2} \Psi' \frac{\mathcal{J}}{R^2} |\nabla \psi|^2 \right\} \\ &= -g^2 \mathcal{J}^{-1} \left[\left(\frac{\Psi'}{g} \frac{\mathcal{J}}{R^2} |\nabla \psi|^2 \right)_{\psi} + \left(\frac{\Psi'}{g} \frac{\mathcal{J}}{R^2} \nabla \psi \cdot \nabla \theta \right)_{\theta} \right]. \end{aligned} \quad (18.3)$$

18.3 Cylindrical tokamak

For a large aspect-ratio, circular cross section tokamak, the R on a magnetic surface is nearly constant, $R \approx R_0$. The poloidal angle dependence of the magnetic field can be neglected, i.e., $B_{\phi}(r, \theta) \approx B_{\phi}(r)$, and $B_p(r, \theta) \approx B_p(r)$, where r is the minor radius of the relevant magnetic surface. Using these, the safety factor in Eq. (9.5) is approximated to

$$q = \frac{1}{2\pi} \oint \frac{1}{R} \frac{B_{\phi}}{B_p} d\ell_p \approx \frac{1}{2\pi} \frac{B_{\phi}(r)}{B_p(r)} \frac{1}{R_0} \oint d\ell_p = \frac{1}{2\pi} \frac{B_{\phi}(r)}{B_p(r)} \frac{1}{R_0} 2\pi r = \frac{r}{R_0} \frac{B_{\phi}(r)}{B_p(r)}, \quad (18.4)$$

18.4 Coils system of EAST tokamak

18.4.1 Poloidal field (PF) coils

EAST has 14 superconducting poloidal field (PF) coils (only 12 of them are independently powered). The layout is shown in Fig. 18.1.

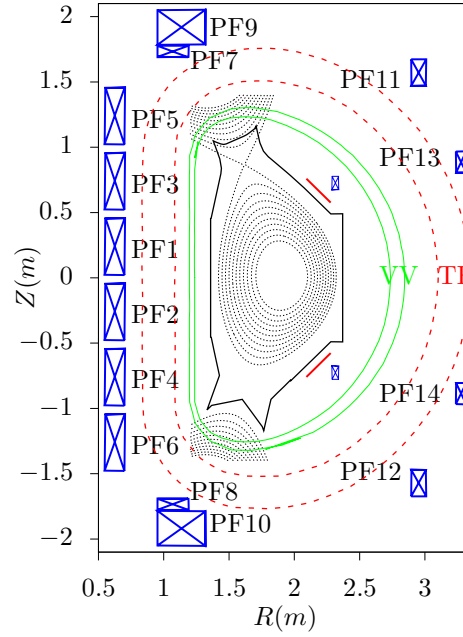


Figure 18.1. Coils system of EAST tokamak. Coils PF1 to PF6 are Central Solenoid (CS) coils with 140 turns/coil. Both PF11 and PF12 have 64 turns, Both PF13 and PF14 have 32 turns. PF7 and PF9 are adjacent to each other and connected in series and thus are considered as one independent coil, with total turns being 248. The same situation applies for PF8 and PF10. Maximum current per turn in PF coils is 14.5kA. Locations of PF coils are from Refs. [26][9]. The inner green D-shaped structure corresponds to the vacuum vessel wall and the outer red dashed D-shape corresponds to the TF-coils. Note that PF1-14 coils are all located outside of the TF-coils. The small blue circles are “flux loops” measuring the poloidal magnetic flux. Red coils are RMP copper coils, which generate 3D magnetic perturbations.

All the PF coils can be considered as shaping coils since they all have effects in shaping the plasmas. In practice, they are further classified according to their main roles. PF1 to PF6 form a solenoid in the center of the torus and thus called Central Solenoid (CS) coils. Their main role is to induce electric field to drive current in the plasma and heat the plasma. As a result, they are often called “Ohm heating coils”. PF13 and PF14 are mainly used to control (slow) vertical

plasma displacement and thus are often called “vertical field coils” or “position control coils”. PF11 and PF12 are used to triangularize the plasma and thus is called “shaping coils”. In order to squeeze the plasma to form desired triangularity, their currents need to be in the opposite direction of plasma current (since two opposite currents repel each other). PF7+PF9 and PF8+PF10 are often called (by EAST operators) as “big coils” or “divertor coils” since they have the largest number of turns and current and are used to elongate the plasma to divertor configurations.

Besides the 16 superconducting PF coils outside vacuum vessel, EAST has two small copper coils within the vacuum vessel (2turn/coil), which are connected in anti-series and thus have opposite currents. They are closer to the plasma (than other PF coils) and are used to control fast plasma displacements, specifically VDEs (vertical displacement events). They are often called “fast control coils”.

18.4.2 Toroidal magnetic field (TF) coils and vacuum toroidal magnetic field

Using Ampere’s circuital law

$$\oint \mathbf{B} \cdot d\mathbf{l} = \mu_0 I, \quad (18.5)$$

along the toroidal direction and assuming perfect toroidal symmetry, we obtain

$$2\pi R B_\phi = \mu_0 I, \quad (18.6)$$

i.e.,

$$B_\phi = \frac{\mu_0 I}{2\pi R}. \quad (18.7)$$

Neglecting the poloidal current contributed by the plasma, the poloidal current is determined solely by the current in the TF coils. The EAST tokamak has 16 groups of TF coils with 132turns/coil (I got to know the number of turns from ZhaoLiang Wang: $\varphi \times R = 12 \times 11 = 132$). Denote the current in a single turn by I_s , then Eq. (18.7) is written

$$B_\phi = \frac{\mu_0 \times 16 \times 132 \times I_s}{2\pi R} = 4.224 \times 10^{-4} \frac{I_s}{R} \quad (18.8)$$

Using this formula, the strength of the toroidal magnetic field at $R = 1.8m$ for $I_s = 10^4 A$ is calculated to be $B_\phi = 2.34T$. This was one of the two scenarios often used in EAST experiments (another scenario is $I_s = 8 \times 10^3 A$). (The limit of the current in a single turn of the TF coils is 14.5kA (from B. J. Xiao’s paper [31]).

Note that the exact equilibrium toroidal magnetic field B_ϕ is given by $B_\phi = g(\Psi)/R$. Compare this with Eq. (18.7), we know that the approximation made to obtain Eq. (18.8) is equivalent to $g(\Psi) \approx \mu_0 I_{TF}/2\pi$, i.e. assuming g is a constant. The poloidal plasma current density j_{pol} is related to g by $j_{pol} = g'(\Psi)B_p/\mu_0$. The constant g corresponds to zero plasma poloidal current, which is consistent to the assumption used to obtain Eq. (18.8).

Let us estimate the safety factor value near the plasma edge using the total plasma current and the current in a single turn of TF coils I_s . For divertor magnetic configuration, the plasma edge is at the separatrix, where $q \rightarrow \infty$. To get a characteristic safety factor value that is finite, one often chooses the edge to be the magnetic surface that encloses 95% of the poloidal magnetic flux. Denote this surface by S_{95} and the value of q at this surface by q_{95} , which is given by

$$q_{95} \approx \frac{B_{\phi, \text{axis}}}{\bar{B}_p} \frac{a}{R_{\text{axis}}}, \quad (18.9)$$

where a is the minor radius of the surface S_{95} , and R_{axis} the major radius of the magnetic axis, $B_{\phi, \text{axis}}$ is the the magnitude of toroidal magnetic field at the magnetic axis, and \bar{B}_p is the average poloidal magnetic field on the surface, $\bar{B}_p \approx \mu_0 I_p / (2\pi a)$. Using Eq. (18.8), Eq. (18.9) is written as

$$q_{95} \approx \frac{4.224 \times 10^{-4} I_s}{\mu_0 I_p} \frac{2\pi a^2}{R_{\text{axis}}^2}, \quad (18.10)$$

For EAST, typically $R_{\text{axis}} = 1.85\text{m}$ and $a = 0.45\text{m}$. Using this, we obtain

$$q_{95} \approx 125 \frac{I_s}{I_p}. \quad (18.11)$$

18.4.3 RMP coils of EAST

The so-called resonant magnetic perturbation (RMP) coils are 3D coils that are used to suppress or mitigate edge localized modes. The shape and location of RMP coils of EAST tokamak are plotted in Fig. 18.2.

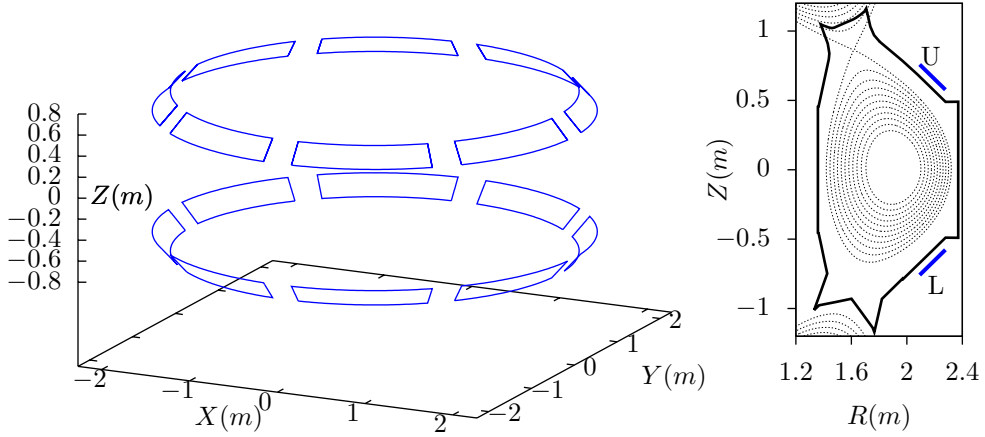


Figure 18.2. Location of the RMP coils on EAST tokamak in 3D view (left) and poloidal view (right).

18.5 Comparison of major tokamaks in the world

The size of EAST is similar to that of DIII-D tokamak. The main parameters are summarized in Table 18.1. A significant difference between EAST and DIII-D is that DIII-D has a larger minor radius, which makes DIII-D able to operate with a larger toroidal current than that EAST can do for the same current density. Another significant difference between EAST and DIII-D is that the coils of EAST are superconducting while the coils of DIII-D are not. The superconducting coils enable EAST to operate at longer pulse.

	EAST	DIII-D[21]	KSTAR[19]	SPARC	WEST	JET
Major radius R_0	1.85m	1.67m	1.8m	1.85m	2.5m	2.96m
minor radius a	0.45m	0.67m	0.5m	0.57m	0.5m	0.9m
elongation						
Plasma volume				20m ³		
No. of TF coils, turns, current	16, 130, 14.5kA	24, 6, 126kA	16, 56, 35.2kA			
B_t at R_0	3.26T	2.17T	3.5T	12.2T	3.7T	3.45T
CS coil module \times turn \times current	6 \times 120 \times 14.5kA					
No. of independent PF coils	6+6	?+18				
Available solenoid magnetic flux	12Vs	10.5Vs	17Vs			
Maximum plasma current	1.0MA	3.0MA	2MA	8.7MA	1MA	5MA
Pulse length	400s	10s	300s			
superconducting?	Yes	No	Yes		Yes	No

Table 18.1. Comparison of main parameters of EAST, DIII-D, JET, and ITER tokamaks. The B_t of EAST is calculated at $R=1.85m$ by using Eq. (18.8) with $I_s=14.5kA$ (the maximal current allowed). The currents listed in the table are maximum plasma current whereas typical plasma currents for EAST are 0.5MA and for DIII-D are 2MA or less.

	ITER[1]	CFETR(old version)	CFETR (new)	BEST
Major radius R_0	6.2m	5.7m	7.2m	3.6m
minor radius a	2.0m	1.6m	2.2m	
elongation				
No. of TF coils, turns, current	18, 134, 68kA	16, 132, 67.5kA	16, ?, ?	16, 152, 45.6kA
B_t at R_0	5.29T	5.00T	6.5T	
CS coil module \times turn \times current				
No. of independent PF coils				
Available solenoid magnetic flux				
Maximum plasma current	15MA	10MA	14MA	
Pulse length	400s			
superconducting?	Yes	Yes	Yes	Yes

Table 18.2. Continued from Table 18.1.

	ASDEX-U	HL-2M	NSTX	MAST
Major radius R_0	1.65m	1.78m	0.85m	0.9m
minor radius a	0.7m	0.65m	0.68m	0.6m
elongation				
No. of TF coils, turns, current	16,?,?	20,7,190kA		
B_t at R_0		2.99T	0.3T	0.55T
CS coil module \times turn \times current		1,?,?		
No. of independent PF coils		1+16		
Available solenoid magnetic flux		14Vs		
typical plasma current	1.6MA	2.5MA		
Pulse length		5s		
superconducting?	No	No	No	

Table 18.3. Continued from Table 18.2.

DIII-D has 24 groups of TF coils with 6turns/coil, i.e., total turns are $24 \times 6 = 144$, with a maximum current of $I_s = 126\text{kA}$ in a single turn[21]. Using formula (18.7), the toroidal field at $R = 1.67\text{m}$ can be calculated, giving $2.17T$.

DIII-D is special in that its poloidal field (PF) coils are located inside of the TF-coils, which makes the PF-coils more close to the plasma and thus more efficient in shaping the plasma. However, this nested structure is difficult to assemble. In superconducting tokamaks (e.g., EAST, KSTAR, ITER), PF coils are all placed outside of the TF-coils.

I noticed that HL-2M also has the PF coils located within the TF-coils, similar to DIII-D. This remind me that this layout may apply to all non-superconducting tokamaks (to be confirmed, No, non-superconducting tokamak ASDEX-U has PF coils outside of TF coils).

KSTAR has 16 TF coils and 14 PF coils. Both of the TF and PF coil system use internally cooled superconductors. The nominal current in TF coils is 35.2kA / turn with 56turns/coil and all coils connected in series[25]. Using these information and formula (18.7), the toroidal field at $R = 1.8\text{m}$ can be calculated, giving $3.5T$. The PF coil system consists of 8 Central Solenoid (CS) coils and 6 outer PF coils and can provide 17 V-sec.

ITER has 18 TF coils with number of turns in one coil being 134 and current per turn 68kA [5]. Using these information and formula (18.7), the toroidal field at $R = 6.2\text{m}$ can be calculated, giving $5.29T$.

18.6 Miller's formula for shaped flux surfaces

According to Refs. [8, 22], Miller's formula for a series of shaped flux surfaces is given by

$$R = R_0(r) + r \cos\{\theta + \arcsin[\delta(r)\sin\theta]\}, \quad (18.12)$$

$$Z = \kappa(r)r \sin\theta, \quad (18.13)$$

where $\kappa(r)$ and $\delta(r)$ are elongation and triangularity profile, $R_0(r)$ is the

Shafranov shift profile, which is given by

$$R_0(r) = R_0(a) - \frac{aR'_0}{2} \left[1 - \left(\frac{r}{a} \right)^2 \right], \quad (18.14)$$

where R'_0 is a constant, $R_0(a)$ is the major radius of the center of the boundary flux surface. The triangularity profile is

$$\delta(r) = \delta_0 \left(\frac{r}{a} \right)^2, \quad (18.15)$$

and the elongation profile is

$$\kappa(r) = \kappa_0 - 0.3 + 0.3 \left(\frac{r}{a} \right)^4. \quad (18.16)$$

The nominal ITER parameters are $\kappa_0 = 1.8$, $\delta_0 = 0.5$ and $R'_0 = -0.16$. I wrote a code to plot the shapes of the flux surface (/home/yj/project/miller_flux_surface). An example of the results is given in Fig. 18.3.

[⟨image|/home/yj/project/miller_flux_surface/plt.eps||||⟩](#)

Figure 18.3. Flux-surfaces given by Eqs. (18.12) and (18.13) with r/a varying from 0.1 to 1.0 (corresponding boundary surface). Other parameters are $R_0(a)/a = 3$, $\kappa_0 = 1.8$, $\delta_0 = 0.5$, $R'_0 = -0.16$.

18.7 Double transport barriers pressure profile

An analytic expression for the pressure profile of double (inner and external) transport barriers is given by

$$P(\psi) = a_i \left(1 + \tanh \left(\frac{-(\psi - \psi_i)}{w_i} \right) \right) + a_e \left(1 + \tanh \left(\frac{-(\psi - \psi_e)}{w_e} \right) \right) - c \quad (18.17)$$

where ψ is the normalized poloidal flux, w_i and w_e are the width of the inner and external barriers, ψ_i and ψ_e are the locations of the barriers, a_i and a_e is the height of the barriers, c is a constant to ensure $P(\psi) = 0$ at $\psi = 1$.

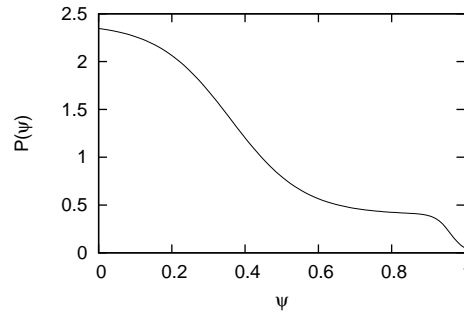


Figure 18.4. Pressure profile of double (inner and external) transport barriers given by Eq. (18.17) with $a_i = 1$, $b_i = 0.2$, $\psi_i = 0.36$, $\psi_e = 0.96$, $w_i = 0.2$, $w_e = 0.04$, $c = 0$.

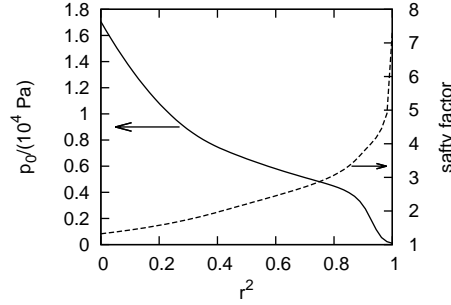


Figure 18.5. Equilibrium pressure profile for EAST discharge #38300 at 3.9s (reconstructed by EFIT code, gfile name: g038300.03900), which shows a boundary transport barrier.

18.8 Ballooning transformation

To construct a periodic function about θ , we introduce a function $\bar{z}(\theta)$ which is defined over $-\infty < \theta < \infty$ and vanishes sufficiently fast as $|\theta| \rightarrow \infty$ so that the following infinite summation converge:

$$\sum_{l=-\infty}^{\infty} \bar{z}(\theta + 2\pi l). \quad (18.18)$$

If we use the above sum to define a function

$$z(\theta) = \sum_{l=-\infty}^{\infty} \bar{z}(\theta + 2\pi l), \quad (18.19)$$

then it is obvious that

$$z(\theta + 2\pi) = z(\theta), \quad (18.20)$$

i.e., $z(\theta)$ is a periodic function about θ with period of 2π .

If we use the right-hand-side of Eq. (18.19) to represent $z(\theta)$, then we do not need to worry about the periodic property of $z(\theta)$ (the periodic property is guaranteed by the representation)

A mics

A.1 Shape parameters of a closed magnetic surface

Let us introduce parameters characterizing the shape of a magnetic surface in the poloidal plane. The “midplane” is defined as the plane that passes through the magnetic axis and is perpendicular to the symmetric axis (Z axis). For

a up-down symmetric (about the midplane) magnetic surface, its shape can be roughly characterized by four parameters, namely, the R coordinate of the innermost and outermost points in the midplane, R_{in} and R_{out} ; the (R, Z) coordinators of the highest point of the magnetic surface, $(R_{\text{top}}, Z_{\text{top}})$. These four parameters are indicated in Fig. A.1.

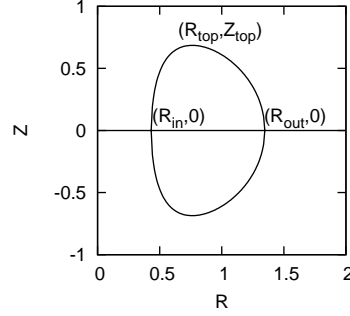


Figure A.1. Four parameters characterizing the shape of a flux surface: the R coordinate of the innermost and outermost points in the middle-plane, R_{in} and R_{out} ; the (R, Z) coordinators of the highest point of the flux surface, $(R_{\text{top}}, Z_{\text{top}})$.

In terms of these four parameters, we can define the major radius of a magnetic surface

$$R_0 = \frac{R_{\text{in}} + R_{\text{out}}}{2}, \quad (\text{A.1})$$

(which is the R coordinate of the geometric center of the magnetic surface), the minor radius of a magnetic surface

$$a = \frac{R_{\text{out}} - R_{\text{in}}}{2}, \quad (\text{A.2})$$

the triangularity of a magnetic surface

$$\delta_t = \frac{R_0 - R_{\text{top}}}{a}, \quad (\text{A.3})$$

and, the ellipticity (elongation) of a magnetic surface

$$\kappa = \frac{Z_{\text{top}}}{a}. \quad (\text{A.4})$$

Usually, we specify the value of R_0 , a , δ_t , and κ , instead of $(R_{\text{in}}, R_{\text{out}}, R_{\text{top}}, Z_{\text{top}})$, to characterize the shape of a magnetic surface. The value of the triangularity δ_t is usually positive in traditional tokamak operations, but negative triangularity is achievable and potentially useful, which is under active investigation.

Besides, using a and R_0 , we can define another useful parameter $\varepsilon \equiv a/R_0$, which is called the inverse aspect ratio. Note that the major radius R_0 of the LCFS is usually different from R_{axis} (the R coordinate of the magnetic axis). Usually we have $R_{\text{axis}} > R_0$ due to the so-called Shafranov shift.

A.2 Ψ is a covariant component of \mathbf{A} in cylindrical coordinates

We note that $\Psi \equiv A_\phi R$ is the covariant toroidal component of \mathbf{A} in cylindrical coordinates (R, ϕ, Z) . The proof is as follows. Note that the covariant form of \mathbf{A} should be expressed in terms of the contravariant basis vector $(\nabla R, \nabla \phi, \text{ and } \nabla Z)$, i.e.,

$$\mathbf{A} = A_1 \nabla R + A_2 \nabla \phi + A_3 \nabla Z. \quad (\text{A.5})$$

where A_2 is the covariant toroidal component of \mathbf{A} . To obtain A_2 , we take scalar product of Eq. (A.5) with $\partial \mathbf{r} / \partial \phi$ and use the orthogonality relation (10.7), which gives

$$\mathbf{A} \cdot \frac{\partial \mathbf{r}}{\partial \phi} = A_2. \quad (\text{A.6})$$

In cylindrical coordinates (R, ϕ, Z) , the position vector is written as

$$\mathbf{r}(R, Z, \phi) = R\hat{\mathbf{R}}(\phi) + Z\hat{\mathbf{Z}} + 0\hat{\phi} \quad (\text{A.7})$$

where $\hat{\mathbf{R}}$, $\hat{\mathbf{Z}}$, and $\hat{\phi}$ are unit vectors along $\partial \mathbf{r} / \partial R$, $\partial \mathbf{r} / \partial Z$, and $\partial \mathbf{r} / \partial \phi$, respectively, i.e.

$$\hat{\mathbf{R}} = \frac{\partial \mathbf{r}}{\partial R} \left| \frac{\partial \mathbf{r}}{\partial R} \right|^{-1}, \hat{\mathbf{Z}} = \frac{\partial \mathbf{r}}{\partial Z} \left| \frac{\partial \mathbf{r}}{\partial Z} \right|^{-1}, \hat{\phi} = \frac{\partial \mathbf{r}}{\partial \phi} \left| \frac{\partial \mathbf{r}}{\partial \phi} \right|^{-1} \quad (\text{A.8})$$

Using this, we obtain

$$\frac{\partial \mathbf{r}}{\partial \phi} = R\hat{\phi}, \quad (\text{A.9})$$

Use Eq. (A.9) in Eq. (A.6) giving

$$A_2 = A_\phi R, \quad (\text{A.10})$$

with A_ϕ defined by $A_\phi = \mathbf{A} \cdot \hat{\phi}$. Equation (A.10) indicates that $\Psi = A_\phi R$ is the covariant toroidal component of the vector potential.

A.3 Solovév equilibrium

For most choices of $P(\Psi)$ and $g(\Psi)$, the GS equation (5.13) has to be solved numerically. For the specific choice of P and g profiles given by

$$\frac{dP}{d\Psi} = -\frac{c_1}{\mu_0}, \quad (\text{A.11})$$

$$g \frac{dg}{d\Psi} = -c_2 R_0^2, \quad (\text{A.12})$$

where c_1 , c_2 , and R_0 are constants, there is an analytical solution, which is given by [16]

$$\Psi = \frac{1}{2}(c_2 R_0^2 + c_0 R^2)Z^2 + \frac{1}{8}(c_1 - c_0)(R^2 - R_0^2)^2, \quad (\text{A.13})$$

where c_0 is a constant. [Proof: By direct substitution, we can verify Ψ of this form is indeed a solution to the GS equation (5.13).] A useful choice for tokamak application is to set $c_0 = B_0 / (R_0^2 \kappa_0 q_0)$, $c_1 = B_0(\kappa_0^2 + 1) / (R_0^2 \kappa_0 q_0)$, and $c_2 = 0$. Then Eq. (A.13) is written

$$\Psi = \frac{B_0}{2R_0^2 \kappa_0 q_0} \left[R^2 Z^2 + \frac{\kappa_0^2}{4} (R^2 - R_0^2)^2 \right]. \quad (\text{A.14})$$

For this case, the toroidal field function g is a constant. (For the Solovév equilibrium (A.14), I found numerically that the value of the safety factor at the magnetic axis ($R = R_0, Z = 0$) is equal to $q_0 g / (R_0 B_0)$. This result should be able to be proved analytically. I will do this later. In calculating the safety factor, we also need the expression of $|\nabla \Psi|$, which is given analytically by

$$\begin{aligned} |\nabla \Psi| &= \sqrt{\left(\frac{\partial \Psi}{\partial R} \right)^2 + \left(\frac{\partial \Psi}{\partial Z} \right)^2} \\ &= \frac{B_0}{2R_0^2 \kappa_0 q_0} \sqrt{[2RZ^2 + \kappa_0^2(R^2 - R_0^2)R]^2 + (2R^2 Z)^2}. \end{aligned} \quad (\text{A.15})$$

)

Define $\Psi_0 = B_0 R_0^2$, and $\bar{\Psi} = \Psi / \Psi_0$, then Eq. (A.14) is written as

$$\bar{\Psi} = \frac{1}{2\kappa_0 q_0} \left[\bar{R}^2 \bar{Z}^2 + \frac{\kappa_0^2}{4} (\bar{R}^2 - 1)^2 \right], \quad (\text{A.16})$$

where $\bar{R} = R / R_0$, $\bar{Z} = Z / R_0$. From Eq. (A.16), we obtain

$$\bar{Z} = \pm \frac{1}{\bar{R}} \sqrt{2\kappa_0 q_0 \bar{\Psi} - \frac{\kappa_0^2}{4} (\bar{R}^2 - 1)^2}. \quad (\text{A.17})$$

Given the value of κ_0 , q_0 , for each value of $\bar{\Psi}$, we can plot a magnetic surface on (\bar{R}, \bar{Z}) plane. An example of the nested magnetic surfaces is shown in Fig. A.2.

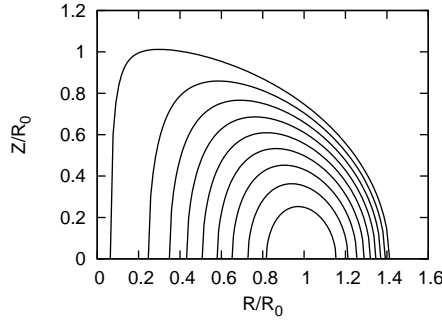


Figure A.2. Flux surfaces of Solovév equilibrium for $\kappa_0 = 1.5$ and $q_0 = 1.5$, with $\bar{\Psi}$ varying from zero (center) to 0.123 (edge). The value of $\bar{\Psi}$ on the edge is determined by the requirement that the minimum of \bar{R} is equal to zero. (To prevent “divided by zero” that appears in Eq. (A.17) when $R = 0$, the value of $\bar{\Psi}$ on the edge is shifted to $0.123 - \varepsilon$ when plotting the above figure, where ε is a small number, $\varepsilon = 10^{-3}$ in this case.)

Equation (A.14) can be solved to give explicit form of the contour of Ψ in (R, Z) plane:

$$Z = \pm \frac{1}{R} \sqrt{\frac{2R_0^2 \kappa_0 q_0}{B_0} \Psi - \frac{\kappa_0^2}{4} (R^2 - R_0^2)^2}. \quad (\text{A.18})$$

The minor radius of a magnetic surface of the Solovév equilibrium can be calculated by using Eq. (A.18), which gives

$$R_{\text{in}} = \sqrt{R_0^2 - \sqrt{A\Psi}}, \quad (\text{A.19})$$

$$R_{\text{out}} = \sqrt{R_0^2 + \sqrt{A\Psi}}, \quad (\text{A.20})$$

and thus

$$a = \frac{R_{\text{out}} - R_{\text{in}}}{2} = \frac{\sqrt{R_0^2 + \sqrt{A\Psi}} - \sqrt{R_0^2 - \sqrt{A\Psi}}}{2}. \quad (\text{A.21})$$

where $A = 8R_0^2 q_0 / (B_0 \kappa_0)$. In my code of constructing Solovév magnetic surface, the value of a is specified by users, and then Eq. (A.21) is solved numerically to obtain the value of Ψ of the flux surface. Note that the case $\Psi = 0$ corresponds to $R_{\text{in}} = R_{\text{out}} = R_0$, i.e., the magnetic axis, while the case $\Psi = R_0^2 B_0 \kappa_0 / (8q_0)$ corresponds to $R_{\text{in}} = 0$. Therefore, the reasonable value of Ψ of a magnetic surface should be in the range $0 \leq \Psi < R_0^2 B_0 \kappa_0 / (8q_0)$. This range is used as the interval bracketing a root in the bisection root finder.

Using Eq. (A.21), the inverse aspect ratio of a magnetic surface labeled by Ψ can be approximated as [16]

$$\varepsilon \approx \sqrt{\frac{2q_0 \Psi}{\kappa_0 R_0^2 B_0}}. \quad (\text{A.22})$$

Therefore, the value of Ψ of a magnetic surface with the inverse aspect ratio ε is approximately given by

$$\Psi = \frac{\varepsilon^2 \kappa_0 R_0^2 B_0}{2q_0}. \quad (\text{A.23})$$

A.4 Plasma rotation

In deriving the Grad-Shafranov equation, we have assumed that there is no plasma flow. Next, let us examine whether this assumption is justified for plasmas in EAST tokamak.

The complete momentum equation is given by

$$\rho_m \left[\frac{\partial \mathbf{U}}{\partial t} + \mathbf{U} \cdot \nabla \mathbf{U} \right] = \rho_q \mathbf{E} + \mathbf{J} \times \mathbf{B} - \nabla \cdot \mathbb{P}, \quad (\text{A.24})$$

where $\rho_q \mathbf{E}$ term can be usually neglected due to either $\rho_q \approx 0$ or $\mathbf{E} \approx 0$, \mathbb{P} is a pressure tensor, which is different from the scalar pressure considered in this note. The equilibrium with pressure tensor can be important for neutral beam heating plasma, where pressure contributed by NBI fast ions can be a tensor. With plasma flow and scalar pressure and neglecting electric force term, the steady state momentum equation is written

$$\rho_m \mathbf{U} \cdot \nabla \mathbf{U} = \mathbf{J} \times \mathbf{B} - \nabla P, \quad (\text{A.25})$$

where the term on the left-hand side is the contribution of plasma flow to the force balance. Let us estimate the magnitude of this term. Macroscopic flows in tokamak are usually along the toroidal direction (the poloidal flow is usually heavily damped). The toroidal flow usually has the same toroidal angular frequency on a magnetic surface, i.e., the flow can be written as

$$\mathbf{U} = R\omega_T(\psi)\mathbf{e}_\phi, \quad (\text{A.26})$$

where $\omega_T = \omega_T(\psi)$ is the toroidal angular frequency of the flow, which can have radial variation. Using this expression, the left-hand side of Eq. (A.25) is written as

$$\begin{aligned} \rho_m \mathbf{U} \cdot \nabla \mathbf{U} &= \rho_m R\omega_T \mathbf{e}_\phi \cdot \nabla (R\omega_T \mathbf{e}_\phi) \\ &= \rho_m R\omega_T \frac{1}{R} \frac{\partial}{\partial \phi} (R\omega_T \mathbf{e}_\phi) \\ &= -\rho_m R\omega_T^2 \mathbf{e}_R, \end{aligned} \quad (\text{A.27})$$

which is just the centripetal force. For typical EAST plasma, the rotation frequency $f_T = \omega_T / 2\pi$ is less than 10kHz. For $f_T = 10\text{kHz}$, $R = 1.8\text{m}$ and $\rho_m = 1.3 \times 10^{-7} \text{kg} / \text{m}^3$ [Mass density of EAST#38300@3.9s, $\rho_m = n_D m_D = 4 \times 10^{19} \text{m}^{-3} \times 2 \times 1.6726 \times 10^{-27} \text{kg} = 1.3 \times 10^{-7} \text{kg} / \text{m}^3$], the above fore is about 9.23×10^2 newton. On the other hand, the pressure gradient force in Eq. (A.25) is about 4×10^4 newton, which is one order larger than the force contributed by the rotation. [Pressure gradient force is estimated by using $\nabla P \approx P_0 / a$, where P_0 is the thermal pressure at the magnetic axis and a is the minor radius of plasma. For typical EAST plasmas (EAST#38300@3.9s), $P_0 \approx 2 \times 10^4 \text{Pa}$, $a = 0.45\text{m}$. Then $\nabla P \approx P_0 / a = 4 \times 10^4 \text{N} / \text{m}^3$.] This indicates the rotation has little influence on the force balance. In other words, the EAST tokamak equilibrium can be well described by the static equilibrium without rotation.

A.5 Poloidal plasma current

As is discussed in Sec. (), to satisfy the force balance, $g \equiv RB_\phi$ must be a magnetic surface function, i.e., $g = g(\Psi)$. Using this, expression (4.2) and (4.3) are written

$$\mu_0 J_R = -\frac{1}{R} \frac{dg}{d\Psi} \frac{\partial \Psi}{\partial Z} = \frac{dg}{d\Psi} B_R, \quad (\text{A.28})$$

and

$$\mu_0 J_Z = \frac{1}{R} \frac{dg}{d\Psi} \frac{\partial \Psi}{\partial R} = \frac{dg}{d\Psi} B_z, \quad (\text{A.29})$$

respectively. The above two equations imply that

$$\frac{J_R}{J_Z} = \frac{B_R}{B_Z}, \quad (\text{A.30})$$

which implies that the projections of \mathbf{B} lines and \mathbf{J} lines in the poloidal plane are identical to each other. This indicates that the \mathbf{J} surfaces coincide with the magnetic surfaces.

The poloidal plasma current density is usually small (compared with the toroidal plasma current density) but is important for some cases of interest and thus could not be safely neglected. Many model equilibria (e.g., Solovév equilibria, DIII-D cyclone base cases) frequently used in simulations assume that g is a spatial constant, i.e., neglecting the poloidal plasmas current. The conclusions drawn from these simulations could be misleading.

Using this and $\nabla \cdot \mathbf{J} = 0$, and following the same steps in Sec. 2.7, we obtain

$$I_{\text{pol}} = \frac{1}{\mu_0} 2\pi [g(\Psi_2) - g(\Psi_1)], \quad (\text{A.31})$$

where I_{pol} is the poloidal current enclosed by the two magnetic surfaces, the positive direction of I_{pol} is chosen to be in the clockwise direction when observers look along $\hat{\phi}$. Equation (A.31) indicates that the difference of g between two magnetic surface is proportional to the poloidal current. For this reason, g is usually call the “poloidal current function”.

In the above, we see that the relation of g with the poloidal electric current is similar to that of Ψ with the poloidal magnetic flux. This similarity is due to the following differential relations:

$$\begin{cases} \mathbf{B} = \nabla \times \mathbf{A} \\ \Psi = R A_\phi \end{cases} \quad \begin{cases} \mu_0 \mathbf{J} = \nabla \times \mathbf{B} \\ g = R B_\phi \end{cases}$$

The poloidal plasma current density \mathbf{J}_p can be further written as

$$\begin{aligned} \mathbf{J}_p &\equiv J_R \hat{\mathbf{R}} + J_Z \hat{\mathbf{Z}} \\ &= \frac{1}{\mu_0} \left(-\frac{1}{R} \frac{\partial g}{\partial Z} \hat{\mathbf{R}} + \frac{1}{R} \frac{\partial g}{\partial R} \hat{\mathbf{Z}} \right) \\ &= \frac{1}{\mu_0} \nabla g \times \nabla \phi \end{aligned} \quad (\text{A.32})$$

Using $g = g(\Psi)$, Eq. (A.32) can also be written as

$$\begin{aligned}\mathbf{J}_p &= \frac{1}{\mu_0} \frac{dg}{d\Psi} \nabla\Psi \times \nabla\phi \\ &= \frac{1}{\mu_0} \frac{dg}{d\Psi} \mathbf{B}_p.\end{aligned}\tag{A.33}$$

A.6 Plasma beta

Plasma β is the ratio of thermal pressure to magnetic pressure, i.e.,

$$\beta = \frac{p}{B^2/(2\mu_0)}.\tag{A.34}$$

Since pressure in tokamak plasmas is not uniform, volume averaged pressure is used to define the beta. The toroidal beta β_t and the poloidal beta β_p are defined, respectively, by

$$\beta_t = \frac{\langle p \rangle}{B_{t0}^2/(2\mu_0)},\tag{A.35}$$

$$\beta_p = \frac{\langle p \rangle}{B_a^2/(2\mu_0)},\tag{A.36}$$

where $\langle \dots \rangle$ is the volume average, B_{t0} is the vacuum toroidal magnetic field at the magnetic axis (or geometrical center of the plasma), $B_a = \mu_0 I_p / l$ is the flux surface averaged poloidal magnetic field, $l = \oint dl$ is the length of the poloidal perimeter of the boundary flux surface. Then β_p can be written as

$$\beta_p = 2l^2 \frac{\langle p \rangle}{\mu_0 I_p^2}.\tag{A.37}$$

An alternative definition of β_p use the LCFS cross-sectional average of p rather than the volume average p (Wesson tokamaks). This definition is adopted in many codes, including HEQ code I developed

A.7 Beta limit

Beta can be considered as a quantity characterizing the efficiency of the magnetic field of tokamaks in confining plasmas.

In tokamaks, the toroidal magnetic field is dominant and thus the toroidal beta β_t (not β_p) is the usual way to characterize the efficiency of the magnetic field in confining plasmas. (Why do we need β_p ? The short answer is that β_p is proportional to an important current, the bootstrap current, which is important for tokamak steady state operation.)

Tokamak experiments have found that it is easier to achieve higher β_t in low B_t plasmas than in higher B_t plasmas, which indicates that the efficiency of the magnetic field in confining plasma is a decreasing function of the magnitude of the magnetic field.

Beta limit means there is a limit for the value of beta beyond which the plasma will encounter a serious disruption. Early calculation of the beta limit on JET shows that the maximal β_t obtained is proportional to $I_p / (10^6 a B_{t0})$, where all quantities are in SI units. This scaling relation $\beta_{t\max} = C_T I_p / (10^6 a B_{t0})$ is often called Troyon scaling, where the coefficient C_T was determined numerically by Troyon to 0.028. Often C_T is expressed in percent, in which case $C_T = 2.8$. This motivates us to define

$$\beta_N = 10^8 \frac{a B_{t0}}{I_p} \beta_t. \quad (\text{A.38})$$

which is called “normalized beta”. The normalized beta β_N is an operational parameter indicating how close the plasma is to reach destabilizing major MHD activities. Its typical value is of order unit. As mentioned above, β_N calculated by Troyon is 2.8. Empirical evaluation from the data of different tokamaks raises this value slightly to 3.5, although significantly higher values, e.g., $\beta_N = 7.2$, have been achieved in the low aspect ratio tokamak NSTX[24].

The value of β_N indicates how close one is to the onset of deleterious instability. The ability to increase the value of β_N can be considered as the ability of controlling the major MHD instabilities, and thus can be used to characterize how well a tokamak device is operated. One goal of EAST tokamak during 2015-2016 is to sustain a plasma with $\beta_N \geq 2$ for at least 10 seconds.

(check** The tearing mode, specifically the neoclassical tearing mode (NTM) is expected to set the beta limit in a reactor.)

(**check: Tokamak experiments have found that it is easier to achieve high β_N in large I_p plasmas than in small I_p plasmas. However, experiments found it is easier to achieve high β_p in small I_p plasmas than in large I_p plasmas. Examining the expression of β_N and β_p given by Eqs. (A.37) and Eq. (), respectively, we recognize that pressure limit should have a scaling of $\langle p \rangle \propto I_p^\alpha$ with $1 < \alpha < 2$.)

β_p is the ratio of the pressure to the square of plasma current, and thus characterizes the efficiency of the plasma current in confining the plasma. Is there a limit for β_p ?

A.8 Why bigger tokamaks with larger plasma current are better for fusion

As is mentioned in Sec. A.6, the beta limit study on JET tokamak shows that the maximal β_t obtained is proportional to $I_p / a B_{t0}$. This means the maximal plasmas pressure obtained is proportional to I_p / a , i.e.,

$$\langle p \rangle \propto \frac{I_p}{a} \quad (\text{A.39})$$

The total plasma energy is given by $E \approx \langle p \rangle 2\pi R \pi a^2$, where R is the major radius of the device. Using Eq. (A.39), we obtain

$$E \propto I_p a R. \quad (\text{A.40})$$

Since fusion power is proportional to the plasma energy, the above relation indicates, to obtain larger fusion power, we need bigger tokamaks with larger plasma current.

The reason why larger plasma current is desired can also be appreciated by examining an empirical scaling of the the energy confinement time τ_E given by

$$\tau_E \propto \frac{I^2}{T}, \quad (\text{A.41})$$

which is proportional to I^2 .

Another fundamental reason for building larger tokamaks is that the energy confinement time $\tau_E \sim a^2 / \chi$ increases with the machine size, where χ is the heat diffusivity. In addition, the heat diffusivity χ decreases with increasing machine size if the diffusivity satisfies the gyro-Bohm scaling, which is given by

$$\chi_{GB} = \frac{\sqrt{m_i} T_i^{3/2}}{a B^2 q_i^2}, \quad (\text{A.42})$$

which is inverse proportional to the machine size a . However, if the diffusivity satisfies the Bohm scaling, which is given by

$$\chi_B = \frac{T}{|q| B}, \quad (\text{A.43})$$

then, the diffusivity is independent of the machine size. The Bohm diffusivity χ_B is a / ρ_s times larger than the gyro-Bohm diffusivity χ_{GB} , where ρ_s is the gyro-radius. Heat diffusivity scaling in the low confinement operation (L mode) in present-day tokamaks is observed to be Bohm or worse than Bohm.

A.9 Density limit

The maximum density that can be obtained in stable plasma operations (without disruption) is empirically given by

$$n_e \approx 1.5 n_G, \quad (\text{A.44})$$

where n_G is the Greenwalt density, which is given by

$$n_G = 10^{14} \frac{I_p}{\pi a^2} \quad (\text{A.45})$$

where I_p is the plasma current, a is the minor radius, all physical quantities are in SI units. The $1.5 n_G$ gives the density limit that can be achieved for a tokamak operation scenario with plasma current I_p and plasma minor radius a . The Greenwalt density limit is an empirical one, which, like other empirical limits, can be exceeded in practice. Equation (A.45) indicates that the Greenwalt density is proportional to the current density. Therefore the ability to operate in large plasma current density means the ability to operate with high plasma density.

Note that neither the pressure limit nor the density limit is determined by the force-balance constraints. They are determined by the stability of the equilibrium. On the other hand, since the stability of the equilibrium is determined by the equilibrium itself, the pressure and density limit is determined by the equilibrium.

A.10 Normalized internal inductance

The self-inductance of a current loop is defined as the ratio of the magnetic flux Φ traversing the loop and its current I :

$$L = \frac{\Phi}{I}, \quad (\text{A.46})$$

where

$$\Phi = \int_S \mathbf{B} \cdot d\mathbf{S}, \quad (\text{A.47})$$

and \mathbf{B} is generated by the current I . It can be proved that L is independent of the current I in the loop, i.e., L is fully determined by the shape of the loop.

On the other hand, the energy contained in the magnetic field produced by the loop current is given by

$$W = \int_{V_0} \frac{B^2}{2\mu_0} dV, \quad (\text{A.48})$$

where the volume includes all space where B is not negligible. It can be proved that (to be proved) W , L , and I are related to each other by:

$$W = \frac{1}{2} L I^2, \quad (\text{A.49})$$

i.e.,

$$L = \frac{2W}{I^2}, \quad (\text{A.50})$$

which can be considered an equivalent definition of the self-inductance.

The internal inductance L_i of tokamak plasma is defined in such a way that W only includes the magnetic energy within the plasma. Specifically, L_i is defined by

$$L_i \equiv \frac{2W_i}{I^2} = \frac{2}{I^2} \int_P \frac{B^2}{2\mu_0} dV, \quad (\text{A.51})$$

where the integration over the plasma volume P . Its complement is the external inductance ($L = L_i + L_e$).

The normalized internal inductance l_i is defined as

$$l_i \equiv \frac{L_i}{\mu_0 \bar{R}/2}, \quad (\text{A.52})$$

where \bar{R} is the surface averaged major radius. Using Eq. (A.51), expression (A.52) is written as

$$l_i = \frac{1}{\mu_0 \bar{R}/2} \frac{2}{I^2} \int_P \frac{B_\theta^2}{2\mu_0} dV = \frac{2V}{I^2 \mu_0^2 \bar{R}} \langle B_\theta^2 \rangle, \quad (\text{A.53})$$

which is the definition of l_i used in the ITER design. Using the definition of \bar{R} , i.e.,

$$\bar{R} = \frac{\int R dS}{\int dS} = \frac{V}{2\pi A}, \quad (\text{A.54})$$

where A is the cross section of boundary flux surface, expression (A.53) is written as

$$l_i = \frac{4\pi A}{\mu_0^2 I^2} \langle B_\theta^2 \rangle. \quad (\text{A.55})$$

Another way of defining the normalized internal inductance is

$$l_i = \frac{\langle B_\theta^2 \rangle}{\langle B_\theta^2 \rangle_s}, \quad (\text{A.56})$$

where $\langle \dots \rangle_s$ is the surface average over the plasma boundary. Using Ampere's law, we obtain

$$\langle B_\theta^2 \rangle_s \approx \langle B_\theta \rangle_s^2 = \left(\frac{\mu_0 I}{l} \right)^2. \quad (\text{A.57})$$

Using this Eq. (A.56) is written as

$$l_i = \frac{l^2}{\mu_0^2 I^2} \langle B_\theta^2 \rangle \quad (\text{A.58})$$

For circular cross section, $l^2 = 4\pi A$. Then the above expression is written as

$$l_i = \frac{4\pi A}{\mu_0^2 I^2} \langle B_\theta^2 \rangle,$$

which agrees with Eq. (A.55).

The normalized internal inductance reflects the peakness of the current density profile in the toroidal plasma: smaller value of l_i corresponds to broader current profile.

A.11 Axisymmetric equilibrium current density

Since $\mathbf{J} = \mu_0^{-1} \nabla \times \mathbf{B}$, the current density \mathbf{J} can be inferred from a given magnetic field. The components of \mathbf{J} (expressed in terms of g and Ψ) are given by Eqs. (4.2), (4.3) and (4.6). These expressions can be further simplified by using the equilibrium constraints, such as $g = g(\Psi)$ and $\triangle^* \Psi = -\mu_0 R^2 \frac{dP}{d\Psi} - \frac{dg}{d\Psi} g$. The simplified \mathbf{J} expressions are given in A.12.

On the other hand, in the kinetic equilibrium reconstruction[20], it is the current that is first (partially) specified (e.g., by summing sources of current drive and bootstrap current) and then the current is used as constraints for the GS equation, i.e, constraints for the magnetic field.

A.12 Relation of plasma current density to pressure gradient

Due to the force balance condition, the plasma current is related to the plasma pressure gradient:

$$J_\phi = R \frac{dP}{d\Psi} + \frac{1}{\mu_0 R} \frac{dg}{d\Psi} g. \quad (\text{A.59})$$

The parallel (to the magnetic field) current density is written as

$$\begin{aligned} J_\parallel &\equiv \frac{\mathbf{J} \cdot \mathbf{B}}{B} \\ &= \frac{J_\phi B_\phi + \mathbf{J}_p \cdot \mathbf{B}_p}{B} \\ &= \frac{\left(R \frac{dP}{d\Psi} + \frac{1}{\mu_0 R} \frac{dg}{d\Psi} g \right) \frac{g}{R} + \frac{1}{\mu_0} \frac{dg}{d\Psi} \left(\frac{\nabla \Psi}{R} \right)^2}{B} \\ &= \frac{g \frac{dP}{d\Psi} + \frac{1}{\mu_0} \frac{dg}{d\Psi} \left[\left(\frac{g}{R} \right)^2 + \left(\frac{\nabla \Psi}{R} \right)^2 \right]}{B} \\ &= \frac{g \frac{dP}{d\Psi} + \frac{1}{\mu_0} \frac{dg}{d\Psi} B^2}{B}. \\ &= g \frac{dP}{d\Psi} \frac{1}{B} + \frac{1}{\mu_0} \frac{dg}{d\Psi} B. \end{aligned} \quad (\text{A.60})$$

For later use, define

$$\begin{aligned} \sigma &\equiv \frac{J_\parallel}{B} \\ &= g \frac{dP}{d\Psi} \frac{1}{B^2} + \frac{1}{\mu_0} \frac{dg}{d\Psi}. \end{aligned} \quad (\text{A.61})$$

Equation (A.61) is used in GTAW code to calculate J_\parallel / B (actually calculated is $\mu_0 J_\parallel / B$) [15]. Note that the expression for J_\parallel / B in Eq. (A.61) is not a magnetic surface function. Define σ_{ps} as

$$\begin{aligned} \sigma_{\text{ps}} &\equiv \sigma - \langle \sigma \rangle \\ &= g \frac{dP}{d\Psi} \left[\frac{1}{B^2} - \left\langle \frac{1}{B^2} \right\rangle \right] \end{aligned} \quad (\text{A.62})$$

$$\equiv \frac{J_\parallel^{\text{ps}}}{B}, \quad (\text{A.63})$$

where $J_\parallel^{\text{ps}} = g \frac{dP}{d\Psi} \left[\frac{1}{B} - B \left\langle \frac{1}{B^2} \right\rangle \right]$ is called Pfirsch-Schluter (PS) current. In cylindrical geometry, due to the poloidal symmetry, the Pfirsch-Schluter current is zero. In toroidal geometry, due to the poloidal asymmetry, the PS current is generally nonzero. Thus, this quantity characterizes a toroidal effect.

Another useful quantity is $\mu_0 \langle \mathbf{J} \cdot \mathbf{B} \rangle$, which is written as

$$\mu_0 \langle \mathbf{J} \cdot \mathbf{B} \rangle = \mu_0 g \frac{dP}{d\Psi} + \frac{dg}{d\Psi} \langle B^2 \rangle, \quad (\text{A.64})$$

where $\langle \dots \rangle$ is flux surface averaging operator.

A.13 Vacuum magnetic field (not finished)

In the vacuum region that is between the plasma and the first wall, there is no current, i.e.,

$$\nabla \times \mathbf{B} = 0. \quad (\text{A.65})$$

Next, let us examine what constraint this condition imposes on the magnetic field. Using expression (2.10), the above equation is written as

$$\nabla \times (\nabla \Psi \times \nabla \phi) + \nabla g \times \nabla \phi = 0, \quad (\text{A.66})$$

It is not obvious how to draw useful information from the above equation.

In the above, we use the vector potential approach. Next, let us try the scalar potential approach:

$$\mathbf{B} = \nabla \Phi, \quad (\text{A.67})$$

then the constraint $\nabla \cdot \mathbf{B} = 0$ is written as

$$\nabla^2 \Phi = 0. \quad (\text{A.68})$$

A.14 Discussion about the poloidal current function, check!

[check***As discussed in Sec. (), the force balance equation of axisymmetric plasma requires that $\mathbf{B} \cdot \nabla g = 0$. From this and the fact $\mathbf{B} \cdot \nabla \Psi = 0$, we conclude that g is a function of Ψ , i.e., $g = g(\Psi)$. However, this reasoning is not rigorous. Note the concept of a function requires that a function can not be a one-to-more map. This means that $g = g(\Psi)$ indicates that the values of g must be equal on two different magnetic field lines that have the same value of Ψ . However, the two equations $\mathbf{B} \cdot \nabla g = 0$ and $\mathbf{B} \cdot \nabla \Psi = 0$ do not require this constraint. To examine whether this constraint removes some equilibria from all the possible ones, we consider a system with an X point. Inside one of the magnetic islands, we use

$$g = \Psi^2 / (B_0 R_0^3), \quad (\text{A.69})$$

and inside the another, we use

$$g = \Psi^3 / (B_0^2 R_0^5), \quad (\text{A.70})$$

Then solve the two GS equations respectively within the boundary of the two islands. It is easy to obtain two magnetic surfaces that have the same value of Ψ respectively inside the two islands. Equations (A.69) and (A.70) indicate that the values of g on the two magnetic surfaces are different from each other. It is obvious the resulting equilibrium that contain the two islands can not be recovered by directly solving a single GS equation with a given function $g(\Psi)$.**check]

A.15 Field-aligned structure of non-axisymmetric perturbations

On both an irrational surface and a rational surface, there are infinite number of magnetic field lines that are not connected with each other. It is wrong to say there is only one magnetic field line on a irrational surface.

Consider a perturbation f that satisfies $\mathbf{B} \cdot \nabla f = 0$, i.e., the value f is a constant along any one of the magnetic field lines (field-aligned structure). Now comes the question: whether the values of f on different field lines are equal to each other?

To answer this question, we choose a direction that is different from \mathbf{B} on the magnetic surface and examine whether Ψ is constant along this direction, i.e., whether $\mathbf{k} \cdot \nabla f$ equals zero, where \mathbf{k} is the chosen direction. For axisymmetric magnetic surfaces, then $\mathbf{k} = \hat{\phi}$ is a direction in the magnetic surface and it is usually not identical with \mathbf{B}/B . Then we obtain

$$\mathbf{k} \cdot \nabla f = \hat{\phi} \cdot \nabla f = \frac{1}{R} \frac{\partial f}{\partial \phi}. \quad (\text{A.71})$$

If f is non-axisymmetric, then Eq. (A.71) indicates that $\mathbf{k} \cdot \nabla f \neq 0$, i.e., the values of f on different magnetic field lines on the same magnetic surface are not equal to each other. This is the case for the α coordinates discussed in Sec. 15.1.

Realistic perturbations in tokamak plasmas only have approximate field-aligned structure, i.e., $\mathbf{B} \cdot \nabla f \approx 0$. Put it in other words, $k_{\parallel} \ll k_{\perp}$.

This reasoning is for the case of axisymmetric magnetic surfaces. It is ready to do the same reasoning for non-axisymmetric magnetic surface after we find a convenient direction \mathbf{k} on the magnetic surface.

A.16 tmp check!

(In practice, I choose the positive direction of θ and ϕ along the direction of toroidal and poloidal magnetic field (i.e., $\mathbf{B} \cdot \nabla \phi$ and $\mathbf{B} \cdot \nabla \theta$ are always positive in (ψ, θ, ϕ) coordinates system). Then, the q_{local} defined by Eq. (10.82) is always positive. It follows that q_{global} should be also positive. Next, let us examine whether this property is correctly preserved by Eq. (10.88). Case 1: The radial coordinate ψ is chosen as $\Psi' \equiv d\Psi/d\psi > 0$. Then the factor before the integration in Eq. (10.88) is negative. We can further verify that \mathcal{J} is always negative for either the case that $\nabla \Psi$ is pointing inward or outward. Therefore the r.h.s. of Eq. (10.88) is always positive for this case. Case 2: The radial coordinate ψ is chosen as $\Psi' \equiv d\Psi/d\psi < 0$. Then the factor before the integration in Eq. (10.88) is positive. We can further verify that \mathcal{J} is always positive for either the case that $\nabla \Psi$ is pointing inward or outward. The above two cases include all possibilities. Therefore, the positivity of q_{global} is always guaranteed)

A.17 Radial coordinate to be deleted

We know that the toroidal flux ψ_t , safety factor q , and the Ψ in the GS equation are related by the following equations:

$$d\psi_t = 2\pi q d\Psi \quad (\text{A.72})$$

$$\Rightarrow \psi_t = 2\pi \int_0^\Psi q d\Psi \quad (\text{A.73})$$

Define:

$$\rho \equiv \sqrt{\frac{\psi_t}{\pi}} \quad (\text{A.74})$$

(In the Toray_ga code, the radial coordinate ρ is defined as

$$\rho \equiv \sqrt{\frac{\psi_t}{\pi B_{t0}}}, \quad (\text{A.75})$$

where B_{t0} is a constant factor. ρ defined this way is of length dimension, which is an effective geometry radius obtained by approximating the flux surface as circular.)

I use Eq. (A.74) to define ρ . Then we have

$$\psi_t = \pi \rho^2 \quad (\text{A.76})$$

$$\Rightarrow \frac{d\psi_t}{d\rho} = 2\pi\rho \quad (\text{A.77})$$

$$\Rightarrow \frac{d\psi_t}{d\psi} \frac{d\psi}{d\rho} = 2\pi\rho \quad (\text{A.78})$$

$$\Rightarrow 2\pi q \frac{d\psi}{d\rho} = 2\pi\rho \quad (\text{A.79})$$

$$\Rightarrow \frac{d\psi}{d\rho} = \frac{\rho}{q} \quad (\text{A.80})$$

Eq. (A.80) is used to transform between ψ and ρ .

$$\begin{aligned} d\rho &= \frac{1}{\sqrt{\Phi/\pi R_0^2 B_0}} \frac{1}{2} \frac{1}{\pi B_0 R_0^2} d\Phi = \frac{1}{\rho} \frac{1}{2} \frac{1}{\pi B_0 R_0^2} 2\pi q d\psi = \frac{1}{\rho} \frac{1}{B_0 R_0^2} q d\psi \\ &\Rightarrow d\psi = \frac{\rho B_0 R_0^2}{q} d\rho (\pi a^2) \end{aligned}$$

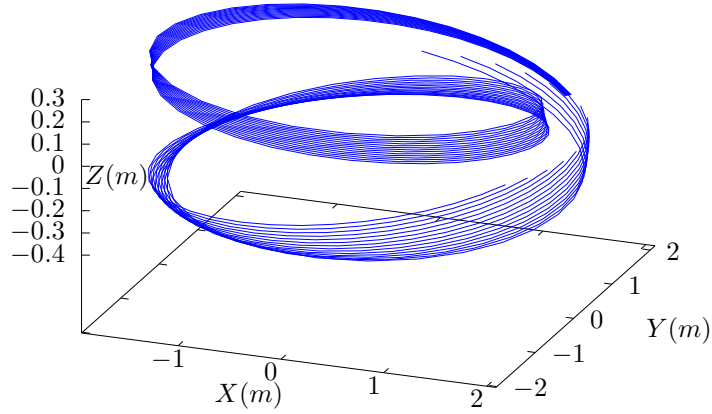


Figure A.3. to be deleted, Isosurface of $\alpha = 2\pi/8$. The surface is made of a family of contours of $\alpha = 2\pi/8$, which are all magnetic field lines. These field lines are traced by starting from a series of points on the low-field-side midplane ($\theta = 0$) at different radial locations and the field lines are followed by a complete poloidal loop. Magnetic field from EAST discharge #59954@3.03s.

A.18 Toroidal elliptic operator in magnetic surface coordinate system

If (ψ, θ, ϕ) are magnetic surface coordinates, i.e., $\partial\Psi/\partial\theta = 0$, then the toroidal elliptic operator in Eq. (17.2) is reduced to

$$\Delta^*\Psi = \frac{R^2}{\mathcal{J}} \left[\left(\Psi_\psi \frac{\mathcal{J}}{R^2} |\nabla\psi|^2 \right)_\psi + \left(\Psi_\psi \frac{\mathcal{J}}{R^2} \nabla\psi \cdot \nabla\theta \right)_\theta \right], \quad (\text{A.81})$$

and the GS equation, Eq. (17.5), is reduced to

$$\frac{R^2}{\mathcal{J}} \left[\left(\Psi_\psi \frac{\mathcal{J}}{R^2} |\nabla\psi|^2 \right)_\psi + \left(\Psi_\psi \frac{\mathcal{J}}{R^2} \nabla\psi \cdot \nabla\theta \right)_\theta \right] = -\mu_0 R^2 \frac{dP}{d\Psi} - \frac{dg}{d\Psi} g(\Psi). \quad (\text{A.82})$$

A.19 Grad-Shafranov equation in (r, θ, ϕ) coordinates

A.19.1 Definition of (r, θ, ϕ) coordinates

Define (r, θ, ϕ) coordinates by

$$R = R_0 + r \cos\theta, \quad (\text{A.83})$$

$$Z = r \sin\theta, \quad (\text{A.84})$$

where (R, ϕ, Z) are the cylindrical coordinates and R_0 is a constant. The above transformation is shown graphically in Fig. A.4.

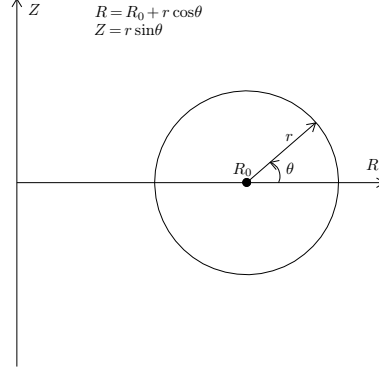


Figure A.4. The relation between coordinates (r, θ) and (R, Z) .

The Jacobian of (r, θ, ϕ) coordinates can be calculated using the definition. Using $x = R \cos \phi$, $y = R \sin \phi$, and $z = Z$, the Jacobian (with respect to the Cartesian coordinates (x, y, z)) is written as

$$\begin{aligned}
 \mathcal{J} &= \begin{vmatrix} \frac{\partial x}{\partial r} & \frac{\partial x}{\partial \theta} & \frac{\partial x}{\partial \phi} \\ \frac{\partial y}{\partial r} & \frac{\partial y}{\partial \theta} & \frac{\partial y}{\partial \phi} \\ \frac{\partial z}{\partial r} & \frac{\partial z}{\partial \theta} & \frac{\partial z}{\partial \phi} \end{vmatrix} = \begin{vmatrix} \frac{\partial R \cos \phi}{\partial r} & \frac{\partial R \cos \phi}{\partial \theta} & \frac{\partial R \cos \phi}{\partial \phi} \\ \frac{\partial R \sin \phi}{\partial r} & \frac{\partial R \sin \phi}{\partial \theta} & \frac{\partial R \sin \phi}{\partial \phi} \\ \frac{\partial Z}{\partial r} & \frac{\partial Z}{\partial \theta} & \frac{\partial Z}{\partial \phi} \end{vmatrix} \\
 &= \begin{vmatrix} \cos \theta \cos \phi & -r \sin \theta \cos \phi & -R \sin \phi \\ \cos \theta \sin \phi & -r \sin \theta \sin \phi & R \cos \phi \\ \sin \theta & r \cos \theta & 0 \end{vmatrix} \\
 &= \sin \theta (-Rr \sin \theta \cos^2 \phi - Rr \sin \theta \sin^2 \phi) \\
 &\quad + r \cos \theta (-R \sin^2 \phi \cos \theta - R \cos^2 \phi \cos \theta) \\
 &= -Rr \sin^2 \theta - Rr \cos^2 \theta \\
 &= -Rr.
 \end{aligned} \tag{A.85}$$

A.19.2 Toroidal elliptic operator $\Delta^* \Psi$ in (r, θ, ϕ) coordinate system

Next, we transform the GS equation from (R, Z) coordinates to (r, θ) coordinates. Using the relations $R = R_0 + r \cos \theta$ and $Z = r \sin \theta$, we have

$$r = \sqrt{(R - R_0)^2 + Z^2} \Rightarrow \frac{\partial r}{\partial Z} = \frac{Z}{r} = \sin \theta \tag{A.86}$$

$$\sin \theta = \frac{Z}{\sqrt{(R - R_0)^2 + Z^2}} \Rightarrow \cos \theta \frac{\partial \theta}{\partial Z} = \frac{r - Z \frac{Z}{r}}{r^2}. \tag{A.87}$$

$$\Rightarrow \frac{\partial \theta}{\partial Z} = \frac{r - Z \frac{Z}{r}}{r(R - R_0)} = \frac{1 - \sin^2 \theta}{R - R_0} = \frac{\cos^2 \theta}{R - R_0} \quad (\text{A.88})$$

$$\frac{\partial \sin \theta}{\partial Z} = \frac{r - Z \frac{Z}{r}}{r^2} = \frac{1 - \sin^2 \theta}{r} = \frac{\cos^2 \theta}{r} \quad (\text{A.89})$$

The GS equation in (R, Z) coordinates is given by

$$\frac{\partial^2 \Psi}{\partial Z^2} + R \frac{\partial}{\partial R} \left(\frac{1}{R} \frac{\partial \Psi}{\partial R} \right) = -\mu_0 R^2 \frac{dP}{d\Psi} - \frac{dg}{d\Psi} g(\Psi). \quad (\text{A.90})$$

The term $\partial \Psi / \partial Z$ is written as

$$\begin{aligned} \frac{\partial \Psi}{\partial Z} &= \frac{\partial \Psi}{\partial r} \frac{\partial r}{\partial Z} + \frac{\partial \Psi}{\partial \theta} \frac{\partial \theta}{\partial Z} \\ &= \frac{\partial \Psi}{\partial r} \sin \theta + \frac{\partial \Psi}{\partial \theta} \frac{\cos^2 \theta}{R - R_0}. \end{aligned} \quad (\text{A.91})$$

Using Eq. (A.91), $\partial^2 \Psi / \partial Z^2$ is written as

$$\begin{aligned} \frac{\partial^2 \Psi}{\partial Z^2} &= \frac{\partial}{\partial Z} \left(\frac{\partial \Psi}{\partial r} \sin \theta \right) + \frac{\partial}{\partial Z} \left(\frac{\partial \Psi}{\partial \theta} \frac{\cos^2 \theta}{R - R_0} \right) \\ &= \sin \theta \frac{\partial}{\partial Z} \left(\frac{\partial \Psi}{\partial r} \right) + \frac{\partial \Psi}{\partial r} \frac{\partial}{\partial Z} (\sin \theta) + \frac{\cos^2 \theta}{R - R_0} \frac{\partial}{\partial Z} \left(\frac{\partial \Psi}{\partial \theta} \right) + \frac{\partial \Psi}{\partial \theta} \frac{\partial}{\partial Z} \left(\frac{\cos^2 \theta}{R - R_0} \right) \\ &= \sin \theta \left(\frac{\partial^2 \Psi}{\partial r^2} \sin \theta + \frac{\partial^2 \Psi}{\partial r \partial \theta} \frac{\cos^2 \theta}{R - R_0} \right) + \frac{\partial \Psi}{\partial r} \frac{\cos^2 \theta}{r} + \frac{\cos^2 \theta}{R - R_0} \left(\frac{\partial^2 \Psi}{\partial \theta \partial r} \sin \theta + \right. \\ &\quad \left. \frac{\partial^2 \Psi}{\partial \theta^2} \frac{\cos^2 \theta}{R - R_0} \right) \\ &\quad - \frac{\partial \Psi}{\partial \theta} \frac{1}{R - R_0} 2 \cos \theta \sin \theta \frac{\cos^2 \theta}{R - R_0} \end{aligned} \quad (\text{A.92})$$

$$\frac{\partial r}{\partial R} = \frac{\partial}{\partial R} \sqrt{(R - R_0)^2 + Z^2} = \frac{R - R_0}{r} = \cos \theta \quad (\text{A.93})$$

$$\sin \theta = \frac{Z}{\sqrt{(R - R_0)^2 + Z^2}}.$$

$$\cos \theta \frac{\partial \theta}{\partial R} = -Z \frac{R - R_0}{r^3}$$

$$\frac{\partial \theta}{\partial R} = -\frac{Z}{r^2}. \quad (\text{A.94})$$

$$\cos \theta = \frac{R - R_0}{\sqrt{(R - R_0)^2 + Z^2}}$$

$$\frac{\partial}{\partial R} \cos \theta = \frac{r - \frac{R - R_0}{r} (R - R_0)}{r^2} = \frac{1 - \cos^2 \theta}{r} = \frac{\sin^2 \theta}{r} \quad (\text{A.95})$$

$$\begin{aligned}
R \frac{\partial}{\partial R} \left(\frac{1}{R} \frac{\partial \Psi}{\partial R} \right) &= R \frac{\partial}{\partial R} \left[\frac{1}{R} \left(\frac{\partial \Psi}{\partial r} \frac{\partial r}{\partial R} + \frac{\partial \Psi}{\partial \theta} \frac{\partial \theta}{\partial R} \right) \right] \\
&= R \frac{\partial}{\partial R} \left[\frac{1}{R} \left(\frac{\partial \Psi}{\partial r} \cos \theta - \frac{\partial \Psi}{\partial \theta} \frac{Z}{r^2} \right) \right] \\
&= \frac{\partial}{\partial R} \left(\frac{\partial \Psi}{\partial r} \cos \theta - \frac{\partial \Psi}{\partial \theta} \frac{Z}{r^2} \right) + R \left(\frac{\partial \Psi}{\partial r} \cos \theta - \frac{\partial \Psi}{\partial \theta} \frac{Z}{r^2} \right) \left(-\frac{1}{R^2} \right) \\
&= \left(\frac{\partial^2 \Psi}{\partial r^2} \frac{\partial r}{\partial R} + \frac{\partial^2 \Psi}{\partial r \partial \theta} \frac{\partial \theta}{\partial R} \right) \cos \theta + \frac{\partial \Psi}{\partial r} \frac{\partial}{\partial R} \cos \theta - \left(\frac{\partial^2 \Psi}{\partial \theta \partial r} \frac{\partial r}{\partial R} + \right. \\
&\quad \left. \frac{\partial^2 \Psi}{\partial \theta^2} \frac{\partial \theta}{\partial R} \right) \frac{Z}{r^2} - \frac{\partial \Psi}{\partial \theta} \frac{\partial}{\partial R} \left(\frac{Z}{r^2} \right) - \frac{1}{R} \left(\frac{\partial \Psi}{\partial r} \cos \theta - \frac{\partial \Psi}{\partial \theta} \frac{Z}{r^2} \right) \\
&= \left(\frac{\partial^2 \Psi}{\partial r^2} \cos \theta - \frac{\partial^2 \Psi}{\partial r \partial \theta} \frac{Z}{r^2} \right) \cos \theta + \frac{\partial \Psi}{\partial r} \frac{\sin^2 \theta}{r} - \left(\frac{\partial^2 \Psi}{\partial \theta \partial r} \cos \theta - \right. \\
&\quad \left. \frac{\partial^2 \Psi}{\partial \theta^2} \frac{Z}{r^2} \right) \frac{Z}{r^2} + \frac{\partial \Psi}{\partial \theta} Z \frac{1}{r^3} 2 \cos \theta - \frac{1}{R} \left(\frac{\partial \Psi}{\partial r} \cos \theta - \frac{\partial \Psi}{\partial \theta} \frac{Z}{r^2} \right) \\
&= \frac{\partial^2 \Psi}{\partial r^2} \cos^2 \theta + \frac{\partial^2 \Psi}{\partial \theta^2} \frac{\sin^2 \theta}{r^2} - 2 \frac{\partial^2 \Psi}{\partial r \partial \theta} \frac{Z}{r^2} \cos \theta + \frac{\partial \Psi}{\partial r} \frac{\sin^2 \theta}{r} + \\
&\quad \frac{\partial \Psi}{\partial \theta} Z \frac{1}{r^3} 2 \cos \theta \tag{A.96} \\
&- \frac{1}{R} \left(\frac{\partial \Psi}{\partial r} \cos \theta - \frac{\partial \Psi}{\partial \theta} \frac{1}{r} \sin \theta \right) \tag{A.97}
\end{aligned}$$

Summing the the right-hand-side of Eq. (A.92) and the expression on line (A.96) yields

$$\frac{\partial^2 \Psi}{\partial r^2} + \frac{\partial \Psi}{\partial r} \frac{1}{r} + \frac{1}{r^2} \frac{\partial^2 \Psi}{\partial \theta^2}. \tag{A.98}$$

Using these, the GS equation is written as

$$\begin{aligned}
&\frac{\partial^2 \Psi}{\partial r^2} + \frac{\partial \Psi}{\partial r} \frac{1}{r} + \frac{1}{r^2} \frac{\partial^2 \Psi}{\partial \theta^2} - \frac{1}{R_0 + r \cos \theta} \left(\frac{\partial \Psi}{\partial r} \cos \theta - \frac{\partial \Psi}{\partial \theta} \frac{1}{r} \sin \theta \right) = -\mu_0 (R_0 + \\
&r \cos \theta)^2 \frac{dP}{d\Psi} - \frac{dg}{d\Psi} g(\Psi),
\end{aligned}$$

which can be arranged in the form

$$\begin{aligned}
&\left(\frac{1}{r} \frac{\partial}{\partial r} r \frac{\partial}{\partial r} + \frac{1}{r^2} \frac{\partial^2}{\partial \theta^2} \right) \Psi - \frac{1}{R_0 + r \cos \theta} \left(\frac{\partial \Psi}{\partial r} \cos \theta - \frac{\partial \Psi}{\partial \theta} \frac{1}{r} \sin \theta \right) = -\mu_0 (R_0 + \\
&r \cos \theta)^2 \frac{dP}{d\Psi} - \frac{dg}{d\Psi} g(\Psi), \tag{A.99}
\end{aligned}$$

which agrees with Eq. (3.6.2) in Wesson's book[29], where f is defined by $f = RB_\phi / \mu_0$, which is different from $g \equiv RB_\phi$ by a $1/\mu_0$ factor.

A.20 Large aspect ratio expansion

Consider the case that the boundary flux surface is circular with radius $r = a$ and the center of the circle at $(R = R_0, Z = 0)$. Consider the case $\varepsilon = r/R_0 \rightarrow 0$. Expanding Ψ in the small parameter ε ,

$$\Psi = \Psi_0 + \Psi_1 \quad (\text{A.100})$$

where $\Psi_0 \sim O(\varepsilon^0)$, $\Psi_1 \sim O(\varepsilon^1)$. Substituting Eq. (A.100) into Eq. (A.99), we obtain

$$\begin{aligned} & \frac{1}{r} \frac{\partial}{\partial r} r \frac{\partial \Psi_0}{\partial r} + \frac{1}{r} \frac{\partial}{\partial r} r \frac{\partial \Psi_1}{\partial r} + \frac{1}{r^2} \frac{\partial^2 \Psi_0}{\partial \theta^2} + \frac{1}{r^2} \frac{\partial^2 \Psi_1}{\partial \theta^2} - \frac{1}{R_0 + r \cos \theta} \left(\frac{\partial \Psi_0}{\partial r} \cos \theta - \right. \\ & \left. \frac{\partial \Psi_0}{\partial \theta} \frac{1}{r} \sin \theta \right) - \frac{1}{R_0 + r \cos \theta} \left(\frac{\partial \Psi_1}{\partial r} \cos \theta - \frac{\partial \Psi_1}{\partial \theta} \frac{1}{r} \sin \theta \right) = -\mu_0 (R_0 + r \cos \theta)^2 P'(\Psi_0 + \Psi_1) \\ & - g'(\Psi_0 + \Psi_1) g(\Psi_0 + \Psi_1) \end{aligned}$$

Multiplying the above equation by R_0^2 , we obtain

$$\begin{aligned} & R_0^2 \frac{1}{r} \frac{\partial}{\partial r} r \frac{\partial \Psi_0}{\partial r} + R_0^2 \frac{1}{r} \frac{\partial}{\partial r} r \frac{\partial \Psi_1}{\partial r} + R_0^2 \frac{1}{r^2} \frac{\partial^2 \Psi_0}{\partial \theta^2} + R_0^2 \frac{1}{r^2} \frac{\partial^2 \Psi_1}{\partial \theta^2} - \frac{R_0^2}{R_0 + r \cos \theta} \left(\frac{\partial \Psi_0}{\partial r} \cos \theta - \right. \\ & \left. \frac{\partial \Psi_0}{\partial \theta} \frac{1}{r} \sin \theta \right) - \frac{R_0^2}{R_0 + r \cos \theta} \left(\frac{\partial \Psi_1}{\partial r} \cos \theta - \frac{\partial \Psi_1}{\partial \theta} \frac{1}{r} \sin \theta \right) = -\mu_0 R_0^2 (R_0 + r \cos \theta)^2 P'(\Psi_0 + \Psi_1) \\ & - R_0^2 g'(\Psi_0 + \Psi_1) g(\Psi_0 + \Psi_1) \end{aligned} \quad (\text{A.101})$$

Further assume the following orderings (why?)

$$R_0 \frac{\partial \Psi}{\partial r} \sim O(\varepsilon^{-1}) \Psi, \quad (\text{A.102})$$

and

$$\frac{\partial \Psi}{\partial \theta} \sim O(\varepsilon^0) \Psi. \quad (\text{A.103})$$

Using these orderings, the order of the terms in Eq. (A.101) can be estimated as

$$R_0^2 \frac{1}{r} \frac{\partial}{\partial r} r \frac{\partial \Psi_0}{\partial r} \sim \frac{\Psi_0}{\varepsilon^2} \sim O(\varepsilon^{-2}) \quad (\text{A.104})$$

$$R_0^2 \frac{1}{r} \frac{\partial}{\partial r} r \frac{\partial \Psi_1}{\partial r} \sim \frac{\Psi_1}{\varepsilon^2} \sim O(\varepsilon^{-1}) \quad (\text{A.105})$$

$$R_0^2 \frac{1}{r^2} \frac{\partial^2 \Psi_0}{\partial \theta^2} \sim \frac{1}{\varepsilon^2} \Psi_0 \sim O(\varepsilon^{-2}) \quad (\text{A.106})$$

$$R_0^2 \frac{1}{r^2} \frac{\partial^2 \Psi_1}{\partial \theta^2} \sim \frac{\Psi_1}{\varepsilon^2} \sim O(\varepsilon^{-1}) \quad (\text{A.107})$$

$$\frac{R_0}{R_0 + r \cos \theta} \approx 1 - \frac{r}{R_0} \cos \theta \quad (\text{A.108})$$

$$R_0 \frac{\partial \Psi_0}{\partial r} \cos \theta \sim \frac{\Psi_0}{\varepsilon} \sim O(\varepsilon^{-1}) \quad (\text{A.109})$$

$$R_0 \frac{\partial \Psi_0}{\partial \theta} \frac{1}{r} \sin \theta \sim \frac{\Psi_0}{\varepsilon} \sim O(\varepsilon^{-1}) \quad (\text{A.110})$$

$$R_0 \frac{\partial \Psi_1}{\partial r} \cos \theta \sim \frac{\Psi_1}{\varepsilon} = O(\varepsilon^0) \quad (\text{A.111})$$

$$R_0 \frac{\partial \Psi_1}{\partial \theta} \frac{1}{r} \sin \theta \sim \frac{\Psi_1}{\varepsilon} = O(\varepsilon^0) \quad (\text{A.112})$$

The leading order (ε^{-2} order) balance is given by the following equation:

$$R_0^2 \frac{1}{r} \frac{\partial}{\partial r} r \frac{\partial \Psi_0}{\partial r} + R_0^2 \frac{1}{r^2} \frac{\partial^2 \Psi_0}{\partial \theta^2} = -\mu_0 R_0^4 P'(\Psi_0) - R_0^2 g'(\Psi_0) g(\Psi_0), \quad (\text{A.113})$$

It is reasonable to assume that Ψ_0 is independent of θ since Ψ_0 corresponds to the limit $a/R \rightarrow 0$. (The limit $a/R \rightarrow 0$ can have two cases, one is $r \rightarrow 0$, another is $R \rightarrow \infty$. In the former case, Ψ must be independent of θ since Ψ should be single-valued. The latter case corresponds to a cylinder, for which it is reasonable (really?) to assume that Ψ_0 is independent of θ .) Then Eq. (A.113) is written

$$\frac{1}{r} \frac{\partial}{\partial r} r \frac{\partial \Psi_0}{\partial r} = -\mu_0 R_0^2 P'(\Psi_0) - g'(\Psi_0) g(\Psi_0). \quad (\text{A.114})$$

(My remarks: The leading order equation (A.114) does not corresponds strictly to a cylinder equilibrium because the magnetic field $\mathbf{B} = \nabla \Psi_0 \times \nabla \phi + g \nabla \phi$ depends on θ .) The next order (ε^{-1} order) equation is

$$R_0^2 \frac{1}{r} \frac{\partial}{\partial r} r \frac{\partial \Psi_1}{\partial r} + R_0^2 \frac{1}{r^2} \frac{\partial^2 \Psi_1}{\partial \theta^2} - R_0 \frac{\partial \Psi_0}{\partial r} \cos \theta = -\mu_0 R_0^2 2R_0 r \cos \theta P'(\Psi_0) - \mu_0 R_0^4 P''(\Psi_0) \Psi_1 - R_0^2 [g'(\Psi_0) g(\Psi_0)]' \Psi_1$$

$$R_0^2 \frac{1}{r} \frac{\partial}{\partial r} r \frac{\partial \Psi_1}{\partial r} + R_0^2 \frac{1}{r^2} \frac{\partial^2 \Psi_1}{\partial \theta^2} + \{\mu_0 R_0^4 P''(\Psi_0) + R_0^2 [g'(\Psi_0) g(\Psi_0)]'\} \Psi_1 = -\mu_0 R_0^2 2R_0 r \cos \theta P'(\Psi_0) + R_0 \frac{\partial \Psi_0}{\partial r} \cos \theta \quad (\text{A.115})$$

$$R_0^2 \frac{1}{r} \frac{\partial}{\partial r} r \frac{\partial \Psi_1}{\partial r} + R_0^2 \frac{1}{r^2} \frac{\partial^2 \Psi_1}{\partial \theta^2} + \frac{d}{dr} \{\mu_0 R_0^4 P'(\Psi_0) + R_0^2 g'(\Psi_0) g(\Psi_0)\} \frac{dr}{d\Psi_0} \Psi_1 = -\mu_0 R_0^2 2R_0 r \cos \theta P'(\Psi_0) + R_0 \frac{\partial \Psi_0}{\partial r} \cos \theta \quad (\text{A.116})$$

It is obvious that the simple poloidal dependence of $\cos \theta$ will satisfy the above equation. Therefore, we consider Ψ_1 of the form

$$\Psi_1 = \Delta(r) \frac{d\Psi_0(r)}{dr} \cos \theta, \quad (\text{A.117})$$

where $\Delta(r)$ is a new function to be determined. Substitute this into the Eq. (A.116), we obtain an equation for $\Delta(r)$,

$$R_0^2 \frac{1}{r} \frac{d}{dr} \left(r \frac{d\Psi_0}{dr} \frac{d\Delta}{dr} + r \Delta \frac{d^2 \Psi_0}{dr^2} \right) - R_0^2 \frac{1}{r^2} \Delta \frac{d\Psi_0(r)}{dr} + \frac{d}{dr} \{\mu_0 R_0^4 P'(\Psi_0) + R_0^2 g'(\Psi_0) g(\Psi_0)\} \frac{dr}{d\Psi_0} \Delta \frac{d\Psi_0(r)}{dr} = -\mu_0 R_0^2 2R_0 r P'(\Psi_0) + R_0 \frac{d\Psi_0}{dr} \quad (\text{A.118})$$

$$R_0^2 \frac{1}{r} \frac{d}{dr} \left(r \frac{d\Psi_0}{dr} \frac{d\Delta}{dr} \right) + R_0^2 \frac{1}{r} \frac{d}{dr} \left(r \Delta \frac{d^2\Psi_0}{dr^2} \right) - R_0^2 \frac{1}{r^2} \Delta \frac{d\Psi_0(r)}{dr} + \frac{d}{dr} \{ \mu_0 R_0^4 P'(\Psi_0) + R_0^2 g'(\Psi_0) g(\Psi_0) \} \Delta = -\mu_0 R_0^2 2R_0 r P'(\Psi_0) + R_0 \frac{d\Psi_0}{dr} \quad (\text{A.119})$$

$$R_0^2 \frac{1}{r} \frac{d}{dr} \left(r \frac{d\Psi_0}{dr} \frac{d\Delta}{dr} \right) + \Delta R_0^2 \frac{1}{r} \frac{d}{dr} \left(r \frac{d^2\Psi_0}{dr^2} \right) + R_0^2 \frac{d^2\Psi_0}{dr^2} \frac{d\Delta}{dr} - R_0^2 \frac{1}{r^2} \Delta \frac{d\Psi_0(r)}{dr} + \frac{d}{dr} \{ \mu_0 R_0^4 P'(\Psi_0) + R_0^2 g'(\Psi_0) g(\Psi_0) \} \Delta = -\mu_0 R_0^2 2R_0 r P'(\Psi_0) + R_0 \frac{d\Psi_0}{dr} \quad (\text{A.120})$$

$$R_0^2 \frac{1}{r} \frac{d}{dr} \left(r \frac{d\Psi_0}{dr} \frac{d\Delta}{dr} \right) + \Delta R_0^2 \left[\frac{1}{r} \frac{d}{dr} \left(r \frac{d^2\Psi_0}{dr^2} \right) - \frac{1}{r^2} \frac{d\Psi_0(r)}{dr} \right] + R_0^2 \frac{d^2\Psi_0}{dr^2} \frac{d\Delta}{dr} + \frac{d}{dr} \{ \mu_0 R_0^4 P'(\Psi_0) + R_0^2 g'(\Psi_0) g(\Psi_0) \} \Delta = -\mu_0 R_0^2 2R_0 r P'(\Psi_0) + R_0 \frac{d\Psi_0}{dr} \quad (\text{A.121})$$

Using the identity

$$\frac{d}{dr} \left[\frac{1}{r} \frac{d}{dr} \left(r \frac{d\Psi_0}{dr} \right) \right] = \frac{1}{r} \frac{d}{dr} \left(r \frac{d^2\Psi_0}{dr^2} \right) - \frac{1}{r^2} \frac{d\Psi_0(r)}{dr},$$

equation () is written as

$$R_0^2 \frac{1}{r} \frac{d}{dr} \left(r \frac{d\Psi_0}{dr} \frac{d\Delta}{dr} \right) + \Delta R_0^2 \frac{d}{dr} \left[\frac{1}{r} \frac{d}{dr} \left(r \frac{d\Psi_0}{dr} \right) \right] + R_0^2 \frac{d^2\Psi_0}{dr^2} \frac{d\Delta}{dr} + \frac{d}{dr} \{ \mu_0 R_0^4 P'(\Psi_0) + R_0^2 g'(\Psi_0) g(\Psi_0) \} \Delta = -\mu_0 R_0^2 2R_0 r P'(\Psi_0) + R_0 \frac{d\Psi_0}{dr} \quad (\text{A.122})$$

Using the leading order equation (), we know that the second and fourth term on the l.h.s of the above equation cancel each other, giving

$$R_0^2 \frac{1}{r} \frac{d}{dr} \left(r \frac{d\Psi_0}{dr} \frac{d\Delta}{dr} \right) + R_0^2 \frac{d^2\Psi_0}{dr^2} \frac{d\Delta}{dr} = -\mu_0 R_0^2 2R_0 r P'(\Psi_0) + R_0 \frac{d\Psi_0}{dr} \quad (\text{A.123})$$

$$\Rightarrow \frac{1}{r} \frac{d}{dr} \left(r \frac{d\Psi_0}{dr} \frac{d\Delta}{dr} \right) + \frac{d^2\Psi_0}{dr^2} \frac{d\Delta}{dr} = -\mu_0 2R_0 r P'(\Psi_0) + \frac{1}{R_0} \frac{d\Psi_0}{dr} \quad (\text{A.124})$$

Using the identity

$$\frac{1}{r} \frac{dr}{d\Psi_0} \frac{d}{dr} \left[r \left(\frac{d\Psi_0}{dr} \right)^2 \frac{d\Delta}{dr} \right] = \frac{1}{r} \frac{d}{dr} \left(r \frac{d\Psi_0}{dr} \frac{d\Delta}{dr} \right) + \frac{d^2\Psi_0}{dr^2} \frac{d\Delta}{dr}, \quad (\text{A.125})$$

equation (A.124) is written

$$\frac{1}{r} \frac{dr}{d\Psi_0} \frac{d}{dr} \left[r \left(\frac{d\Psi_0}{dr} \right)^2 \frac{d\Delta}{dr} \right] = -\mu_0 2R_0 r P'(\Psi_0) + \frac{1}{R_0} \frac{d\Psi_0}{dr}, \quad (\text{A.126})$$

$$\Rightarrow \frac{1}{r} \frac{d}{dr} \left[r \left(\frac{d\Psi_0}{dr} \right)^2 \frac{d\Delta}{dr} \right] = -\mu_0 2R_0 r \frac{dP}{dr} + \frac{1}{R_0} \left(\frac{d\Psi_0}{dr} \right)^2, \quad (\text{A.127})$$

Using

$$B_{\theta 0} = \frac{1}{R_0} \frac{d\Psi_0}{dr} \quad (\text{A.128})$$

equation (A.127) is written

$$\frac{1}{r} \frac{d}{dr} \left[r B_{\theta 0}^2 \frac{d\Delta}{dr} \right] = -\mu_0 2 \frac{1}{R_0} r \frac{dP}{dr} + \frac{B_{\theta 0}^2}{R_0}. \quad (\text{A.129})$$

$$\Rightarrow \frac{d}{dr} \left[r B_{\theta 0}^2 \frac{d\Delta}{dr} \right] = \frac{r}{R_0} \left(-2\mu_0 r \frac{dP(\Psi_0)}{dr} + B_{\theta 0}^2 \right), \quad (\text{A.130})$$

which agrees with equation (3.6.7) in Wessson's book[29].

A.21 (s, α) parameters

The normalized pressure gradient, α , which appears frequently in tokamak literature, is defined by[3]

$$\alpha = -R_0 q^2 \frac{1}{B_0^2 / 2\mu_0} \frac{dp}{dr}, \quad (\text{A.131})$$

which can be further written

$$\alpha = -R_0 q^2 \frac{d\bar{p}}{dr}, \quad (\text{A.132})$$

where $\bar{p} = p / (B_0^2 / 2\mu_0)$. Equation (A.132) can be further written as

$$\alpha = -\frac{1}{\varepsilon_a} q^2 \frac{d\bar{p}}{d\bar{r}}, \quad (\text{A.133})$$

where $\varepsilon_a = a / R_0$, $\bar{r} = r / a$, and a is the minor radius of the boundary flux surface. (Why is there a q^2 factor in the definition of α ?)

The global magnetic shear s is defined by

$$s = \frac{r}{q} \frac{dq}{dr}, \quad (\text{A.134})$$

which can be written

$$s = \frac{\bar{r}}{q} \frac{dq}{d\bar{r}}. \quad (\text{A.135})$$

In the case of large aspect ratio and circular flux surface, the leading order equation of the Grad-Shafranov equation in (r, θ) coordinates is written

$$\frac{1}{r} \frac{d}{dr} r \frac{d\Psi}{dr} = -\mu_0 R_0 J_\phi(r), \quad (\text{A.136})$$

which gives concentric circular flux surfaces centered at $(R = R_0, Z = 0)$. Assume that J_ϕ is uniform distributed, i.e., $|J_\phi| = I / (\pi a^2)$, where I is the total current within the flux surface $r = a$. Further assume the current is in the opposite direction of $\nabla \phi$, then $J_\phi = -I / (\pi a^2)$. Using this, Eq. (A.136) can be solved to give

$$\Psi = \frac{\mu_0 I}{4\pi a^2} R_0 r^2. \quad (\text{A.137})$$

Then it follows that the normalized radial coordinate $\rho \equiv (\Psi - \Psi_0) / (\Psi_b - \Psi_0)$ relates to \bar{r} by $\bar{r} = \sqrt{\rho}$ (I check this numerically for the case of EAST discharge #38300). Since in my code, the radial coordinate is Ψ , I need to transform the derivative with respect to \bar{r} to one with respect to Ψ , which gives

$$\alpha = -\frac{1}{\varepsilon} q^2 \frac{d\bar{p}}{d\bar{r}} = -\frac{1}{\varepsilon} q^2 \frac{d\bar{p}}{d\sqrt{\rho}} = -\frac{1}{\varepsilon} q^2 \frac{d\bar{p}}{d\rho} \frac{1}{2\sqrt{\rho}} = -\frac{1}{\varepsilon} q^2 \frac{d\bar{p}}{d\Psi} \frac{1}{2\sqrt{\rho}} (\Psi_b - \Psi_0). \quad (\text{A.138})$$

$$s = \frac{\bar{r}}{q} \frac{dq}{d\bar{r}} = \frac{\sqrt{\rho}}{q} \frac{dq}{d\Psi} \frac{1}{2\sqrt{\rho}} (\Psi_b - \Psi_0) = \frac{1}{2q} \frac{dq}{d\Psi} (\Psi_b - \Psi_0). \quad (\text{A.139})$$

The necessary condition for the existence of TAEs with frequency near the upper tip of the gap is given by[3]

$$\alpha < -s^2 + \varepsilon, \quad (\text{A.140})$$

which is used in my paper on Alfvén eigenmodes on EAST tokamak[15]. Equations (A.138) and (A.139) are used in the GTAW code to calculate s and α .

B Computing magnetic field and vector potential generated by coils

Magnetic field (e.g., equilibrium poloidal field, RMP field, ripple field) and vector potential generated by coils can be calculated in the following way.

B.1 Magnetic field

The Biot-Savart law for a zero-thickness wire is given by

$$\mathbf{B}(\mathbf{r}) = \frac{\mu_0}{4\pi} \int I \frac{d\mathbf{l}(\mathbf{r}') \times (\mathbf{r} - \mathbf{r}')}{|\mathbf{r} - \mathbf{r}'|^3}, \quad (\text{B.1})$$

where $d\mathbf{l}(\mathbf{r}')$ is a line element along the wire (the freedom of choosing which one of the two possible directions along the wire is up to users), I is the current in the wire (I is positive if the current in the same direction of $d\mathbf{l}$, otherwise, negative).

B.2 Magnetic vector potential

Given a current source $\mathbf{J}(\mathbf{r}, t)$, the vector potential can be calculated using

$$\mathbf{A}(\mathbf{r}, t) = \frac{\mu_0}{4\pi} \int_{\Omega} \frac{\mathbf{J}(\mathbf{r}', t')}{|\mathbf{r} - \mathbf{r}'|} d^3\mathbf{r}', \quad (\text{B.2})$$

where

$$t' = t - \frac{|\mathbf{r} - \mathbf{r}'|}{c}, \quad (\text{B.3})$$

is called the retarded time. For a steady-state source, $\mathbf{J}(\mathbf{r}', t') = \mathbf{J}(\mathbf{r})$. Then Eq. (B.2) is simplified as

$$\mathbf{A}(\mathbf{r}) = \frac{\mu_0}{4\pi} \int_{\Omega} \frac{\mathbf{J}(\mathbf{r}')}{|\mathbf{r} - \mathbf{r}'|} d^3\mathbf{r}'. \quad (\text{B.4})$$

For a current flowing in a thin wire, the above equation is written as

$$\mathbf{A}(\mathbf{r}) = \frac{\mu_0}{4\pi} \int \frac{\mathbf{J}(\mathbf{r}')}{|\mathbf{r} - \mathbf{r}'|} dS(\mathbf{r}') dl(\mathbf{r}'), \quad (\text{B.5})$$

where dS is a surface element perpendicular to the wire and dl is a line element along the wire. Using $\mathbf{J}(\mathbf{r}')dS(\mathbf{r}') = \mathbf{I}(\mathbf{r}')$, the above equation is written as

$$\begin{aligned} \mathbf{A}(\mathbf{r}) &= \frac{\mu_0}{4\pi} \int \frac{\mathbf{I}(\mathbf{r}')}{|\mathbf{r} - \mathbf{r}'|} dl(\mathbf{r}') \\ &= \frac{\mu_0}{4\pi} \int \frac{I(\mathbf{r}')}{|\mathbf{r} - \mathbf{r}'|} d\mathbf{l}(\mathbf{r}'). \end{aligned} \quad (\text{B.6})$$

In cylindrical coordinates, the toroidal component of \mathbf{A} , $A_\phi \equiv \mathbf{A} \cdot \mathbf{e}_\phi(\mathbf{r})$, is written as

$$A_\phi(\mathbf{r}) = \frac{\mu_0}{4\pi} \int \frac{I(\mathbf{r}')}{|\mathbf{r} - \mathbf{r}'|} d\mathbf{l}(\mathbf{r}') \cdot \mathbf{e}_\phi(\mathbf{r}). \quad (\text{B.7})$$

(A_ϕ is needed in several applications. In solving the free-boundary equilibrium problem, we need to calculate A_ϕ generated by the PF coils. In studying the effects of RMP on particles, we need to calculate P_ϕ , the canonical toroidal angular momentum, whose definition involves A_ϕ . So we need to calculate A_ϕ generated by the RMP coils.)

B.3 For a toroidal wire

In terms of the cylindrical basis, the line element $d\mathbf{l}'$ of a toroidal curve is given by $d\mathbf{l}' = R' d\phi' \hat{\mathbf{e}}'_\phi$. Using Cartesian coordinate basis vectors, $d\mathbf{l}'$ is written as

$$d\mathbf{l}' = R' d\phi' (-\sin\phi' \hat{\mathbf{e}}_x + \cos\phi' \hat{\mathbf{e}}_y), \quad (\text{B.8})$$

and the position vector \mathbf{r}' is written as

$$\mathbf{r}' = R' \cos\phi' \hat{\mathbf{e}}_x + R' \sin\phi' \hat{\mathbf{e}}_y + Z' \hat{\mathbf{e}}_z \quad (\text{B.9})$$

where a global Cartesian coordinates with x axis in $\phi = 0$ plane is assumed.

Let us consider a full toroidal coil at (R', Z') with current I (a filamentary current loop). Since the problem is axisymmetric, the magnetic field/potential is independent of ϕ . For calculation ease, we select $\phi = 0$ plane and calculate \mathbf{A} and \mathbf{B} values in this plane. Then

$$\mathbf{e}_\phi(\mathbf{r}) = \hat{\mathbf{e}}_y, \quad (\text{B.10})$$

$$\mathbf{r} = R \hat{\mathbf{e}}_x + 0 \hat{\mathbf{e}}_y + Z \hat{\mathbf{e}}_z, \quad (\text{B.11})$$

Using these, we obtain

$$d\mathbf{l}' \cdot \mathbf{e}_\phi(\mathbf{r}) = R' d\phi' \cos\phi'. \quad (\text{B.12})$$

and Eq. (B.7) is written as

$$A_\phi(R, Z, \phi = 0) = \frac{\mu_0 I}{4\pi} \int_0^{2\pi} \frac{R' \cos\phi' d\phi'}{\sqrt{(Z - Z')^2 + (R - R' \cos\phi')^2 + (R' \sin\phi')^2}}. \quad (\text{B.13})$$

Because A_ϕ is axsymmetric, the above formula applies to all values of ϕ . Multiply A_ϕ by R and set $I=1$, we get Green's function for Ψ :

$$\begin{aligned}
& G(R', Z', R, Z) \\
&= RA_\phi \\
&= \frac{\mu_0}{4\pi} \int_0^{2\pi} \frac{RR' \cos \phi' d\phi'}{\sqrt{(Z-Z')^2 + (R-R' \cos \phi')^2 + (R' \sin \phi')^2}} \\
&= \frac{\mu_0}{4\pi} \int_0^{2\pi} \frac{RR' \cos \phi' d\phi'}{\sqrt{(Z-Z')^2 + R^2 + R'^2 - 2RR' \cos \phi'}}. \tag{B.14}
\end{aligned}$$

This expression can be directly used in numerical codes to compute the Green function table. From this formula, we can see that the source location and observation location are symmetric, i.e., $G(R', Z', R, Z) = G(R, Z, R', Z')$.

One can also write the above integration to the elipitic integrals and use library to compute these inegreals. Let us write the above expresion in this form. Define $\theta = (\pi - \phi) / 2$, then $\cos \phi' = \cos(\pi - 2\theta) = -\cos(2\theta) = 2 \sin^2 \theta - 1$. Using this Eq. (B.14) is written as

$$\begin{aligned}
& G(R', Z', R, Z) \\
&= \frac{\mu_0}{4\pi} \int_{\pi/2}^{-\pi/2} \frac{-2RR'(2\sin^2 \theta - 1)d\theta}{\sqrt{(Z-Z')^2 + R^2 + R'^2 - 2RR'(2\sin^2 \theta - 1)}} \\
&= \frac{\mu_0}{4\pi} \int_0^{\pi/2} \frac{4RR'(2\sin^2 \theta - 1)d\theta}{\sqrt{(Z-Z')^2 + R^2 + R'^2 - 2RR'(2\sin^2 \theta - 1)}} \\
&= \frac{\mu_0}{4\pi} \int_0^{\pi/2} \frac{4RR'(2\sin^2 \theta - 1)d\theta}{\sqrt{(Z-Z')^2 + (R+R')^2 - 4RR' \sin^2 \theta}} \tag{B.15}
\end{aligned}$$

Define

$$k^2 = \frac{4RR'}{(Z-Z')^2 + (R+R')^2} \tag{B.16}$$

Then

$$\begin{aligned}
& G(R', Z', R, Z) \\
&= \frac{\mu_0}{4\pi} \int_0^{\pi/2} \frac{4RR'(2\sin^2 \theta - 1)d\theta}{\sqrt{(Z-Z')^2 + (R+R')^2} \sqrt{1 - k^2 \sin^2 \theta}} \\
&= \frac{\mu_0 \sqrt{RR'}}{2\pi} \int_0^{\pi/2} \frac{k(2\sin^2 \theta - 1)d\theta}{\sqrt{1 - k^2 \sin^2 \theta}} \\
&= \frac{\mu_0 \sqrt{RR'}}{2\pi k} \left[\int_0^{\pi/2} \frac{2 - k^2}{\sqrt{1 - k^2 \sin^2 \theta}} d\theta - \int_0^{\pi/2} \frac{2 - 2k^2 \sin^2 \theta}{\sqrt{1 - k^2 \sin^2 \theta}} d\theta \right] \\
&= \frac{\mu_0 \sqrt{RR'}}{2\pi k} \left[\int_0^{\pi/2} \frac{2 - k^2}{\sqrt{1 - k^2 \sin^2 \theta}} d\theta - 2 \int_0^{\pi/2} \sqrt{1 - k^2 \sin^2 \theta} d\theta \right] \\
&= \frac{\mu_0 \sqrt{RR'}}{2\pi k} [(2 - k^2)K(k) - 2E(k)]. \tag{B.17}
\end{aligned}$$

where

$$E(k) = \int_0^{\pi/2} \sqrt{1 - k^2 \sin^2 \theta} d\theta,$$

$$K(k) = \int_0^{\pi/2} \frac{1}{\sqrt{1 - k^2 \sin^2 \theta}} d\theta$$

are the elliptic integrals of the first and second kind.

Similarly, we can calculate the magnetic field:

$$\mathbf{B}(\mathbf{r}) = \frac{\mu_0 I}{4\pi} \oint \frac{d\mathbf{l}' \times (\mathbf{r} - \mathbf{r}')}{|\mathbf{r} - \mathbf{r}'|^3}, \quad (\text{B.18})$$

where the cross product is written as

$$\begin{aligned} d\mathbf{l}' \times (\mathbf{r} - \mathbf{r}') &= \begin{vmatrix} \hat{\mathbf{e}}_x & \hat{\mathbf{e}}_y & \hat{\mathbf{e}}_z \\ -R' d\phi' \sin \phi' & R' d\phi' \cos \phi' & 0 \\ R - R' \cos \phi' & -R' \sin \phi' & Z - Z' \end{vmatrix} \\ &= \hat{\mathbf{e}}_x R' d\phi' \cos \phi' (Z - Z') + \hat{\mathbf{e}}_y R' d\phi' \sin \phi' (Z - Z') \\ &\quad + \hat{\mathbf{e}}_z (R'^2 - R R' \cos \phi') d\phi' \end{aligned}$$

The $\hat{\mathbf{e}}_R(\mathbf{r})$ and $\hat{\mathbf{e}}_Z(\mathbf{r})$ components of the above result are written as

$$\begin{aligned} \hat{\mathbf{e}}_R \cdot d\mathbf{l}' \times (\mathbf{r} - \mathbf{r}') &= R' (Z - Z') \cos \phi' d\phi' \\ \hat{\mathbf{e}}_Z \cdot d\mathbf{l}' \times (\mathbf{r} - \mathbf{r}') &= (R'^2 - R R' \cos \phi') d\phi' \end{aligned}$$

Using these in Eq. (B.18), $B_R(\mathbf{r})$ and $B_Z(\mathbf{r})$ are written as

$$B_R = \frac{\mu_0 I}{4\pi} \int_0^{2\pi} \frac{R' (Z - Z') \cos \phi'}{(\sqrt{(Z - Z')^2 + (R - R' \cos \phi')^2 + (R' \sin \phi')^2})^3} d\phi',$$

$$B_Z = \frac{\mu_0 I}{4\pi} \int_0^{2\pi} \frac{R'^2 - R R' \cos \phi'}{(\sqrt{(Z - Z')^2 + (R - R' \cos \phi')^2 + (R' \sin \phi')^2})^3} d\phi',$$

Dropping I in the above expressions gives the corresponding Green's function:

$$G_{B_R}(R', Z', R, Z) = \frac{\mu_0}{2\pi} \int_0^\pi \frac{R' (Z - Z') \cos \phi'}{(\sqrt{(Z - Z')^2 + R^2 + R'^2 - 2R R' \cos \phi'})^3} d\phi', \quad (\text{B.19})$$

$$G_{B_Z}(R', Z', R, Z) = \frac{\mu_0}{2\pi} \int_0^\pi \frac{R'^2 - R R' \cos \phi'}{(\sqrt{(Z - Z')^2 + R^2 + R'^2 - 2R R' \cos \phi'})^3} d\phi', \quad (\text{B.20})$$

One can also try to write the above formula to ellipticity integral form. The result is not compact as the formula for RA_ϕ . So I directly use Eqs. (B.18) and (B.19) in HEQ code. Alternatively, one can directly take the finite difference of G to get G_{B_R} and G_{B_Z} in a numerical code.

B.4 For wires in poloidal plane

For a curve in the poloidal plane, the line element $d\mathbf{l}$ in terms of the cylindrical basis is written as $d\mathbf{l} = dR\hat{\mathbf{e}}_R(\phi) + dZ\hat{\mathbf{e}}_z$. Using Cartesian coordinate basis vectors, $d\mathbf{l}$ is written as

$$d\mathbf{l} = dR \cos\phi \hat{\mathbf{e}}_x + dR \sin\phi \hat{\mathbf{e}}_y + dZ \hat{\mathbf{e}}_z. \quad (\text{B.21})$$

Using Eq. (B.21) and (), we obtain

$$d\mathbf{l} \times (\mathbf{r} - \mathbf{r}') = \begin{vmatrix} \hat{\mathbf{e}}_x & \hat{\mathbf{e}}_y & \hat{\mathbf{e}}_z \\ dR \cos\phi & dR \sin\phi & dZ \\ (x - x') & (y - y') & (z - z') \end{vmatrix}. \quad (\text{B.22})$$

19 About this document

This document initially contains notes I took when learning tokamak equilibrium theory. As a result of the on-going learning, the document is evolving. I enjoy seeing the continuous improvement of this document over a long time scale (10 years). Most of the content is elementary but I still found I got something totally wrong in the first version. Let me know if you spot something specious.

This document was written by using TeXmacs[27], a structured wysiwyw (what you see is what you want) editor for scientists. The HTML version is generated by first converting the TeXmacs file to TeX format and then using `htlatex` to convert the TeX to HTML.

Bibliography

- [1] R Aymar, P Barabaschi, and Y Shimomura. The ITER design. *Plasma Physics and Controlled Fusion*, 44(5):519–565, apr 2002.
- [2] M. A. Beer, S. C. Cowley, and G. W. Hammett. Field-aligned coordinates for nonlinear simulations of tokamak turbulence. *Phys. Plasmas (1994-present)*, 2(7):2687–2700, 1995.
- [3] H. L. Berk, J. W. Van Dam, D. Borba, J. Candy, G. T. A. Huysmans, and S. Sharapov. More on core localized toroidal alfvén eigenmodes. *Phys. Plasmas*, 2(9):3401–3406, 1995.
- [4] Allen H. Boozer. Physics of magnetically confined plasmas. *Rev. Mod. Phys.*, 76:1071–1141, Jan 2005.
- [5] R. Gallix, C. Jong, J. Knaster, N. Mitchell C. Sborchia, Y. Fu. Design and specifications of the iter tf coils. *IEEE TRANSACTIONS ON APPLIED SUPERCONDUCTIVITY*, 18(2):463, 2008.
- [6] Yang Chen and Scott E. Parker. A delta-f particle method for gyrokinetic simulations with kinetic electrons and electromagnetic perturbations. *Journal of Computational Physics*, 189(2):463–475, 2003.
- [7] Yang Chen and Scott E. Parker. Electromagnetic gyrokinetic δf particle-in-cell turbulence simulation with realistic equilibrium profiles and geometry. *Journal of Computational Physics*, 220(2):839–855, 2007.

- [8] Yang Chen, Scott E. Parker, J. Lang, and G.-Y. Fu. Linear gyrokinetic simulation of high- n toroidal alfvén eigenmodes in a burning plasma. *Phys. Plasmas*, 17(10):102504, 2010.
- [9] Fu Peng, Gao Ge Chen Yuan-Yang, Bao Xiao-Hua. Plasma shape optimization for east tokamak using orthogonal method. *Chinese Physics B*, 28(1):15201, 2019.
- [10] C.Z Cheng and M.S Chance. Nova: a nonvariational code for solving the mhd stability of axisymmetric toroidal plasmas. *J. of Comput. Phys.*, 71(1):124–146, 1987.
- [11] J DeLucia, S.C Jardin, and A.M.M Todd. An iterative metric method for solving the inverse tokamak equilibrium problem. *Journal of Computational Physics*, 37(2):183–204, 1980.
- [12] A. M. Dimits. Fluid simulations of tokamak turbulence in quasibalooning coordinates. *Phys. Rev. E*, 48:4070–4079, Nov 1993.
- [13] T. Görler, N. Tronko, W. A. Hornsby, A. Bottino, R. Kleiber, C. Nordsieck, V. Grandgirard, F. Jenko, and E. Sonnendrücker. Intercode comparison of gyrokinetic global electromagnetic modes. *Physics of Plasmas*, 23(7):72503, 2016.
- [14] J. van der Hoeven et al. GNU TeXmacs. <https://www.texmacs.org>, 1998.
- [15] Youjun Hu, Guoqiang Li, N. N. Gorelenkov, Huishan Cai, Wenjun Yang, Deng Zhou, and Qilong Ren. Numerical study of alfvén eigenmodes in the experimental advanced superconducting tokamak. *Phys. Plasmas*, 21(5):0, 2014.
- [16] Stephen C. Jardin. *Computational methods in plasma physics*. CRC Press, 2010.
- [17] Young Mu Jeon. Development of a Free-boundary Tokamak Equilibrium Solver for Advanced Study of Tokamak Equilibria. *Journal of the Korean Physical Society*, 67(5):843–853, 09 2015.
- [18] L.L. Lao, H. St. John, R.D. Stambaugh, A.G. Kellman, and W. Pfeiffer. Reconstruction of current profile parameters and plasma shapes in tokamaks. *Nucl. Fusion*, 25(11):1611, 1985.
- [19] G.S. Lee, M. Kwon, C.J. Doh, B.G. Hong, K. Kim, M.H. Cho, W. Namkung, C.S. Chang, Y.C. Kim, J.Y. Kim, H.G. Jhang, D.K. Lee, K.I. You, J.H. Han, M.C. Kyum, J.W. Choi, J. Hong, W.C. Kim, B.C. Kim, J.H. Choi, S.H. Seo, H.K. Na, H.G. Lee, S.G. Lee, S.J. Yoo, B.J. Lee, Y.S. Jung, J.G. Bak, H.L. Yang, S.Y. Cho, K.H. Im, N.I. Hur, I.K. Yoo, J.W. Sa, K.H. Hong, G.H. Kim, B.J. Yoo, H.C. Ri, Y.K. Oh, Y.S. Kim, C.H. Choi, D.L. Kim, Y.M. Park, K.W. Cho, T.H. Ha, S.M. Hwang, Y.J. Kim, S. Baang, S.I. Lee, H.Y. Chang, W. Choe, S.G. Jeong, S.S. Oh, H.J. Lee, B.H. Oh, B.H. Choi, C.K. Hwang, S.R. In, S.H. Jeong, I.S. Ko, Y.S. Bae, H.S. Kang, J.B. Kim, H.J. Ahn, D.S. Kim, C.H. Choi, J.H. Lee, Y.W. Lee, Y.S. Hwang, S.H. Hong, K.-H. Chung, D.-I. Choi, and KSTAR Team. Design and construction of the KSTAR tokamak. *Nuclear Fusion*, 41(10):1515–1523, oct 2001.
- [20] G Q Li, Q L Ren, J P Qian, L L Lao, S Y Ding, Y J Chen, Z X Liu, B Lu, and Q Zang. Kinetic equilibrium reconstruction on east tokamak. *Plasma Phys. Controlled Fusion*, 55(12):125008, 2013.
- [21] J.L. Luxon. A design retrospective of the DIII-D tokamak. *Nuclear Fusion*, 42(5):614–633, may 2002.
- [22] R. L. Miller, M. S. Chu, J. M. Greene, Y. R. Lin-Liu, and R. E. Waltz. Noncircular, finite aspect ratio, local equilibrium model. *Phys. Plasmas*, 5(4):973–978, 1998.
- [23] M. Ottaviani. An alternative approach to field-aligned coordinates for plasma turbulence simulations. *Physics Letters A*, 375(15):1677–1685, 2011.
- [24] S.A. Sabbagh, A.C. Sontag, J.M. Bialek, D.A. Gates, A.H. Glasser, J.E. Menard, W. Zhu, M.G. Bell, R.E. Bell, A. Bondeson, C.E. Bush, J.D. Callen, M.S. Chu, C.C. Hegna, S.M. Kaye, L.L. Lao, B.P. LeBlanc, Y.Q. Liu, R. Maingi, D. Mueller, K.C. Shaing, D. Stutman, K. Tritz, and C. Zhang. Resistive wall stabilized operation in rotating high beta nstx plasmas. *Nucl. Fusion*, 46(5):635, 2006.
- [25] I. Song, C. Choi, and M. Cho. Quench protection system for the superconducting coil of the kstar tokamak. *IEEE Transactions on Applied Superconductivity*, 17(1):1–6, March 2007.

- [26] Youwen Sun. Tokamak geometry and equilibrium. http://theory.ipp.ac.cn/~yj/other/TOKAMAK_geometry_and_equilibrium-Youwen_Sun_201208.pdf, 2012. [Online; Institute of Plasma Physics, Chinese Academy of Sciences].
- [27] Joris van der Hoeven. Gnu texmacs, a structured wysiwyw (what you see is what you want) editor for scientists. <http://www.texmacs.org/>, 2007. [Online].
- [28] W. X. Wang, Z. Lin, W. M. Tang, W. W. Lee, S. Ethier, J. L. V. Lewandowski, G. Rewoldt, T. S. Hahm, and J. Manickam. Gyro-kinetic simulation of global turbulent transport properties in tokamak experiments. *Physics of Plasmas*, 13(9):92505, 2006.
- [29] John Wesson. *Tokamaks*. Oxford University Press, 2004.
- [30] R. B. White and M. S. Chance. Hamiltonian guiding center drift orbit calculation for plasmas of arbitrary cross section. *The Physics of Fluids*, 27(10):2455–2467, 1984.
- [31] B J Xiao, D A Humphreys, and M L Walker. East plasma control system. *Fusion Engineering and Design*, 83:181, 2008.
- [32] B. J. Xiao. The first diverted plasma on east tokamak. *34th EPS Conference on Plasma Phys*, 2007.